frontiers | Research Topics

# Clinical impact of fast platforms and laboratory automation for the rapid diagnosis of infectious diseases and detection of antimicrobial resistance determinants

**Edited by**
Antonella Mencacci, Fabio Arena
and Paola Bernaschi

**Published in**
Frontiers in Cellular and Infection Microbiology

ISSN 1664-8714
ISBN 978-2-8325-4153-1
DOI 10.3389/978-2-8325-4153-1

## About Frontiers

Frontiers is more than just an open access publisher of scholarly articles: it is a pioneering approach to the world of academia, radically improving the way scholarly research is managed. The grand vision of Frontiers is a world where all people have an equal opportunity to seek, share and generate knowledge. Frontiers provides immediate and permanent online open access to all its publications, but this alone is not enough to realize our grand goals.

## Frontiers journal series

The Frontiers journal series is a multi-tier and interdisciplinary set of open-access, online journals, promising a paradigm shift from the current review, selection and dissemination processes in academic publishing. All Frontiers journals are driven by researchers for researchers; therefore, they constitute a service to the scholarly community. At the same time, the *Frontiers journal series* operates on a revolutionary invention, the tiered publishing system, initially addressing specific communities of scholars, and gradually climbing up to broader public understanding, thus serving the interests of the lay society, too.

## Dedication to quality

Each Frontiers article is a landmark of the highest quality, thanks to genuinely collaborative interactions between authors and review editors, who include some of the world's best academicians. Research must be certified by peers before entering a stream of knowledge that may eventually reach the public - and shape society; therefore, Frontiers only applies the most rigorous and unbiased reviews. Frontiers revolutionizes research publishing by freely delivering the most outstanding research, evaluated with no bias from both the academic and social point of view. By applying the most advanced information technologies, Frontiers is catapulting scholarly publishing into a new generation.

## What are Frontiers Research Topics?

Frontiers Research Topics are very popular trademarks of the *Frontiers journals series*: they are collections of at least ten articles, all centered on a particular subject. With their unique mix of varied contributions from Original Research to Review Articles, Frontiers Research Topics unify the most influential researchers, the latest key findings and historical advances in a hot research area.

Find out more on how to host your own Frontiers Research Topic or contribute to one as an author by contacting the Frontiers editorial office: frontiersin.org/about/contact

# Clinical impact of fast platforms and laboratory automation for the rapid diagnosis of infectious diseases and detection of antimicrobial resistance determinants

**Topic editors**

Antonella Mencacci – University of Perugia Dept of Medicine and Surgery, Italy
Fabio Arena – University of Foggia, Italy
Paola Bernaschi – Bambino Gesù Children's Hospital (IRCCS), Italy

**Citation**

Mencacci, A., Arena, F., Bernaschi, P., eds. (2023). *Clinical impact of fast platforms and laboratory automation for the rapid diagnosis of infectious diseases and detection of antimicrobial resistance determinants*. Lausanne: Frontiers Media SA. doi: 10.3389/978-2-8325-4153-1

# Table of contents

frontiers | Frontiers in Cellular and Infection Microbiology

TYPE Editorial
PUBLISHED 04 December 2023
DOI 10.3389/fcimb.2023.1321663



OPEN ACCESS

EDITED AND REVIEWED BY
Costas C Papagiannitsis,
University of Thessaly, Greece

*CORRESPONDENCE
Antonella Mencacci
antonella.mencacci@unipg.it

RECEIVED 14 October 2023
ACCEPTED 27 November 2023
PUBLISHED 04 December 2023

CITATION
Arena F, Bernaschi P and Mencacci A (2023) Editorial: Clinical impact of fast platforms and laboratory automation for the rapid diagnosis of infectious diseases and detection of antimicrobial resistance determinants.
*Front. Cell. Infect. Microbiol.* 13:1321663.
doi: 10.3389/fcimb.2023.1321663



# Editorial: Clinical impact of fast platforms and laboratory automation for the rapid diagnosis of infectious diseases and detection of antimicrobial resistance determinants

Fabio Arena[1], Paola Bernaschi[2] and Antonella Mencacci[3,4]*

[1]Department of Clinical and Experimental Medicine, University of Foggia, Foggia, Italy, [2]Microbiology and Diagnostic Immunology Unit, Bambino Gesù Children's Hospital, Istituto di Ricovero e Cura a Carattere Scientifico (IRCCS), Rome, Italy, [3]Microbiology and Clinical Microbiology, Department of Medicine and Surgery, University of Perugia, Perugia, Italy, [4]Microbiology, Perugia General Hospital, Perugia, Italy

KEYWORDS

**clinical outcome, innovation, next-generation sequencing, artificial intelligence, new diagnostics**

Editorial on the Research Topic
Clinical impact of fast platforms and laboratory automation for the rapid diagnosis of infectious diseases and detection of antimicrobial resistance determinants

Infectious diseases remain a significant global health threat, exacerbated by the emergence of antimicrobial resistance (Centers for Disease Control and Prevention, 2019; Baquero et al., 2021; European Centre for Disease Prevention and Control, 2022; World Health Organization, 2022). Accurate and timely microbiological diagnosis is vital for effective patient management, infection control, and antimicrobial stewardship (Morency-Potvin et al., 2019).

The availability of fast platforms and laboratory automation have revolutionized clinical microbiology improving the speed and precision of diagnosing infectious diseases (Özenci and Rossolini, 2019; Trotter et al., 2019). Traditional diagnostic methods, such as culture-based techniques, are time-consuming and may take several days to yield results. In contrast, automated platforms like polymerase chain reaction (PCR) and next-generation sequencing (NGS) can rapidly identify pathogens directly from clinical specimens. This rapidity allows for the prompt initiation of appropriate treatment, reducing the risk of complications and transmission to other patients, all while aligning with the principles of diagnostic stewardship (Dien Bard and McElvania, 2020; Hilt and Ferrieri, 2022).

Diagnostic stewardship is a healthcare concept and practice that focuses on the responsible and judicious use of diagnostic tests and procedures to improve patient care, enhance clinical outcomes, and optimize resource utilization. It is closely related to antimicrobial stewardship, which primarily deals with the appropriate use of antibiotics to combat antimicrobial resistance. Diagnostic stewardship, on the other hand,

encompasses a broader spectrum of diagnostic tests and procedures beyond just antibiotics (Patel and Fang, 2018).

Prioritizing laboratory practices in a patient-oriented approach can be used to optimize technology advances for improved patient care. Laboratory automation optimizes workflow in clinical microbiology laboratories, reducing the manual labor needed for sample processing and analysis. This not only expedites diagnostic turnaround times but also maximizes resource utilization. Automation diminishes the risk of human error, enhances result reproducibility, and frees laboratory personnel to concentrate on more intricate tasks. All these aspects are discussed in a "Perspective" paper published in this Research Topic (Menacci et al.).

Beside this, several contributions in this Research Topic have focused on how innovative and rapid diagnostic approaches could improve the diagnosis of neglected infective diseases or the detection of slow growing/fastidious pathogens, enhancing the quality of care provided to patients.

For example, an "Original research" paper described the functioning and the performances of a new DNA microarray chip assay which provides a simple, rapid, high-throughput, and reliable method for the diagnosis of cutaneous mycobacterial infections with potential for clinical application (Yu et al.). In another research paper, a recombinase-aided amplification assay targeting the 16S rRNA gene was developed for rapid detection of *Burkholderia cepacia* complex in patients with an uncharacterized infection who are immunocompromised or have underlying diseases, thereby providing guidance for effective treatment (Fu et al.). Finally, a novel automated antifungal susceptibility testing system, Droplet 48, which detects the fluorescence of microdilution wells in real time and fits growth characteristics using fluorescence intensity over time has been described (Yu et al.).

Another group of original research papers focused on how NGS approaches can be adapted to the diagnosis of infectious diseases and can empower clinicians to create personalized treatment strategies by providing comprehensive information about the infecting pathogen and its resistance profile in a timely manner. An original research paper showed how metagenomic NGS could represent a valuable supplement of conventional microbiological tests for the pathogen detection responsible of community acquired pulmonary infection (Lin et al.). A similar experience underscored that, in some cases metagenomic NGS (using Illumina short reads) was more sensitive than the conventional culture method in the detection of fastidious pathogens such as *Pneumocystis jirovecii* and Mucoraceae form blood samples, bronchoalveolar lavage fluid, cerebrospinal fluid, sputum, and ascitic fluid of immunocompromised patients (Li et al.). In another study the Nanopore sequencing approach (long reads) together with a set of multiple independent predictors, enabled the discrimination of uropathogens from colonizing bacteria in a large set of urinary tract infections (Jiang et al.). An original research provided insights on how metagenomic NGS can provide additional information to improve the diagnosis of *Cutibacterium acnes* orthopedic implant-associated infections. Taken together, metagenomic NGS was able to detect *C. acnes* DNA in more samples compared to culture and could be used to identify cases of suspected *C. acnes* orthopedic implant-associated infections, in particular, regarding possible polymicrobial infections, where the growth of *C. acnes* might be compromised due to a fast-growing bacterial species (Ponraj et al.).

Finally, a "METHODS article" published in this Research Topic showed how automated systems can empower healthcare facilities to establish robust surveillance programs for infectious diseases. In this paper a combination of real-time PCR assay with a strain typing method based on mid-infrared radiation associated with Fourier transform IR spectroscopy was adopted for rapid detection and typing of the emerging pathogen *Candida auris* (Contreras and Morgan).

As we move forward in the field of clinical microbiology, continuous research and development are vital. Challenges such as the integration of new technologies (metagenomic NGS), efficient data management, use of artificial intelligence and standardization of protocols need to be addressed (Hilt EE and Ferrieri, 2022; Egli, 2023). Moreover, ensuring accessibility to these advanced diagnostic tools in resource-limited settings is crucial.

The clinical impact of fast platforms and laboratory automation for the rapid diagnosis of infectious diseases, detection of antimicrobial resistance determinants, and diagnostic stewardship is profound. These technologies have transformed clinical microbiology, enabling healthcare providers to make quicker, more precise diagnoses and treatment decisions while aligning with the principles of diagnostic stewardship. As we continue to advance in this field, the potential to improve patient outcomes, reduce the spread of infectious diseases, combat antimicrobial resistance, and promote responsible diagnostic stewardship holds great promise, ushering in a brighter future for global healthcare.

## Author contributions

FA: Writing – original draft, Writing – review & editing. PB: Writing – review & editing. AM: Writing – review & editing.

## Conflict of interest

The authors declare that the research was conducted in the absence of any commercial or financial relationships that could be construed as a potential conflict of interest.

## Publisher's note

## References


Baquero, F., Martínez JL, F., Lanza, V., Rodríguez-Beltrán, J., Galán, J. C., San Millán, A., et al. (2021). Evolutionary pathways and trajectories in antibiotic resistance. *Clin. Microbiol. Rev.* 34 (4), e0005019. doi: 10.1128/CMR.00050-19

Centers for Disease Control and Prevention (2019). *Antibiotic resistance threats in the United States* (Atlanta, GA: U.S. Department of Health and Human Services, CDC).

Dien Bard, J., and McElvania, E. (2020). Panels and syndromic testing in clinical microbiology. *Clin. Lab. Med.* 40 (4), 393–420. doi: 10.1016/j.cll.2020.08.001

Egli, A. (2023). ChatGPT, GPT-4, and other large language models - the next revolution for clinical microbiology? *Clin. Infect. Dis.*, 77 (9), 1322-1328. doi: 10.1093/cid/ciad407

European Centre for Disease Prevention and Control (2022). *Assessing the health burden of infections with antibiotic-resistant bacteria in the EU/EEA 2016-2020* (Stockholm: ECDC).

Hilt, E. E., and Ferrieri, P. (2022). Next generation and other sequencing technologies in diagnostic microbiology and infectious diseases. *Genes (Basel).* 13 (9), 1566. doi: 10.3390/genes13091566

Morency-Potvin, P., Schwartz, D. N., and Weinstein, R. A. (2016). Antimicrobial stewardship: how the microbiology laboratory can right the ship. *Clin. Microbiol. Rev.* 30 (1), 381–407. doi: 10.1128/CMR.00066-16

Özenci, V., and Rossolini, G. M. (2019). Rapid microbial identification and antimicrobial susceptibility testing to drive better patient care: an evolving scenario. *J. Antimicrob. Chemother.* 74 (Suppl 1), i2–i5. doi: 10.1093/jac/dky529

Patel, R., and Fang, F. C. (2018). Diagnostic stewardship: opportunity for a laboratory-infectious diseases partnership. *Clin. Infect. Dis.* 67 (5), 799–801. doi: 10.1093/cid/ciy077.2

Trotter, A. J., Aydin, A., Strinden, M. J., and O'Grady, J. (2019). Recent and emerging technologies for the rapid diagnosis of infection and antimicrobial resistance. *Curr. Opin. Microbiol.* 51, 39–45. doi: 10.1016/j.mib.2019.03.001.4

World Health Organization (2022). *Global antimicrobial resistance and use surveillance system (GLASS) report 2022* (Geneva: World Health Organization).

frontiers | Frontiers in Cellular and Infection Microbiology

TYPE Methods
PUBLISHED 31 August 2022
DOI 10.3389/fcimb.2022.887754



OPEN ACCESS

EDITED BY
Yun F. (Wayne) Wang,
Emory University, United States

REVIEWED BY
Marie Desnos-Ollivier,
Institut Pasteur, France
Sudha Chaturvedi,
Wadsworth Center, United States

*CORRESPONDENCE
Margie A. Morgan
Margie.Morgan@cshs.org

†These authors have contributed equally to this work

SPECIALTY SECTION
This article was submitted to Clinical Microbiology, a section of the journal Frontiers in Cellular and Infection Microbiology

RECEIVED 01 March 2022
ACCEPTED 30 June 2022
PUBLISHED 31 August 2022

CITATION
Contreras DA and Morgan MA (2022) Surveillance diagnostic algorithm using real-time PCR assay and strain typing method development to assist with the control of *C. auris* amid COVID-19 pandemic.
*Front. Cell. Infect. Microbiol.* 12:887754.
doi: 10.3389/fcimb.2022.887754



# Surveillance diagnostic algorithm using real-time PCR assay and strain typing method development to assist with the control of *C. auris* amid COVID-19 pandemic

Deisy A. Contreras† and Margie A. Morgan*†

Clinical Microbiology Laboratory, Department Pathology and Laboratory Medicine, Cedars-Sinai Medical Center, Los Angeles, CA, United States,

*Candida auris* continues to be a global threat for infection and transmission in hospitals and long-term care facilities. The emergence of SARS-CoV-2 has rerouted attention and resources away from this silent pandemic to the frontlines of the ongoing COVID-19 disease. Cases of *C. auris* continue to rise, and clinical laboratories need a contingency plan to prevent a possible outbreak amid the COVID-19 pandemic. Here, we introduce a two-tier *Candida auris* surveillance program that includes, first, a rapid qualitative rt-PCR for the identification of high-risk patients and, second, a method to analyze the isolated *C. auris* for strain typing using the Fourier-Transform Infrared spectroscopy. We have performed this two-tier surveillance for over 700 at-risk patients being admitted into our hospital and have identified 28 positive specimens (4%) over a 1-year period. Strain typing analysis by the IR spectrum acquisition typing method, supplemented by whole genome sequencing, has shown grouping of two significant clusters. The majority of our isolates belong to circulating African lineage associated with *C. auris* Clade III and an isolated strain grouping differently belonging to South Asian lineage *C. auris* Clade I. Low numbers of genomic variation point to local and ongoing transmission within the Los Angeles area not specifically within the hospital setting. Collectively, clinical laboratories having the ability to rapidly screen high-risk patients for *C. auris* and to participate in outbreak investigations by offering strain typing will greatly assist in the control of *C. auris* transmission within the hospital setting.

KEYWORDS

***candida auris*, surveillance pcr, strain typing, epidemiology, algorithm**

## Introduction

*Candida auris* continues to be a major public health threat, due to the unrelenting nosocomial spread in long-term and acute care medical facilities. This fungal pathogen causes a wide array of clinical presentations ranging from invasive nosocomial bloodstream to deep wound infections usually affecting the most vulnerable immunocompromised patient population resulting in high mortality rates (Du et al., 2020). The first incident of *C. auris* was in an unrecognized case of candidemia in South Korea dating back to as early as 1996 (Forsberg et al., 2019) followed by its first identified official report in 2009 in Japan (Satoh et al., 2009). To date, there are five different clades of *C. auris* that have been identified globally, in which four out of the five have been reported in the United States, attributing their introduction through international travel and medical tourism (Chow et al., 2018). In addition to its elusive nature and spread, this yeast exhibits resistance patterns in all the three widely used classes of antifungals including azoles, echinocandins, and polyenes, making it a critical antibiotic resistance threat in the US. The Centers for Disease Control and Prevention (CDC, 2019) stresses the need for the implementation of accurate diagnostic methods and infection prevention mitigation measures in US medical institutions.

While hospitals were preparing to combat this emerging yeast pathogen, the world was confronted by another novel agent causing a severe pneumonia-like illness, which was first identified in Wuhan, Hubei province, China in January 2020 as SARS-CoV-2 (Wu et al., 2020). This viral agent and succeeding variants were defined by increased transmissibility and high mortality rates, leaving patients in intensive care units supported on ventilators and immunosuppressive drugs vulnerable. Hospitals were soon met with an overwhelmingly need to focus all resources on preventing the spread of SARS-CoV-2, leaving them and their immune paralyzed patient population susceptible to secondary nosocomial infections such as those caused by *C. auris*. As the medical community learned to better treat and contain COVID-19 infections, hospitals were observing an increase in *C. auris* cases. By January 2021, cases of *C. auris* infections and transmission were at the frontline of most hospitals, specifically in those patients who have spent time in long-term acute care hospitals (LTACH). Containment of *C. auris* among patients, specifically residents of high-acuity long-term care facilities and ventilator-equipped skilled nursing facilities (vSNF), remains a critical public health priority, predominantly in the context of the current COVID-19 pandemic.

The Department of Public Health put out a health advisory for healthcare facilities alerting them of this need to contain nosocomial transmission rates of *C. auris*. The current guidelines called for active surveillance for the rapid identification of high-risk patients colonized with *C. auris* and implementation of infection control measures. Rapid identification could be achieved by the employment of highly sensitive real-time polymerase chain reaction (rt-PCR) platform. In addition to rapid identification of colonized patients, an alternative strain typing method was needed to aid in outbreak investigations within the clinical setting. In this context, the laboratory turned to spectroscopy-based technique, particularly the IR Biotyper (Bruker Daltonics, Germany), which utilizes mid-infrared (IR) radiation associated with Fourier transform IR (FTIR) spectroscopy. This direct IR radiation generates vibration patterns, primarily in the C-O stretching of biomolecules such as carbohydrates (800–1,300 $cm^{-1}$) within the biochemical structure of these prokaryotic cell. These vibration patterns generate strain-specific absorbance fingerprints within the IR spectrum (Vatanshenassan et al., 2020), which can be used to differentiate among isolates. Literature has shown extensive reports illustrating the discriminatory power among both Gram-positive and Gram-negative bacteria, particularly *Listeria* spp., *Bacillus* spp., *Pseudomonas* spp., *Klebsiella* spp., and *Salmonella* spp., both at the genus and species levels (Quintelas et al., 2018; Hu, et al., 2020; Rakovitsky et al., 2020; Cordovana et al., 2021; Mullie, et al., 2022; Pascale, et al., 2022; Wang-Wang, et al., 2022). The IR Biotyper has proven to be an effective tool for microbial strain typing, specifically for those pathogens that are associated with nosocomial outbreaks within the hospital setting (Deidda et al., 2021; Lombardo, et al., 2021; Guerro-Lozano, et al., 2022; Hadas, et al., 2022; Li, et al., 2022; Passaris, et. al., 2022).

In this study, we aim to discuss implementation for enhanced detection and further prevention of transmission of *Candida auris* through 1) active surveillance by rt-PCR and 2) strain typing by IR Biotyper. This two-tier diagnostic algorithm assesses the status of patients being admitted into the hospital for those individuals identified to be at highest risk for *C. auris* before being admitted to the hospital.

## Materials and methods

### Study design and participants

This study was conducted at a 900-bed tertiary care hospital and affiliate 200-bed community hospital in the coastal and westside communities of Los Angeles. Specimens were prospectively collected and *Candida auris* isolates were recovered from combined axilla/groin surveillance specimens testing positive by rt-PCR (n = 19) and from microbiological cultures from infections including wound (n = 2), respiratory (n = 4), and blood (n = 3). The surveillance rt-PCR assay was implemented as a tool to aid in the detection of *C. auris* from high-risk groups starting in August of 2021 for both our main campus and affiliate hospital. The high-risk criteria for patient inclusion in surveillance testing were established following discussion with our local public health department. Since

initial studies, the microbiology laboratory has recovered an additional 28 C. *auris* isolates that were included in this study. *C. auris* isolates were recovered from critically ill patients with complicated clinical conditions that had a history of medical care in intensive care units and long-term care facilities. Patients ages range from 41 to 60 (n = 10), 61 to 70 (n = 6), and >70 (n = 12) with an equal distribution of both male and female patients.

## *C. auris* real-time surveillance PCR assay

The surveillance PCR assay utilizes the BioGX *Candida auris* rt-PCR reagents (BioGX, Inc., USA) for use with the BD MAX™ open testing system. The assay uses single vial, lyophilized ITS2 primer/probe set (Leach et al., 2018), which are used in conjunction with the BD MAX™ ExK DNA-3 extraction kit (BD Inc., USA). The assay extraction and PCR settings were used according to the manufacturer. In brief, the sample extraction parameters were set as follows: lysis heat time, temperature, sample tip height, and volume were all set to manufacturer default settings, with the exception, of sample volume that was set to 700 µl. The PCR parameters were set to the manufacturer recommendations with the 585/630 detector channel set for *C. auris* and the 680/715 detector channel for the sample processing control sequence from *Drosophila melanogaster* (GenBank, AC246436) with a default cross threshold setting of 200 for both fluorophore channels. The cycling conditions for the assay included an initial hold of 99°C for 300 s, followed by 40 cycles of 99°C for 10 s, 58°C for 30 s, and 70°C for 15 s. To avoid any type of amplicon or high-titer cross contamination, unidirectional workflow was established by keeping specimen preparation and reagent preparation separate.

## IR Biotyper strain typing

Any positive *C. auris* surveillance PCR specimen was inoculated on inhibitory mold agar (Becton Dickinson, USA) and CHROM™ Candida + auris (Hardy Diagnostics, USA) to isolate *C. auris.* Once isolate identification was confirmed to be *C. auris* using MALDI-TOF MS (Bruker Daltonics, USA), it was then plated on Sabouraud Dextrose (SabDex) agar (Becton Dickinson, USA) and incubated at 35°C for 24 h to prepare for strain typing. *Candida auris* isolates recovered from culture were directly inoculated on SabDex agar and incubated at designated standardized temperature and incubation period as stated above. As recommended by the manufacturer, two loopfuls using a 10 µl inoculation loop is harvested from the confluent portion of the yeast colony and added to a 1.5-ml suspension vial filled with 70 µl of freshly prepared 70% ethanol. According to the manufacturer, the amount of yeast colony does not need to be exact, but the pellet should be visible to ensure that there is enough biomass for processing. The suspension vials contain metal cylinders to aid in sample homogenization. The inoculated suspension vial is then vortexed for 10 min. Once initial resuspension of the organism is complete, and then, equal volume of deionized water is added to the suspension vial and vortexed for an additional 5 min. In parallel, IRTS1 and IRTS2 control vials are prepared by adding 90 µl of deionized water to each vial and mixing by vortex for 10 min and then adding undiluted ethanol in equal volume. The suspension was homogenized for an additional 5 min. To perform spectrum acquisition, 15 µl of the processed specimen was plated at a minimum plated in quintuplicates on the silicone sample plate and allowed to airdry on the silicone microtiter plate and allowed to air-dry. Spectra was recorded using an IR Biotyper spectrometer (Bruker Daltonik, USA). The recorded spectra were then visualized and processed by OPUS v8.2 software. To expand on differences between spectra of different isolates, the second derivative FTIR spectra in the carbohydrate adsorption region, as standardized by the manufacturer, were normalized. Hierarchical clustering (HCA) and principal component analysis of the normalized second derivative of each of the isolates were performed using Client Software v3.0 (Bruker Daltonik, USA). Standardization of media type, temperature, and incubation time allows for interpretation of specimens processed at different times. Following specimen preparation, the average time for result is 2 h. Whole genome sequencing (WGS) was utilized to assess the validity of spectral data analysis and not as a strict comparator method.

# Results

## Two-step clinical surveillance diagnostic algorithm *C. auris*

### *C. auris* surveillance PCR assay

While the COVID-19 pandemic was impacting the operations in microbiology laboratories, *C. auris* was appearing in medical facilities as an emerging nosocomial threat. The development, maintenance, and funding of a *C. auris* surveillance and outbreak investigation program was necessary for the control of *C. auris* mitigation within the hospital setting. The microbiology laboratory developed a two-step surveillance program to first detect patients colonized with *C. auris* and then provide nosocomial transmission information from analysis of the cultured yeast (Figure 1). With the cooperation of our local public health department and our epidemiology team, criteria were established for the patient population needing surveillance. All had one or more of the following risk factors: admission from skilled nursing facility (SNF), long-term care hospital (LTACH), and patients that are chronically ventilated or with a tracheostomy. Daily PCR testing runs were performed from axilla/groin specimens collected from patients admitted with risk factors using an Eswab (BD, Inc.,

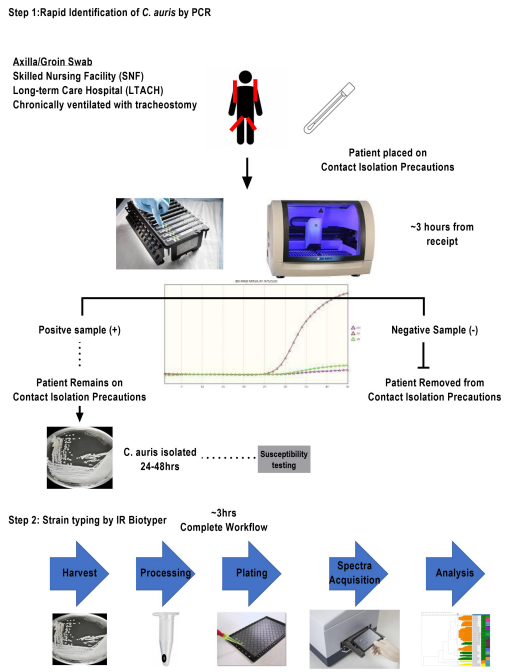


FIGURE 1
Two-tier clinical surveillance diagnostic algorithm for the detection of *C. auris*. This two-step procedure illustrated includes a rapid identification qualitative RT-PCR with an approximate turnaround time of 3 h for at-risk patient population meeting the criteria of transferring from SNF and LTACH or being chronically ventilated with tracheostomy. Any identified PCR-positive specimens are reflexed to fungal culture for isolation of organism. Once a pure culture *C. auris* is obtained, the laboratory sets up a susceptibility panel and a second pure culture isolate is prepared for strain typing.

USA) and analyzed using the BioGX Candida auris rt-PCR reagents for the BD™ MAX open testing system. The limit of detection (LOD) was established using quantitative *C. auris* template control with a known total concentration of $10^5$ copies/ml. Assay sensitivity was found to be set at 100 copies/ml using a total of 40 amplification cycles as set forth and optimized by the manufacturer based on the utilization of the BD™ Extk DNA-3 extraction protocol. On the basis of the established analytical sensitivity, a cycle threshold (Ct) value of ≤ 36 was reported as detected for *C. auris* and a Ct value of greater than 36 would need chart review by the medical director or designee. The coefficient variance was found to be less than 8% when Ct values across different concentrations were measured and compared. Consistent range of Ct values was established, making the assay reliable and highly reproducible. Utilization of CDC and FDA Antibiotic Resistance Isolate Bank *Candida auris* Panel was utilized to establish analytical specificity. The panel consisted of confirmed *C. auris* strains as well as close and distant genetic strains such as *Candida duobushaemulonii*, *C. haemulonii*, *C. krusei*, *C. lusitaniae*, and *Saccharomyces cerevisiae*. It was found that the qualitative RT-PCR was highly specific and sensitive (Table 1). Over the past year, we have successfully screened a total of 716 high-risk patients with a positivity rate of 3.9% (n = 28). Taken together, the data support the findings put forth by Leach and colleagues.

## Fourier transform infrared Biotyper for strain typing

The second tier of our *C. auris* surveillance program was the ability to actively perform strain typing of all *C. auris* strains in real time. Whole genome typing data were used to assess the validity of the spectra analysis acquired by the IR Biotyper. First, we wanted to test the discriminatory power of the IR Biotyper among different clinically relevant yeast species, including *Candida albicans*, *Candida glabrata*, *Candida auris*, and *Cryptococcus neoformans*. Hierarchical cluster and principal component analysis allowed for the successful differentiation of different yeast isolates, which formed distinct clusters both at the genus and species levels (Figure 2). To assess the variability and similarity among the identified *Candida auris* isolates (n = 28), spectra acquisition (n = 420) was acquired by the IR Biotyper spectrometer, and its normalized second derivative was analyzed using Client Software v3.0. Whole genome single-nucleotide polymorphism (SNP)–based phylogenetic analysis of the *C. auris* sequenced genomes was used as reference for the IR-based spectrum typing method. Although these two platforms are measuring different output reads, there were clonal relationships that were found to be significant and were confirmed by both SNP-based phylogenetic and IR-based spectrum typing analysis. K-mer SNP analysis was conducted on the 28 sequenced genomes using previously *C. auris* sequences available on GenBank (Chow et al., 2020). This analysis showed assignment of the 28 C. *auris* isolates into two distinct lineages. Most of the *C. auris* isolates (n = 27) were closely related to African lineage (Clade III) apart from one *C. auris* isolate that was found to be genetically distinct. This single-isolate cluster was closely related to a *C. auris* isolate from the South Asian lineage (Clade I). IR-based spectrum typing analysis of all 28 C. *auris* isolates consistently confirmed the separation of the two specified clusters: Cluster 1, demonstrating isolates belonging to the African lineage, and Cluster 2, single-isolate cluster belonging to South Asian Clade (Figure 3). Further phylogenetic k-mer SNP analysis of *C. auris* isolates in Cluster 1 to its closest ancestral relative showed less than 30-SNP difference among the strains, which contained isolates from both the main hospital and its affiliated clinical center. IR spectra typing analysis distance matrix supported the WGS reference data that the isolates found in Cluster 1 were from both affiliated hospitals. Together, these data demonstrate that the genetic background of isolates from Cluster 1 between both hospitals are very similar. Given the fact that the evolutionary rate of *C. auris* is approximately $5.7 \times 10^{-5}$ substitutions per site per year and that the majority of circulating *C. auris* strains are

TABLE 1 CDC and FDA AMR *C. auris* rt-PCR data showing high specificity and sensitivity.

| CDC ARBank# | Organism name | Clade | Specimen name | BD MAX BioGX *C. auris* Result | | Agreement (Y/N) |
|---|---|---|---|---|---|---|
| | | | | *C. auris POS (+)* | *C. auris NEG (-)* | |
| 381 | *Candida auris* | East Asia | CAU 1 | x | | Y |
| 382 | *Candida auris* | South Asia | CAU 2 | x | | Y |
| 383 | *Candida auris* | Africa | CAU 3 | x | | Y |
| 384 | *Candida auris* | Africa | CAU 4 | x | | Y |
| 385 | *Candida auris* | South America | CAU 5 | x | | Y |
| 386 | *Candida auris* | South America | CAU 6 | x | | Y |
| 387 | *Candida auris* | South Asia | CAU 7 | x | | Y |
| 388 | *Candida auris* | South Asia | CAU 8 | x | | Y |
| 389 | *Candida auris* | South Asia | CAU 9 | x | | Y |
| 390 | *Candida auris* | South Asia | CAU 10 | x | | Y |
| 391 | *Candida duobushaemulonii* | NA | 391 | | x | Y |
| 392 | *Candida duobushaemulonii* | NA | 392 | | x | Y |
| 393 | *Candida haemulonii* | NA | 393 | | x | Y |
| 394 | *Candida duobushaemulonii* | NA | 394 | | x | Y |
| 396 | *Kodameae ohmeri* | NA | 396 | | x | Y |
| 397 | *Candida krusei* | NA | 397 | | x | Y |
| 398 | *Candida lusitaniae* | NA | 398 | | x | Y |
| 399 | *Saccharomyces cerevisiae* | NA | 399 | | x | Y |
| 400 | *Saccharomyces cerevisiae* | NA | 400 | | x | Y |
| 931 | *Candida auris* | South American | CAU21 | x | | Y |
| 932 | *Candida haemulonii* | NA | 932 | | x | Y |
| 1097 | *Candida auris* | Iranian | CAU23 | x | | Y |
| 1099 | *Candida auris* | Iranian | CAU24 | x | | Y |
| 1100 | *Candida auris* | Iranian | CAU25 | x | | Y |
| 1101 | *Candida auris* | East Asian | CAU26 | x | | Y |
| 1102 | *Candida auris* | African | CAU27 | x | | Y |
| 1103 | *Candida auris* | African | CAU28 | x | | Y |
| 1104 | *Candida auris* | South American | CAU29 | x | | Y |
| 1105 | *Candida auris* | South American | CAU30 | x | | Y |
| | *Concordance* | | | 100% | | |

NA, Not Applicable.

genetically very similar suggests that population genetics are geospatial specific in origin with subsequent spread, making transmission within a hospital setting very hard to definitively conclude without the support of additional epidemiological evidence. Collectively, IR spectrum typing analysis performed on the IR Biotyper spectrometer was able to successfully differentiate clinically relevant yeast species both at the genus and species levels as well as differentiate between distinctly different clusters belonging to two different lineages of *C. auris* strains.

## Discussion

*Candida auris* has emerged as a critical multi-drug resistant pathogen having significant clinical impact. Dealing with a silent critical pathogen such as *Candida auris* amid a COVID-19 pandemic requires immediate action from the clinical and laboratory team. Here, we describe a two-tier *Candida auris* surveillance diagnostic algorithm composed of a surveillance rt-PCR for the rapid detection of the organism complemented by a strain typing platform to dissect clonal relatedness in real-time.

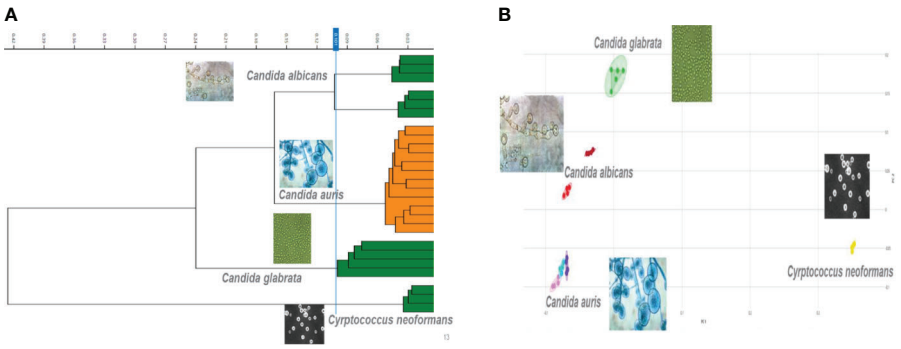


FIGURE 2
Discriminatory power of the IR Biotyper for the differentiation of yeast isolates. **(A)** Dendogram illustrating hierarchical cluster analysis (HCA) and principal component analysis **(B)** of clinically relevant yeast species including *Candida albicans*, *Candida glabrata*, *Candida auris*, and *Cryptococcus neoformans*. In the scatterplot, each isolate is displayed by a different color, and each geometric form represents a single spectrum.

The BioGX *Candida auris* rt-PCR reagents for the BD™ MAX direct from specimen testing were found to have great sensitivity, specificity, and reproducibility in the rapid detection of *C. auris*. It has allowed the clinical laboratory to work alongside our epidemiology team to identify cases and implement infection control measures to prevent transmission within the hospital setting. The *C. auris* rt-PCR has provided rapid results with minimal hands-on time within 2.5 h of setup, which is considerably more rapid than the standard culture method that can take anywhere from 48 to 96 h to isolate and identify. The assay was highly sensitive with LOD of 100 copies/ml, associated with a Ct value of 36. Most importantly, the BioGX RT-PCR was found to be highly specific (100%) having no cross-reactivity with genetically similar yeast relatives such as *Candida duobushaemulonii*, *C. haemulonii*, *C. krusei*, *C. lusitaniae*, and *Saccharomyces cerevisiae*. Our RT-PCR was able to successfully detect *C. auris* isolates from different clades (CDC strains), showing it will be able to detect new genetic variants associated specifically within a lineage clade. This is important because the WGS data have shown us that there is geospatial genetic variation within a regional population as seen in the Los Angeles area and across the country (Chybowska et al., 2020).

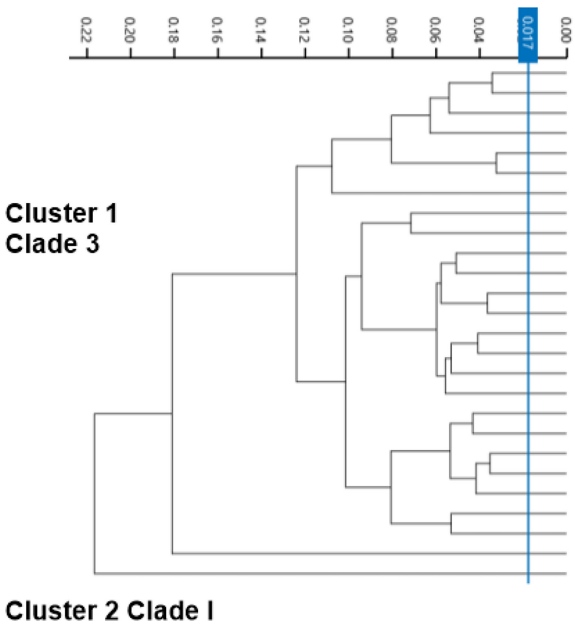


FIGURE 3
Spectra analysis using the IR Biotyper for strain typing. Dendogram illustrating hierarchical cluster analysis (HCA) of identified *C. auris* strains from two affiliated hospitals over a 1-year period showing two distinct significant clusters. Cluster 1 is *C. auris* isolates belonging to African lineage (Clade III), major circulating strain within the Los Angeles area. Cluster 2 was identified to belong to South Asian Lineage (Clade I).

The second part in controlling the spread of *Candida auris* within the clinical setting is having the ability to conduct outbreak investigations and tracking any new variant strain circulation. The IR Biotyper has proven to show its potential in microbial strain typing when using WGS as a reference method and validity. When it comes to IR Biotyper application of yeast isolate differentiation, data are limited, and, to our knowledge, this is the first report of its application for the differentiation of different yeast species, including *Canida auris*. It was found that the IR Biotyper was able to allow for the successful discrimination of various yeast isolates, which included *Candida albicans*, *Candida glabrata*, *Candida auris*, and *Cryptococcus neoformans*. Furthermore, IR spectrum typing method distributed the processed *C. auris* isolates into two different lineages, as supported by phylogenetic genomic analysis. It was able to separate the isolates into two distinct lineages with the majority of the circulating strains

belonging to common ancestral strain belonging to African lineage (Clade III) and a single-isolate cluster to South Asian lineage (Clade I), which furthers support the running hypothesis of Los Angeles County *C. auris* strains primarily belonging to African lineage (Price et al., 2021). The IR Biotyper is a great alternative for moderate to high-complexity laboratories looking for strain typing platform that is moderately priced, technically friendly with post-analysis ease. The IR Biotyper provides spectra within the 2 h of processing, and it does not require extensive prior knowledge of FTIR technology. Since the IR Biotyper is a phenotypic method, it is important to standardize, especially for yeast, the growth conditions such as temperature and growth media to reduce technical variability (Szekely et al., 2019). In order to ensure a high level of technical reproducibility, all samples were processed in quintuplicates. The new IR Biotyper Software v3.0 allows for AI learning capability. This will allow a laboratory to create its own patient database and identify any trends or shifts in the genetic lineage of the yeast in real-time.

In summary, *C. auris* surveillance PCR for detection of colonized patients paired with the Bruker IR Biotyper for fungal strain typing provides a two-step algorithm that has proven to be effective in the control of nosocomial spread of *C. auris* transmission in our hospital amid the COVID-19 pandemic.

## Data availability statement

The original contributions presented in the study are included in the article/supplementary material. Further inquiries can be directed to the corresponding author.

## Author contributions

All authors listed have made a substantial, direct, and intellectual contribution to the work, and approved it for publication.

## Funding

Supported in part by the Special Pathogens Grant (235461) from California Department of Public Health. The contents are solelythe responsibility of the authors and do not necessarilyrepresent the official views of the CDPH.

## Conflict of interest

The authors declare that the research was conducted in the absence of any commercial or financial relationships that could be construed as a potential conflict of interest.

## Publisher's note

All claims expressed in this article are solely those of the authors and do not necessarily represent those of their affiliated organizations, or those of the publisher, the editors and the reviewers. Any product that may be evaluated in this article, or claim that may be made by its manufacturer, is not guaranteed or endorsed by the publisher.

## References

CDC (2019). *Antibiotic resistance threats in the united states*. Atlanta: U.S. Department of Health and Human Services.

Chow, N. A., Gade, L., Tsay, S. V., Forsberg, K., Greenko, J. A., Southwick, K. L., et al. (2018). Multiple introductions and subsequent transmission of multidrug-resistant candida auris in the USA: a molecular epidemiological survey. *Lancet Infect. Dis.* 18, 1377–84. doi: 10.1016/S1473-3099(18)30597-8

Chow, N. A., Muñoz, J. F., Gade, L., Berkow, E. L., Li, X., and Welsh, R. M. (2020). Tracing the evolutionary history and global expansion of candida auris using population genomic analyses. *mBio.* 11, e03364–e03319. doi: 10.1128/mBio.03364-19

Chybowska, A. D., Childers, D. S., and Farrer, R. A. (2020). Nine things genomics can tell us about *Candida auris*. *Front. Gen.* 11. doi: 10.3389/fgene.2020.00351

Cordovana, M., Mauder, N., Kostrzewa, M., Wille, A., Rojak, S., Hagen, R. M., et al (2021). Classification of Salmonella enterica of the (Para-)Typhoid Fever Group by Fourier-Transform Infrared (FTIR) Spectroscopy. *Microorganisms* doi: 10.3390/microorganisms9040853

Deidda, F., Cionci, N. B., Cordovana, M., Campedelli, I., Fracchetti, F., Di Gioia, D., et al (2021). Bifidobacteria Strain Typing by Fourier Transform Infrared Spectroscopy. *Front Microbiol.* doi: 10.3389/fmicb.2021.692975

Du, H., Bing, J., Hu, T., Ennis, C. L., Nobile, C. J., and Huang, G. (2020). *Candida auris*: Epidemiology, biology, antifungal resistance, and virulence. *PloS Pathog.* 16, 10. doi: 10.1371/journal.ppat.1008921

Forsberg, K., Woodworth, K., Walters, M., Berkow, EL, Jackson, B, Chiller, T, et al. (2019). Candida auris: The recent emergence of a multidrug-resistant fungal pathogen. *Med. Mycol.* 57, 1. doi: 10.1093/mmy/myy054

Guerrero-Lozano, I., Galán-Sánchez, F., and Rodríguez-Iglesias, M. (2020). Fourier transform infrared spectroscopy as a new tool for surveillance in local stewardship antimicrobial program: a retrospective study in a nosocomial Acinetobacter baumannii outbreak. *Brazil J. Microbiol.* doi: 10.1007/s42770-022-00774-6

Hadas, K., Elizabeth, T., Polet, E., Alona, K. P., Debby, B. D., Ronza, N. D., et al (2022). Analysis of four carbapenem-resistant Acinetobacter baumannii outbreaks using Fourier-transform infrared spectroscopy. *Infection Control Hosp Epidemiol.* doi: 10.1017/ice.2022.109

Hu, Y., Zhou, H., Lu, J., Sun, Q., Liu, C., Zeng, Y., et al. (2020). Evaluation of the IR biotyper for Klebsiella pneumoniae typing and its potentials in hospital hygiene management. *Microb. Biotechnol.* doi: 10.1111/1751-7915.13709

Leach, L., Russell, A., Zhu, Y., Chaturvedi, S., and Chaturvedi, V. (2018). Development and validation of a real-time PCR assay for rapid detection of candida auris from surveillance samples. *J. Clin. Microbiol.* 56, 2. doi: 10.1128/JCM.01223-17

Li, X., Zhu, L., Wang, X., Li, J., and Tang, B. (2022). Evaluation of IR Biotyper for Lactiplantibacillus plantarum Typing and Its Application Potential in Probiotic Preliminary Screening. *Front. Microbiol.* doi: 10.3389/fmicb.2022.823120

Lombardo, D., Cordovana, M., Deidda, F., Pane, M., and Ambretti, S. (2021). Application of Fourier transform infrared spectroscopy for real-time typing of

Acinetobacter baumannii outbreak in intensive care unit. *Future Microbiol*. doi: 10.2217/fmb-2020-0276

Mullié, C., Lemonnier, D., Adjidé, C. C., Maizel, J., Mismacque, G., Cappe, A., et al (2022). Nosocomial outbreak of monoclonal VIM carbapenemase-producing Enterobacter cloacae complex in an intensive care unit during the COVID-19 pandemic: an integrated approach. *J Hosp Infection*. doi: 10.1016/j.jhin.2021.11.017

Pascale, M. R., Bisognin, F., Mazzotta, M., Girolamini, L., Marino, F., Dal Monte, P., et al (2022). Use of Fourier-Transform Infrared Spectroscopy With IR Biotyper® System for Legionella pneumophila Serogroups Identification. *Front Microbiol*. doi: 10.3389/fmicb.2022.866426

Passaris, I., Mauder, N., Kostrzewa, M., Burckhardt, I., Zimmermann, S., van Sorge, N. M., et al (2022). Validation of Fourier Transform Infrared Spectroscopy for Serotyping of Streptococcus pneumoniae. *J Clin Microbiol*. doi: 10.1128/JCM.00325-22

Price, T. K., Mirasol, R., Ward, K. W., Dayo, A. J., Hilt, E. E., Chandrasekaran, S., et al. (2021). Genomic characterizations of clade III lineage of *Candida auris*, California, USA. *Emerg. Infect. Dis.* 27, 4. doi: 10.3201/eid2704.204361

Quintelas, C., Ferreira, E. C., Lopes, J. A., and Sousa, C. (2018). An overview of the evolution of infrared spectroscopy applied to bacterial typing. *Med. Biotech.* 13, 1–10. doi: 10.1002/biot.201700449

Rakovitsky, N., Frenk, S., Kon, H., Schwartz, D., Temkin, E., Solter, E., et al. (2020). Fourier transform infrared spectroscopy is a new option for outbreak investigation: a retrospective analysis of an extended-spectrum-beta lactamase-producing Klebsiella pneumoniae outbreak in a neonatal intensive care unit. *J. Clin. Microbiol.* 58 (5), e00098–20. doi: 10.1128/JCM.00098-20

Satoh, K., Makimura, K., Hasumi, Y., Nishiyama, Y., Uchida, K., and Yamaguchi, H. (2009). Candida auris sp. nov., a novel ascomycetous yeast isolated from the external ear canal of an inpatient in a japanese hospital. *Microbiol. Immunol.* 53, 1. doi: 10.1111/j.1348-0421.2008.00083.x

Szekely, A., Borman, A. M., and Johnson, E. M. (2019). *Candida auris* isolates of the southern Asian and south African lineages exhibit different phenotypic and antifungal susceptibility profiles *in vitro*. *J. Clin. Micro.* 57, 5. doi: 10.1128/JCM.02055-18

Vatanshenassan, M., Boekhout, T., Mauder, N., Robert, V., Maier, T., and Meis, J. F (2020). Evaluation of Microsatellite Typing, ITS Sequencing, AFLP Fingerprinting, MALDI-TOF MS, and Fourier-Transform Infrared Spectroscopy Analysis of Candida auris. *J. Fungi* 6, 1461–29. doi: 10.3390/jof6030146

Wang-Wang, J. H., Bordoy, A. E., Martró, E, Quesada, M. D., Pérez-Vázquez, M., Guerrero-Murillo, M., et al (2022). Evaluation of Fourier Transform Infrared Spectroscopy as a First-Line Typing Tool for the Identification of Extended-Spectrum β-Lactamase-Producing Klebsiella pneumoniae Outbreaks in the Hospital Setting. *Front Microbiol*. doi: 10.3389/fmicb.2022.897161

Wu, F., Zhao, S., Yu, B., Chen, Y., Wang, W., Song, Z., et al. (2020). A new coronavirus associated with human respiratory disease in China. *Nature*. 12, 265–69. doi: 10.1038/s41586-020-2008-3

frontiers | Frontiers in Cellular and Infection Microbiology

TYPE Original Research
PUBLISHED 05 September 2022
DOI 10.3389/fcimb.2022.984140



OPEN ACCESS

EDITED BY
Zhanhui Wang
China Agricultural University, China

REVIEWED BY
Lei Ma,
Anyang Institute of Technology, China
Todd Steck,
University of North Carolina at Charlotte, United States

*CORRESPONDENCE
Jing Yuan
yuanjing6216@163.com
Ling Cao
caoling9919@163.com

†These authors have contributed equally to this work

SPECIALTY SECTION
This article was submitted to Clinical Microbiology, a section of the journal Frontiers in Cellular and Infection Microbiology

RECEIVED 01 July 2022
ACCEPTED 18 August 2022
PUBLISHED 05 September 2022

CITATION
Fu H, Gan L, Tian Z, Han J, Du B, Xue G, Feng Y, Zhao H, Cui J, Yan C, Feng J, Fan Z, Fu T, Xu Z, Zhang R, Cui X, Du S, Zhou Y, Zhang Q, Cao L and Yuan J (2022) Rapid detection of *Burkholderia cepacia* complex carrying the *16S rRNA* gene in clinical specimens by recombinase-aided amplification. *Front. Cell. Infect. Microbiol.* 12:984140. doi: 10.3389/fcimb.2022.984140



# Rapid detection of *Burkholderia cepacia* complex carrying the *16S rRNA* gene in clinical specimens by recombinase-aided amplification

Hanyu Fu[1,2†], Lin Gan[1†], Ziyan Tian[1], Juqiang Han[3], Bing Du[1], Guanhua Xue[1], Yanling Feng[1], Hanqing Zhao[1], Jinghua Cui[1], Chao Yan[1], Junxia Feng[1], Zheng Fan[1], Tongtong Fu[1], Ziying Xu[1], Rui Zhang[1], Xiaohu Cui[1], Shuheng Du[1], Yao Zhou[1], Qun Zhang[1], Ling Cao[2*] and Jing Yuan[1*]

[1]Department of Bacteriology, Capital Institute of Pediatrics, Beijing, China, [2]Department of Pulmonology, The Affiliated Children's Hospital, Capital Institute of Pediatrics, Beijing, China, [3]Institute of Hepatology, Chinese People Liberation Army General Hospital, Beijing, China

The *Burkholderia cepacia* complex (BCC) is a group of opportunistic pathogens, including *Burkholderia cepacia, Burkholderia multivorans, Burkholderia vietnamiensis* and *Burkholderia ambifaria*, which can cause severe respiratory tract infections and lead to high mortality rates among humans. The early diagnosis and effective treatment of BCC infection are therefore crucial. In this study, a novel and rapid recombinase-aided amplification (RAA) assay targeting the *16S rRNA* gene was developed for BCC detection. The protocol for this RAA assay could be completed in 10 min at 39°C, with a sensitivity of 10 copies per reaction and no cross-reactivity with other pathogens. To characterize the effectiveness of the RAA assay, we further collected 269 clinical samples from patients with bacterial pneumonia. The sensitivity and specificity of the RAA assay were 100% and 98.5%, respectively. Seven BCC-infected patients were detected using the RAA assay, and three BCC strains were isolated from the 269 clinical samples. Our data showed that the prevalence of BCC infection was 2.60%, which is higher than the 1.40% reported in previous studies, suggesting that high sensitivity is vital to BCC detection. We also screened a patient with *B. vietnamiensis* infection using the RAA assay in clinic, allowing for appropriate treatment to be initiated rapidly. Together, these data indicate that the RAA assay targeting the *16S rRNA* gene can be applied for the early and rapid detection of BCC pathogens in patients with an uncharacterized infection who are immunocompromised or have underlying diseases, thereby providing guidance for effective treatment.

KEYWORDS

***Burkholderia cepacia* complex, recombinase-aided amplification, rapid detection, 16S rRNA, infection**

## Introduction

The *Burkholderia cepacia* complex (BCC) is a group of over 20 phenotypically similar but genetically different Gram-negative, non-fermenting, bacteria that includes *Burkholderia cepacia*, *Burkholderia multivorans*, *Burkholderia vietnamiensis* and *Burkholderia ambifaria* (Depoorter et al., 2016; Sfeir, 2018; Tavares et al., 2020). Members of the BCC are opportunistic pathogens that can cause severe respiratory infections in immunocompromised patients (such as those with congenital immunodeficiency, HIV, and cancer patients receiving chemotherapy) or patients with underlying diseases such as cystic fibrosis (CF) and chronic granulomatous (Kalish et al., 2006; Greenberg et al., 2009; Tavares et al., 2020). According to a previous study in Nepal, the infection rate of BCC was 1.4% in patients who received more than 48 hours of mechanical ventilation (Baidya et al., 2021). The 2017 CF Foundation Annual Report on Patient Registrations showed that the occurrence of BCC was 2.4% in CF patients (Blanchard and Waters, 2019). Although the BCC only accounts for a small proportion of lung infections in CF patients, BCC infection accelerates lung function deterioration, which leads to a poor prognosis and high mortality (Whiteford et al., 1995; Stephenson et al., 2015). This high mortality is generally caused by the progression of "cepacia syndrome", which is clinically characterized by necrotizing pneumonia, sepsis, hyperthermia, and even severe progressive respiratory failure (Lord et al., 2020; Lauman and Dennis, 2021). In view of the significant morbidity and mortality associated with BCC infection, rapid and accurate detection is vital to initiate timely and effective treatment. Currently, BCC identification mainly involves isolation on selective media and DNA-based detection methods such as PCR and qPCR (De Volder et al., 2021). However, novel methods that offer high sensitivity and specificity, while being quick and easy to perform, are much needed (Ahn et al., 2020).

Recombinase-aided amplification (RAA) is a rapid, specific, sensitive and reliable isothermal gene amplification technology (Wang et al., 2021). At present, RAA has been widely used in the detection of various pathogens such as SARS-CoV-2, adenovirus, hepatitis B virus, *Escherichia coli*, *Klebsiella pneumoniae*, *Mycoplasma pneumoniae*, *Salmonella* and *Vibrio parahaemolyticus* (Zhang et al., 2017; Shen et al., 2019; Wang et al., 2019; Xue et al., 2020; Mu et al., 2021; Zhang et al., 2021; Zheng et al., 2021; Feng et al., 2022). RAA achieves DNA amplification by employing recombinase UvsX, DNA polymerase and single-stranded DNA binding protein at 35°C–42°C, replacing the traditional thermal cycling process (Fan et al., 2020). With the addition of 6-carboxyfluorescein (FAM)-labeled probes and biotin-labeled primers, double-labeled amplification products can be obtained, making the assay sensitive and specific (He et al., 2021).

In this study, pairs of primers and probes targeting the *16S rRNA* gene, which is highly conserved and specific for BCC species, were designed, and a rapid and intuitive RAA assay with high sensitivity and specificity for BCC detection was established. To assess the applicability of the RAA assay in clinic, 269 clinical samples were detected, and conventional PCR was also performed for comparison.

## Material and methods

### Ethical approval

This study was performed in compliance with the Helsinki Declaration (Ethical Principles for Medical Research Involving Human Subjects) and was approved by the research board of the Ethics Committee of the Capital Institute of Pediatrics, Beijing, China (SHERLLM2022004). All specimens used in this study are part of routine patient management without any additional collection, and all patient data were anonymously reported.

### Bacterial strains

The RAA assay was evaluated with 12 clinically-common pathogens, including *Haemophilus influenzae*, *Mycobacterium tuberculosis*, *Staphylococcus aureus*, *Pseudomonas aeruginosa*, *K. pneumoniae*, *E. coli*, *M. pneumoniae*, *B. cepacia*, *B. multivorans*, *B. vietnamiensis*, *B. ambifaria* and *B. gladioli*. The details of these strains are shown in Table S1.

### DNA extraction and BCC isolation of clinical samples

A total of 269 bronchoalveolar lavage fluid, throat swab or sputum samples from patients with bacterial pneumonia were randomly collected. Total DNA was extracted from the 269 collected samples using the QIAamp DNA Mini Kit (Qiagen, Hilden, Germany) and was stored at −80°C. BCC standard strains and the clinical samples were plated onto *B. cepacia* selective agar (BCSA) for 2 days at 35°C, followed by 3 days of incubation at room temperature (Martina et al., 2020).

### Recombinant plasmid construction

The PCR amplification product of the *16S rRNA* gene (*BCC*, GenBank accession number: LC496395) was cloned into the vector pGM-T (Tiangen Biotech, Beijing, China) according to the manufacturer's instructions. The primers used for amplification are shown in Table 1. The concentration of

plasmid was detected using a NanoDrop spectrophotometer. Then, the standard recombinant plasmids were prepared at 10-fold dilutions ranging from $10^6$ copies/μL to $10^0$ copies/μL for sensitivity analysis. The plasmid concentration and copy number were determined using the formula: DNA copy number (copy number/μL) = [$6.02\times10^{23}$ × plasmid concentration (ng/μL) ×$10^{-9}$]/[DNA length (in nucleotides) × 660]. The length of the DNA (3226 bp) was the sum of the plasmid fragment length (211 bp) and the vector length (3015 bp).

## RAA primer design

The sequence of the *16S rRNA* gene was used for RAA primer design. According to the principles of RAA primer and probe design (primer length between 30 to 35 bp, probe length between 46 to 52 bp), four sets of primers and probes were manually designed in highly-conserved regions. Primer and probe specificities were analyzed using NCBI Primer-BLAST, and the formation of primer dimers and secondary structures (hairpins) was predicted using the Website OligoEvaluator (http://www.oligoevaluator.com/LoginServlet). The primers and probes were synthesized and purified using high-performance liquid chromatography (Sangon Biotech, Shanghai, China).

## RAA assay

The RAA assay was performed in a 50 μL reaction volume using a commercial RAA kit (Qitian, Jiangsu, China). The reaction mixture included 2 μL extracted DNA template, 25 μL reaction buffer, 15.7 μL DNase-free water, 2.1 μL primer F/R, 0.6 μL of probe and 2.5 μL of magnesium acetate. The reaction mixture was added to the tube containing the RAA enzyme mixture in lyophilized form. The test tubes were placed in a B6100 shaking mixer (QT-RAA-B6100, Qitian), incubated for 4 min, mixed briefly, centrifuged, and finally transferred to a fluorescence detector (QT-RAA-1620, Qitian), and measured at 39°C for 10 min.

## Sensitivity and specificity of the RAA assay

The sensitivity of the RAA assay was assessed using a series of diluted recombinant plasmids ranging from $10^6$ to $10^0$ copies/μL. The specificity was evaluated by detecting four strains of different BCC subspecies, one strain of *B. gladioli* (which does not belong to the BCC) and seven clinically-common pathogens, as presented in Table S1. The positive control was *16S rRNA*-positive plasmid, and the negative control was nucleic acid-free water.

## PCR assay

PCR primers were designed according to primer design principles (Table 1). The conventional PCR assay was performed in a 25 μL reaction system containing 12.5 μL 2 × Taq PCR MasterMix (Tiangen Biotech), 1.0 μL of each primer and 2 μL of extracted DNA template. The reaction program was set as 95°C for 10 min, followed by 35 cycles of 30 s at 95°C, 30 s at 55°C and 1 min at 72°C, and a final extension step for 10 min at 72°C. PCR products were visualized on a 1.5% agarose gel and stained with GeneGreen. Images were acquired with a Gel Doc EQ imaging system (Bio-Rad, Hercules, USA), and the amplified product was sequenced (Sangon Biotech).

## Evaluating the RAA assay on clinical samples

Established RAA assay was evaluated using 269 clinical samples from patients with bacterial pneumoniae. The RAA assay results were compared to conventional PCR assay. The formulas for evaluating RAA assay were as follows: consistency between RAA and conventional PCR assays = (true positives + true negatives)/(true positives + true negatives + false positives + false negatives) × 100%, sensitivity of RAA assay = true positives/(true positives + false negatives) × 100%, specificity of RAA assay = true negatives/(false positives + true negatives) × 100%, and the conventional PCR method was used as gold standard for

TABLE 1 The primer sequences used in the study.

| Primer | Sequence (5' to 3') | Function |
|---|---|---|
| *16S*-F1 | GCAGGCTAGAGTATGGCA | conventional PCR |
| *16S*-R1 | GTTACTAAGGAAATGAATCCC | conventional PCR |
| *16S*-1-F | TAAGACMGATGTGAAATCCCCGGGCTCAACC | RAA assay |
| *16S*-1-R | GCTGCCTTCGCCATCGGTATTCCTCCACATCT | RAA assay |
| *16S*-1-P | CTAGAGTATGGCAGAGGGGGGTAGAATTCCACG [FAM-dT][THF][BHQ-dT]AGCAGTGAAATGCGT | RAA assay |

identification (Gautam et al., 2017). A case was also used for assessing the clinical application of RAA assay for detecting BCC infection in this study. The pus sample extracted from the patient's neck abscess and sputum were used for BCC isolation, RAA and metagenomic sequencing (Vison Medicals, Guangzhou, China).

## Genome sequencing and analysis

BCC isolates were subjected to DNA extraction using the Wizard Genome DNA Purification Kit (Promega, Madison, USA) and sequenced on the Illumina HiSeq PE150 platform (Novogene, Beijing, China). The genome sequences were assembled and annotated by software SOAP denovo and Prokka. Multilocus sequence typing (MLST) identification was performed using the Institute Pasteur database (https://bigsdb.pasteur.fr/klebsiella/klebsiella.html) by analyzing the sequences of seven housekeeping genes (*atpD*, *gltB*, *gyrB*, *recA*, *lepA*, *phaC* and *trpB*) (Diancourt et al., 2005). The core genome single-nucleotide polymorphisms (SNPs) of BCC strains were detected using the software Snippy and Gubbins, as previously described (Gan et al., 2022). The extracted SNPs were used for phylogenetic tree construction by software MEGA. Strains MSMB384WGS and FL_2_3_10_S3_D0 were used as reference strains for *B. cepacia* phylogenetic tree and *B. vietnamiensis* phylogenetic tree, respectively (Croucher et al., 2015). Strain ATCC10248 (*B. gladioli*) was included as an outgroup. All strains used for constructing the phylogenetic tree are listed in Table S2.

# Results

## Primers and probes designed for the RAA assay

Four sets of RAA primers and probes named *16S*-1 (Figure 1 and Table 1), *16S*-2, *16S*-3 and *16S*-4 (Table S3) were manually designed against the conserved region of the *16S rRNA* gene of BCC. No cross-reactivity with other species was predicted by the BLAST tool. The amplification efficiencies of the four sets of primers and probes were compared, and the recombinant *16S rRNA* plasmid was used as the positive template and nucleic acid-free water was used as the negative template. All reactions were performed in triplicate. Under the same reaction condition and system, *16S*-1 exhibited the highest amplification efficiency compared to other sets (Supplementary Figure 1). Therefore, *16S*-1 was chosen as the primers and probe for the subsequent analysis.

## Sensitivity of the RAA assay

The template concentration of the recombinant plasmid determined by the NanoDrop spectrophotometer was 153.6 ng/μL, and the converted copy number was $4.34\times10^{10}$ copies/μL. The 10-fold serially diluted recombinant plasmids ranged in concentration from $10^6$ to $10^0$ copies/μL. The results of sensitivity analysis are shown in Figure 2A. The RAA assay detected the *16S rRNA* gene within 10 min at 39°C at a sensitivity of 10 copies/μL. The minimum concentration of conventional PCR was $10^3$ copies/μL.

## Specificity of the RAA assay

The specificity of the RAA assay was confirmed by the detection of four strains of different BCC subspecies and eight clinically-common pathogens (Table S1). Only *B. cepacia*, *B. multivorans*, *B. vietnamiensis* and *B. ambifaria* produced fluorescence signals (Figure 2B), while the other strains tested, including *B. gladioli* that does not belong to the BCC, were negative (Figures 2B, C). No cross-reactivity with strains of other species being detected in this RAA assay targeted *16S rRNA*.

## Evaluation of the RAA assay using clinical samples

A total of 269 specimens collected from patients with bacterial pneumonia were simultaneously detected by RAA

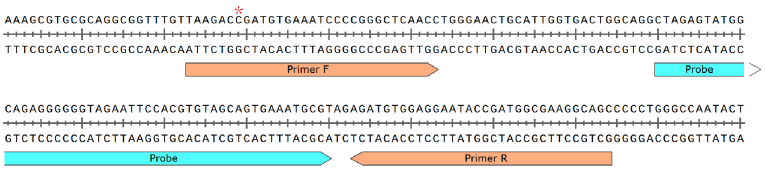


FIGURE 1
Primer and probe sequences used in RAA detection. * denotes the site with multiple subtypes between BCC species, *Burkholderia cepacia* is C, *Burkholderia multivorans* is A or C, *Burkholderia vietnamiensis* is C, and *Burkholderia ambifaria* is C.

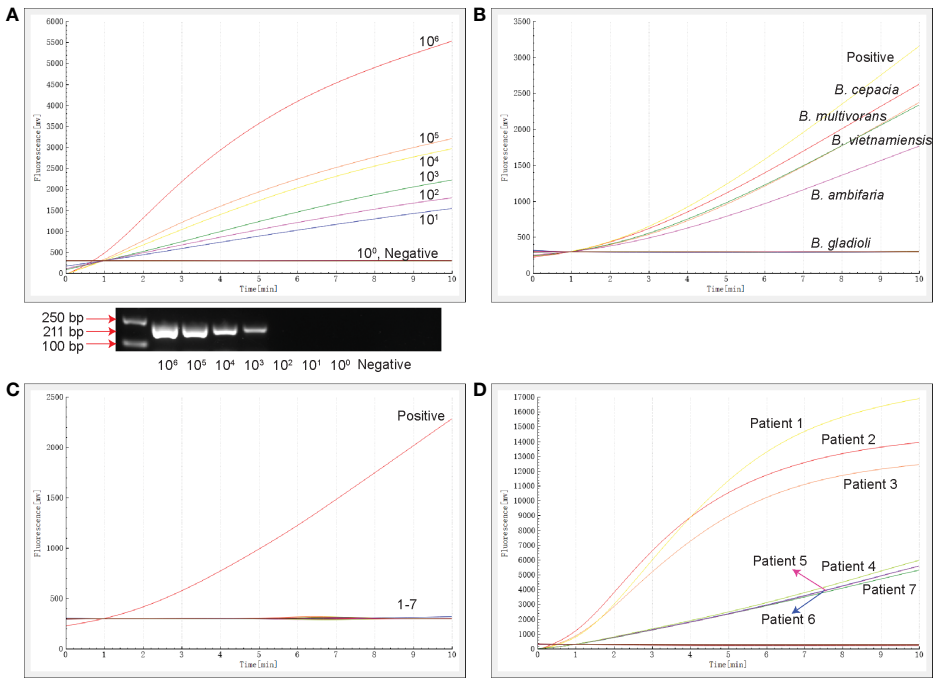


FIGURE 2
The sensitivity, specificity and clinical testing of the RAA assay. **(A)** The sensitivity of RAA and conventional PCR assays. The results of RAA are shown by an amplification curve, and the PCR amplification products are shown following separation on a 1.5% agarose gel. **(B)** The specificity of the RAA assay for members of the *Burkholderia* family. **(C)** The specificity of RAA for clinically-common pathogens. 1: *Haemophilus influenzae* ATCC10211, 2: *M. tuberculosis* ATCC25618, 3: *Staphylococcus aureus* ATCC29213, 4: *Pseudomonas aeruginosa* ATCC27853, 5: *K. pneumoniae* ATCC BAA-2146, 6: *E. coli* ATCC25922, 7: *Mycoplasma pneumoniae* M129 ATCC 29342. **(D)** Seven samples tested positive by the RAA assay. The positive control was *16S rRNA*-positive plasmid, and the negative control was nucleic acid-free water.

and conventional PCR assays (Table 2). Seven samples (2.6%) tested positive and 262 samples tested negative for the BCC by the RAA assay (Figure 2D), whereas three cases (1.1%) tested positive and 266 cases tested negative in conventional PCR assay. Among them, four samples were positive by RAA and negative by the conventional PCR assay. The percentage consistency between RAA and PCR assays was 98.5%. Compared with the gold standard PCR method, the RAA assay had a sensitivity of 100% and a specificity of 98.5%.

To investigate the value of the RAA assay in terms of clinical application, we also analyzed a patient with *B. vietnamiensis* infection in detail. The 7-year-old girl was diagnosed with chronic granulomatous disease. To determine the cause of infection, cervical lymph node puncture sample was collected for metagenomic sequencing, and the results indicated *B. vietnamiensis* infection. Meanwhile, BCC infection was further confirmed by the RAA assay targeting the *16S rRNA* gene, and a BCC isolate was successfully isolated from a pus sample, confirming the reliability of RAA assay for clinical diagnosis.

TABLE 2 Testing of clinical samples.

| Results | PCR positive | PCR negative | Total |
|---|---|---|---|
| RAA positive | 3 | 4 | 7 |
| RAA negative | 0 | 262 | 262 |
| Total | 3 | 266 | 269 |

The prevalence of BCC infection among patients with pneumonia was 2.60%, and three strains were isolated from these positive samples. Isolates BC1 (ST608, Genome accession number SAMN29388125) and BC2 (ST608, Genome accession number SAMN29388126) belonged to *B. cepacia*, and isolate Vit1 (Genome accession number SAMN29388124) belonged to *B. vietnamiensis* (*atpD* type 27, *gltB* type 231, *gyrB* type 16, *recA* type 22, *lepA* type 12, *phaC* 5 type 6 and *trpB* type 268, which was a new sequence type). In the phylogenetic tree of *B. cepacia*, isolates BC1 and BC2 clustered with strains collected from patients in China (toggle2 and toggle3), suggesting that these four strains from China were closely related phylogenetically and potentially shared epidemiological characteristics (Figure 3A). In the *B. vietnamiensis* phylogenetic tree, isolate Vit1 was separate from the Chinese strains, indicating that it shared no phylogenetic or epidemiological characteristics (Figure 3B).

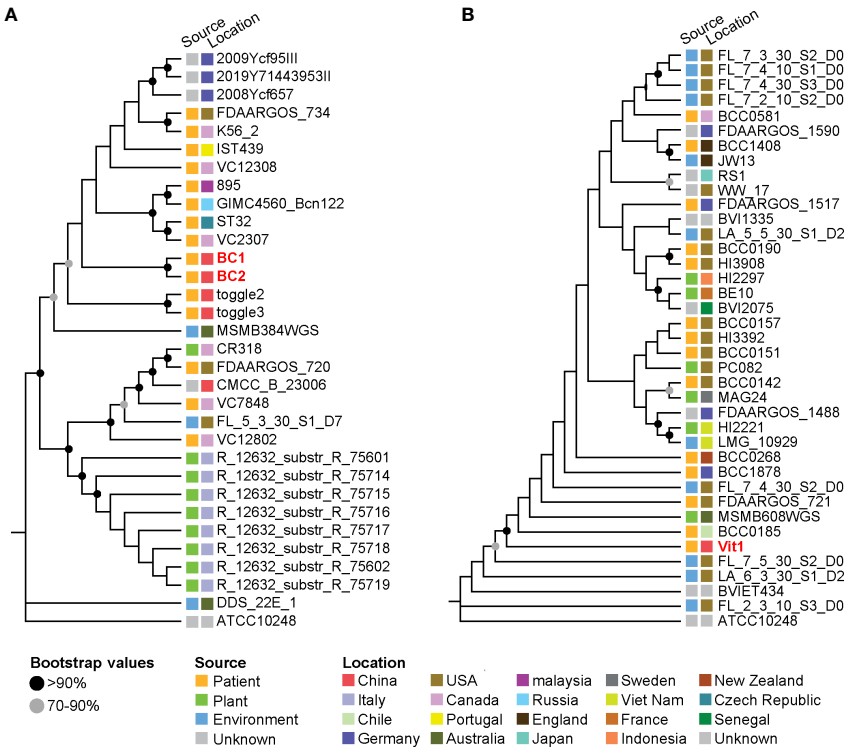


FIGURE 3
Phylogenetic trees of *Burkholderia* strains based on core single-nucleotide polymorphisms. **(A)** Phylogenetic tree of *B. cepacia* strains. **(B)** Phylogenetic tree of *B. vietnamiensis* strains. The squares beside the strains denote the source and location of the strains.

## Discussion

BCC pathogens are an important cause of secondary severe pulmonary infection in patients with a congenital immunodeficiency or existing underlying disease, and earlier identification of pathogens means more rapid intervention and therefore better clinical outcomes. However, BCC pathogens typically require 48 to 72 hours of incubation for colonies to appear on selective media (Brown and Govan, 2007). Currently, BCC identification mainly depends on molecular methods (Drevinek et al., 2008), but the sensitivity of PCR assays varies widely. Moreover, BCC diagnosis also faces challenges posed by non-BCC *Burkholderia* species, such as *B. gladioli* (Brown and Govan, 2007), and a detection method is urgently needed to distinguish these organisms. In recent years, RAA has been successfully applied to the detection of many pathogens and SNPs (Qin et al., 2021). Because of its fast speed, low cost and high sensitivity, RAA is potentially suitable for clinical application.

Multiple copies of *rRNA* genes are present throughout the bacterial genome. Therefore, *16S rRNA* gene-based PCR assays generally have higher sensitivity than PCR assays targeting single-copy genes such as *recA* (Brown and Govan, 2007). In this study, the gene *16S rRNA* of BCC was selected through detailed analysis of conserved regions in multiple sequence alignments. The *16S rRNA* gene shows no cross-homology and meets the requirements for designing BCC-specific RAA primers. The specificity and sensitivity of the RAA primers were verified by BLAST analysis and subsequent experiments.

The RAA assay targeting the *16S rRNA* gene of BCC has the ability to detect a minimum template of 10 copies/μL, and the sensitivity is similar to that of RAA detection of other pathogens (Xiao et al., 2021), which was more sensitive than conventional PCR, qPCR and LAMP assays of BCC (Daddy Gaoh et al., 2021). Compared with conventional PCR ($45/sample, >2 h detection speed) (Pliakos et al., 2018), RAA has a lower cost ($5/sample), faster detection speed (10 min) and simpler reaction conditions, not requiring complex instruments. For samples with 10 copies/μL of BCC, a positive result can be obtained within 10 min under a constant temperature of 39°C. The RAA assay in this study did not cross-react with eight other species of pathogens tested, including one species of non-BCC *Burkholderia* and seven clinically-common species. Of note, we employed four species of the BCC and one non-BCC *Burkholderia* species (*B. gladioli*) to verify the specificity of the method, and the results showed that this method can effectively distinguish between BCC and non-BCC species.

To evaluate the clinical applicability of this method, we further collected 269 clinical samples for BCC detection. The

assay had a sensitivity of 100% and a specificity of 98.5%, which was superior to other reported assays (Daddy Gaoh et al., 2021). In particular, the four samples that tested negative for conventional PCR but positive for RAA also exhibited low peak values for the RAA assay. Moreover, previous studies have shown a low rate of infection with BCC (Baidya et al., 2021), but the results of the RAA assay in this study suggest a higher prevalence. BCC screening in specific populations may be strengthened through the application of the RAA assay in the future.

We carried out a case study of a child with *B. vietnamiensis* infection to test the applicability of RAA for clinical detection. The patient underwent recurrent infection as a result of congenital immunodeficiency, chronic granulomatous disease and the heavy use of antibiotics. The RAA assay in this study was able to detect *B. multivorans*, *B. vietnamiensis* and other common clinical BCC members (Rhodes and Schweizer, 2016). Thus, if patients with a similar course of disease were observed in clinic in the future, our RAA assay could be applied to quickly detect BCC infection. It is worth noting that the treatment of BCC infection relies on ceftazidime and other broad-spectrum cephalosporins (Rhodes and Schweizer, 2016). Although imipenem (a broad-spectrum β-lactam antibiotic) can be effective with clinical recovery occurring at a later stage, doctors often employ a large number of antibiotics to target a range of pathogens when the causative pathogen is unknown at an early stage. In the future, the aim would be to achieve early and rapid pathogen detection through RAA, enabling early targeted treatment and thereby avoiding the overuse of antibiotics.

Taken together, we established an RAA assay for BCC detection, which has high specificity and sensitivity. RAA has the advantages of simple reaction conditions, a short reaction time and low cost. The applicability of the assay was also verified in clinic. However, future studies are needed to analyze a greater number of clinical samples to further verify the effectiveness of the assay in the early detection of BCC infection.

## Data availability statement

The datasets presented in this study can be found in online repositories. The names of the repository/repositories and accession number(s) can be found in the article/Supplementary Material.

## Ethics statement

The studies involving human participants were reviewed and approved by This study was performed in compliance with the Helsinki Declaration (Ethical Principles for Medical Research Involving Human Subjects) and was approved by the research board of the Ethics Committee of the Capital Institute of Pediatrics, Beijing, China (SHERLLM2022004). All specimens used in this study are part of routine patient management without any additional collection, and all patient data were anonymously reported. Written informed consent to participate in this study was provided by the participants' legal guardian/next of kin.

## Author contributions

JY and LC designed the study and revised the manuscript. HF, LG, ZT, JH, BD, GX, YF, HZ, JC, CY, JF, ZF, TF, ZX, RZ, XC, SD, YZ and QZ performed the experiments. JH and YF collected the clinical samples. HF and LG analyzed the results. HF and LG wrote the manuscript. All authors contributed to the article and approved the submitted version.

## Funding

This work was financially supported by grants from the National Natural Science Foundation (82002191, 82130065 and 32170201), Public service development and reform pilot project of Beijing Medical Research Institute (BMR2019-11) and Feng Foundation (FFBR 202103).

## Conflict of interest

The authors declare that the research was conducted in the absence of any commercial or financial relationships that could be construed as a potential conflict of interest.

## Publisher's note



## Supplementary material

The Supplementary Material for this article can be found online at: https://www.frontiersin.org/articles/10.3389/fcimb.2022.984140/full#supplementary-material

SUPPLEMENTARY FIGURE 1
Four sets of primers and probes used for RAA assay. The DNA template used in this assay was extracted from recombinant plasmid, and the negative control was nucleic acid-free water.

# References

Ahn, Y., Gibson, B., Williams, A., Alusta, P., Buzatu, D., Lee, Y., et al. (2020). A comparison of culture-based, real-time PCR, droplet digital PCR and flow cytometric methods for the detection of burkholderia cepacia complex in nuclease-free water and antiseptics. *J. Ind. Microbiol. Biotechnol.* 47, 475–484. doi: 10.1007/s10295-020-02287-3

Baidya, S., Sharma, S., Mishra, S., Kattel, H., Parajuli, K., and Sherchand, J. (2021). Biofilm formation by pathogens causing ventilator-associated pneumonia at intensive care units in a tertiary care hospital: An armor for refuge. *BioMed. Res. Int.* 2021, 8817700. doi: 10.1155/2021/8817700

Blanchard, A., and Waters, V. (2019). Microbiology of cystic fibrosis airway disease. *Semin. Respir. Crit. Care Med.* 40, 727–736. doi: 10.1055/s-0039-1698464

Brown, A., and Govan, J. (2007). Assessment of fluorescent *in situ* hybridization and PCR-based methods for rapid identification of burkholderia cepacia complex organisms directly from sputum samples. *J. Clin. Microbiol.* 45, 1920–1926. doi: 10.1128/JCM.00147-07

Croucher, N., Page, A., Connor, T., Delaney, A., Keane, J., Bentley, S., et al. (2015). Rapid phylogenetic analysis of large samples of recombinant bacterial whole genome sequences using gubbins. *Nucleic Acids Res.* 43, e15. doi: 10.1093/nar/gku1196

Daddy Gaoh, S., Kweon, O., Lee, Y., Lipuma, J., Hussong, D., Marasa, B., et al. (2021). Burkholderia cepaciaLoop-mediated isothermal amplification (LAMP) assay for detecting complex in non-sterile pharmaceutical products. *Pathogens* 10 (9), 1071. doi: 10.3390/pathogens10091071

Depoorter, E., Bull, M., Peeters, C., Coenye, T., Vandamme, P., and Mahenthiralingam, E. (2016). Burkholderia: an update on taxonomy and biotechnological potential as antibiotic producers. *Appl. Microbiol. Biotechnol.* 100, 5215–5229. doi: 10.1007/s00253-016-7520-x

De Volder, A., Teves, S., Isasmendi, A., Pinheiro, J., Ibarra, L., Breglia, N., et al. (2021). Distribution of burkholderia cepacia complex species isolated from industrial processes and contaminated products in Argentina. *Int. microbiol.: Off. J. Spanish Soc. Microbiol.* 24, 157–167. doi: 10.1007/s10123-020-00151-z

Diancourt, L., Passet, V., Verhoef, J., Grimont, P., and Brisse, S. (2005). Multilocus sequence typing of klebsiella pneumoniae nosocomial isolates. *J. Clin. Microbiol.* 43, 4178–4182. doi: 10.1128/JCM.43.8.4178-4182.2005

Drevinek, P., Baldwin, A., Dowson, C., and Mahenthiralingam, E. (2008). Diversity of the parB and repA genes of the burkholderia cepacia complex and their utility for rapid identification of burkholderia cenocepacia. *BMC Microbiol.* 8, 44. doi: 10.1186/1471-2180-8-44

Fan, X., Li, L., Zhao, Y., Liu, Y., Liu, C., Wang, Q., et al. (2020). Clinical validation of two recombinase-based isothermal amplification assays (RPA/RAA) for the rapid detection of African swine fever virus. *Front. Microbiol.* 11, 1696. doi: 10.3389/fmicb.2020.01696

Feng, Z., Li, J., Zhang, J., Li, F., Guan, H., Zhang, R., et al. (2022). Development and evaluation of a sensitive recombinase aided amplification assay for rapid detection of vibrio parahaemolyticus. *J. Microbiol. Methods* 193, 106404. doi: 10.1016/j.mimet.2021.106404

Gan, L., Yan, C., Cui, J., Xue, G., Fu, H., Du, B., et al. (2022). Genetic diversity and pathogenic features in klebsiella pneumoniae isolates from patients with pyogenic liver abscess and pneumonia. *Microbiol. Spectr.* 10, e0264621. doi: 10.1128/spectrum.02646-21

Gautam, V., Sharma, M., Singhal, L., Kumar, S., Kaur, P., Tiwari, R., et al. (2017). MALDI-TOF mass spectrometry: An emerging tool for unequivocal identification of non-fermenting gram-negative bacilli. *Indian J. Med. Res.* 145, 665–672. doi: 10.4103/ijmr.IJMR_1105_15

Greenberg, D., Goldberg, J., Stock, F., Murray, P., Holland, S., and Lipuma, J. (2009). Recurrent burkholderia infection in patients with chronic granulomatous disease: 11-year experience at a large referral center. *Clin. Infect. dis.: an Off. Publ. Infect. Dis. Soc. America* 48, 1577–1579.

He, Y., Chen, W., Fan, J., Fan, S., Ding, H., Chen, J., et al. (2021). Recombinase-aided amplification coupled with lateral flow dipstick for efficient and accurate detection of porcine parvovirus. *Life (Basel)* 11 (8), 762. doi: 10.3390/life11080762

Kalish, L., Waltz, D., Dovey, M., Potter-Bynoe, G., Mcadam, A., Lipuma, J., et al. (2006). Impact of burkholderia dolosa on lung function and survival in cystic fibrosis. *Am. J. Respir. Crit. Care Med.* 173, 421–425. doi: 10.1164/rccm.200503-344OC

Lauman, P., and Dennis, J. (2021). Burkholderia cepaciaAdvances in phage therapy: Targeting the complex. *Viruses.* 13 (7), 1331. doi: 10.3390/v13071331

Lord, R., Jones, A., and Horsley, A. (2020). Antibiotic treatment for burkholderia cepacia complex in people with cystic fibrosis experiencing a pulmonary exacerbation. *Cochrane Database Syst. Rev.* 4, CD009529. doi: 10.1002/14651858.CD009529.pub4

Martina, P., Martinez, M., Rivas, S., Leguizamón, L., Von Specht, M., and Ferreras, J. (2020). Burkholderia cepacia complex: 11 years of surveillance in patients with cystic fibrosis in posadas, Argentina. *Rev. Argent. Microbiol.* 52, 176–182. doi: 10.1016/j.ram.2019.08.002

Mu, D., Zhou, D., Xie, G., Liu, J., Xiong, Q., Feng, X., et al. (2021). The fluorescent probe-based recombinase-aided amplification for rapid detection of escherichia coli O157:H7. *Mol. Cell. Probes* 60, 101777. doi: 10.1016/j.mcp.2021.101777

Pliakos, E., Andreatos, N., Shehadeh, F., Ziakas, P., and Mylonakis, E. (2018). The cost-effectiveness of rapid diagnostic testing for the diagnosis of bloodstream infections with or without antimicrobial stewardship. *Clin. Microbiol. Rev.* 31 (3), e00095–17. doi: 10.1128/CMR.00095-17

Qin, Z., Xue, L., Cai, W., Gao, J., Jiang, Y., Yang, J., et al. (2021). Development of a recombinase-aided amplification assay for rapid detection of human norovirus GII.4. *BMC Infect. Dis.* 21, 248. doi: 10.1186/s12879-021-05942-x

Rhodes, K., and Schweizer, H. (2016). Antibiotic resistance in burkholderia species. *Drug resist. updates: Rev. commentaries antimicrob. Anticancer chemother.* 28, 82–90.

Sfeir, M. M. (2018). Burkholderia cepacia complex infections: More complex than the bacterium name suggest. *J. Infect.* 77, 166–170. doi: 10.1016/j.jinf.2018.07.006

Shen, X., Qiu, F., Shen, L., Yan, T., Zhao, M., Qi, J., et al. (2019). A rapid and sensitive recombinase aided amplification assay to detect hepatitis b virus without DNA extraction. *BMC Infect. Dis.* 19, 229. doi: 10.1186/s12879-019-3814-9

Stephenson, A., Sykes, J., Berthiaume, Y., Singer, L., Aaron, S., Whitmore, G., et al. (2015). Clinical and demographic factors associated with post-lung transplantation survival in individuals with cystic fibrosis. *J. Heart Lung Transplant.* 34, 1139–1145. doi: 10.1016/j.healun.2015.05.003

Tavares, M., Kozak, M., Balola, A., and Sa-Correia, I. (2020). Burkholderia cepacia complex bacteria: a feared contamination risk in water-based pharmaceutical products. *Clin. Microbiol. Rev.* 33 (3), e00139–19. doi: 10.1128/CMR.00139-19

Wang, W., Wang, C., Zhang, Z., Zhang, P., Zhai, X., Li, X., et al. (2021). Recombinase-aided amplification-lateral flow dipstick assay-a specific and sensitive method for visual detection of avian infectious laryngotracheitis virus. *Poultry Sci.* 100, 100895. doi: 10.1016/j.psj.2020.12.008

Wang, R., Zhang, H., Zhang, Y., Li, X., Shen, X., Qi, J., et al. (2019). Development and evaluation of recombinase-aided amplification assays incorporating competitive internal controls for detection of human adenovirus serotypes 3 and 7. *Virol. J.* 16, 86. doi: 10.1186/s12985-019-1178-9

Whiteford, M., Wilkinson, J., Mccoll, J., Conlon, F., Michie, J., Evans, T., et al. (1995). Outcome of burkholderia (Pseudomonas) cepacia colonisation in children with cystic fibrosis following a hospital outbreak. *Thorax* 50, 1194–1198. doi: 10.1136/thx.50.11.1194

Xiao, X., Lin, Z., Huang, X., Lu, J., Zhou, Y., Zheng, L., et al. (2021). Vibrio vulnificusRapid and sensitive detection of using CRISPR/Cas12a combined with a recombinase-aided amplification assay. *Front. Microbiol.* 12, 767315. doi: 10.3389/fmicb.2021.767315

Xue, G., Li, S., Zhao, H., Yan, C., Feng, Y., Cui, J., et al. (2020). Use of a rapid recombinase-aided amplification assay for mycoplasma pneumoniae detection. *BMC Infect. Dis.* 20, 79. doi: 10.1186/s12879-019-4750-4

Zhang, W., Feng, Y., Zhao, H., Yan, C., Feng, J., Gan, L., et al. (2021). Klebsiella pneumoniaeA recombinase aided amplification assay for rapid detection of the carbapenemase gene and its characteristics in. *Front. Cell. infect. Microbiol.* 11, 746325. doi: 10.3389/fcimb.2021.746325

Zhang, X., Guo, L., Ma, R., Cong, L., Wu, Z., Wei, Y., et al. (2017). Rapid detection of salmonella with recombinase aided amplification. *J. Microbiol. Methods* 139, 202–204. doi: 10.1016/j.mimet.2017.06.011

Zheng, Y., Chen, J., Li, J., Wu, X., Wen, J., Liu, X., et al. (2021). Reverse transcription recombinase-aided amplification assay with lateral flow dipstick assay for rapid detection of 2019 novel coronavirus. *Front. Cell. Infect. Microbiol.* 11, 613304. doi: 10.3389/fcimb.2021.613304

frontiers | Frontiers in Cellular and Infection Microbiology

TYPE Original Research
PUBLISHED 16 March 2023
DOI 10.3389/fcimb.2023.1136588



OPEN ACCESS

EDITED BY
Christoph Gabler,
Freie Universität Berlin, Germany

REVIEWED BY
Abhishek Mishra,
Houston Methodist Research Institute, United States
Feroze A. Ganaie,
University of Alabama at Birmingham, United States
Wenfang Li,
Second Military Medical University, China

*CORRESPONDENCE
Jingwei Lou
jingweilou@biotecan.com
Shouxin Wu
swu@biotecan.com
Hongling Zhang
zhanghonglingysj@163.com

†These authors have contributed equally to this work and share first authorship

SPECIALTY SECTION
This article was submitted to Clinical Microbiology, a section of the journal Frontiers in Cellular and Infection Microbiology

RECEIVED 03 January 2023
ACCEPTED 23 February 2023
PUBLISHED 16 March 2023

CITATION
Lin T, Tu X, Zhao J, Huang L, Dai X, Chen X, Xu Y, Li W, Wang Y, Lou J, Wu S and Zhang H (2023) Microbiological diagnostic performance of metagenomic next-generation sequencing compared with conventional culture for patients with community-acquired pneumonia. *Front. Cell. Infect. Microbiol.* 13:1136588. doi: 10.3389/fcimb.2023.1136588



# Microbiological diagnostic performance of metagenomic next-generation sequencing compared with conventional culture for patients with community-acquired pneumonia

Tianlai Lin[1†], Xueliang Tu[4†], Jiangman Zhao[2,3†], Ling Huang[1], Xiaodong Dai[1], Xiaoling Chen[1], Yue Xu[2,3], Wushuang Li[2,3], Yaoyao Wang[2,3], Jingwei Lou[2,3*], Shouxin Wu[2*] and Hongling Zhang[1*]

[1]Department of Intensive Care Unit, Quanzhou First Hospital Affiliated to Fujian Medical University, Quanzhou, China, [2]Shanghai Biotecan Pharmaceuticals Co., Ltd., Shanghai, China, [3]Shanghai Zhangjiang Institute of Medical Innovation, Shanghai, China, [4]Department of Clinical Laboratory, Huanghe Sanmenxia Hospital Affiliated to Henan University of Science and Technology, Sanmenxia, China

**Background:** Community-acquired pneumonia (CAP) is an extraordinarily heterogeneous illness, both in the range of responsible pathogens and the host response. Metagenomic next-generation sequencing (mNGS) is a promising technology for pathogen detection. However, the clinical application of mNGS for pathogen detection remains challenging.

**Methods:** A total of 205 patients with CAP admitted to the intensive care unit were recruited, and broncho alveolar lavage fluids (BALFs) from 83 patients, sputum samples from 33 cases, and blood from 89 cases were collected for pathogen detection by mNGS. At the same time, multiple samples of each patient were tested by culture. The diagnostic performance was compared between mNGS and culture for pathogen detection.

**Results:** The positive rate of pathogen detection by mNGS in BALF and sputum samples was 89.2% and 97.0%, which was significantly higher ($P < 0.001$) than that (67.4%) of blood samples. The positive rate of mNGS was significantly higher than that of culture (81.0% vs. 56.1%, $P = 1.052e-07$). A group of pathogens including *Mycobacterium abscessus*, *Chlamydia psittaci, Pneumocystis jirovecii, Orientia tsutsugamushi*, and *all viruses* were only detected by mNGS. Based on mNGS results, *Escherichia coli* was the most common pathogen (15/61, 24.59%) of non-severe patients with CAP, and *Mycobacterium tuberculosis* was the most common pathogen (21/144, 14.58%) leading to severe pneumonia. *Pneumocystis jirovecii* was the most common pathogen (26.09%) in severe CAP patients with an immunocompromised status, which was all detected by mNGS only.

**Conclusion:** mNGS has higher overall sensitivity for pathogen detection than culture, BALF, and sputum mNGS are more sensitive than blood mNGS. mNGS is a necessary supplement of conventional microbiological tests for the pathogen detection of pulmonary infection.

KEYWORDS

metagenomic next-generation sequencing, culture, community-acquired pneumonia, conventional microbiological test, pathogen detection

# 1 Introduction

Infection is a common occurrence among patients in the intensive care unit (ICU) (Vincent et al., 2020), and community-acquired pneumonia (CAP) is the leading infectious disease cause of mortality worldwide (Torres et al., 2021). Severe CAP (SCAP) has a high mortality, and those survivors often have serious sequelae including the reduction of lung, mental, cognitive, and motor functions, especially those with an immunocompromised status (Sangla et al., 2020; Cilloniz et al., 2021). The identification of infected pathogens and prompt and adequate antimicrobial therapy are critical to improve the survival of patients with severe pneumonia (Cilloniz et al., 2021).

The conventional microbiological tests (CMTs) of an infectious disease diagnosis are mainly dependent on culture methodology combined with molecular detection through polymerase chain reaction (PCR) and the enzyme immunoassay (Miller et al., 2018). However, previous literature reported that no pathogen was detected in the majority of patients with pneumonia despite using comprehensive testing methods (Jain et al., 2015; Lu H. et al., 2022), resulting in delayed and inadequate treatment, prolonged stays, and increased mortality. Furthermore, empirical broad-spectrum antibiotic usage for patients without pathogen identification may lead to antimicrobial resistance.

Metagenomic next-generation sequencing (mNGS) is an unbiased approach that enables a broad identification of known and unexpected pathogens and has a special advantage on rare, novel, and atypical etiologies of complicated infectious diseases (Wang et al., 2019). In recent years, increasing studies have demonstrated its clinical value of sensitivity and speed in the pathogen detection of infectious diseases such as pneumonia (Chen et al., 2020; Wu et al., 2020; Peng et al., 2021; Sun et al., 2021). However, there are still limitations of mNGS for pathogen detection such as a high human host background, infection from colonization, and microbial contaminants limiting its sensitivity and specificity (Gu et al., 2019). On the other hand, it is still challenging for the interpretation of mNGS results, especially when they are inconsistent with clinical symptoms or CMT results. Thus, further investigation with a larger cohort across different geographical areas could promote the establishment of the clinical application standard of mNGS.

In this study, the results of the mNGS and conventional culture of 205 patients with CAP admitted to the ICU were retrospectively analyzed. This study aims to comprehensively evaluate and compare the diagnostic performance of mNGS and culture methods in patients with severe and non-severe CAP.

# 2 Methods

## 2.1 Study patients

A total of 205 patients with a diagnosis of community-acquired CAP admitted into the ICU were retrospectively included in this study from September 2019 to September 2021 in Quanzhou First Hospital. SCAP was defined as who included either one major criterion or no less than three minor criteria according to the Infectious Diseases Society of America/American Thoracic Society criteria (Metlay et al., 2019). The immunocompromised status was defined following the previous study (Wu et al., 2020). This study involving human participants was approved by the Ethical Committee of Quanzhou First Hospital (No. 2018220). Informed consent was obtained from each subject, and this study conforms to the ethical guidelines of the latest version of the Declaration of Helsinki.

The samples of broncho alveolar lavage fluid (BALF) from 83 patients, sputum samples from 33 cases, and blood from 89 cases were collected for pathogen detection by mNGS. At the same time, multiple samples of each patient were used for the CMT (Miller et al., 2018) such as microscopy with routine laboratory staining and the cultures of bacteria and fungi. The samples included BALF, sputum, blood, ascites, urine, and feces. Among 205 patients, 186 patients' sample type of mNGS and the CMT was consistent.

## 2.2 Clinical data and treatment

The clinical data of each participant were collected from hospital electronic medical records combined with a questionnaire. Sequential Organ Failure Assessment (SOFA), Confusion, Urea, Respiratory Rate, Blood Pressure and Age Above or Below 65 Years (CURB-65) score, and Acute

Physiologic Assessment and Chronic Health Evaluation II (APACHE II) scores were calculated to assess the severity degree and mortality risk in patients with pneumonia admitted to the ICU. The laboratory test results of blood routine examination were recorded including C-reactive protein, white blood cell and neutrophil count, serum creatinine, and blood lactic acid. Among 205 participants, 188 cases have received empirical antibiotic therapy prior to ICU admission. Then, the therapeutic regimens were adjusted based on the results of microbiology tests and mNGS combined with the clinical symptoms, imaging, and other infection indicators.

## 2.3 Sample collection and DNA extraction

At least 5 ml of BALF was collected by bronchoscopy following the standard clinical procedure (Chen et al., 2020) in a dry sterile tube. In a dry sterile tube, 1–3 ml of sputum was collected, which was liquefied with 0.1% dithiothreitol (DTT) at room temperature for 30 min before DNA extraction. Then, the DNA of BALF and sputum was extracted by the HostZEROTM Microbial DNA Kit (D4310, ZYMO RESEARCH) according to the kit instructions. No less than 5 ml of blood was collected using a cell-free DNA storage tube (CW2815M, CWBIO); then, plasma was separated by centrifugation at 1,600 g for 10 min. Cell-free DNA was extracted by the HiPure circulating DNA MIDI kit (D3182-03B, Magen). All samples were transported in drikold and cryopreserved until the experiment.

## 2.4 Metagenomic next-generation sequencing

The Kapa HyperPlus library preparation kit (kk8514, Kapa) was used to construct a library based on 1 ng DNA of each sample, following the manufacturer's protocol. The length of the fragments of the library was analyzed by the Agilent 2100 Bioanalyzer, and the concentration of the library was controlled using the qubit dsDNA HS assay kit (Q32854, Thermo Fisher Scientific Inc.). The qualified library was loaded into the flow cell and sequenced on the NextSeq CN500 platform (Illumina). For each test, the negative control of no-template water was set to detect the contamination of the environment, reagent, and cross-sample in the process of the experiment. A historical positive sample was used as positive control. An internal control of specific molecular tags was put into sample to join in extraction to supervise the whole process of the experiment.

## 2.5 Bioinformatic analysis

Clean data were input into the follow-up analysis after removing the adapter, the low-quality and short reads, and reads with ≥10% N using Fastp software (v0.19.5) (Chen et al., 2018). Low-complexity reads were removed by Seqtk_sdust software (v1.3-r106). Then, human host sequences mapped to the human reference genome (GRCh38.p12) were subtracted using bowtie2 software (v 2.3.4.1). The remaining data were classified and annotated through alignment to four microbial genome databases consisting of bacteria, fungi, viruses, and parasites by Burrows–Wheeler Alignment software (v0.7.15). The databases were downloaded from the National Center for Biotechnology Information (NCBI) Refseq (ftp://ftp.ncbi.nlm.nih.gov/genomes/refseq/) including 17,822 microorganisms.

## 2.6 Criteria of positive metagenomic next-generation sequencing analysis results

The suspected background microorganisms from the microbial list were removed referring to the in-house background database. For the remaining microorganisms, the following criteria were used to identify infectious pathogens according to previous studies (Chen et al., 2020; Sun et al., 2021; Lu H. et al., 2022). Positive results were annotated if one of the following criteria were met. (1) For bacterium, the number of reads stringently mapped to pathogen species ≥50 or the suspected pathogens with reads<50 should be supported by a conventional culture result (Wang et al., 2019). (2) A fungus/mycoplasma/chlamydia/virus with at least three reads mapped to pathogen species, or supported by clinical culture (Chen et al., 2020). (3) *Mycobacterium tuberculosis* (MTB) with at least one read mapped to either the species or genus level due to the difficulty of DNA extraction and low possibility for contamination (Miao et al., 2018). (4) A non-tuberculous mycobacterium (NTM) was identified as a positive pathogen if the relative abundance of mapping reads in the genus or species level was in the top 10 of bacteria list, due to the balance of hospital-to-laboratory environmental contamination, which is commonly found in the environment (Miao et al., 2018). Mixed pulmonary infection was defined when two or more infectious pathogens were detected.

## 2.7 Statistical analysis

IBM SPSS Statistics 22 (IBM, NY, USA) was used for statistical analysis. R project (R 4.0.2, R Core Team; https://www.R-Project.org) and GraphPad Prism 6 (GraphPad Software, Inc., San Diego, CA, USA) were employed to plot graphics. Categorical variables were presented in the count number and percentage, which were compared with the chi-square test or Fisher exact test. Continuous variables were presented in mean ± standard deviation and were compared between two groups by a t-test if the data follow a normal distribution. If not, the median and interquartile range were presented and a non-parametric Mann–Whitney U test was performed. $P < 0.05$ indicated a statistically significant difference.

10.3389/fcimb.2023.1136588

TABLE 1 Baseline characteristics and clinical manifestation of 205 patients with community-acquired pneumonia in the study on admission.

| Clinical characteristics | Total | Non-severe CAP (n = 61) | SCAP (n = 144) | *P*- value |
|---|---|---|---|---|
| **Gender** | | | | 0.009 |
| Male | 164 | 42 (68.9%) | 122 (84.7%) | |
| Female | 41 | 19 (31.1%) | 22 (15.3%) | |
| **Age (mean ± SD)** | 65.41 ± 14.19 | 61.59 ± 14.92 | 67.06 ± 13.585 | 0.011 |
| **BMI (mean ± SD)** | 22.00 ± 2.97 | 22.05 ± 2.61 | 21.98 ± 3.12 | 0.876 |
| **Smoking history** | | | | 0.060 |
| No | 135 | 46 (75.4%) | 89 (61.8%) | |
| Yes | 70 | 15 (24.6%) | 55 (38.2%) | |
| **Drinking history** | | | | 0.785 |
| No | 167 | 49 (80.3%) | 118 (81.9%) | |
| Yes | 38 | 12 (19.7%) | 26 (18.1%) | |
| **Immunocompromised** | | | | 0.010 |
| No | 180 (87.8%) | 59 (96.7%) | 121 (84.0%) | |
| Yes | 25 (12.2%) | 2 (3.3%) | 23 (16.0) | |
| Underlying disease | | | | |
| Cardiovascular diseases | 111 | 31 (50.8%) | 80 (55.6%) | 0.534 |
| Diabetes mellitus | 50 | 18 (29.5) | 32 (22.2%) | 0.267 |
| COPD | 30 | 4 (6.6%) | 26 (18.1%) | 0.033 |
| Malignant | 30 | 7 (11.5%) | 23 (16.0%) | 0.405 |
| **Fever** | | | | 0.009 |
| No | 64 (31.2%) | 27 (44.3%) | 37 (25.7%) | |
| Yes | 141 (68.8%) | 34 (55.7%) | 107 (74.3%) | |
| Severity | | | | |
| SOFA score | 8 (5, 11)) | 7 (4, 11) | 8 (5, 10.75) | 0.755 |
| CURB-65 score | 3 (2, 3) | 2 (1, 3) | 3 (2, 4) | <0.001 |
| APACHE II score | 22 (16, 27) | 20 (13.5, 26) | 22 (16, 8) | 0.098 |
| **WBC, *10^9/L** | 11.34 (7.02, 16.90) | 11.83 (6.93, 17.56) | 11.26 (7.12, 16.84) | 0.900 |
| <4*10^9/L | 22 | 6 (9.8%) | 16 (11.1%) | 0.925 |
| 4–10*10^9/L | 116 | 34 (55.7%) | 82 (56.9%) | |
| >10*10^9/L | 67 | 21 (34.4%) | 46 (31.9%) | |
| **Neutrophil, *10^9/L** | 10.87 (6.04, 18.38) | 9.84 (4.99, 15.41) | 11.55 (6.52, 22.45) | 0.029 |
| <1.8*10^9/L | 14 | 7 (11.5%) | 7 (4.9%) | 0.066 |
| 1.8-6.3*10^9/L | 149 | 38 (62.3%) | 111 (77.1%) | |
| >6.3*10^9/L | 42 | 16 (26.2%) | 26 (18.1%) | |
| **CRP, mg/L** | 86.87 (24.52, 142.32) | 76.28 (16.68, 128.17) | 96.62 (33.27, 149.97) | 0.124 |
| ≤6 mg/L | 22 | 9 (14.8%) | 13 (9.0%) | 0.226 |
| >6 mg/L | 131 | 52 (85.2%) | 131 (91.0%) | |

CAP, community-acquired pneumonia; SCAP, severe community-acquired pneumonia; COPD, chronic obstructive pulmonary disease; WBC, white blood cell; CRP, C-reactive protein; SOFA, Sequential Organ Failure Assessment; CURB-65, Confusion, Urea, Respiratory Rate, Blood Pressure and Age Above or Below 65 Years score; APACHE II Acute Physiologic Assessment and Chronic Health Evaluation II.

# 3 Results

## 3.1 Clinical characteristics of patients with community-acquired pneumonia

The demographic characteristics of patients in this study are shown in Table 1. Among 205 patients with CAP, 144 patients (70.24%) were diagnosed as SCAP, and 25 patients (12.2%) were immunocompromised. SCAP patients had elder age ($P = 0.011$) and a significant higher prevalence of an immunocompromised status (16.0% vs. 3.3%, $P = 0.010$) than that of non-severe CAP patients. 141 patients (68.8%) had a symptom of fever, and a higher ratio of patients with SCAP had a fever than patients with non-severe CAP patients (74.3% vs. 55.7%, $P$=0.009).

## 3.2 Comparison of positive rate between metagenomic next-generation sequencing and culture methods

For mNGS technology, the sample type of 83 patients was BALF, 33 patients' samples were sputum, and 89 patients' samples were blood. Generally, a total of 50 pathogens were detected from the BALF samples of 83 patients, and 28 and 23 pathogens were detected from 33 sputum samples and 89 blood samples (Figure 1; Supplementary Table 1). The positive rate of pathogen detection in BALF and sputum samples was 89.2% and 97.0%, which was significantly higher ($P < 0.001$) than that (67.4%) of blood samples (Table 2).

We compared the positive rate of mNGS and culture methods, which is shown in Figure 2A. For all the 205 patients, the positive rate of mNGS was 81.0% which is much higher than that (56.1%) of culture results ($P$ = 1.052e-07). Among 205 patients, 186 patients' sample type of mNGS and culture was consistent. Figure 2B further compares the positive rate between mNGS and culture for samples with a consistent type, which also shows that the positive rate of mNGS was significantly higher than that of culture (82.3% vs. 43.5%, $P$ = 2.527e−14).

## 3.3 Comparison of pathogen detection between metagenomic next-generation sequencing and culture

We analyzed the consistency of pathogens between mNGS and culture methods for 186 patients with a consistent sample type (Figure 2C). The results of mNGS and culture methods were both positive in 80 of 205 cases (43.0%) and both negative in 32 cases (17.2%). The results of 73 cases (39.2%) were only positive in

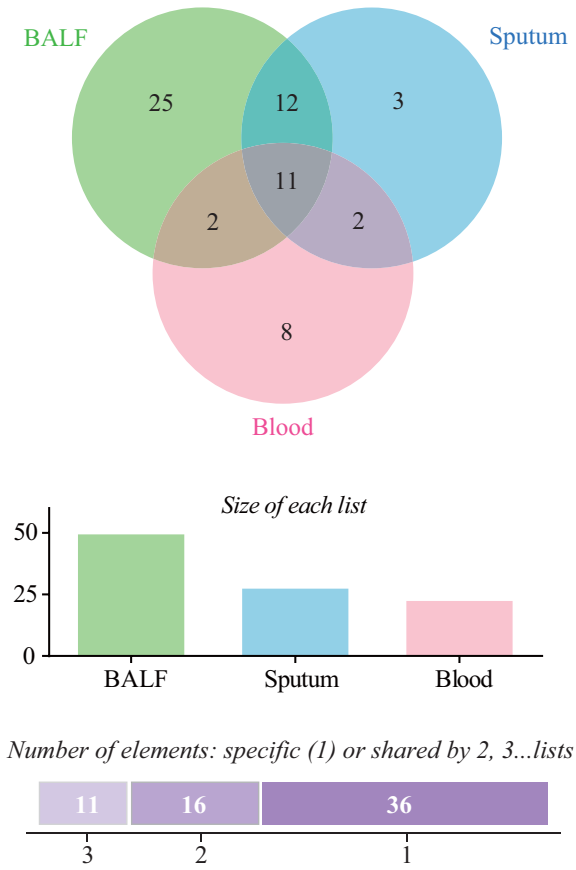


FIGURE 1
Comparison of pathogens detected by metagenomic next-generation sequencing (mNGS) among bronchoalveolar lavage fluid (BALF), sputum, and blood samples.

TABLE 2 Positive rate of pathogens detected by metagenomic next-generation sequencing in different sample types involving bronchoalveolar lavage fluid, sputum, and blood.

| Sample type | Total | Negative | Positive | P- value |
|---|---|---|---|---|
| BALF | 93 | 9 (10.8%) | 74 (89.2%) | <0.001 |
| Sputum | 33 | 1 (3.0%) | 32 (97.0%) | |
| Blood | 89 | 29 (32.6%) | 60 (67.4%) | |

BALF, bronchoalveolar lavage fluid.

mNGS, and one patient's result was only positive by culture. To examine the results' consistency of mNGS and culture, we further compared the detected pathogens between mNGS and culture for 80 patients whose mNGS result and culture result were both positive (Figure 2C, double+). The detected pathogens of mNGS were identical with the results of the culture method in 16 patients and partly matched with culture results in 40 patients. For 24 patients, the pathogens were mismatched between mNGS and culture methods (Figure 2C, right).

## 3.4 Pathogens' profile of all CAP patients according to detection methods

Figure 3 shows the pathogens' profile of 205 CAP patients by mNGS and culture methods. The detected pathogens were divided into three kingdoms, namely, bacteria, fungi, and viruses. A total of 57 bacteria (Figure 3A), 12 fungi (Figure 3B), and 9 viruses (Figure 3C) were detected by mNGS and the CMT.

### 3.4.1 Profile of bacteria

In the bacteria level (Figure 3A), *Escherichia coli* (*E. coli*) was the most common pathogen that was detected in 31 CAP patients. In addition, MTB (n=25), *Klebsiella pneumoniae* (n=22), *Corynebacterium striatum* (n=20), *Acinetobacter baumannii* (n=15), and *Pseudomonas aeruginosa* (n=12) were the common pathogens of CAP patients. A total of 23 bacteria were only detected by mNGS, including *Mycobacterium abscessus* (*M. abscessus*, n=8), *Chlamydia psittaci* (*C. psittaci*, n=5), *Burkholderia cenocepacia* (n=2), and *Chlamydia abortus* (n=2). A total of 12 bacteria were only detected by culture, including *Klebsiella aerogenes* (n=3), and *Acinetobacter calcoaceticus* (n=1). A total of 22 bacteria were detected by both mNGS and culture.

### 3.4.2 Profile of fungi

In the fungi level (Figure 3B), *Candida albicans* (*C. albicans*) detected in 40 patients was the most frequent fungus, and 27 of cases were only detected by mNGS. *Pneumocystis jirovecii* (*P. jirovecii*) was the second common fungus detected in 12 cases by mNGS only.

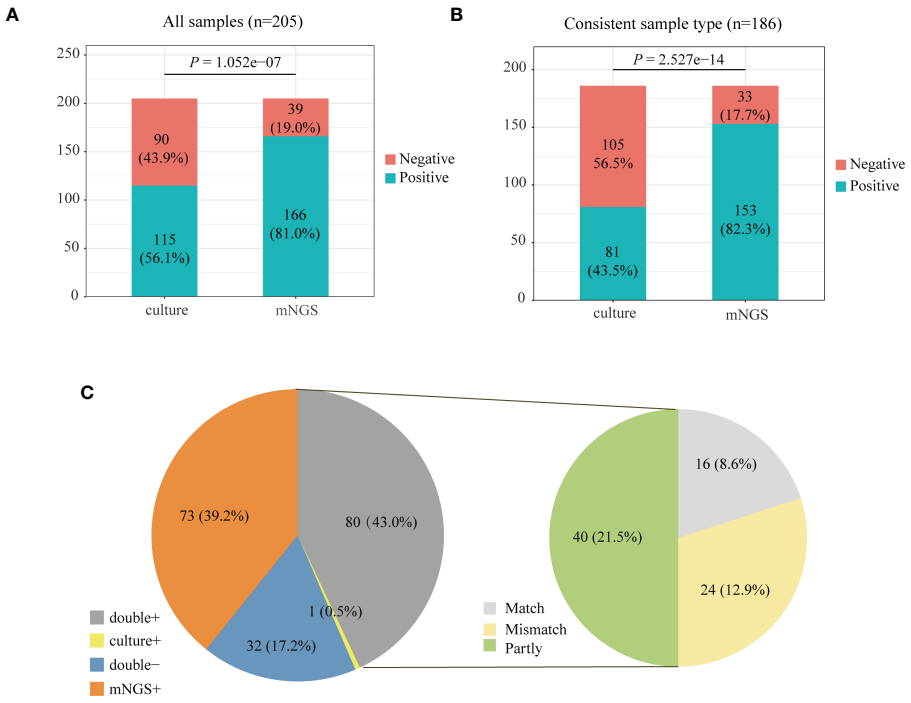


FIGURE 2
Positive rate comparison between metagenomic next-generation sequencing (mNGS) and laboratory culture for 205 community-acquired pneumonia (CAP) patients **(A)** and 186 pneumonia patients whose sample type was consistent for mNGS and culture **(B)**. **(C)** The positivity distribution of mNGS and culture for 186 patients with a consistent sample type. For the double-positive subgroup, the cases were divided into matched, mismatched, and partly matched groups based on the consistency of pathogens detected by the two methods.

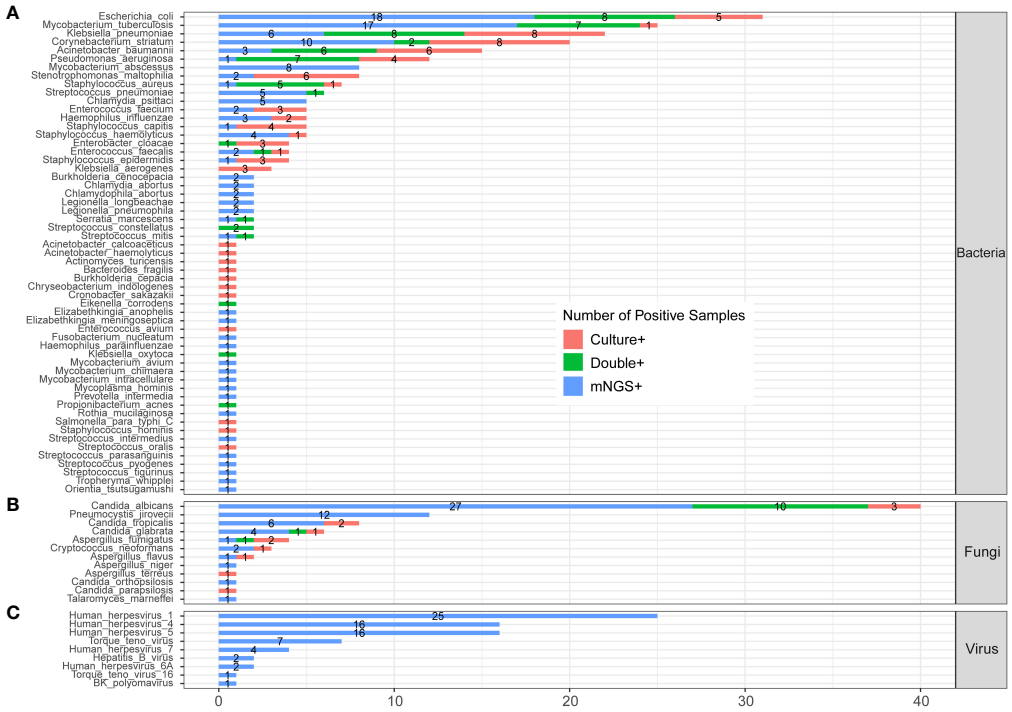


FIGURE 3
The comparison and overlap of infected pathogens between mNGS and laboratory culture in all 205 patients with CAP. **(A)** Bacteria levels; **(B)** fungi level; and **(C)** virus level.

### 3.4.3 Profile of virus

All the nine viruses were all detected by the mNGS method. *Human herpesvirus* (HHV) was the most recurrent virus, including 25 cases of HHV-1, 16 cases of HHV-4, 16 cases of HHV -5, 4 cases of HHV-7, and 2 cases of HHV-6A (Figure 3D). The heatmap in Supplementary Figure 1 shows the relative abundance of all nine viruses in 60 virus-infected patients.

We compared the results of the clinical culture test and mNGS from 186 CAP patients whose sample type was consistent between two methods, which is shown in Supplementary Figure 2. It had an overall consistency with the results of Figure 3.

## 3.5 Comparison of pathogens detected by metagenomic next-generation sequencing between severe and non-severe community-acquired pneumonia patients

To further evaluate the clinical significance of mNGS in patients with pulmonary infection, we compared the infected pathogens identified by mNGS between severe and non-severe CAP patients (Figure 4; Supplementary Table 2). A total of 45 bacteria were identified by mNGS in 205 CAP patients. There were 14 bacteria found in both severe and non-severe CAP patients, 5 bacteria were found only in infected non-severe patients, and 26 bacteria were only detected in SCAP patients (Figure 4A). *E. coli* is the most common infected bacteria in non-severe CAP patients (24.5%); the infection rate was significantly higher than that (7.64%) in the SCAP group ($P$ = 0.001, Supplementary Table 2). MTB was the most common infected bacteria in SCAP patients (14.58%, Supplementary Table 2).

All five *C. psittaci* infected cases were from the SCAP group. From Figure 3, we can see that *C. psittaci* from five infected cases were all identified by mNGS only with negative culture results. In addition, all five *Staphylococcus haemolyticus (S. haemolyticus)*–infected cases belonged to the SCAP group. *S. haemolyticus* in four cases were identified by mNGS only, and one case was detected by culture. These results indicated that *C. psittaci* and *S. haemolyticus* were the common pathogens that had an almost entire probability leading to severe disease. mNGS has a very high clinical value on the identification of these two pathogens in SCAP patients with negative CMT results.

## 3.6 Comparison of pathogens between immunocompromised and immunocompetent patients with severe community-acquired pneumonia

The positive rates of mNGS and culture for both immunocompromised and immunocompetent patients with SCAP are illustrated in Figure 5A. The positive rate of mNGS in the immunocompetent group was significantly higher than that of culture (80.17% vs. 54.55%, $P$ = 3.911e-05). However, there was no significant differences in the diagnostic positive rate between mNGS and culture in the immunocompromised group (86.96% vs. 69.57%, $P$=0.2835, Figure 5A). In addition, there was no significant difference in both the mixed pathogen rate (57% vs. 45%, $P$ = 0.6744) and the

diagnostic positive rate (87% vs. 80%, $P = 0.9401$) of mNGS between immunocompromised and immunocompetent patients with SCAP (Figure 5B).

The profile of infected pathogens identified by mNGS in 144 SCAP patients is shown in Figure 6 and Supplementary Table 3 according to patients with or without an immunocompromised status. A total of 40 bacteria were identified by mNGS from 144 SCAP patients. Among them, 29 bacteria were detected in immunocompetent cases only, 3 bacteria were detected in immunocompromised cases only, and 8 bacteria were found in both immunocompetent and immunocompromised groups. MTB was the most common infected bacterium both in immunocompetent (15.70%) and immunocompromised (8.70%) patients with SCAP. There was no significant difference in the positive rate of every bacterium between patients with or without an immunocompromised status (Supplementary Table 3).

A total of nine fungi were detected by mNGS in SCAP patients. Among them, three fungi were specifically identified in immunocompetent cases, one fungus was specifically detected in immunocompromised cases, and five fungi were found in both immunocompetent and immunocompromised groups. *C. albicans* was the most frequently infected fungus in the immunocompetent (20.66%) SCAP group. *P. jirovecii* was the most common pathogen (26.09%) in SCAP patients with an immunocompromised status. We found that the positive rate of *P. jirovecii* in immunocompromised patients with SCAP was obviously higher than that in immunocompetent cases (26.09% vs. 4.13%, $P<0.001$, Supplementary Table 3). All the *P. jirovecii*– infected patients were identified by mNGS only (Figure 3).

# 4 Discussion

In this study, we systematically compared the effectiveness of pathogen detection between mNGS and culture in a pairwise manner from 205 patients with CAP in the ICU. Firstly, we found that mNGS performed differently on pathogen detection for BALF, sputum, and blood samples. The mNGS of BALF and sputum samples had a higher sensitivity of pathogen detection than blood ($P < 0.001$), which was consistent with previous literature (Chen et al., 2020; Lu H. et al., 2022). Compared to sputum, BALF has the following advantages: reflecting the component at the level of alveoli and avoiding the contamination of oropharyngeal flora (Dubourg et al., 2015). Thus, BALF was suggested as the appropriate sample for the pathogen detection of SCAP patients because of its high sensitivity, good tolerance, and easily acquisition *via* bedside bronchoscopy (Hertz et al., 1991). Hence, if the BALF samples are not available for some patients with pneumonia, sputum is suggested as the second-rate choice. Xu Chen et al. (2020) reported that blood mNGS detected more viruses than BALF mNGS overall, but no similar phenomenon was observed in our study.

As the previous literature reported, our data also indicated that mNGS had overall higher sensitivity for pathogen detection compared with culture. In this study, MTB was the second most frequent pathogen (25/205, 12.2%) in the overall CAP cohort but the most common pathogen for the SCAP group. MTB is a main pathogen causing CAP in developing countries (Wei et al., 2020). A systematic review reported that more than 10% of patients with CAP in Asia were caused by MTB, which was consistent with our

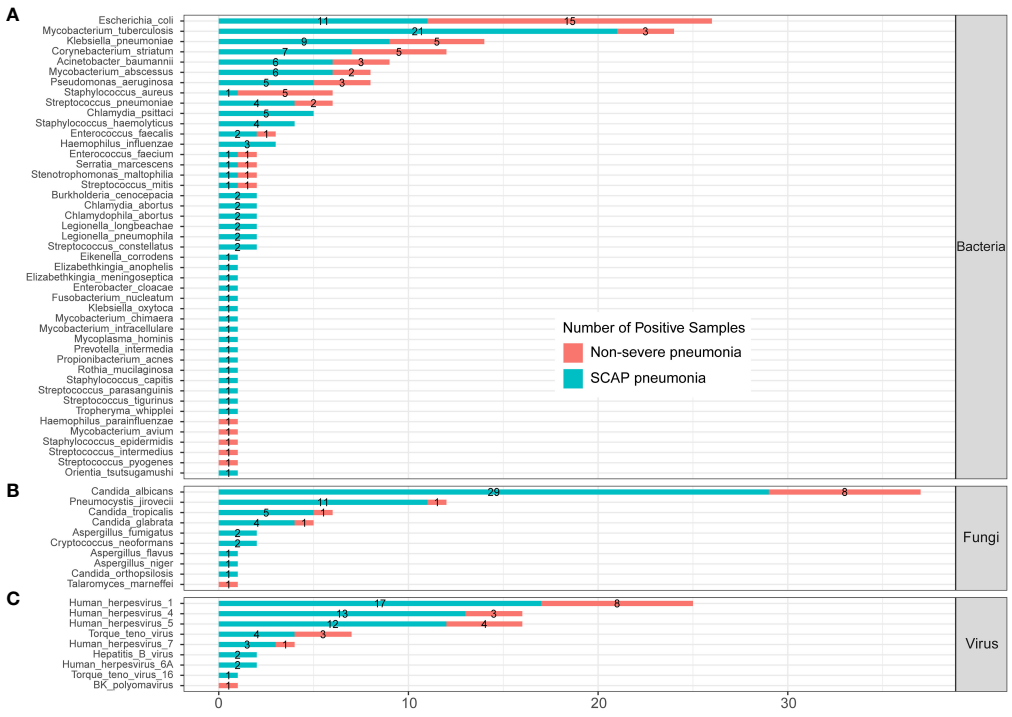


FIGURE 4
Infected pathogens detected by mNGS in severe and non-severe patients with CAP. **(A)** bacteria levels; **(B)** fungi level; **(C)** protozoa level; and (**C**) virus level.

results (Peto et al., 2014). Previous literature showed that mNGS produced a similar sensitivity with Xpert and culture for MTB detection (Zhou et al., 2019; Shi et al., 2020). Some researchers suggested that the sensitivity of mNGS is not superior to that of culture for identifying common bacteria (excluding MTB and anaerobes) (Miao et al., 2018), and culture could identify the vast majority (74%) of bacterium-associated pneumonia (Toma et al., 2014). Our study showed mNGS had advantages over culture for MTB and NTM. For example, eight *M. abscessus*– infected patients were all diagnosed by mNGS only. *M. abscessus* is reported as the second most common non-tuberculous mycobacterial lung disease pathogen (Griffith and Daley, 2022), which is often regarded as one of the most antibiotic-resistant mycobacteria, leaving clinicians with few therapeutic options (Johansen et al., 2020). Thus, mNGS has a very high clinical value on the identification of MTB and NTM in patients with pulmonary infection, whose conventional microbiological tests give negative results.

In the cohort of our study, five patients with SCAP were identified as *C. psittaci* infection by mNGS. For all the five cases, culture gave the negative results. *C. psittaci* is an obligatory intracellular Gram-negative bacterium that typically infects birds; infections in humans mainly present as CAP (Hogerwerf et al., 2017). Conventional laboratory tests for *C. psittaci* include culture, a serological assay, and PCR. Culture is low efficient and requires a P3 facility (Balsamo et al., 2017); serological tests are only appropriate for a retrospective diagnosis (Tuuminen et al., 2000). Molecular detection by PCR is the specific and fastest method but needs the prejudgment of *C. psittaci* infection, which tends to be overlooked due to relatively low awareness by physicians. Our study accumulated evidence that mNGS is a useful tool to diagnose *C. psittaci* infection. Moreover, mNGS could even provide semiquantitative information (based on sequence reads) about the load of *C. psittaci*, which could be really important for judging whether it is the causative pathogen in mixed infected samples (Gu et al., 2020). CY Kong et al.'s study (Kong et al., 2021) suggested that poultry exposure history, high fever, elevated inflammatory biomarkers, and elevated lactate dehydrogenase, combined with air-containing bronchial shadow consolidation with little or no secretions, may guide the early clinical diagnosis of *C. psittaci* pneumonia.

In this study, *P. jirovecii* was the most common pathogen in SCAP patients with an immunocompromised status, whose infected frequency was significantly higher than that of immunocompetent patients with SCAP. Previous researchers reported that the asymptomatic lung colonization of *P. jirovecii* could occur in people with normal immune systems (Truong and Ashurst, 2022). They may unknowingly become asymptomatic carriers for the spread of *Pneumocystis* to immunocompromised individuals through an airborne route (Truong and Ashurst, 2022). Patients with *P. jirovecii* pneumonia may have the symptoms of fever, cough, dyspnea, and respiratory failure in severe cases. The diagnosis of *P. jirovecii* pneumonia is multifactorial and may include the laboratory tests of BALF and sputum, chest radiograph, chest computed tomography, or lung biopsies (Langevin and Saleh, 2016). A definitive diagnosis of *P. jirovecii* pneumonia requires identifying the organism by the PCR of respiratory specimens, dye staining, or fluorescein antibody staining (Limper et al., 1989). Since *Pneumocystis* cannot be cultured, in this study, all patients infected with *P. jirovecii* were diagnosed by mNGS. Our study demonstrated that mNGS could quickly and accurately diagnose *P. jirovecii* pneumonia, which was also approved by other reseachers (Liu et al., 2021; Lu X. et al., 2022; Sun et al., 2022; Wang et al., 2022; Zhao et al., 2022). A combination of clinical symptoms, laboratory testing, and imaging examination is suggested to make a comprehensive judgment along with the mNGS test.

There are some limitations in our study. Firstly, mNGS in this study was only performed on the DNA level without concomitant RNA-seq data. It will miss the RNA virus and microbial transcriptome information. Comprehensive mNGS- based DNA-seq combined with RNA-seq could further improve the sensitivity of pathogen detection. In addition, the sample types were varied including BALF, sputum, and blood, and the detection efficiency of virus sample types was different. The lack of a consistent sample-collecting method and site affected the results of mNGS. To further

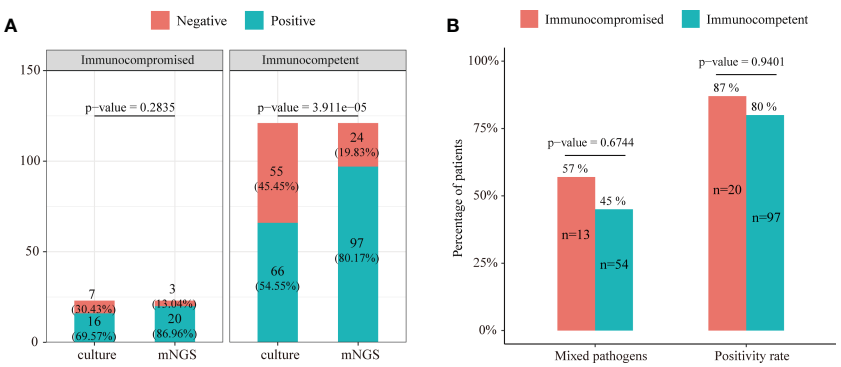


FIGURE 5
**(A)** The positive rate comparison between mNGS and the conventional test in immunocompetent and immunocompromised patients with severe pneumonia. **(B)** Comparison of the positive rate and ratio of mixed pathogen infection between immunocompetent and immunocompromised severe pneumonia patients.

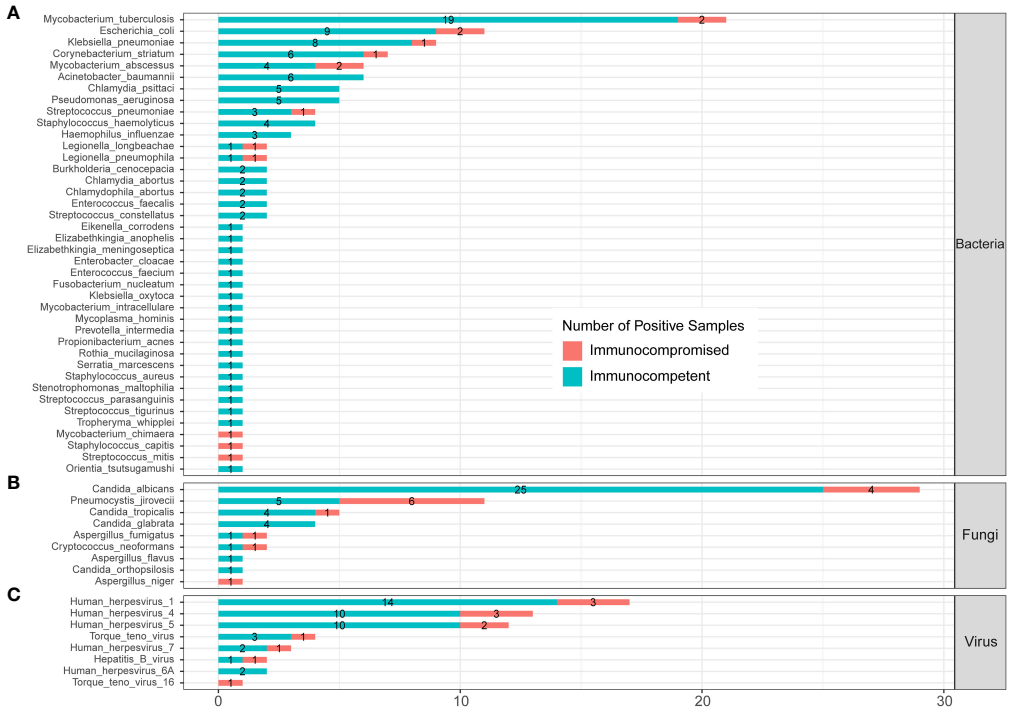


FIGURE 6
Infected pathogens detected by mNGS in immunocompetent and immunocompromised patients with severe pneumonia. **(A)** Bacteria levels; **(B)** fungi level; and **(C)** virus level.

comprehensively evaluate the application value of mNGS in the diagnosis of pulmonary infections, multicenter prospective studies with a larger number of participants are required. Further research is needed to evaluate the possible improvement in clinical outcomes and the cost-effectiveness of mNGS for infectious diseases.

## Conclusions

In conclusion, this study demonstrated that mNGS had higher overall sensitivity for the pathogen identification of pulmonary infections than culture. BALF and sputum mNGS had advantage over blood mNGS in pathogen detection. mNGS is superior in detecting MTB, NTM, viruses, *P. jirovecii*, and chlamydia. Thus, mNGS is a necessary complement of conventional microbiological tests and helps clinicians to make treatment decisions for patients with an unknown clinical diagnosis.

## Data availability statement

The original contributions presented in the study are publicly available. This data can be found here: NCBI SRA under project ID: PRJNA917446.

## Ethics statement

The studies involving human participants were reviewed and approved by the Ethical Committee of Quanzhou First Hospital. The patients/participants provided their written informed consent to participate in this study.

## Author contributions

TL, JL, and HZ designed the project. LH, XD, and XC collected samples and clinical data. YX, WL, and YW performed experiments and analyzed the data. TL, JZ, and XT wrote the manuscript. All authors read and approved the final manuscript.

## Funding

This work was supported by National key Research & Development plan (2018YFE0102400), Shanghai Special Project for Artificial Intelligence Innovation and Development (2020-RGZN-02039), and Quanzhou Guiding Science and Technology Project in Medical and Health Field (2021N062S).

## Conflict of interest

JZ, YX, WL, YW, and JL were employed by Shanghai Biotecan Pharmaceuticals Co., Ltd.

The remaining authors declare that the research was conducted in the absence of any commercial or financial relationships that could be construed as a potential conflict of interest.

## Publisher's note

All claims expressed in this article are solely those of the authors and do not necessarily represent those of their affiliated organizations, or those of the publisher, the editors and the reviewers. Any product that may be evaluated in this article, or claim that may be made by its manufacturer, is not guaranteed or endorsed by the publisher.

## Supplementary material

The Supplementary Material for this article can be found online at: https://www.frontiersin.org/articles/10.3389/fcimb.2023.1136588/full#supplementary-material

## References

Balsamo, G., Maxted, A. M., Midla, J. W., Murphy, J. M., Wohrle, R., Edling, T. M., et al. (2017). Compendium of measures to control chlamydia psittaci infection among humans (Psittacosis) and pet birds (Avian chlamydiosis). *J. Avian Med. Surg.* 31, 262–282. doi: 10.1647/217-265

Chen, X., Ding, S., Lei, C., Qin, J., Guo, T., Yang, D., et al. (2020). Blood and bronchoalveolar lavage fluid metagenomic next-generation sequencing in pneumonia. *Can. J. Infect. Dis. Med. Microbiol.* 2020, 6839103. doi: 10.1155/2020/6839103

Chen, S., Zhou, Y., Chen, Y., and Gu, J. (2018). Fastp: an ultra-fast all-in-one FASTQ preprocessor. *Bioinf.* 34(17), i884–i890. doi: 10.1093/bioinformatics/bty560

Cilloniz, C., Torres, A., and Niederman, M. S. (2021). Management of pneumonia in critically ill patients. *BMJ* 375, e065871. doi: 10.1136/bmj-2021-065871

Dubourg, G., Abat, C., Rolain, J. M., and Raoult, D. (2015). Correlation between sputum and bronchoalveolar lavage fluid cultures. *J. Clin. Microbiol.* 53, 994–996. doi: 10.1128/JCM.02918-14

Griffith, D. E., and Daley, C. L. (2022). Treatment of mycobacterium abscessus pulmonary disease. *Chest* 161, 64–75. doi: 10.1016/j.chest.2021.07.035

Gu, L., Liu, W., Ru, M., Lin, J., Yu, G., Ye, J., et al. (2020). The application of metagenomic next-generation sequencing in diagnosing chlamydia psittaci pneumonia: a report of five cases. *BMC Pulm. Med.* 20, 65. doi: 10.1186/s12890-020-1098-x

Gu, W., Miller, S., and Chiu, C. Y. (2019). Clinical metagenomic next-generation sequencing for pathogen detection. *Annu. Rev. Pathol.* 14, 319–338. doi: 10.1146/annurev-pathmechdis-012418-012751

Hertz, M. I., Woodward, M. E., Gross, C. R., Swart, M., Marcy, T. W., and Bitterman, P. B. (1991). Safety of bronchoalveolar lavage in the critically ill, mechanically ventilated patient. *Crit. Care Med.* 19, 1526–1532. doi: 10.1097/00003246-199112000-00015

Hogerwerf, L., Gier., B. D. E., Baan, B., and Van DER Hoek, W. (2017). Chlamydia psittaci (psittacosis) as a cause of community-acquired pneumonia: a systematic review and meta-analysis. *Epidemiol. Infect.* 145, 3096–3105. doi: 10.1017/S0950268817002060

Jain, S., Self, W. H., Wunderink, R. G., Fakhran, S., Balk, R., Bramley, A. M., et al. (2015). Community-acquired pneumonia requiring hospitalization among U. *S. Adults N. Engl. J. Med.* 373, 415–427. doi: 10.1056/NEJMoa1500245

Johansen, M. D., Herrmann, J. L., and Kremer, L. (2020). Non-tuberculous mycobacteria and the rise of mycobacterium abscessus. *Nat. Rev. Microbiol.* 18, 392–407. doi: 10.1038/s41579-020-0331-1

Kong, C. Y., Zhu, J., Lu, J. J., and Xu, Z. H. (2021). Clinical characteristics of chlamydia psittaci pneumonia. *Chin. Med. J. (Engl)* 134, 353–355. doi: 10.1097/CM9.0000000000001313

Langevin, B., and Saleh, M. (2016). Radiological presentation of pneumocystis jiroveci pneumonia mimicking bacterial pneumonia. *BMJ Case Rep.* doi: 10.1136/bcr-2016-215207

Limper, A. H., Offord, K. P., Smith, T. F., and Martin, W. J.2nd (1989). Pneumocystis carinii pneumonia. differences in lung parasite number and inflammation in patients with and without AIDS. *Am. Rev. Respir. Dis.* 140, 1204–1209. doi: 10.1164/ajrccm/140.5.1204

Liu, L., Yuan, M., Shi, Y., and Su, X. (2021). Clinical performance of BAL metagenomic next-generation sequence and serum (1,3)-beta-D-Glucan for differential diagnosis of pneumocystis jirovecii pneumonia and pneumocystis jirovecii colonisation. *Front. Cell Infect. Microbiol.* 11, 784236. doi: 10.3389/fcimb.2021.784236

Lu, H., Ma, L., Zhang, H., Feng, L., Yu, Y., Zhao, Y., et al. (2022). The comparison of metagenomic next-generation sequencing with conventional microbiological tests for identification of pathogens and antibiotic resistance genes in infectious diseases. *Infect. Drug Resist.* 15, 6115–6128. doi: 10.2147/IDR.S370964

Lu, X., Zhang, J., Ma, W., Xing, L., Ning, H., and Yao, M. (2022). Pneumocystis jirovecii pneumonia diagnosis *via* metagenomic next-generation sequencing. *Front. Med. (Lausanne)* 9, 812005. doi: 10.3389/fmed.2022.812005

Metlay, J. P., Waterer, G. W., Long, A. C., Anzueto, A., Brozek, J., Crothers, K., et al. (2019). Diagnosis and treatment of adults with community-acquired pneumonia. an official clinical practice guideline of the American thoracic society and infectious diseases society of America. *Am. J. Respir. Crit. Care Med.* 200, e45–e67. doi: 10.1164/rccm.201908-1581ST

Miao, Q., Ma, Y., Wang, Q., Pan, J., Zhang, Y., Jin, W., et al. (2018). Microbiological diagnostic performance of metagenomic next-generation sequencing when applied to clinical practice. *Clin. Infect. Dis.* 67, S231–S240. doi: 10.1093/cid/ciy693

Miller, J. M., Binnicker, M. J., Campbell, S., Carroll, K. C., Chapin, K. C., Gilligan, P. H., et al. (2018). A guide to utilization of the microbiology laboratory for diagnosis of infectious diseases: 2018 update by the infectious diseases society of America and the American society for microbiology. *Clin. Infect. Dis.* 67, e1–e94. doi: 10.1093/cid/ciy381

Peng, J. M., Du, B., Qin, H. Y., Wang, Q., and Shi, Y. (2021). Metagenomic next-generation sequencing for the diagnosis of suspected pneumonia in immunocompromised patients. *J. Infect.* 82, 22–27. doi: 10.1016/j.jinf.2021.01.029

Peto, L., Nadjm, B., Horby, P., Ngan, T. T., van Doorn, R., Van Kinh, N., et al. (2014). The bacterial aetiology of adult community-acquired pneumonia in Asia: a systematic review. *Trans. R. Soc. Trop. Med. Hyg.* 108, 326–337. doi: 10.1093/trstmh/tru058

Sangla, F., Legouis, D., Marti, P. E., Sgardello, S. D., Brebion, A., Saint-Sardos, P., et al. (2020). One year after ICU admission for severe community-acquired pneumonia of bacterial, viral or unidentified etiology. *What are outcomes? PloS One* 15, e0243762. doi: 10.1371/journal.pone.0243762

Shi, C. L., Han, P., Tang, P. J., Chen, M. M., Ye, Z. J., Wu, M. Y., et al. (2020). Clinical metagenomic sequencing for diagnosis of pulmonary tuberculosis. *J. Infect.* 81, 567–574. doi: 10.1016/j.jinf.2020.08.004

Sun, H., Wang, F., Zhang, M., Xu, X., Li, M., Gao, W., et al. (2022). Diagnostic value of bronchoalveolar lavage fluid metagenomic next-generation sequencing in pneumocystis jirovecii pneumonia in non-HIV immunosuppressed patients. *Front. Cell Infect. Microbiol.* 12, 872813. doi: 10.3389/fcimb.2022.872813

Sun, T., Wu, X., Cai, Y., Zhai, T., Huang, L., Zhang, Y., et al. (2021). Metagenomic next-generation sequencing for pathogenic diagnosis and antibiotic management of severe community-acquired pneumonia in immunocompromised adults. *Front. Cell Infect. Microbiol.* 11, 661589. doi: 10.3389/fcimb.2021.661589

Toma, I., Siegel, M. O., Keiser, J., Yakovleva, A., Kim, A., Davenport, L., et al. (2014). Single-molecule long-read 16S sequencing to characterize the lung microbiome from mechanically ventilated patients with suspected pneumonia. *J. Clin. Microbiol.* 52, 3913–3921. doi: 10.1128/JCM.01678-14

Torres, A., Cilloniz, C., Niederman, M. S., Menendez, R., Chalmers, J. D., Wunderink, R. G., et al. (2021). Pneumonia. *Nat. Rev. Dis. Primers* 7, 25. doi: 10.1038/s41572-021-00259-0

Truong, J., and Ashurst, J. V. (2022). Pneumocystis jirovecii pneumonia. *StatPearls Treasure Island (FL).*

Tuuminen, T., Palomaki, P., and Paavonen, J. (2000). The use of serologic tests for the diagnosis of chlamydial infections. *J. Microbiol. Methods* 42, 265–279. doi: 10.1016/S0167-7012(00)00209-8

Vincent, J. L., Sakr, Y., Singer, M., Martin-Loeches, I., Machado, F. R., Marshall, J. C., et al. (2020). Prevalence and outcomes of infection among patients in intensive care units in 2017. *JAMA* 323, 1478–1487. doi: 10.1001/jama.2020.2717

Wang, D., Fang, S., Hu, X., Xu, Q., Chu, X., Mei, X., et al. (2022). Metagenomic next-generation sequencing is highly efficient in diagnosing pneumocystis jirovecii pneumonia in the immunocompromised patients. *Front. Microbiol.* 13, 913405. doi: 10.3389/fmicb.2022.913405

Wang, J., Han, Y., and Feng, J. (2019). Metagenomic next-generation sequencing for mixed pulmonary infection diagnosis. *BMC Pulm. Med.* 19, 252. doi: 10.1186/s12890-019-1022-4

Wei, M., Yongjie, Z., Zhuoyu, Q., Biao, Y., Xi, J., Wei, J., et al. (2020). Pneumonia caused by mycobacterium tuberculosis. *Microbes Infect.* 22, 278–284. doi: 10.1016/j.micinf.2020.05.020

Wu, X., Li, Y., Zhang, M., Li, M., Zhang, R., Lu, X., et al. (2020). Etiology of severe community-acquired pneumonia in adults based on metagenomic next-generation sequencing: A prospective multicenter study. *Infect. Dis. Ther.* 9, 1003–1015. doi: 10.1007/s40121-020-00353-y

Zhao, M., Yue, R., Wu, X., Gao, Z., He, M., and Pan, L. (2022). The diagnostic value of metagenomic next-generation sequencing for identifying pneumocystis jirovecii infection in non-HIV immunocompromised patients. *Front. Cell Infect. Microbiol.* 12, 1026739. doi: 10.3389/fcimb.2022.1026739

Zhou, X., Wu, H., Ruan, Q., Jiang, N., Chen, X., Shen, Y., et al. (2019). Clinical evaluation of diagnosis efficacy of active mycobacterium tuberculosis complex infection *via* metagenomic next-generation sequencing of direct clinical samples. *Front. Cell Infect. Microbiol.* 9, 351. doi: 10.3389/fcimb.2019.00351

frontiers | Frontiers in Cellular and Infection Microbiology

TYPE Original Research
PUBLISHED 24 April 2023
DOI 10.3389/fcimb.2023.1170687



OPEN ACCESS

EDITED BY
Rodolfo García-Contreras,
Department of Microbiology and Parasitology, National Autonomous University of Mexico, Mexico

REVIEWED BY
Kokila Kota,
Ramapo College, United States
Gangfeng Yan,
Fudan University, China

*CORRESPONDENCE
Hong Zhang
zhanghong20070703@163.com

SPECIALTY SECTION
This article was submitted to Clinical Microbiology, a section of the journal Frontiers in Cellular and Infection Microbiology

RECEIVED 21 February 2023
ACCEPTED 27 March 2023
PUBLISHED 24 April 2023

CITATION
Li X, Liang S, Zhang D, He M and Zhang H (2023) The clinical application of metagenomic next-generation sequencing in sepsis of immunocompromised patients. *Front. Cell. Infect. Microbiol.* 13:1170687. doi: 10.3389/fcimb.2023.1170687



# The clinical application of metagenomic next-generation sequencing in sepsis of immunocompromised patients

Xingxing Li, Shunda Liang, Dan Zhang, Miao He and Hong Zhang*

Department of Emergency Medicine, The First Affiliated Hospital of Anhui Medical University, Anhui, Hefei, China

**Background:** Metagenomic next-generation sequencing (mNGS) was commonly applied given its ability to identify and type all infections without depending upon culture and to retrieve all DNA with unbiasedness. In this study, we strive to compare outcomes of mNGS with conventional culture methods in adults with sepsis, investigate the differences between the immunocompromised and control group, and assess the clinical effects of mNGS.

**Methods:** In our study, 308 adult sepsis patients were included. We used both mNGS and conventional culture methods to analyze diagnostic results, pathogens, and sample types. The correlation between some laboratory tests and the frequency of pathogens by groups was also analyzed. Furthermore, the clinical impacts of mNGS were estimated.

**Results:** 308 samples were assigned to an immunocompromised group (92/308,29.9%) and a control group (216/308,70.1%). There was the sensitivity of mNGS considered greater than that of the culture method in all samples (88.0% vs 26.3%; $P < 0.001$), in the immunocompromised group (91.3% vs 26.1%; $P < 0.001$), and the control group (86.6% vs 26.4%; $P < 0.001$), particularly in all sample types of blood ($P < 0.001$), BALF ($P < 0.001$), CSF ($P < 0.001$), sputum ($P < 0.001$) and ascitic fluid ($P = 0.008$). When examining the mNGS results between groups, Pneumocystis jirovecii ($P < 0.001$), Mucoraceae ($P = 0.014$), and Klebsiella ($P = 0.045$) all showed significant differences. On the whole, mNGS detected more pathogens than culture methods (111 vs 25), found 89 organisms that were continuously overlooked in entire samples by culture methods, and showed a favorable positive clinical effect in 76.3% (235 of 308) of patients. In 185 (60.1%) patients, mNGS prompted a modification in the course of management, which included antibiotic de-escalation in 61(19.8%) patients.

**Conclusions:** The research discovered that mNGS was more sensitive than the culture method, particularly in samples of blood, BALF, CSF, sputum, and ascitic fluid. When examining the mNGS results, Pneumocystis jirovecii and Mucoraceae were the pathogens seen more commonly in immunocompromised patients with sepsis, which required more attention from clinicians. There was a

substantial benefit of mNGS in enhancing the diagnosis of sepsis and advancing patient treatment.

KEYWORDS

metagenomic next-generation sequencing, sepsis, immunocompromised patients, diagnostic, sensitivity, clinical effect

# 1 Introduction

Sepsis is a serious medical problem that affects people all over the world and is accompanied by a high incidence of morbidity and mortality. Despite the significant improvements in the care of immunocompromised patients over the past few decades, sepsis remains to be the main reason for death in this population. The diagnosis and management of severe infections may be more problematic due to patients' limited capacity to manifest the clinical symptoms that normally accompany sepsis, but essential to salvaging the patient outcomes (McCreery et al., 2020). The microbiology laboratory, as the first line of pathogen detection, contributes significantly to controlling infections by microscopy, culture, classification, drug sensitivity, and other means (Zhou et al., 2016). Nevertheless, pathogens can be undiagnosed in roughly 60% of samples as a result of the limitations of molecular diagnostics and genotyping approaches (Ewig et al., 2002; van Gageldonk-Lafeber et al., 2005; Schlaberg et al., 2017). When microorganisms fail to be identified in time, broad-spectrum antibiotics may be used unnecessarily, which leads to the development of resistance and an increase in medical expenses (Miao et al., 2018).

An unbiased molecular technique called metagenomics next-generation sequencing (mNGS) may concurrently identify bacteria, viruses, fungi, and parasites in clinical specimens by detecting all of their DNA and/or RNA content (Chiu and Miller, 2019). Previous research has shown that mNGS, distinguished by high accuracy, extreme sensitivity, and rapidly detectable time, may identify pathogens in an array of specimens (Chiu and Miller, 2019; Wilson et al., 2019; Chen et al., 2021; Gu et al., 2021). It has important benefits for identifying pathogens that cause severe infections, mixed infections, and uncommon and novel pathogen infections in immunocompromised patients (Chiu and Miller, 2019). Whereas, it is unknown whether mNGS is effective in the etiological diagnosis and management of immunocompromised individuals with sepsis.

Thus, we analyzed sensitivities between the mNGS method and the conventional culture method to identify pathogens and evaluated the effects of mNGS detection outcomes on the diagnosis and management of immunocompromised patients with sepsis in our study.

# 2 Materials and methods

## 2.1 Enrolled patients

A total of 308 adult patients with sepsis were enrolled in this study at The First Affiliated Hospital of Anhui Medical University in Anhui, China, from January 2021 to December 2021. The diagnosis of sepsis met the diagnostic criteria set out by the Society of Critical Care Medicine (SCCM) and the European Society of Intensive Care Medicine (ESICM) (Singer et al., 2016). According to immunological status, the patients were split into an immunocompromised group and a control group.

Based on the previous study, the following definition of the immunocompromised state (Hill, 2020) was used: ① hematological malignancies; ② solid organ transplantation or hematopoietic stem cell transplantation (HCT); ③ solid tumors recently treated with chemotherapeutic agents; ④ primary immunodeficiency disease; ⑤ HIV infection with a CD4+ T-lymphocyte count <200 cells/ul; ⑥ taken immunosuppressants, biological immunomodulators, and anti-rheumatic drugs (e.g., methotrexate, cyclophosphamide, and cyclosporin); ⑦ taken 20 mg of glucocorticoids daily for more than 14 days (or 700 mg of prednisolone cumulatively, or equivalent doses of other corticosteroids).

## 2.2 Clinical data and sample collection

Two experienced resident physicians collected clinical data independently. Baseline data from electronic medical records were obtained, including demographic characteristics, past illness history, immunocompromised state, laboratory test, treatment procedure, and prognosis. A group of three senior doctors reviewed the data.

Samples from the infected location were collected from sepsis patients by standard procedures. Blood samples were obtained if the primary infection site was not known or its sample was not available. Each sample of blood, BALF, or urine contained a minimum of 5 ml, and each sample of CSF, sputum or other sterile liquid had at least 3 ml. Pathogen detection was carried out on entire specimens using mNGS and conventional culture methods simultaneously.

## 2.3 Etiological diagnosis

The conventional culture methods include bacterial culture, fungal culture, acid-fast bacterial culture, and blood culture. Blood cultures contain aerobic and anaerobic cultures. We performed conventional culture and mNGS methods according to the patient's medical conditions, and finally selected cases with the same specimens for examination to be included in this study. However, it was not required that all types of cultures be performed on each patient. Microbial culture and automated microbial identification systems were utilized.

Following standard operating procedures, nucleic acid extraction, nucleic acid fragmentation, end repair, end adenylation, primer ligation, and purification were performed from each sample to form a sequencing library using kits from an automated workstation (Amar et al., 2021). Libraries were assessed for quality using kits quantified by real-time PCR and loaded onto an illumina Nextseq CN500 sequencer for 75 cycles of single-end sequencing, producing approximately 20 million reads per library (Miller et al., 2019). Furthermore, peripheral hematopoietic cell specimens from healthy donors were used as negative controls simultaneously, and sterile deionized water was represented as non-template controls concurrently with each batch (Miller et al., 2019).

## 2.4 Bioinformatics analyses

All original sequence reads are eliminated by the bioinformatics analysis software for low-quality and complex reads, duplicate reads, reads shorter than 50bp, contamination reads, and human sequence data (Li and Durbin, 2009; Bolger et al., 2014). In the end, there were approximately 13,000 genomes included in the final database. The remaining sequence data were aligned to a microbial database (including bacteria, viruses, fungi, and parasites) designed by a technology company, which is comparable to the National Center for Biotechnology Information (NCBI) Nucleotide and Genome databases, to determine the species and relative abundance of pathogens. Pathogen lists were chosen based on three references: 1) Manual of Clinical Microbiology, 2) Johns Hopkins ABX Guide, and 3) clinical case reports or academic studies recently appeared in peer-reviewed publications. RPM-r was defined as the reads per million (RPM) of a particular organism in the clinical sample divided by the RPM of the negative control. If the RPM-r was ≥ 5, and the RPM for bacteria and fungi were more than 10 and 2 respectively, there was a reported positive detection for the certain pathogen (Miller et al., 2019; Zinter et al., 2019). A viral detection result was considered positive when three or more non-overlapping areas of the genome were covered.

## 2.5 Definition of clinical effect

In this study, the identification of pathogenic microorganisms was carried out independently by a group of three senior doctors. They made this diagnosis based on clinical manifestations, laboratory tests, mNGS results, imaging studies, and treatment adjustments from patients. Any disputes between clinicians are resolved by further discussion.

A positive effect was defined as the use of mNGS results to support etiology diagnosis and adjust the anti-infective management, including change in antibiotic treatment, antibiotic de-escalation, and continuation of the empirical antibiotic treatment. A negative effect was defined as the use of mNGS results to make a mistaken diagnosis resulting in unnecessary or inadequate antibiotic treatment. A negative mNGS result and an incorrect or insignificant mNGS result were deemed to have no clinical effect.

## 2.6 Statistic analysis

The SPSS 23.0 software was employed to statistically analyze the data. Normal distribution of continuous variables used the Kolmogorov-Smirnov test and measurement data in accord with normal distribution was performed as mean ± standard deviation. An independent sample t-test was utilized between groups. Non-normal distribution measurement data were represented as median (lower quartile, upper quartile), and we applied a nonparametric test for comparison between groups. Comparative analysis was carried out by Pearson's $\chi 2$ test. P values below 0.05 were regarded as significant.

# 3 Results

## 3.1 Characteristics of patients and samples

A total of 308 patients were enrolled in our study, of whom 92 patients were in the immunocompromised group and 216 patients were in the control group. The majority of patients in the immunocompromised group (n=92) had hematological malignancies (39/92, 42.3%), followed by rheumatic diseases (14/92,15.2%), non-rheumatic diseases with long-period glucocorticoid (13/92,14.1%), solid tumors recently treated with chemotherapeutic agents (11/92,12.0%), solid organ transplantation (11/92,12.0%), HIV infection with a CD4+ T-lymphocyte count < 200cells/ul (3/92,3.3%), and hematopoietic stem cell transplantation (HCT) (1/92,1.1%) (Figure 1). Blood made up the majority of our samples (111/308, 36.0%), followed by BALF (68/308, 22.1%), CSF (54/308, 17.5%), and sputum (42/308, 13.6%), as well as ascitic fluid (15/308, 4.9%), pus (6/308, 1.9%), pleural fluid (6/308, 1.9%), tissue (2/308, 0.6%), urine (2/308, 0.6%), hydropericardium (1/308, 0.3%), bone marrow (1/308, 0.3%) (Figure 2A). The majority of infectious sites were confirmed with the respiratory system (174/308,56.5%), followed by the central nervous system (52/308,16.9%), bloodstream (42/308, 13.6%), abdominal (23/308,7.5%), urinary system (8/308,2.6%), skin and soft tissue (8/308,2.6%), pericarditis (1/308,0.3%) (Figure 2B).

In Table 1, the fundamental clinical data about the patients is displayed. The immunocompromised patients were substantially younger than those in the control group, indicating that age could be a risk factor for sepsis in immunocompromised patients. Furthermore, the proportion of patients receiving glucocorticoids and blood products

10.3389/fcimb.2023.1170687

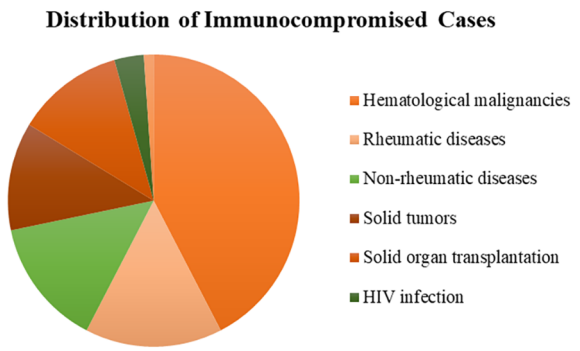


FIGURE 1
The distribution of immunocompromised patients. Most had hematological malignancies (42.3%), followed by rheumatic diseases (15.2%), non-rheumatic diseases (14.1%), solid tumors (12.0%), solid organ transplantation (12.0%), HIV infection (3.3%), and hematopoietic stem cell transplantation (1.1%). HIV, human immunodeficiency virus.

was statistically greater in the immunocompromised group than those in the control group, suggesting that immunocompromised patients with sepsis were more prone to anemia, coagulation disorders, and immunomodulatory therapy. Although there were no statistically significant differences between groups in case fatality rate, there were more patients in the control group with higher SOFA and APACHE II scores, were receiving vasoactive drugs and mechanical ventilation than in the immunocompromised group, implying that these patients were more prone to severe infection, mechanical ventilation, and shock.

## 3.2 Comparison of mNGS and culture's diagnostic performance

In this study, Figure 3 shows the results of mNGS and culture methods. There were significant differences between the culture and mNGS method of all patients (P<0.001), of the immunocompromised group (P<0.001) and control group (P<0.001), in the chi-square test of positive rate. The results demonstrated that the sensitivity (positive number/number) was increased by roughly 62% in all samples (88.0% vs. 26.3%; P < 0.001), 65% in the immunocompromised group (91.3% vs. 26.1%; P < 0.001), and 60% in the control group (86.6% vs. 26.4%; P < 0.001) when mNGS was used in place of culture method. In all samples, there was considerably higher sensitivity in mNGS detection than those in the culture method in the types of blood (P < 0.001), BALF (P < 0.001), CSF (P < 0.001), sputum (P < 0.001) and ascitic fluid (P = 0.008). However, in the subtypes of pus, pleural fluid, tissue, urine, hydro pericardium, and bone marrow, there were no substantial differences in sensitivity between the two techniques owing to the limited sample size. The results of the control group were identical to those of the above (P < 0.001 in blood, P < 0.001 in BALF, P < 0.001 in CSF, P = 0.004 in sputum, P = 0.016 in ascitic fluid). Nevertheless, in the immunocompromised group, mNGS detection demonstrated considerably more sensitivity than the culture method in the types of blood (P < 0.001), and sputum (P =0.004). There was no apparent difference between the sensitivity of the two methods in the types of others due to the limited sample size.

Both mNGS and culture method contribute to 81 of 308 (26.3%) cases of positive results and 37 of 308 (12.0%) cases of negative results in this study. Only mNGS detection was positive in 190 cases (61.7%), whereas only culture result was positive in 0 cases (0%). (Figure 4). The detection consequences were totally matched in 8 of 81 cases (overlap of all pathogens) and completely mismatched in 9 of 81 cases (overlap of no pathogen) in double-positive cases. The other 64 samples were characterized as "partly matched", meaning that at least one but not all overlapped pathogens were founded in polymicrobial results. In 227 of 308 cases, mNGS detected one (n = 87), two (n = 57), or three or more (n = 46) organisms in each sample, while culture failed to identify any organism (Table 2). Conversely, in 37 cases where mNGS was negative, the culture method did not detect organisms. Consequently, compared with the culture method, mNGS detected more bacterial (79 vs 17), fungal (20 versus 8), and viral (12 versus 0) microorganisms (Figure 5).

The pathogen identification outcomes of mNGS and culture are displayed in Figure 6. The most frequently identified bacteria were Klebsiella (n = 63) and Acinetobacter baumannii (n = 63) among the microbes identified using two methods, followed by Pseudomonas

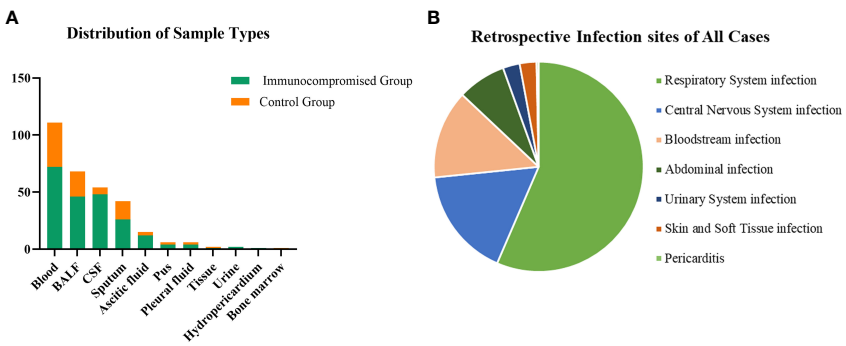


FIGURE 2
The distribution of sample types and infection sites. **(A)** In samples of this study, 36.0% were from the blood which was the most, 22.1% from BALF, 17.5% from CSF, and the others were from sputum (13.6%), ascitic fluid (4.9%), pus (1.9%), pleural fluid (1.9%), tissue (0.6%), urine (0.6%), hydropericardium (0.3%), bone marrow (0.3%). **(B)** Most infection sites were respiratory system infections (174/308,56.5%) and followed by central nervous system infections (52/308,16.9%), bloodstream infections (42/308, 13.6%), abdominal infections (23/308,7.5%), urinary system infections (8/308,2.6%), skin and soft tissue infections (8/308,2.6%), pericarditis (1/308,0.3%). CSF, cerebrospinal fluid; BALF, bronchoalveolar lavage fluid.

TABLE 1 The basic clinical information of patients.

| | Immunocompromised group (n = 92) | Control group (n = 216) | P-value |
|---|---|---|---|
| **Men (%)** | 54 (58.69%) | 141 (65.28%) | 0.273 |
| **Age (year)** | 55 (48-66) | 62.5 (49-71) | 0.010 |
| Clinical indicators | | | |
| SOFA score | 5.00 (3.00-8.75) | 6.00 (3.00-10.00) | 0.226 |
| APACHII score | 14.00 (10.00-22.00) | 16.00 (11.00-21.00) | 0.497 |
| Length of stay (day) | 28.00 (19.00-39.00) | 24.00 (14.00-37.00) | 0.058 |
| Admission to ICU (%) | 35 (38.04%) | 117 (54.17%) | 0.010 |
| Length of ICU stay (day) | 13.00 (7.00-23.00) | 17.00 (11.50-28.00) | 0.083 |
| Treatments | | | |
| Mechanical ventilation (%) | 29 (31.52%) | 105 (48.61%) | 0.006 |
| Duration of mechanical ventilation (day) | 11 (4.5-20) | 14 (8-22) | 0.132 |
| Renal replacement therapy (%) | 15 (16.30%) | 40 (18.52%) | 0.642 |
| Duration of renal replacement therapy (hour) | 114.50 (39.50-262.75) | 70.38 (41.25-167.75) | 0.427 |
| Vasoactive medications (%) | 36 (39.13%) | 108 (50.00%) | 0.080 |
| Glucocorticoids (%) | 82 (89.13%) | 127 (58.80%) | 0.000 |
| Blood products (%) | 79 (85.87%) | 155 (71.76%) | 0.008 |
| **Case fatality rate (%)** | 28 (30.43%) | 62 (28.70%) | 0.760 |

(n = 47), Enterococcus (n = 36), Escherichia coli (n = 32), Staphylococcus (n = 29), and Mycobacterium tuberculosis (n = 17). Additionally, there were Candida (n = 63) detected most frequently, followed by Aspergillus (n = 45) and Pneumocystis jirovecii (n = 19) in fungal organisms detected among the microbes.

There were 89 and 3 organisms detected respectively only by mNGS or culture. Microbes that were thought to induce sepsis and detected only by mNGS included Rickettsiae, Legionella, Nocardia, Mycobacterium tuberculosis, Mucoraceae, Pneumocystis jirovecii, and others. Furthermore, mNGS also detected viruses including HHV, EBV, and CMV, that were not identified by culture. There were only 3 organisms identified only by culture: Staphylococcus warneri, Candida lusitaniae, and Pichia ohmeri which were considered pathogens in this study. The followings are some plausible explanations for the missing species: either there was an extremely poor microbial loading of the specimen that was under the detection limit of mNGS or the microorganisms were excluded by the software as being part of the normal flora or environmental contaminants. There were substantial differences in the mNGS results between immunocompromised and control groups for Pneumocystis jirovecii($P < 0.001$), Mucoraceae ($P = 0.014$), Klebsiella ($P = 0.045$).

## 3.3 Comparison of laboratory tests in immunocompromised and control group

In this study, we compared the laboratory results between the immunocompromised group and control group on the diagnosis day of sepsis using complete blood count, hepatorenal function, coagulation function, CRP, and PCT tests. There were statistically significant differences in hemocyte, hepatic and renal function, coagulation function, and procalcitonin between the immunocompromised group and control group according to the results (Table 3).

## 3.4 Clinical effects of mNGS result on diagnosis and management

When mNGS results were examined for impacts on patient treatment, they were found to have a positive or no effect in 235 (76.3%) and 66 (21.4%) patients separately, while a negative effect was reported in 7 patients (2.3%). Positive mNGS results made for a definite diagnosis in the 235 positive effect samples. However, mNGS failed to identify any extra pathogens in 37 patients, and its consequences in 29 patients were considered contaminated or insubstantial, in the patients without effects (Table 4).

In the light of treatment, mNGS result caused a directly shift in management (185 of 235 positive effect patients) or a definite diagnosis that allowed the continued empirical treatment (50 of 235 positive effect patients). 61 of 185 patients, where the course of treatment was altered due to the mNGS results, issued in a de-escalation of antibiotics.

Notably, there were 7 cases of mNGS results with negative impact. In 5 of these cases, there were patients infected with RNA viruses (eg, SFTSV, Encephalitis B virus, hantaan virus), while mNGS only performed DNA detection without RNA detection in this study. The case detected Streptococcus suis covered by antibiotics before, which of the clinical impact was effectless but

10.3389/fcimb.2023.1170687

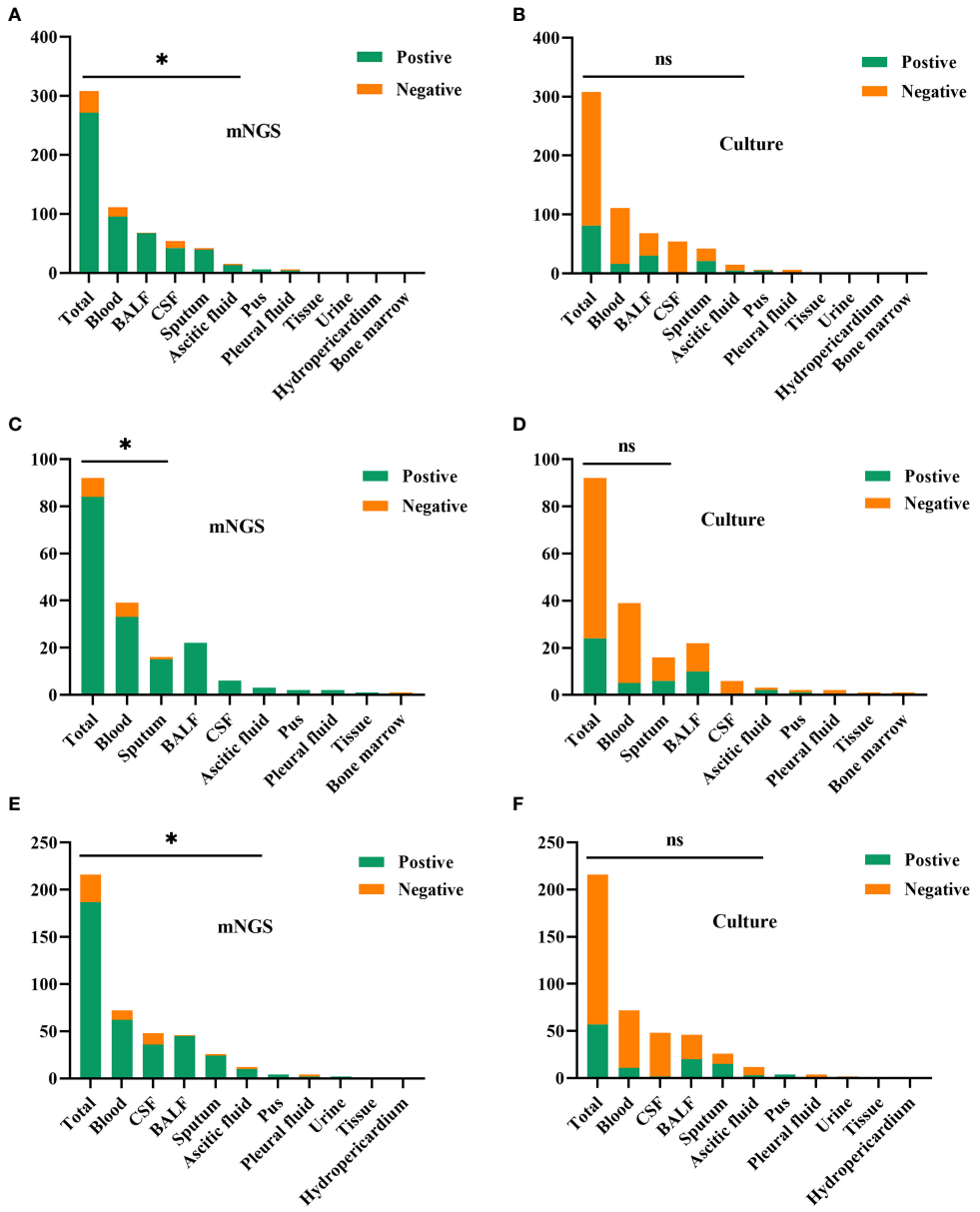


FIGURE 3
The comparison of positive rates between mNGS and culture method in sample types. **(A, B)** In all samples, there was considerably higher sensitivity in mNGS than those in the culture method in the types of blood ($P < 0.001$), BALF ($P < 0.001$), CSF ($P < 0.001$), sputum ($P < 0.001$) and ascitic fluid ($P = 0.008$). **(C, D)** In the immunocompromised group, mNGS results demonstrated more sensitivity than the culture method in the types of blood ($P < 0.001$), and sputum ($P = 0.004$). **(E, F)** In the control group, there was more sensitivity in mNGS than those in the culture method in the types of blood ($P < 0.001$), BALF ($P < 0.001$), CSF ($P < 0.001$), sputum ($P = 0.004$) and ascitic fluid ($P = 0.016$). mNGS, metagenomic next-generation sequencing; BALF, bronchoalveolar lavage fluid; CSF, cerebrospinal fluid. * $p < 0.05$; ns, no significant difference.

was improved after empirical antibiotic escalation. In addition, there was a case clinically diagnosed as tuberculous pleurisy, which reported Bacteroides, leading to not replacing with anti-tuberculosis drugs in time.

## 4 Discussion

Sepsis in immunocompromised patients has increased with the rise in the immunocompromised population, and the resultant septic shock and multiple organ dysfunction syndrome become the major reasons for mortality (Ramirez et al., 2020). Given the influence of immune function and underlying diseases, there are frequently conditional pathogens, uncommon pathogens, and mixed infections where these infections are characteristic of untypical clinical manifestations, rapid clinical progression, and severe death (Linden, 2009). Furthermore, the use of various anti-infective drugs results in a poor incidence of infection detection using conventional methods during the period of their diseases. Consequently, it is a clinical challenge to develop a timely and precise pathogen diagnosis. MNGS has been widely used to identify new pathogens and diagnose infections in humans since it analyzes the whole

10.3389/fcimb.2023.1170687

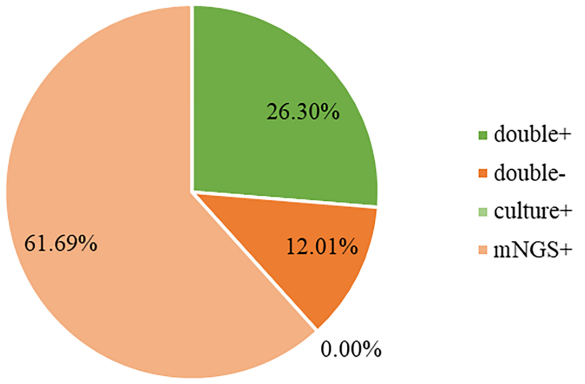


FIGURE 4
Concordance between mNGS and culture for pathogen detection. The pie chart demonstrated the positivity distribution of mNGS and culture for all samples. 61.69% were positive by mNGS, 0% by culture, 26.30% by both, and 12.01% were both negative. mNGS, metagenomic next-generation sequencing.

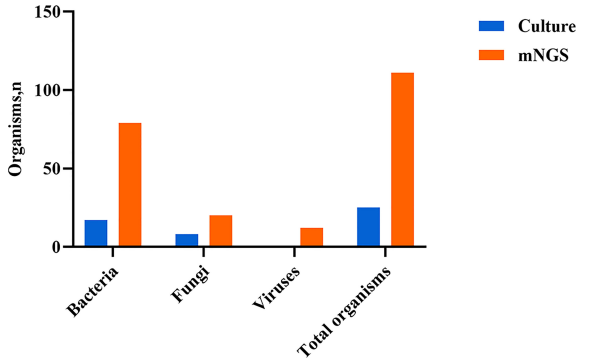


FIGURE 5
Type of organisms detected by mNGS compared with culture method. mNGS, metagenomic next-generation sequencing.

microbiome in patient samples (Lefterova et al., 2015). Thus, we investigated the utilization and differences between mNGS and the conventional culture method in adult sepsis, particularly in immunocompromised patients. In our study, samples from 308 patients with sepsis were collected and submitted to mNGS and conventional culture methods in a pairwise manner, where the samples included blood, BALF, CSF, sputum, pus, pleural fluid, tissue, urine, or bone marrow. Then, we thoroughly compared the clinical characteristics and consequences of the conventional culture method with mNGS, especially for immunocompromised patients.

The result showed that there were substantial differences in ages, receiving mechanical ventilation, glucocorticoids, and blood products, as well as admission to ICU, between the two groups. It was also suggested that the sensitivity of mNGS was greater than that of the conventional culture method. Additionally, a group of researchists observed that mNGS identified potential pathogens more quickly and sensitively than pathology and culture (Li et al., 2018). According to Miao's study (Miao et al., 2018), it was observed that mNGS exhibited a higher sensitivity for the infectious disease diagnosis than the conventional culture method (50.7% vs. 35.2%) and that it had significant advantages for the identification of MTB, Nocardia, anaerobic bacteria, virus, and fungi in particular. The above findings were compatible with our study, which revealed that the sensitivity of mNGS was considerably greater than that of the culture method (88.0% vs 26.3%). The extreme sensitivity of mNGS may be attributed to a lengthy plasma survival time of pathogen DNA and the fact that antibiotic treatment has a minor impact on mNGS results, but a significant impact on conventional culture. In this research, the sensitivity of mNGS in samples of blood ($P < 0.001$), BALF ($P < 0.001$), CSF ($P < 0.001$), sputum ($P < 0.001$), and ascitic fluid ($P = 0.008$) was substantially higher than that of the culture method.

Our study emphasizes important situations in which mNGS enabled species-level pathogen identification, acting as the sole diagnostic tool or complementing standard results. One such field dealt with usual pathogens that cause infections but were not identified by culture method. This study also identified Nocardia species, Tropheryma whipplei, and anaerobic bacteria, which had poor yields by conventional culture but were detectable by mNGS.

The capability of mNGS to identify viruses that are currently not routinely examined in patients with sepsis in China is another advantage, where mNGS produced definitive diagnoses and improved patient cares in these cases. Most notably, the capacity to identify atypical bacteria, where microorganisms are undetectable in conventional culture methods and routine molecular testing is limited, is one of the critical obstacles that mNGS overcame for conventional culture methods. In this study, Rickettsiae, Legionella, and Chlamydia Psittaci were among the atypical bacteria detected through mNGS that were undetected through conventional culture methods. Legionella is a slow-growing bacterium that can cause extrapulmonary symptoms and severe community-acquired pneumonia, while also being useless to β-lactam antibiotic therapy, requiring a prompt diagnosis (Bradley and Bryan, 2019). Previously, the diagnosis has relied on a time-consuming culture necessitating a specialized medium and urine antigen testing that can barely detect a serogroup since molecular methods are neither

TABLE 2 mNGS and culture results for each specimen: Comparison of microorganisms detected.

| | | Culture (n=25 microorganisms) | | | |
|---|---|---|---|---|---|
| | | Negative | 1 | 2 | 3+ |
| mNGS (n=111 microorganisms) | Negative | 37 | 0 | 0 | 0 |
| | 1 | 87 | 11 | 0 | 0 |
| | 2 | 57 | 14 | 0 | 0 |
| | 3+ | 46 | 49 | 7 | 0 |

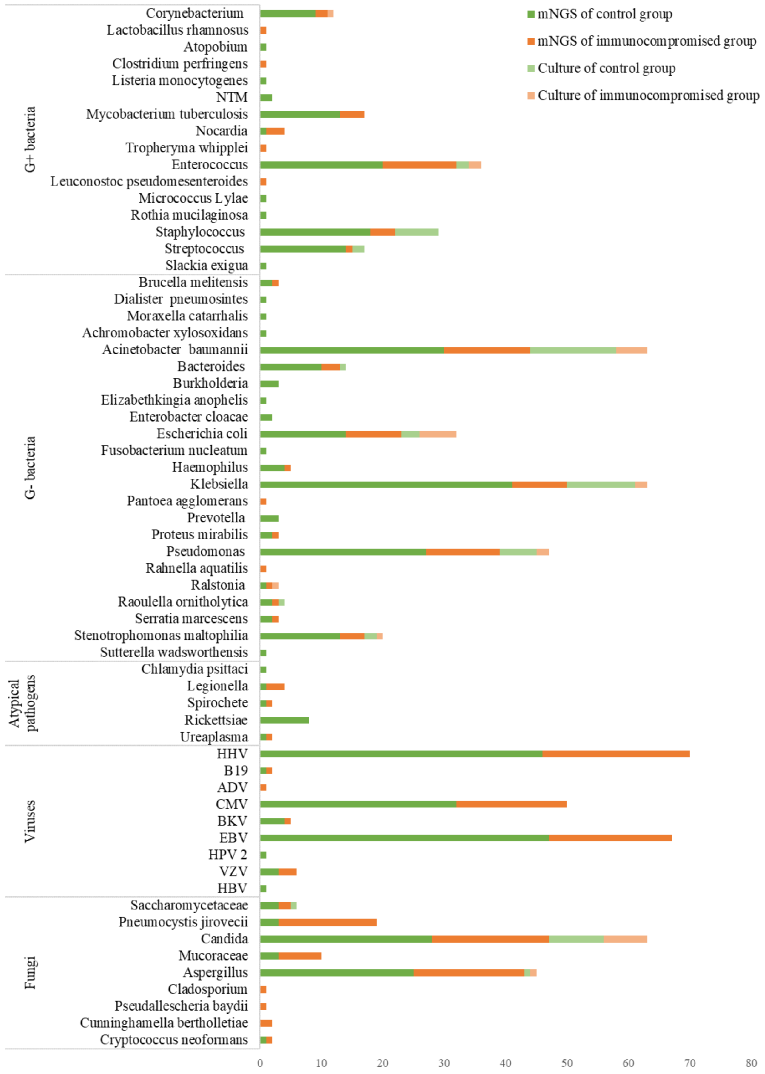


FIGURE 6
The distribution of detected pathogens of all patients by mNGS and culture method. The mNGS results were shown in dark green (control group) and orange (immunocompromised group), and the results of the culture method were shown in light green (control group) and orange (immunocompromised group). mNGS, metagenomic next-generation sequencing.

generally accessible nor standardized (Bradley and Bryan, 2019). Currently, identification and molecular epidemiology investigations of Legionella have both shown promise when using direct sequencing from samples (Coscollá and González-Candelas, 2009). Psittacosis is brought on by the zoonotic pathogen Chlamydia psittaci, which is spread from birds to humans (Knittler et al., 2014). Although Chlamydia psittaci is a challenging organism to be detected, mNGS has been utilized to diagnose a case of sepsis and multi-organ failure caused by this organism previously (Zhang et al., 2020), emphasizing the importance of mNGS in this process. It is this fact that mNGS also identified Mycobacterium tuberculosis, which was undetectable by conventional culture methods in 17 cases, resulting in a clear diagnosis, further emphasizing the power of mNGS for species-level detection.

In addition, it is difficult that fungal infections to be identified by the conventional culture method. When compared with histology, mNGS has been reported to exhibit a higher specificity for detecting fungal pathogens in specimens and allows reliable species-level identification (Guarner and Brandt, 2011). It is sluggish and laborious to cultivate fungi, and a pure isolate with sporulation and distinguishing characteristics is required for their identification by macroscopic and microscopic morphology (Larkin et al., 2020). When the clinical microbiological method was negative, other research indicated the identification value of mNGS for Coccidioides and Aspergillus (Gu et al., 2021). In this research, mNGS (which identified Aspergillus in 36 patients) offered an excellent complement to culture (which identified Aspergillus in 2 patients), resulting in an efficient anti-fungal therapy. Except for molds with low recovery rates, other fungi, such as Pneumocystis Jirovecii and Mucoraceae, cannot be cultivated. Opportunistic pathogen Pneumocystis Jirovecii is a significant contributor to sepsis and mortality in immunocompromised people, which the main methods used for diagnosis are an insensitive fluorescent antibody test and, an unstandardized and widely unavailable

TABLE 3 The lab information of patients.

| | Immunocompromised group (n = 92) | Control group (n = 216) | P-value |
|---|---|---|---|
| RBC ($10^{12}$/L) | 2.70 ± 0.87 | 3.54 ± 0.89 | 0.000 |
| Hemoglobin (g/L) | 82.99 ± 25.51 | 107.48 ± 26.56 | 0.000 |
| WBC ($10^9$/L) | 5.90 (1.37-10.01) | 9.46 (6.06-14.27) | 0.000 |
| Neutrophile ($10^{12}$/L) | 3.72 (0.54-7.94) | 8.09 (4.61-12.49) | 0.000 |
| Lymphocyte ($10^{12}$/L) | 0.49 (0.28-1.05) | 0.78 (0.45-1.21) | 0.001 |
| NLR | 4.93 (0.67-15.17) | 10.87 (5.36-19.64) | 0.000 |
| Eosinophil ($10^9$/L) | 0.00 (0.00-0.03) | 0.01 (0.00-0.08) | 0.003 |
| PLT ($10^9$/L) | 74.00 (18.75-140.50) | 143.50 (84.75-210.50) | 0.000 |
| ALT (U/L) | 26.50 (17.00-74.00) | 38.00 (21.25-90.50) | 0.023 |
| AST (U/L) | 29.00 (19.25-53.50) | 40.00 (24.25-85.00) | 0.000 |
| Tbil (umol/L) | 12.95 (10.03-21.70) | 15.60 (10.18-29.20) | 0.208 |
| Albumin (g/L) | 31.85 (28.15-35.10) | 32.70 (28.10-37.83) | 0.213 |
| BUN (mmol/L) | 5.93 (4.15-12.53) | 7.89 (4.96-15.88) | 0.029 |
| Creatinine (umol/L) | 61.45 (43.78-91.70) | 74.00 (53.20-146.58) | 0.001 |
| CRP (mg/L) | 99.88 (45.44-156.49) | 85.95 (32.08-158.45) | 0.415 |
| PCT (ug/L) | 0.49 (0.12-2.00) | 0.84 (0.21-5.18) | 0.022 |
| Fibrinogen (mg/dl) | 3.81 (2.53-5.23) | 4.31 (3.07-5.86) | 0.035 |
| PT (S) | 14.20 (13.30-15.78) | 14.90 (13.83-16.30) | 0.010 |
| APTT (S) | 39.20 (33.35-45.85) | 42.70 (36.60-48.00) | 0.014 |
| D- dimer (ug/L) | 2.04 (0.96-5.11) | 2.82 (1.41-6.59) | 0.069 |
| PTA (%) | 82.10 (66.30-92.00) | 77.50 (65.25-89.00) | 0.137 |

Pneumocystis Jirovecii PCR (Sokulska et al., 2015). In our study, mNGS identified an extra 19 cases of Pneumocystis Jirovecii that conventional methods had missed (3 patients in the control group and 16 patients in the immunocompromised group). Pneumocystis jirovecii was also involved in 17 of the positive effect patients where mNGS detected multiple pathogens demanding different antibiotics, demonstrating the usefulness of mNGS in directing proper treatment coverage. Mucoraceae is also an opportunistic pathogen that disseminated infections caused by often involving the gastrointestinal tract, skin, lungs, orbit, paranasal sinuses, and central nervous system with lethality in immunocompromised patients. The diagnosis is based mainly on histopathology and a Mucoraceae PCR that has become less regularly used in clinical settings (Vallabhaneni and Mody, 2015), which can result in missed diagnoses. In our study, 10 patients of Mucoraceae (3 patients in the control group and 7 patients in the immunocompromised group) were detected through mNGS that were undetected through conventional culture methods, further emphasizing the role of mNGS in the diagnosis of this fungi.

Overall, in 235 (76.3%) patients, the mNGS results resulted in a positive effect, including the detection of more pathogens, a clear diagnosis, and assurance for antibiotic de-escalation therapy when a

TABLE 4 Clinical effects of mNGS results on diagnosis and management.

| Clinical effect | Role of mNGS result | Treatment changes owing to mNGS |
|---|---|---|
| Positive effect (n=235; 76.3%) | Contributed to definitive diagnosis (n=235; 76.3%) | Treatment adjusted without de-escalation (n =124; 40.3%) |
| | | Antibiotic de-escalated (n = 61; 19.8%) |
| | | Empirical treatment continued (n=50; 16.2%) |
| Negative effect (n =7; 2.3%) | False-positive result led to incorrect diagnosis (n=7; 2.3%) | Incorrect antibiotic treatment |
| No effect (n=66; 21.4%) | No additional pathogen detected (n=37; 12.0%) | No changes |
| | Results deemed false or insignificant (n=29; 9.4%) | |

patient's condition improves. There were only 7 cases of the negative effect, notably false-positive mNGS results that caused a misdiagnosis and inappropriate treatment. In those cases, there were five patients infected with RNA viruses which mNGS did not detect, suggesting that mNGS RNA testing should be considered if the patient was suspected of RNA virus infection. Noticeably, one case of Mycobacterium tuberculosis was missed by mNGS. Further investigation revealed that it was most likely that the mNGS DNA extraction procedure utilized in this study was insufficient since it did not include a committed step, which may have helped more thoroughly break down the mycobacteria's cell wall. This serves as a reminder that regardless of downstream molecular methods used, specimen preprocessing optimization is crucial for organism recovery. Our research suggests the utilization of both conventional culture methods and mNGS to increase organism recovery and diagnostic precision. In one case, Streptococcus suis was identified through mNGS but the culture result came back negative. Antibiotics for Streptococcus suis were administered to the patient without success and eventually, the patient was improved after empirical antibiotic escalation. Furthermore, regardless of the rigorous algorithms incorporated into the bioinformatic software that ruled out potential contamination, mNGS consequences in 29 patients were considered as normal flora or contamination.

Some studies showed that it can be difficult to distinguish between colonization and human or environmental contamination because mNGS detects unbiased and broad-spectrum microbial DNA (de Goffau et al., 2018; Oechslin et al., 2018). Colonization and background contamination are specifically significant for samples with poorer pathogenic bacterial loads (Marsh et al., 2018). When employing the mNGS method solely, there is currently an unstandardized methodology for separating true etiological pathogens, colonization, and contamination. In order to avoid these problems, a rigorous bioinformatics threshold would be founded to rule out lab contaminants and shorten within-run spillover from highly positive specimens, as well as negative control may be incorporated at every stage of the specimen preparation and sequencing procedure (Salter et al., 2014). Additionally, clinical presentation and concurrent laboratory results including bacterial and fungal cultures should be taken into consideration when evaluating mNGS results. However, problems occur when mNGS results disagree with those of the gold-standard method. In this research, doctors utilized clinical judgments to determine whether to rely on the mNGS results, the conventional culture method results, or both. Even though unavoidable due to the continuously evolving techniques, the standardization of mNGS methods and analyses, and recognition of the main limits of mNGS, can start to address these difficulties. When numerous organisms are identified, transient microbial DNA, which may represent either dead or live microorganisms in the sample source area, could potentially complicate mNGS result and demand interpretations with great caution (Hogan et al., 2021). Even though some susceptibility information may be obtained by sequencing, the culture method is required for extensive susceptibility tests since pathogens exhibit varied resistance patterns that call for susceptibility testing (Metlay et al., 2019; Yang et al., 2019).

It is noteworthy that we discovered that mNGS had no impact on 66 (21.4%) patients, mostly because the majority of these patients had no additional pathogens detected by mNGS. It could partially account for the major drawback of this research, which was that mNGS only sequenced DNA, not RNA and that the samples were not entirely aligned with the infection sites. In this study, the second drawback was that the software utilized assumed that any microorganisms whose sequence reads fell below a predetermined threshold were contaminated and eliminated. It is the unsatisfied fact that real infections can develop owing to the complexity of infections and the uncertainty of function of normal flora species in some circumstances, even at low abundance (sequence reads). Therefore, the clinical situation must be taken into account while interpreting the results. It is crucial to note that a frequent issue with the mNGS method is background microbial contamination which might be filtered out partially through negative controls, so it calls for clinicians familiar with usual background microorganisms and better result explanations with clinical practices (Fan et al., 2018).

We systematically investigated sample type, sensitivity, and pathogen type between mNGS and conventional culture in this study. Based on this, we also analyzed the differences in sepsis between immunocompromised and control groups. The greatest deficiency of our study was its limited sample size, which led to a variety of results showing certain trends without attaining statistical significance regrettably. As a result, more patients need to be involved in future studies. The study had the additional drawback of not being randomized controlled. This study has certain drawbacks as a retrospective study, such as insufficient data and data accumulations beyond the researcher's control. In addition, there are also numerous drawbacks in this study including limited generalizability resulting from a single-center study, absence of a gold-standard diagnostic comparator, and absence of detailed information on antibiotic usage.

## 5 Conclusion

In conclusion, mNGS showed better sensitivity than conventional culture, particularly in blood, BALF, CSF, and sputum samples, and there was a tendency for greater sensitivity in the detection of Pneumocystis jirovecii, Mucoraceae and Klebsiella in the immunocompromised group. In addition, mNGS offers a considerable impact in enhancing sepsis diagnosis and contributing to better patient treatment. As a consequence of our findings above, as well as additional advantages of mNGS such as rapid results, and less impact of antibiotic exposures, we believe that mNGS should be employed more frequently in the future for early pathogen diagnosis in sepsis patients, especially immunocompromised patients. Nonetheless, it will be challenging for clinicians to interpret mNGS results in guiding clinical therapy of infectious disorders.

## Data availability statement

The original contributions presented in the study are included in the article/supplementary material. Further inquiries can be directed to the corresponding author.

## Ethics statement

The studies involving human participants were reviewed and approved by The Medical Ethics Committee of the First Affiliated Hospital of Anhui Medical University. The patients/participants provided their written informed consent to participate in this study. Written informed consent was obtained from the individual(s) for the publication of any potentially identifiable images or data included in this article.

## Author contributions

HZ contributed to conceptualizing and designing this investigation. XL, SL, DZ, and MH collected and arranged the data. XL and HZ analyzed the data. XL wrote this article. All authors contributed to the article and approved the submitted version.

## Conflict of interest

The authors declare that the research was conducted in the absence of any commercial or financial relationships that could be construed as a potential conflict of interest.

## Publisher's note

All claims expressed in this article are solely those of the authors and do not necessarily represent those of their affiliated organizations, or those of the publisher, the editors and the reviewers. Any product that may be evaluated in this article, or claim that may be made by its manufacturer, is not guaranteed or endorsed by the publisher.

## References

Amar, Y., Lagkouvardos, I., Silva, R. L., Ishola, O. A., Foesel, B. U., Kublik, S., et al. (2021). Pre-digest of unprotected DNA by benzonase improves the representation of living skin bacteria and efficiently depletes host DNA. *Microbiome* 9 (1), 123. doi: 10.1186/s40168-021-01067-0

Bolger, A. M., Lohse, M., and Usadel, B. (2014). Trimmomatic: A flexible trimmer for illumina sequence data. *Bioinf. (Oxford England).* 30 (15), 2114–2120. doi: 10.1093/bioinformatics/btu170

Bradley, B. T., and Bryan, A. (2019). Emerging respiratory infections: The infectious disease pathology of SARS, MERS, pandemic influenza, and legionella. *Semin. Diagn. Pathol.* 36 (3), 152–159. doi: 10.1053/j.semdp.2019.04.006

Chen, Y., Feng, W., Ye, K., Guo, L., Xia, H., Guan, Y., et al. (2021). Application of metagenomic next-generation sequencing in the diagnosis of pulmonary infectious pathogens from bronchoalveolar lavage samples. *Front. Cell. Infect. Microbiol.* 11. doi: 10.3389/fcimb.2021.541092

Chiu, C. Y., and Miller, S. A. (2019). Clinical metagenomics. nature reviews. *Genetics* 20 (6), 341–355. doi: 10.1038/s41576-019-0113-7

Coscollá, M., and González-Candelas, F. (2009). Direct sequencing of legionella pneumophila from respiratory samples for sequence-based typing analysis. *J. Clin. Microbiol.* 47 (9), 2901–2905. doi: 10.1128/JCM.00268-09

de Goffau, M. C., Lager, S., Salter, S. J., Wagner, J., Kronbichler, A., Charnock-Jones, D. S., et al. (2018). Recognizing the reagent microbiome. *Nat. Microbiol.* 3 (8), 851–853. doi: 10.1038/s41564-018-0202-y

Ewig, S., Torres, A., Angeles Marcos, M., Angrill, J., Rañó, A., de Roux, A., et al. (2002). Factors associated with unknown aetiology in patients with community-acquired pneumonia. *Eur. Respir. J.* 20 (5), 1254–1262. doi: 10.1183/09031936.02.01942001

Fan, S., Ren, H., Wei, Y., Mao, C., Ma, Z., Zhang, L., et al. (2018). Next-generation sequencing of the cerebrospinal fluid in the diagnosis of neurobrucellosis. *Int. J. Infect. Dis.* 67, 20–24. doi: 10.1016/j.ijid.2017.11.028

Gu, W., Deng, X., Lee, M., Sucu, Y. D., Arevalo, S., Stryke, D., et al. (2021). Rapid pathogen detection by metagenomic next-generation sequencing of infected body fluids. *Nat. Med.* 27 (1), 115–124. doi: 10.1038/s41591-020-1105-z

Guarner, J., and Brandt, M. E. (2011). Histopathologic diagnosis of fungal infections in the 21st century. *Clin. Microbiol. Rev.* 24 (2), 247–280. doi: 10.1128/CMR.00053-10

Hill, A. T. (2020). Management of community-acquired pneumonia in immunocompromised adults: A consensus statement regarding initial strategies. *Chest* 158 (5), 1802–1803. doi: 10.1016/j.chest.2020.08.003

Hogan, C. A., Yang, S., Garner, O. B., Green, D. A., Gomez, C. A., Dien Bard, J., et al. (2021). Clinical impact of metagenomic next-generation sequencing of plasma cell-free DNA for the diagnosis of infectious diseases: A multicenter retrospective cohort study. *Clin. Infect. Dis.* 72 (2), 239–245. doi: 10.1093/cid/ciaa035

Knittler, M. R., Berndt, A., Böcker, S., Dutow, P., Hänel, F., Heuer, D., et al. (2014). Chlamydia psittaci: New insights into genomic diversity, clinical pathology, host-pathogen interaction and anti-bacterial immunity. *Int. J. Med. Microbiol.* 304 (7), 877–893. doi: 10.1016/j.ijmm.2014.06.010

Larkin, P. M. K., Multani, A., Beaird, O. E., Dayo, A. J., Fishbein, G. A., and Yang, S. (2020). A collaborative tale of diagnosing and treating chronic pulmonary aspergillosis, from the perspectives of clinical microbiologists, surgical pathologists, and infectious disease clinicians. *J. Fungi (Basel Switzerland).* 6 (3), 106. doi: 10.3390/jof6030106

Lefterova, M. I., Suarez, C. J., Banaei, N., and Pinsky, B. A. (2015). Next-generation sequencing for infectious disease diagnosis and management: A report of the association for molecular pathology. *J. Mol. Diagn.* 17 (6), 623–634. doi: 10.1016/j.jmoldx.2015.07.004

Li, H., and Durbin, R. (2009). Fast and accurate short read alignment with burrows-wheeler transform. *Bioinf. (Oxford England).* 25 (14), 1754–1760. doi: 10.1093/bioinformatics/btp324

Li, H., Gao, H., Meng, H., Wang, Q., Li, S., Chen, H., et al. (2018). Detection of pulmonary infectious pathogens from lung biopsy tissues by metagenomic next-generation sequencing. *Front. Cell. Infect. Microbiol.* 8. doi: 10.3389/fcimb.2018.00205

Linden, P. K. (2009). Approach to the immunocompromised host with infection in the intensive care unit. *Infect. Dis. Clinics North America.* 23 (3), 535–556. doi: 10.1016/j.idc.2009.04.014

Marsh, R. L., Nelson, M. T., Pope, C. E., Leach, A. J., Hoffman, L. R., Chang, A. B., et al. (2018). How low can we go? the implications of low bacterial load in respiratory microbiota studies. *Pneumonia (Nathan Qld.).* 10, 7. doi: 10.1186/s41479-018-0051-8

McCreery, R. J., Florescu, D. F., and Kalil, A. C. (2020). Sepsis in immunocompromised patients without human immunodeficiency virus. *J. Infect. Dis.* 222 (2), 156–165. doi: 10.1093/infdis/jiaa320

Metlay, J. P., Waterer, G. W., Long, A. C., Anzueto, A., Brozek, J., Crothers, K., et al. (2019). Diagnosis and treatment of adults with community-acquired pneumonia. an official clinical practice guideline of the American thoracic society and infectious diseases society of America. *Am. J. Respir. Crit. Care Med.* 200 (7), 45–67. doi: 10.1164/rccm.201908-1581ST

Miao, Q., Ma, Y., Wang, Q., Pan, J., Zhang, Y., Jin, W., et al. (2018). Microbiological diagnostic performance of metagenomic next-generation sequencing when applied to clinical practice. *Clin. Infect. Dis.* 67 (2), 231–240. doi: 10.1093/cid/ciy693

Miller, S., Naccache, S. N., Samayoa, E., Messacar, K., Arevalo, S., Federman, S., et al. (2019). Laboratory validation of a clinical metagenomic sequencing assay for pathogen detection in cerebrospinal fluid. *Genome Res.* 29 (5), 831–842. doi: 10.1101/gr.238170.118

Oechslin, C. P., Lenz, N., Liechti, N., Ryter, S., Agyeman, P., Bruggmann, R., et al. (2018). Limited correlation of shotgun metagenomics following host depletion and routine diagnostics for viruses and bacteria in low concentrated surrogate and clinical samples. *Front. Cell. infect. Microbiol.* 8. doi: 10.3389/fcimb.2018.00375

Ramirez, J. A., Musher, D. M., Evans, S. E., Dela Cruz, C., Crothers, K. A., Hage, C. A., et al. (2020). Treatment of community-acquired pneumonia in immunocompromised adults: A consensus statement regarding initial strategies. *Chest* 158 (5), 1896–1911. doi: 10.1016/j.chest.2020.05.598

Salter, S. J., Cox, M. J., Turek, E. M., Calus, S. T., Cookson, W. O., Moffatt, M. F., et al. (2014). Reagent and laboratory contamination can critically impact sequence-based microbiome analyses. *BMC Biol.* 12, 87. doi: 10.1186/s12915-014-0087-z

Schlaberg, R., Chiu, C. Y., Miller, S., Procop, G. W., Weinstock, G.Professional Practice Committee and Committee on Laboratory Practices of the American Society for Microbiology, et al. (2017). Validation of metagenomic next-generation sequencing tests for universal pathogen detection. *Arch. Pathol. Lab. Med.* 141 (6), 776–786. doi: 10.5858/arpa.2016-0539-RA

Singer, M., Deutschman, C. S., Seymour, C. W., Shankar-Hari, M., Annane, D., Bauer, M., et al. (2016). The third international consensus definitions for sepsis and septic shock (Sepsis-3). *JAMA* 315 (8), 801–810. doi: 10.1001/jama.2016.0287

Sokulska, M., Kicia, M., Wesołowska, M., and Hendrich, A. B. (2015). Pneumocystis jirovecii–from a commensal to pathogen: Clinical and diagnostic review. *Parasitol. Res.* 114 (10), 3577–3585. doi: 10.1007/s00436-015-4678-6

Vallabhaneni, S., and Mody, R. K. (2015). Gastrointestinal mucormycosis in neonates: A review. *Curr. Fungal Infect. Rep.* 9 (4), 269–274. doi: 10.1007/s12281-015-0239-9

van Gageldonk-Lafeber, A. B., Heijnen, M. L., Bartelds, A. I., Peters, M. F., van der Plas, S. M., and Wilbrink, B. (2005). A case-control study of acute respiratory tract infection in general practice patients in the Netherlands. *Clin. Infect. Dis.* 41 (4), 490–497. doi: 10.1086/431982

Wilson, M. R., Sample, H. A., Zorn, K. C., Arevalo, S., Yu, G., Neuhaus, J., et al. (2019). Clinical metagenomic sequencing for diagnosis of meningitis and encephalitis. *New Engl. J. Med.* 380 (24), 2327–2340. doi: 10.1056/NEJMoa1803396

Yang, L., Haidar, G., Zia, H., Nettles, R., Qin, S., Wang, X., et al. (2019). Metagenomic identification of severe pneumonia pathogens in mechanically-ventilated patients: a feasibility and clinical validity study. *Respir. Res.* 20 (1), 265. doi: 10.1186/s12931-019-1218-4

Zhang, H., Zhan, D., Chen, D., Huang, W., Yu, M., Li, Q., et al. (2020). Next-generation sequencing diagnosis of severe pneumonia from fulminant psittacosis with multiple organ failure: a case report and literature review. *Ann. Trans. Med.* 8 (6), 401. doi: 10.21037/atm.2020.03.17

Zhou, K., Lokate, M., Deurenberg, R. H., Tepper, M., Arends, J. P., Raangs, E. G., et al. (2016). Use of whole-genome sequencing to trace, control and characterize the regional expansion of extended-spectrum β-lactamase producing ST15 klebsiella pneumoniae. *Sci. Rep.* 6, 20840. doi: 10.1038/srep20840

Zinter, M. S., Dvorak, C. C., Mayday, M. Y., Iwanaga, K., Ly, N. P., McGarry, M. E., et al. (2019). Pulmonary metagenomic sequencing suggests missed infections in immunocompromised children. *Clin. Infect. Dis.* 68 (11), 1847–1855. doi: 10.1093/cid/ciy802

frontiers | Frontiers in Cellular and Infection Microbiology

TYPE Original Research
PUBLISHED 02 May 2023
DOI 10.3389/fcimb.2023.1149741



OPEN ACCESS

EDITED BY
Antonella Mencacci,
University of Perugia, Italy

REVIEWED BY
Renan M. Mauch,
Lund University, Sweden
Damira Kanayeva,
Nazarbayev University, Kazakhstan

*CORRESPONDENCE
Yifei Li
liyfwcsh@scu.edu.cn
Yimin Hua
nathan_hua@163.com

RECEIVED 22 January 2023
ACCEPTED 18 April 2023
PUBLISHED 02 May 2023

CITATION
Gong X, He Y, Zhou K, Hua Y and Li Y (2023) Efficacy of Xpert in tuberculosis diagnosis based on various specimens: a systematic review and meta-analysis. *Front. Cell. Infect. Microbiol.* 13:1149741. doi: 10.3389/fcimb.2023.1149741



# Efficacy of Xpert in tuberculosis diagnosis based on various specimens: a systematic review and meta-analysis

Xue Gong, Yunru He, Kaiyu Zhou, Yimin Hua* and Yifei Li*

Department of Pediatrics, Ministry of Education Key Laboratory of Women and Children's Diseases and Birth Defects, West China Second University Hospital, Sichuan University, Chengdu, Sichuan, China

**Objective:** The GeneXpert MTB/RIF assay (Xpert) is a diagnostic tool that has been shown to significantly improve the accuracy of tuberculosis (TB) detection in clinical settings, with advanced sensitivity and specificity. Early detection of TB can be challenging, but Xpert has improved the efficacy of the diagnostic process. Nevertheless, the accuracy of Xpert varies according to different diagnostic specimens and TB infection sites. Therefore, the selection of adequate specimens is critical when using Xpert to identify suspected TB. As such, we have conducted a meta-analysis to evaluate the effectiveness of Xpert for diagnosis of different TB types using several specimens.

**Methods:** We conducted a comprehensive search of several electronic databases, including PubMed, Embase, the Cochrane Central Register of Controlled Trials, and the World Health Organization clinical trials registry center, covering studies published from Jan 2008 to July 2022. Data were extracted using an adapted version of the Checklist for Critical Appraisal and Data Extraction for Systematic Reviews of Prediction Modeling Studies. Where appropriate, meta-analysis was performed using random-effects models. The risk of bias and level of evidence was assessed using the Quality in Prognosis Studies tool and a modified version of the Grading of Recommendations Assessment, Development, and Evaluation. RStudio was utilized to analyze the results, employing the *meta4diag*, *robvis*, and *metafor* packages.

**Results:** After excluding duplicates, a total of 2163 studies were identified, and ultimately, 144 studies from 107 articles were included in the meta-analysis based on predetermined inclusion and exclusion criteria. Sensitivity, specificity and diagnostic accuracy were estimated for various specimens and TB types. In the case of pulmonary TB, Xpert using sputum (0.95 95%CI 0.91–0.98) and gastric juice (0.94 95%CI 0.84–0.99) demonstrated similarly high sensitivity, surpassing other specimen types. Additionally, Xpert exhibited high specificity for detecting TB across all specimen types. For bone and joint TB, Xpert, based on both biopsy and joint fluid specimens, demonstrated high accuracy in TB detection. Furthermore, Xpert effectively detected unclassified extrapulmonary TB and tuberculosis lymphadenitis. However, the Xpert accuracy was not satisfactory to distinguish TB meningitis, tuberculous pleuritis and unclassified TB.

**Conclusions:** Xpert has exhibited satisfactory diagnostic accuracy for most TB infections, but the efficacy of detection may vary depending on the specimens analyzed. Therefore, selecting appropriate specimens for Xpert analysis is essential, as using inadequate specimens can reduce the ability to distinguish TB.

**Systematic review registration:** https://www.crd.york.ac.uk/prospero/display_record.php?RecordID=370111, identifier CRD42022370111.

KEYWORDS

Xpert, tuberculosis, specimens, meta-analysis, systematic review

## Introduction

Tuberculosis (TB) infection, caused by Mycobacterium tuberculosis, is a leading cause of mortality worldwide and ranks among the deadliest infectious diseases, including HIV and malaria. Despite global efforts, TB remains a significant public health threat, particularly in developing and underdeveloped countries. The World Health Organization (WHO) has reported that an estimated 10.4 million people contract new TB infections yearly, with 1.8 million TB-related deaths occurring annually (Holmes et al., 2017; Harding, 2020). Furthermore, pediatric patients are particularly vulnerable, with an annual mortality rate of 0.2 million. However, the features of *M. tuberculosis* make it challenging to establish a definitive diagnosis in a timely manner, resulting in over 40% of patients not receiving a prompt diagnosis. Moreover, latent TB infection can lead to substantial morbidity and mortality, with negative socioeconomic consequences (Vitoria et al., 2009). Therefore, improved TB diagnostic procedures and techniques are urgently needed.

Accurate detection of *M. tuberculosis* is crucial for diagnosing TB, a respiratory-transmitted disease that primarily affects the lungs. Additionally, TB infection can result in tissue damage, particularly in young children and adolescents, who have a higher incidence of TB infection than adults (Holmes et al., 2017; Lamb and Starke, 2017). Due to the nonspecific symptoms and the paucibacillary nature of the disease, TB diagnosis is challenging. Diagnostic approaches for TB rely on clinical signs and symptoms. Non-sputum-based tests, such as tuberculin skin tests and chest radiography, have insufficient sensitivity and specificity (Khan and Starke, 1995).

The GeneXpert MTB/RIF assay (Xpert) was the first point-of-care assay for TB, and was endorsed by the WHO in 2010 (WHO Guidelines Approved by the Guidelines Review Committee, 2011). Xpert has demonstrated improved efficacy in detecting intrapulmonary and extrapulmonary TB. However, the sensitivity of Xpert has been found to vary depending on the specimens used for analysis, namely sputum, stool, bronchoalveolar lavage fluid (BALF), gastric juice, interstitial fluid, and biopsies. Xpert's estimated specificity among all specimens is generally higher than 98% (Kay et al., 2020). Moreover, Xpert has improved the efficacy of TB diagnostic procedures, particularly in the early phase of infection. Nevertheless, the accuracy rate of Xpert varies between specimens and specific types of TB. Therefore, selecting optimal specimens is critical for applying Xpert in identifying specific suspected TB infections (Howard-Jones and Marais, 2020; Gaensbauer, 2021; Gebre et al., 2021; Kabir et al., 2021; Maharjan et al., 2021). Accordingly, we conducted a meta-analysis to evaluate the efficacy of Xpert in detecting different types of TB in different samples, aiming to provide evidence of the best specimens for each type of TB infection.

## Materials and methods

### Study protocol

This metanalysis was conducted by following a predetermined protocol in accordance with the recommendations of a guideline for systematic reviews of diagnostic studies. Data collection and reporting followed the Preferred Reporting Items for Systematic Reviews and Meta-Analyses (PRISMA) Statement (PROSPERO; CRD42022370111).

### Search strategy

A comprehensive search strategy was employed to identify relevant publications, utilizing multiple databases, including PubMed, Embase, the Cochrane Central Register of Controlled Trials, and the World Health Organization clinical trials registry center. The search strategy included various Medical Subject Headings (MeSH) terms and keywords related to tuberculosis and Xpert assay. Specifically, the search terms used were "tuberculosis"[All Fields] OR "tuberculosis"[MeSH Terms] OR "tuberculosis"[All Fields] OR "tuberculoses"[All Fields] OR "tuberculosis s"[All Fields] OR ("tuberculosis"[MeSH Terms] OR "tuberculosis"[All Fields] OR ("tuberculosis"[All Fields] AND "infection"[All Fields]) OR "tuberculosis infection"[All Fields] OR "latent tuberculosis"[MeSH Terms] OR ("latent"[All Fields] AND "tuberculosis"[All Fields]) OR "latent tuberculosis"[All Fields] OR ("tuberculosis"[All Fields] AND "infection"[All Fields])) AND ("Xpert"[All Fields] OR ("GeneXpert"[All Fields] AND "mtb rif"[All Fields])). As the technology of Xpert had been introduced in clinical since 2009, the search included publications from Jan 2008 to July 2022.

## Study selection

The citations retrieved from the systematic search were initially screened based on their titles and/or abstracts. Relevant reports were then retrieved as complete manuscripts and evaluated for compliance with the inclusion and exclusion criteria. The following inclusion criteria were used: 1) Xpert examination was performed on any type of specimen in all individuals; 2) the study involved a diagnostic test or performance design; 3) a definitive diagnostic gold standard was provided for TB infection diagnosis in all the studies; 4) the data to obtain the results of true positive (TP), false positive (FP), false negative (FN), and true negative (TN) of Xpert examination were available. Alternatively, sensitivity, specificity, and actual sample size data could be provided, which could be calculated or converted into TP, FP, FN, and TN. The following exclusion criteria were used: 1) inclusion of the same cohort that had been studied in another study, with only the newest cohort data being included; 2) essential data for pooled analysis or quality assessment were not retrievable; 3) absence of a gold standard setup; and 4) exclusion of case reports or conference articles.

## Data collection and assessment of study quality

Initially, we manually searched the reference lists of all included studies, previous systematic reviews, and articles citing the included studies using Google Scholar. Subsequently, relevant reports were obtained as full-text manuscripts and examined for adherence to the inclusion and exclusion criteria. To assess the methodological quality of each study, we employed the 14-item Quality Assessment of Diagnostic Accuracy Studies (QUADAS) checklist. Each item was assessed with a response of "yes," "no," or "unclear" while evaluating the included studies. Because the quality assessment is intricately linked to reporting results, a well-designed study could have received a poor score if the methods and results were not reported in sufficient detail. Therefore, we presented the assessment in a descriptive format rather than as a numerical score.

## Publication bias

The possibility of publication bias was examined using funnel plots and the Risk-of-bias VISualization (*Robvis*) tool in the R programming environment (version 4.2.0). The presence of an asymmetric distribution of data points in the funnel plot and the quantified results obtained from the traffic light plot was used to determine any risk of bias. This plot displays each risk-of-bias judgment in a matrix, with domains along the horizontal and results/studies down the vertical axis, similar to the data set, and a weighted bar plot, which depicts the proportion of information with each risk-of-bias judgment separately for each domain in the specified assessment tool (McGuinness and Higgins, 2021).

## Sensitivity analyses

A sensitivity analysis was performed by systematically excluding one set of study data at a time to investigate whether any individual study was exerting an excessive influence on the overall analysis. The pooled results were then reassessed to determine whether there was a significant alteration in the findings. These analyses were conducted for each study included in this work.

## Statistical analyses

The data were analyzed using R and RStudio software version 4.2.0. The diagnostic efficacy of different specimens of Xpert in distinguishing various types of TB was measured using sensitivity, specificity, diagnostic odds ratio (DOR), and summary receiver operating characteristics (SROC) curve. Sensitivity was defined as the proportion of patients diagnosed with TB by the gold standard correctly identified by the positive results of different specimens using Xpert. Specificity was defined as the non-TB cases correctly identified by the negative results of different samples using Xpert. The crosshair plot for the Xpert data set was generated by displaying the posterior means for each study as the summary points, along with paired lines showing the corresponding 95% confidential intervals (95% CI) for sensitivity and false positive rate (1-specificity). The confidence intervals presented in particular results were related to the confidence level, sample size, and associated factors. The crosshair plot displayed the individual studies in receiver operating characteristic (ROC) space with paired confidence intervals representing sensitivity and specificity (Phillips et al., 2010). The SROC was also plotted based on the sensitivity and specificity combination.

The area under the curve (AUC) value was calculated as a global measurement of diagnostic accuracy performance. Posterior density plots were also generated to estimate the correlation between the two linear predictors. The posterior density plot showed the relative importance of the two-study metrics. The risk of bias was assessed using the *Robvis* and *metafor* packages in RStudio. Pooled sensitivity and specificity, based on various specimens in TB detection using Xpert, were measured using the meta4diag package in RStudio. Moreover, one set of study data was systematically removed to determine whether any single study was incurring undue weight in the analysis. The pooled results for the remaining studies were reanalyzed to determine whether the results had a significant change. Sensitivity analysis was conducted for every study.

# Results

## Study evaluation

A total of 2163 studies were initially identified through literature search and abstracts. Following the application of inclusion and exclusion criteria, 1908 citations were excluded, leaving 207 articles for careful evaluation. Ultimately, 101 articles were excluded, 58 of which did not provide necessary data on TP, FP, FN, and TN. Further, 37 studies did not report the gold standard utilized, 5 studies were designed for TB drug resistance without a diagnostic test design, and 1 article was a case report (Supplementary Figure 1). The essential information and basic

characteristics of the 144 included studies from 107 articles (Armand et al., 2011; Causse et al., 2011; Friedrich et al., 2011; Ligthelm et al., 2011; Malbruny et al., 2011; Vadwai et al., 2011; Moure et al., 2012; Tortoli et al., 2012; Bates et al., 2013; Christopher et al., 2013; Porcel et al., 2013; Van Rie et al., 2013; Weyer et al., 2013; Zmak et al., 2013; Ablanedo-Terrazas et al., 2014; Biadglegne et al., 2014; Coetzee et al., 2014; Javed et al., 2014; Litao et al., 2014; Lusiba et al., 2014; Meldau et al., 2014; Pang et al., 2014; Scott et al., 2014; Theron et al., 2014; Trajman et al., 2014; Coleman et al., 2015; Gu et al., 2015; Kim et al., 2015; Liu et al., 2015; Rufai et al., 2015; Singh et al., 2015; Solomons et al., 2015; Agrawal et al., 2016; Bajrami et al., 2016; Bholla et al., 2016; Chew et al., 2016; Dhooria et al., 2016; Held et al., 2016; Jo et al., 2016; Marcy et al., 2016; Mazzola et al., 2016; Reechaipichitkul et al., 2016; Sauzullo et al., 2016; Arockiaraj et al., 2017; Aslam et al., 2017; Che et al., 2017; Chikaonda et al., 2017; Hasan et al., 2017; Jin et al., 2017; Kawkitinarong et al., 2017; Lu et al., 2017; Massi et al., 2017; Meyer et al., 2017; Rufai et al., 2017; Tang et al., 2017; Tang et al., 2017; Ullah et al., 2017; Walters et al., 2017; Yang et al., 2017; Yu et al., 2017; Bahr et al., 2018; Castro et al., 2018; Christopher et al., 2018; Cresswell et al., 2018; Fan et al., 2018; Kasa Tom et al., 2018; Khan et al., 2018; Li et al., 2018; Lu et al., 2018; Myo et al., 2018; Pereira et al., 2018; Perez-Risco et al., 2018; Rahman et al., 2018; Samuel et al., 2018; Sharma et al., 2018; Akhter et al., 2019; Allahyartorkaman et al., 2019; Creswell et al., 2019; Dahale et al., 2019; Fakey Khan et al., 2019; Galal El-Din et al., 2019; Peize et al., 2019; Piersimoni et al., 2019; Rasheed et al., 2019; Sun et al., 2019; Tadesse et al., 2019; Talib et al., 2019; Wang et al., 2019; Wu et al., 2019; Donovan et al., 2020; Phetsuksiri et al., 2020; Shao et al., 2020; Sharma et al., 2020; Solanki et al., 2020; Ssengooba et al., 2020; Sun et al., 2020; Tiamiyu et al., 2020; Wang et al., 2020; Xia et al., 2020; Yeong et al., 2020; Yu et al., 2020; Zhou et al., 2020b; Zhou et al., 2020a; Kohli et al., 2021; Liu et al., 2021; Parigi et al., 2021; Pierre-Louis et al., 2021) are summarized in Supplementary Table 1.

## Study quality

Quality assessment of diagnostic accuracy studies was conducted using the QUADAS list. Most of the included studies received satisfactory scores on the essential items in the QUADAS list. However, several studies lacked complete reporting on certain items, such as uninterpretable test results and excluded cases (Supplementary Figure 2 and Supplementary Table 2).

## Risk of bias

Assessment of the risk of bias was visualized using the *robvis* (Risk-of-bias VISualization) package (McGuinness and Higgins, 2021). The traffic light plot presents every risk-of-bias judgment in a matrix, while the weighted bar plot displays the proportion of information for each risk-of-bias judgment separately for each domain in the assessment (Figures 1A, B). To evaluate the publication bias of included studies, funnel plots were utilized, with each dot representing a study and the distance between each dot and the horizontal line indicating the bias of each study. The absence of any asymmetric distribution suggested no publication bias, whereas the presence of an asymmetric distribution was indicative of publication bias.

## Efficacy of Xpert in identifying pulmonary TB on various specimens

Pulmonary TB was the predominant type of TB infection. The Xpert assay was mainly used for pulmonary TB detection, and several types of specimens were evaluated to determine their accuracy. This analysis examined bronchoalveolar lavage fluid (BALF), biopsy samples, gastric juice, sputum, and stool using the Xpert assay to differentiate pulmonary TB (Figure 2 and Table 1). Sensitivities, specificities, and SROCs were calculated for each analysis. Nine articles were identified for calculating the diagnostic efficacy of BALF in Xpert assay, with a sensitivity of 0.88 (95% CI 0.79–0.96) and a specificity of 0.94 (95% CI 0.90–0.97). The AUC of BALF in the Xpert assay was 0.879 ± 0.098, with an estimated AUC of 0.924 (Figure 2A). For sputum, 25 articles were eligible for diagnostic efficacy calculation, resulting in a sensitivity of 0.95 (95% CI 0.91–0.98) and a specificity of 0.96 (95%CI 0.93–0.98).

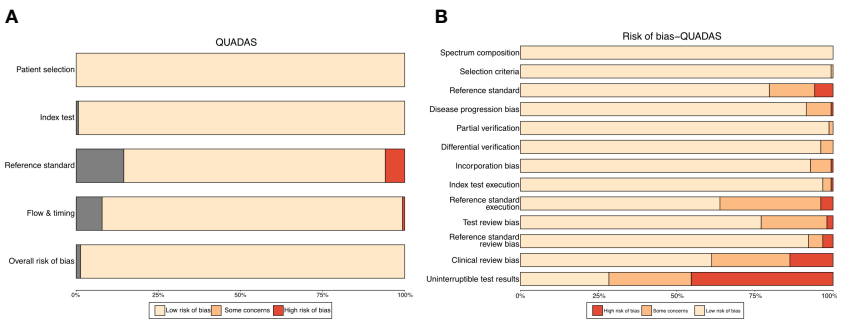


FIGURE 1
Traffic light plot **(A)** for QUADAS-s scores of included studies. Weighted bar plot **(B)** shows the proportion of information with each risk-of-bias judgement separately for each domain in the assessment.

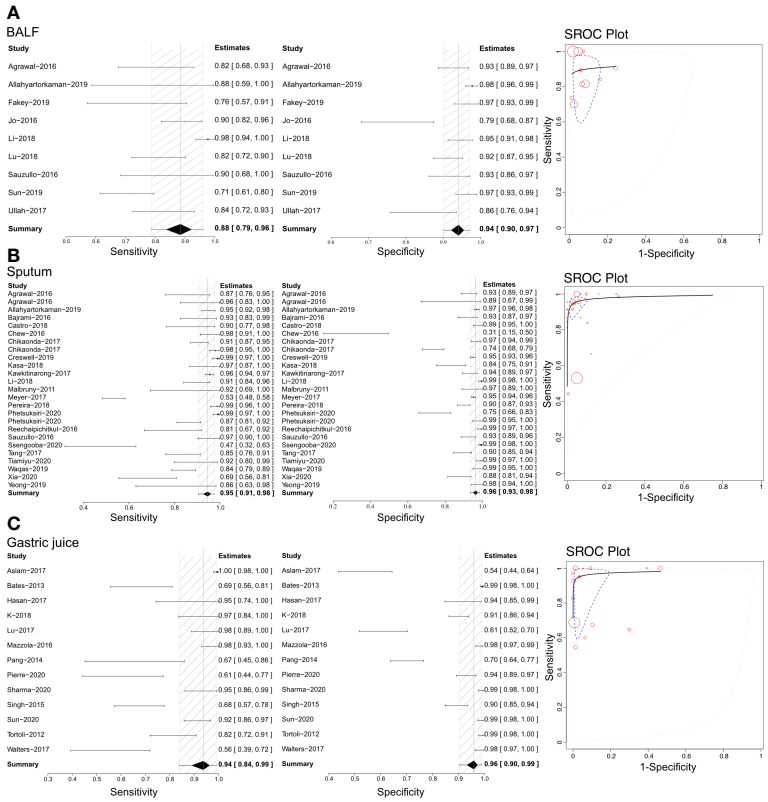


FIGURE 2
The sensitivity, specificity and SROC curve of different samples for diagnosing pulmonary TB. **(A)** The diagnostic efficiency on BALF sample based Xpert analysis; **(B)** The diagnostic efficiency on sputum sample based Xpert analysis; **(C)** The diagnostic efficiency on gastric juice sample based Xpert analysis.

The AUC of sputum in the Xpert assay was 0.981 ± 0.011, with an estimated AUC of 0.983 (Figure 2B). Thirteen articles were eligible to calculate the diagnostic efficacy of gastric juice in the Xpert assay, with a sensitivity of 0.94 (95% CI 0.84–0.98) and a specificity of 0.96 (95% CI 0.93–0.98). The AUC of gastric juice using the Xpert assay was 0.953 ± 0.057, with an estimated AUC of 0.979 (Figure 2C). Two articles were eligible to calculate the diagnostic efficacy of stool samples using the Xpert assay, with a sensitivity of 0.79 (95%CI 0.35–0.98) and a specificity of 0.98 (95% CI 0.93–1.00). The AUC of stool in the Xpert assay was 0.607 ± 0.310, with an estimated AUC of 0.675 (Table 1). Two articles were identified to calculate the diagnostic efficacy of biopsy samples from bronchoscopies in the Xpert assay, with a sensitivity of 0.77 (95% CI 0.57–0.98), but the specificity failed to reach a positive calculated result. The AUC of the biopsy samples taken from a bronchoscopy in the Xpert assay was 0.492 ± 0.431, with an estimated AUC of 0.672 (Table 1). Crosshair and posterior density plots are presented in Supplementary Figures 3, 4, respectively.

## Efficacy of Xpert in identifying bone and joint TB on various specimens

Based on our literature review, Xpert has been used to distinguish bone and joint TB using tissue biopsy samples and joint fluid (Figure 3). Therefore, we calculated each analysis' sensitivities, specificities, and SROCs. Ten articles were eligible for use in calculating the diagnostic efficacy of tissue biopsy samples using Xpert assessment, with a sensitivity of 0.95 (95% CI 0.90–0.99) and specificity of 0.79 (95% CI 0.57–0.93). The AUC of tissue biopsy samples in the Xpert application was 0.959 ± 0.026, with an estimated AUC of 0.970 (Figure 3A). Additionally, nine articles were eligible to calculate the diagnostic efficacy of joint fluid using Xpert assessment, with a sensitivity of 0.96 (95% CI 0.90–0.99) and a specificity of 0.93 (95% CI 0.77–1.00). The AUC of joint fluid in the Xpert application was 0.979 ± 0.030, with an estimated AUC of 0.988 (Figure 3B). Supplementary Figures 5, 6 show the Crosshair and posterior density plots for these analyses, respectively.

## Efficacy of Xpert in identifying tuberculous lymphadenitis

Based on the literature we retrieved, Xpert has been used with lymph node biopsy samples to differentiate tuberculous lymphadenitis (Figure 4). Through our analysis, we calculated sensitivities, specificities, and SROCs. We identified 17 articles eligible for calculating the diagnostic efficacy of lymph node biopsy samples using Xpert assessment. The sensitivity of lymph node biopsy samples in the Xpert assessment for identifying

TABLE 1 Summary of pooled results on pulmonary TB diagnosis.

| Sample for Xpet | Included researches | Sensitivity (95%CI) | Specificity (95%CI) | AUC (mean ± SD) | Publication bias |
|---|---|---|---|---|---|
| BALF | 9 | 0.88 (0.79, 0.96) | 0.94 (0.90, 0.97) | 0.879 ± 0.098 | Potentially exist |
| Sputum | 25 | 0.95 (0.91, 0.98) | 0.96 (0.93, 0.98) | 0.981 ± 0.011 | Absent |
| Gastric juice | 13 | 0.94 (0.84, 0.98) | 0.96 (0.93, 0.98) | 0.953 ± 0.057 | Potentially exist |
| Stool | 2 | 0.79 (0.35, 0.98) | 0.98 (0.93, 1.00) | 0.607 ± 0.310 | Absent |
| Biopsy | 2 | 0.77 (0.57, 0.98) | 0.86 (0.67, 1.00) | 0.492 ± 0.431 | Potentially exist |

BALF, bronchoalveolar lavage fluid; CI, confidential intervals; SD, standard difference.

tuberculous lymphadenitis was 0.84 (95%CI 0.76–0.90), with a specificity of 0.97 (95% CI 0.94–0.99). The AUC of tissue biopsy samples in the Xpert application was 0.753 ± 0.256, and the estimated AUC was 0.857 (Figure 4). Additionally, we found only one article that demonstrated the diagnostic efficacy of lymphoglandula fluid in the Xpert assay, with a sensitivity of 0.89 and a specificity of 0.91. Supplementary Figures 7A, 8A present the Crosshair and posterior density plots, respectively.

## Efficacy of Xpert in identifying tuberculous meningitis

Based on the literature we gathered, Xpert has been utilized with cerebrospinal fluid (CSF) to differentiate tuberculous meningitis (Figure 5). The sensitivities, specificities, and SROCs were computed among the assessments conducted. We identified 12 studies that qualified for evaluating the diagnostic performance of CSF in Xpert analysis. The sensitivity of CSF in Xpert evaluation for detecting tuberculous meningitis was 0.60 (95% CI 0.37–0.81), while its specificity was 0.98 (95% CI 0.95–1.00). Furthermore, the AUC of CSF in the Xpert application was 0.433 ± 0.290, and the estimated AUC was 0.444 (Figure 5). We present the Crosshair and posterior density plots in Supplementary Figures 7B, 8B, respectively.

## Efficacy of Xpert in identifying pleural TB

Based on the literature we retrieved, Xpert has been applied with pleural fluid to differentiate pleural TB (Figure 6). Our analyses calculated sensitivities, specificities, and SROCs. Twenty-five articles were deemed eligible to compute the diagnostic efficacy of pleural fluid in Xpert assessment. The sensitivity of pleural fluid in Xpert assessment to detect pleural TB was 0.30 (95% CI 0.21–0.40), while its specificity was 0.99 (95% CI 0.94–1.00). Additionally, the AUC of tissue biopsy samples in the Xpert application was 0.776 ± 0.205, with an estimated AUC of 0.718 (Figure 6). Supplementary Figures 7C, 8C present the Crosshair and posterior density plots, respectively.

## Efficacy of Xpert in identifying unclassified extrapulmonary TB

Based on the literature we retrieved, Xpert has been used to differentiate unclassified extrapulmonary TB using compound

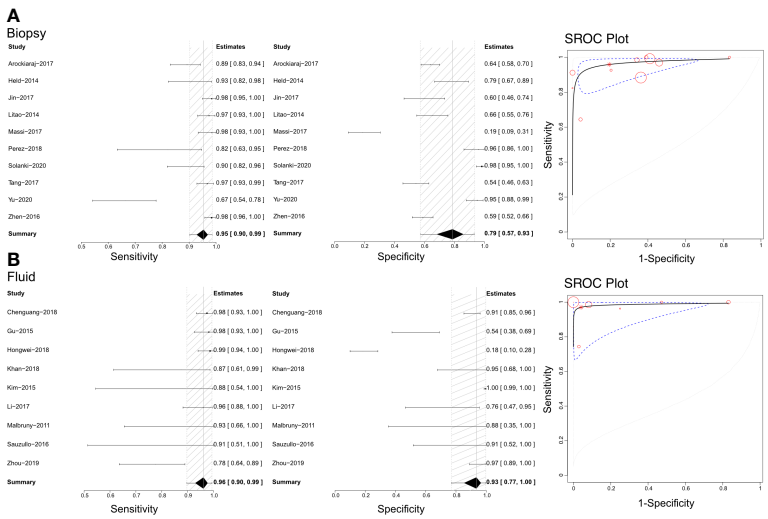


FIGURE 3
The sensitivity, specificity and SROC curve of different samples for diagnosing bone and joint TB. **(A)** The diagnostic efficiency on biopsy sample based Xpert analysis; **(B)** The diagnostic efficiency on joint fluid sample based Xpert analysis.

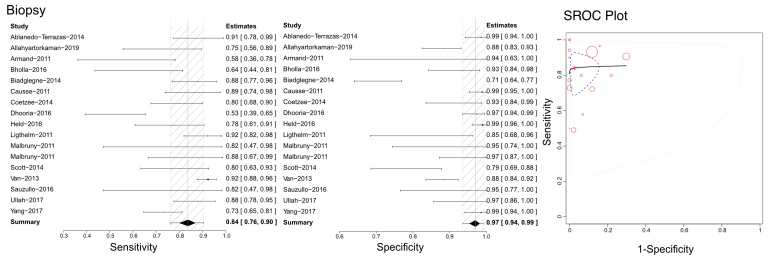


FIGURE 4
The sensitivity, specificity and SROC curve of different samples for diagnosing tuberculous lymphadenitis on biopsy sample based Xpert analysis.

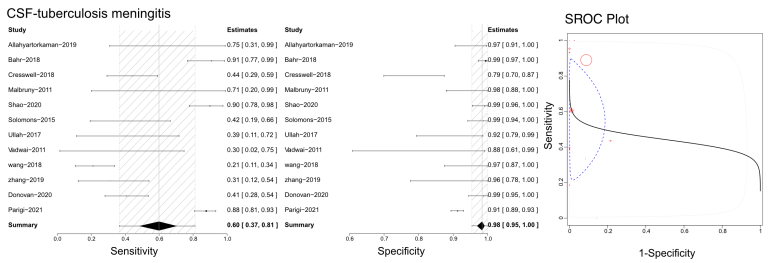


FIGURE 5
The sensitivity, specificity and SROC curve of different samples for diagnosing tuberculosis meningitis on cerebrospinal fluid sample based Xpert analysis.

specimens (Figure 7). Sensitivities, specificities, and SROCs were computed among the analyses. Twelve articles were deemed eligible to determine the diagnostic efficacy of compound specimens in Xpert assessment of unclassified extrapulmonary TB. The sensitivity of compound specimens in Xpert assessment for identifying unclassified extrapulmonary TB was 0.90 (95% CI 0.81–0.97), while its specificity was 0.98 (95%CI 0.94–1.00). The AUC of samples in the Xpert application was 0.416 ± 0.387, and the estimated AUC was 0.876 (Figure 7). Supplementary Figures 7D, 8D present the Crosshair and posterior density plots, respectively, for the diagnostic efficacy of compound specimens in Xpert assessment of unclassified extrapulmonary TB.

## Efficacy of Xpert in identifying other types of TB

In accordance with our pre-defined inclusion and exclusion criteria, we have identified several studies that have demonstrated the diagnostic accuracy of Xpert in identifying various forms of TB. One study reported on the diagnostic efficacy of urine in urinary TB, with a sensitivity of 0.69 and specificity of 1.00 (Table 2). Another study investigated the diagnostic efficacy of stool samples in intestinal TB, with a sensitivity of 0.36 and specificity of 0.75 (Table 2). Furthermore, we identified three articles that were eligible for calculating the diagnostic efficacy of ascitic fluid in peritoneal

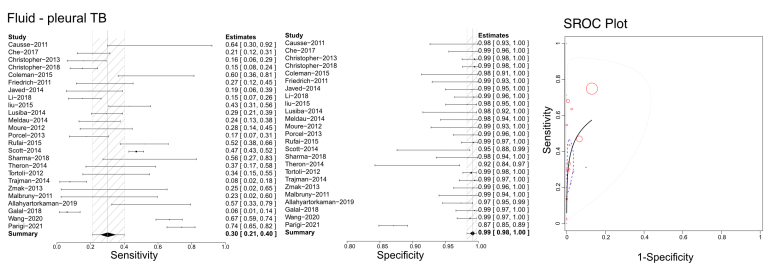


FIGURE 6
The sensitivity, specificity and SROC curve of different samples for diagnosing pleural TB on fluid sample based Xpert analysis.

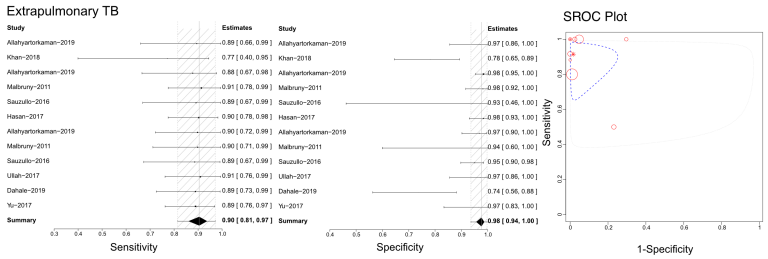


FIGURE 7
The sensitivity, specificity and SROC curve of different samples for diagnosing extrapulmonary TB based Xpert analysis.

TB. The sensitivity of using ascitic fluid to diagnose peritoneal TB was found to be 0.65 (95% CI 0.44–0.83), while the specificity was 0.99 (95% CI 0.95–1.00). Therefore, the AUC of ascitic fluid in peritoneal TB for Xpert application was calculated to be 0.638 ± 0.367, with an estimated AUC of 0.824 (Table 2). Crosshair and posterior density plots are provided in Supplementary Figure 7E and Supplementary Figure 8E, respectively. Additionally, one article was eligible for determining the diagnostic efficacy of ascitic biopsy in peritoneal TB. The study reported a sensitivity of 1.00 and a specificity of 0.70 (Table 2).

## Discussion

This meta-analysis aimed to evaluate the diagnostic efficacy of Xpert in identifying different types of TB infections based on the use of various specimens. Based on the results obtained from this meta-analysis, we aimed to provide recommendations for selecting the optimal specimen for detecting suspected TB infections. We conducted a comprehensive literature review to identify all types of TB and the specimens used in each Xpert application. We then calculated the pooled sensitivities, specificities, and SROCs for each pair of the applied specimen and suspected TB infection. The findings of this meta-analysis offer valuable insights for clinical practice. Since its introduction in 2010, Xpert has been shown to possess superior characteristics in identifying TB pathogens and has been applied to various clinical diseases, including COVID-19 (Lee and Song, 2021). Several meta-analyses have demonstrated the efficacy of Xpert in TB diagnosis. However, previous meta-analyses have mainly focused on a specific type of TB infection or the accuracy of Xpert with compound specimen applications or a specific specimen among unclassified types of TB infection (Steingart et al., 2014; Kohli et al., 2018; Ssengooba et al., 2020; Wang et al., 2020; Sharma et al., 2021). This study is the first meta-analysis to provide an integrative assessment of Xpert's diagnostic efficacy in identifying different types of TB based on various specimens' applications.

Based on our evaluation of pulmonary TB, all specimens used in the Xpert analysis demonstrated satisfactory specificity. However, there were significant differences in sensitivity assessments among the different specimens. Sputum and gastric juice, commonly used specimens, showed similar sensitivity values, around 0.95. In contrast, Xpert based on BALF had a lower sensitivity of 0.88 and an AUC of 0.879 ± 0.098, which was lower than that of sputum and gastric juice. Importantly, invasive sample harvesting by bronchoscopy is not as simple as obtaining sputum and gastric juice. Harvesting gastric juice is an invasive method, which precludes its use as the primary choice for Xpert analysis. Sputum would be the easiest and most convenient way to detect pulmonary TB but false negative results are expected with this sampling method. To overcome this issue, multiple sputum examinations would be required. Stool or biopsy samples obtained by bronchoscopy had unsatisfactory sensitivities, lower than 0.80. Thus, due to the excellent efficacy of Xpert on sputum and gastric juice samples, repeated Xpert examinations on sputum or gastric juice would be more efficient in achieving a precise diagnosis of pulmonary TB compared to using BALF, stool, and other samples. However, DiNardo et al. (DiNardo et al., 2015) found that 10–85% of individuals with presumed pulmonary TB cannot produce sputum, depending on age and disease status. Therefore, gastric juice could serve as an alternative to diagnostic specimens. Although stool had lower sensitivity, it had the highest specificity. Stool samples are also more accessible than BALF, gastric juice, and biopsies. Because obtaining BALF, gastric juice, and biopsy samples

TABLE 2 Summary of pooled results on other types of TB.

| Sample for Xpet | Included researches | Sensitivity (95%CI) | Specificity (95%CI) | AUC (Mean ± SD) | Publication bias |
|---|---|---|---|---|---|
| Urine in urinary TB | 1 | 0.69 | 1.00 | – | – |
| Stool to intestinal TB | 1 | 0.36 | 0.75 | – | – |
| Ascitic fluid in peritoneal TB | 3 | 0.65 (0.44,0.83) | 0.99 (0.95, 1.00) | 0.638 ± 0.367 | Absent |
| Ascitic biopsy in peritoneal TB | 1 | 1.00 | 0.70 | – | – |

CI, confidential intervals; SD, standard difference.

is invasive, these samples cannot be easily acquired from infants or young children. Additionally, young patients cannot produce enough sputum for Xpert analysis. Therefore, performing Xpert on gastric juice for infants and young children would still be a good alternation. Although stool samples have lower sensitivity, their high specificity implies high accuracy with multiple assessments, as confirmed in a prospective study by Sun et al. in 2021 (Donovan et al., 2020).

TB infection affecting the bone and joints results in significant morbidity and disability due to the damage inflicted on chondrocytes, which lack the ability to regenerate postnatally. Therefore, early bone and joint TB diagnosis is critical in improving patient outcomes. Our results indicate that Xpert effectively detects bone and joint TB using joint fluid and biopsy tissue samples, demonstrating similar diagnostic values. Furthermore, the accuracy of Xpert in identifying bone and joint TB can be enhanced by selecting appropriate tissue biopsy samples. Thus, using joint fluid for Xpert analysis should be considered the primary option. In a previous study, Zhou et al. conducted a retrospective study and found that the positive rate of the Xpert assay was significantly higher when using granulation tissue specimens compared to caseous necrotic tissue, sequestrum, and other necrotic connective tissues for bone and joint TB diagnosis (Zhou et al., 2021).

In evaluating extrapulmonary TB, combining multiple specimens appears to be more helpful than relying on a single sample. Although Shama et al. recommended urine samples for Xpert analysis in extrapulmonary TB diagnosis, our meta-analysis failed to identify any advantages of urine over stool or gastric juice. Given the uncertain nature of extrapulmonary TB, using multiple specimens for Xpert testing would be a superior choice. TB lymphadenitis is the most common extrapulmonary manifestation of the disease and presents diagnostic and therapeutic challenges due to its resemblance to other pathologic processes and inconsistent physical and laboratory findings. Therefore, diagnosis of TB lymphadenitis often requires lymph node biopsy (Mohapatra and Janmeja, 2009). Our analysis confirmed that Xpert analysis of biopsy samples is viable for TB lymphadenitis diagnosis. In recent years, fine-needle aspiration cytology has become a more straightforward outpatient diagnostic procedure that has replaced complete excisional node biopsy and significantly improved diagnostic accuracy (Cataño and Robledo, 2016). However, lymph node biopsy is an invasive approach and its use necessitates a risk evaluation for the recipients. Therefore, alternative specimen options should be considered. A recent study suggested that lymphoglandular fluid could be a promising alternative to conventional biopsy for Xpert analysis. Nonetheless, more studies are required to enhance the evidence and evaluate the accuracy of this approach.

The diagnostic performance of Xpert for TB and tuberculous meningitis was inferior to that for pulmonary TB, as well as bone and joint TB, but both maintained a remarkably high specificity. A meta-analysis by Kohli et al. (Kohli et al., 2018) demonstrated that Xpert achieved a specificity higher than 98% for diagnosing peritoneal TB based on compound samples. In contrast, a retrospective study by Nguyen et al. (Mai and Thwaites, 2017) indicated that Xpert played a crucial role in diagnosing tuberculous meningitis but showed poor sensitivity, which limited its ability to exclude the disease. Nevertheless, our study also confirmed the high specificity of Xpert for these diseases. Given the characteristics of these types of TB, significant improvement of sensitivity remains challenging. Repeating Xpert tests multiple times could enhance its overall sensitivity.

Limitations of this meta-analysis include: 1) possible variations in Xpert policies among different countries that could impact test results, but this factor could not be analyzed. 2) Inclusion of studies involving children or HIV-positive patients expanded our findings' generalizability, as the aim of this study was to explore the diagnostic utility of various specimens in detecting different types of TB infection. However, this issue may affect the results, and it still needs to be considered as a limitation. 3) The meta4diag program package in R software, which was used for the analysis, did not include a heterogeneity test. Therefore, additional studies with more convincing results may be needed for potential influence factor analysis of some studies.

## Conclusion

In conclusion, Xpert has shown satisfactory diagnostic accuracy in most cases of TB infections. Nevertheless, the efficacy of detection varied depending on the specimens used for Xpert analysis. Unselected specimens for Xpert could diminish its ability to differentiate TB. Therefore, we have highlighted the critical role of specimen selection in TB detection using Xpert.

## Data availability statement

The datasets presented in this study can be found in online repositories. The names of the repository/repositories and accession number(s) can be found in the article/Supplementary Material.

## Author contributions

XG, YRH, YMH, KZ, and YL collected the data. XG and YRH reviewed the literature and contributed to manuscript drafting; XG and YL conceptualized and designed the study, coordinated and supervised data collection, and critically reviewed the manuscript for important intellectual content. YL were responsible for the revision of the manuscript for important intellectual content. All authors contributed to the article and approved the submitted version.

## Funding

This work was supported by grants from Technology Project of Sichuan Province of China (2021YFQ0061) and the National Natural Science Foundation of China (82270249). The funding

did not participate in the design of the study and collection, analysis, and interpretation of data and in writing the manuscript.

## Acknowledgments

We thank Dr. Yazhou He from West China Public Health School, Sichuan University to help us evaluate the meta-analysis as a statistician.

## Conflict of interest

The authors declare that the research was conducted in the absence of any commercial or financial relationships that could be construed as a potential conflict of interest.

## Publisher's note



## Supplementary material

The Supplementary Material for this article can be found online at: https://www.frontiersin.org/articles/10.3389/fcimb.2023.1149741/full#supplementary-material

SUPPLEMENTARY TABLE 1
Essential information of included studies.

SUPPLEMENTARY TABLE 2
Traffic light plot (A) for the assessment of potential risk of bias summary, which have 5 columns (D1 for Patient selection, D2 for Index test, D3 for Reference standard, D4 for Flow and time, and 1 for overall judgements, in that order).

SUPPLEMENTARY FIGURE 1
PRISMA flow chart on citations selection.

SUPPLEMENTARY FIGURE 2
Quality assessment of the included articles. QUADAS, Quality Assessment of Diagnostic Accuracy Studies.

SUPPLEMENTARY FIGURE 3
Crosshair plots for pooled results on pulmonary TB diagnosis using Xpert.

SUPPLEMENTARY FIGURE 4
Posterior density plots for pooled results on pulmonary TB diagnosis using Xpert.

SUPPLEMENTARY FIGURE 5
Crosshair plots for pooled results on bone and joint TB diagnosis using Xpert.

SUPPLEMENTARY FIGURE 6
Posterior density plots for pooled results on bone and joint TB diagnosis using Xpert.

SUPPLEMENTARY FIGURE 7
Crosshair plots for pooled results on various TB diagnosis using Xpert. **(A)** Biopsy sample for tuberculous lymphadenitis diagnosis based on Xpert. **(B)** Cerebrospinal fluid sample for tuberculosis meningitis diagnosis based on Xpert. **(C)** Fluid sample for pleural TB diagnosis based on Xpert. **(D)** Extrapulmonary TB diagnosis based on Xpert. **(E)** Ascitic fluid for peritoneal TB diagnosis based on Xpert.

SUPPLEMENTARY FIGURE 8
Posterior density plots for pooled results on various TB diagnosis using Xpert. **(A)** Biopsy sample for tuberculous lymphadenitis diagnosis based on Xpert. **(B)** Cerebrospinal fluid sample for tuberculosis meningitis diagnosis based on Xpert. **(C)** Fluid sample for pleural TB diagnosis based on Xpert. **(D)** Extrapulmonary TB diagnosis based on Xpert. **(E)** Ascitic fluid for peritoneal TB diagnosis based on Xpert.

## References

Ablanedo-Terrazas, Y., Alvarado-de la Barrera, C., Hernández-Juan, R., Ruiz-Cruz, M., and Reyes-Terán, G. (2014). Xpert MTB/RIF for diagnosis of tuberculous cervical lymphadenitis in HIV-infected patients. *Laryngoscope.* 124 (6), 1382–1385. doi: 10.1002/lary.24478

Agrawal, M., Bajaj, A., Bhatia, V., and Dutt, S. (2016). Comparative study of GeneXpert with ZN stain and culture in samples of suspected pulmonary tuberculosis. *J. Clin. Diagn. Res.* 10 (5), Dc09–Dc12. doi: 10.7860/jcdr/2016/18837.7755

Akhter, N., Sumalani, K. K., Chawla, D., and Ahmed Rizvi, N. (2019). Comparison between the diagnostic accuracy of xpert MTB/Rif assay and culture for pleural tuberculosis using tissue biopsy. *ERJ Open Res.* 5 (3), 00065-2019. doi: 10.1183/23120541.00065-2019

Allahyartorkaman, M., Mirsaeidi, M., Hamzehloo, G., Amini, S., Zakiloo, M., and Nasiri, M. J. (2019). Low diagnostic accuracy of xpert MTB/RIF assay for extrapulmonary tuberculosis: a multicenter surveillance. *Sci. Rep.* 9 (1), 18515. doi: 10.1038/s41598-019-55112-y

Armand, S., Vanhuls, P., Delcroix, G., Courcol, R., and Lemaître, N. (2011). Comparison of the xpert MTB/RIF test with an IS6110-TaqMan real-time PCR assay for direct detection of mycobacterium tuberculosis in respiratory and nonrespiratory specimens. *J. Clin. Microbiol.* 49 (5), 1772–1776. doi: 10.1128/jcm.02157-10

Arockiaraj, J., Michael, J. S., Amritanand, R., David, K. S., and Krishnan, V. (2017). The role of xpert MTB/RIF assay in the diagnosis of tubercular spondylodiscitis. *Eur. Spine J.* 26 (12), 3162–3169. doi: 10.1007/s00586-017-5076-9

Aslam, W., Tahseen, S., Schomotzer, C., Hussain, A., Khanzada, F., Ul Haq, M., et al. (2017). Gastric specimens for diagnosing tuberculosis in adults unable to expectorate in rawalpindi, Pakistan. *Public Health Action.* 7 (2), 141–146. doi: 10.5588/pha.16.0126

Bahr, N. C., Nuwagira, E., Evans, E. E., Cresswell, F. V., Bystrom, P. V., Byamukama, A., et al. (2018). Diagnostic accuracy of xpert MTB/RIF ultra for tuberculous meningitis in HIV-infected adults: a prospective cohort study. *Lancet Infect. Dis.* 18 (1), 68–75. doi: 10.1016/s1473-3099(17)30474-7

Bajrami, R., Mulliqi, G., Kurti, A., Lila, G., and Raka, L. (2016). Comparison of GeneXpert MTB/RIF and conventional methods for the diagnosis of tuberculosis in Kosovo. *J. Infect. Dev. Ctries.* 10 (4), 418–422. doi: 10.3855/jidc.7569

Bates, M., O'Grady, J., Maeurer, M., Tembo, J., Chilukutu, L., Chabala, C., et al. (2013). Assessment of the xpert MTB/RIF assay for diagnosis of tuberculosis with gastric lavage aspirates in children in sub-Saharan Africa: a prospective descriptive study. *Lancet Infect. Dis.* 13 (1), 36–42. doi: 10.1016/s1473-3099(12)70245-1

Bholla, M., Kapalata, N., Masika, E., Chande, H., Jugheli, L., Sasamalo, M., et al. (2016). Evaluation of xpert® MTB/RIF and ustar EasyNAT™ TB IAD for diagnosis of tuberculous lymphadenitis of children in Tanzania: a prospective descriptive study. *BMC Infect. Dis.* 16, 246. doi: 10.1186/s12879-016-1578-z

Biadglegne, F., Mulu, A., Rodloff, A. C., and Sack, U. (2014). Diagnostic performance of the xpert MTB/RIF assay for tuberculous lymphadenitis on fine needle aspirates from Ethiopia. *Tuberculosis (Edinb).* 94 (5), 502–505. doi: 10.1016/j.tube.2014.05.002

Castro, A. Z., Moreira, A. R., Oliveira, J., Costa, P. A., Graça, C., Pérez, M. A., et al. (2018). Clinical impact and cost analysis of the use of either the xpert MTB rif test or sputum smear microscopy in the diagnosis of pulmonary tuberculosis in Rio de Janeiro, Brazil. *Rev. Soc. Bras. Med. Trop.* 51 (5), 631–637. doi: 10.1590/0037-8682-0082-2018

Cataño, J. C., and Robledo, J. (2016). Tuberculous lymphadenitis and parotitis. *Microbiol. Spectr.* 4 (6). doi: 10.1128/microbiolspec.TNMI7-0008-2016

Causse, M., Ruiz, P., Gutiérrez-Aroca, J. B., and Casal, M. (2011). Comparison of two molecular methods for rapid diagnosis of extrapulmonary tuberculosis. *J. Clin. Microbiol.* 49 (8), 3065–3067. doi: 10.1128/jcm.00491-11

Che, N., Yang, X., Liu, Z., Li, K., and Chen, X. (2017). Rapid detection of cell-free mycobacterium tuberculosis DNA in tuberculous pleural effusion. *J. Clin. Microbiol.* 55 (5), 1526–1532. doi: 10.1128/jcm.02473-16

Chew, M. Y., Ng, J., Cai, H. M., Lim, T. G., and Lim, T. K. (2016). The clinical utility of xpert® MTB/RIF testing in induced sputum. *Int. J. Tuberc Lung Dis.* 20 (12), 1668–1670. doi: 10.5588/ijtld.16.0123

Chikaonda, T., Nguluwe, N., Barnett, B., Gokhale, R. H., Krysiak, R., Thengolose, I., et al. (2017). Performance of xpert(®) MTB/RIF among tuberculosis outpatients in Lilongwe, Malawi. *Afr J. Lab. Med.* 6 (2), 464. doi: 10.4102/ajlm.v6i2.464

Christopher, D. J., Dinakaran, S., Gupta, R., James, P., Isaac, B., and Thangakunam, B. (2018). Thoracoscopic pleural biopsy improves yield of xpert MTB/RIF for diagnosis of pleural tuberculosis. *Respirology.* 23 (7), 714–717. doi: 10.1111/resp.13275

Christopher, D. J., Schumacher, S. G., Michael, J. S., Luo, R., Balamugesh, T., Duraikannan, P., et al. (2013). Performance of xpert MTB/RIF on pleural tissue for the diagnosis of pleural tuberculosis. *Eur. Respir. J.* 42 (5), 1427–1429. doi: 10.1183/09031936.00103213

Coetzee, L., Nicol, M. P., Jacobson, R., Schubert, P. T., van Helden, P. D., Warren, R. M., et al. (2014). Rapid diagnosis of pediatric mycobacterial lymphadenitis using fine needle aspiration biopsy. *Pediatr. Infect. Dis. J.* 33 (9), 893–896. doi: 10.1097/inf.0000000000000312

Coleman, M., Finney, L. J., Komrower, D., Chitani, A., Bates, J., Chipungu, G. A., et al. (2015). Markers to differentiate between kaposi's sarcoma and tuberculous pleural effusions in HIV-positive patients. *Int. J. Tuberc Lung Dis.* 19 (2), 144–150. doi: 10.5588/ijtld.14.0289

Cresswell, F. V., Bangdiwala, A. S., Bahr, N. C., Trautner, E., Nuwagira, E., Ellis, J., et al. (2018). Can improved diagnostics reduce mortality from tuberculous meningitis? findings from a 6.5-year cohort in Uganda. *Wellcome Open Res.* 3, 64. doi: 10.12688/wellcomeopenres.14610.2

Creswell, J., Qin, Z. Z., Gurung, R., Lamichhane, B., Yadav, D. K., Prasai, M. K., et al. (2019). The performance and yield of tuberculosis testing algorithms using microscopy, chest x-ray, and xpert MTB/RIF. *J. Clin. Tuberc Other Mycobact Dis.* 14, 1–6. doi: 10.1016/j.jctube.2018.11.002

Dahale, A. S., Puri, A. S., Kumar, A., Dalal, A., Agarwal, A., and Sachdeva, S. (2019). Tissue xpert® MTB/RIF assay in peritoneal tuberculosis: to be (Done) or not to be (Done). *Cureus.* 11 (6), e5009. doi: 10.7759/cureus.5009

Dhooria, S., Gupta, N., Bal, A., Sehgal, I. S., Aggarwal, A. N., Sethi, S., et al. (2016). Role of xpert MTB/RIF in differentiating tuberculosis from sarcoidosis in patients with mediastinal lymphadenopathy undergoing EBUS-TBNA: a study of 147 patients. *Sarcoidosis Vasc. Diffuse Lung Dis.* 33 (3), 258–266.

DiNardo, A. R., Hahn, A., Leyden, J., Stager, C., Jo Baron, E., Graviss, E. A., et al. (2015). Use of string test and stool specimens to diagnose pulmonary tuberculosis. *Int. J. Infect. Dis.* 41, 50–52. doi: 10.1016/j.ijid.2015.10.022

Donovan, J., Thu, D. D. A., Phu, N. H., Dung, V. T. M., Quang, T. P., Nghia, H. D. T., et al. (2020). Xpert MTB/RIF ultra versus xpert MTB/RIF for the diagnosis of tuberculous meningitis: a prospective, randomised, diagnostic accuracy study. *Lancet Infect. Dis.* 20 (3), 299–307. doi: 10.1016/s1473-3099(19)30649-8

Fakey Khan, D., Suleman, M., Baijnath, P., Perumal, R., Moodley, V., Mhlane, Z., et al. (2019). Multiple microbiologic tests for tuberculosis improve diagnostic yield of bronchoscopy in medically complex patients. *AAS Open Res.* 2, 25. doi: 10.12688/aasopenres.12980.1

Fan, L., Li, D., Zhang, S., Yao, L., Hao, X., Gu, J., et al. (2018). Parallel tests using culture, xpert MTB/RIF, and SAT-TB in sputum plus bronchial alveolar lavage fluid significantly increase diagnostic performance of smear-negative pulmonary tuberculosis. *Front. Microbiol.* 9. doi: 10.3389/fmicb.2018.01107

Friedrich, S. O., von Groote-Bidlingmaier, F., and Diacon, A. H. (2011). Xpert MTB/RIF assay for diagnosis of pleural tuberculosis. *J. Clin. Microbiol.* 49 (12), 4341–4342. doi: 10.1128/jcm.05454-11

Gaensbauer, J. (2021). Xpert ultra, pediatric pulmonary tuberculosis and stool: forward progress raises new questions. *Clin. Infect. Dis.* 73 (2), 235–236. doi: 10.1093/cid/ciaa589

Galal El-Din, M., Sobh, E., Adawy, Z., and Farghaly, N. (2019). Diagnostic utility of gene X-pert in the diagnosis of tuberculous pleural effusion. *Infect. Dis. (Lond).* 51 (3), 227–229. doi: 10.1080/23744235.2018.1532105

Gebre, M., Cameron, L. H., Tadesse, G., Woldeamanuel, Y., and Wassie, L. (2021). Variable diagnostic performance of stool xpert in pediatric tuberculosis: a systematic review and meta-analysis. *Open Forum Infect. Dis.* 8 (8), ofaa627. doi: 10.1093/ofid/ofaa627

Gu, Y., Wang, G., Dong, W., Li, Y., Ma, Y., Shang, Y., et al. (2015). Xpert MTB/RIF and GenoType MTBDRplus assays for the rapid diagnosis of bone and joint tuberculosis. *Int. J. Infect. Dis.* 36, 27–30. doi: 10.1016/j.ijid.2015.05.014

Harding, E. (2020). WHO global progress report on tuberculosis elimination. *Lancet Respir. Med.* 8 (1), 19. doi: 10.1016/s2213-2600(19)30418-7

Hasan, Z., Shakoor, S., Arif, F., Mehnaz, A., Akber, A., Haider, M., et al. (2017). Evaluation of xpert MTB/RIF testing for rapid diagnosis of childhood pulmonary tuberculosis in children by xpert MTB/RIF testing of stool samples in a low resource setting. *BMC Res. Notes.* 10 (1), 473. doi: 10.1186/s13104-017-2806-3

Held, M., Laubscher, M., Mears, S., Dix-Peek, S., Workman, L., Zar, H., et al. (2016). Diagnostic accuracy of the xpert MTB/RIF assay for extrapulmonary tuberculosis in children with musculoskeletal infections. *Pediatr. Infect. Dis. J.* 35 (11), 1165–1168. doi: 10.1097/inf.0000000000001271

K. K. Holmes, S. Bertozzi, B. R. Bloom and P. Jha (Eds.) (2017). *Major infectious diseases* (Washington (DC: The International Bank for Reconstruction and Development / The World Bank© 2017 International Bank for Reconstruction and Development / The World Bank).

Howard-Jones, A. R., and Marais, B. J. (2020). Tuberculosis in children: screening, diagnosis and management. *Curr. Opin. Pediatr.* 32 (3), 395–404. doi: 10.1097/mop.0000000000000897

Javed, N., Aslam, M., Mushtaq, M. A., Khan, T., and Shaheen, M. Z. (2014). Role of gene xpert in diagnosis of tuberculous pleural effusion: comparison with pleural biopsy. *Eur. Respir. J.* 44 (Suppl 58), P2655.

Jin, Y. H., Shi, S. Y., Zheng, Q., Shen, J., Ying, X. Z., and Wang, Y. F. (2017). Application value of xpert MTB/RIF in diagnosis of spinal tuberculosis and detection of rifampin resistance. *Zhongguo Gu Shang.* 30 (9), 787–791. doi: 10.3969/j.issn.1003-0034.2017.09.002

Jo, Y. S., Park, J. H., Lee, J. K., Heo, E. Y., Chung, H. S., and Kim, D. K. (2016). Discordance between MTB/RIF and real-time tuberculosis-specific polymerase chain reaction assay in bronchial washing specimen and its clinical implications. *PLoS One* 11 (10), e0164923. doi: 10.1371/journal.pone.0164923

Kabir, S., Rahman, S. M. M., Ahmed, S., Islam, M. S., Banu, R. S., Shewade, H. D., et al. (2021). Xpert ultra assay on stool to diagnose pulmonary tuberculosis in children. *Clin. Infect. Dis.* 73 (2), 226–234. doi: 10.1093/cid/ciaa583

Kasa Tom, S., Welch, H., Kilalang, C., Tefuarani, N., Vince, J., Lavu, E., et al. (2018). Evaluation of xpert MTB/RIF assay in children with presumed pulmonary tuberculosis in Papua new Guinea. *Paediatr. Int. Child Health* 38 (2), 97–105. doi: 10.1080/20469047.2017.1319898

Kawkitinarong, K., Suwanpimolkul, G., Kateruttanakul, P., Manosuthi, W., Ubolyam, S., Sophonphan, J., et al. (2017). Real-life clinical practice of using the xpert MTB/RIF assay in Thailand. *Clin. Infect. Dis.* 64 (suppl_2), S171–s178. doi: 10.1093/cid/cix151

Kay, A. W., González Fernández, L., Takwoingi, Y., Eisenhut, M., Detjen, A. K., Steingart, K. R., et al. (2020). Xpert MTB/RIF and xpert MTB/RIF ultra assays for active tuberculosis and rifampicin resistance in children. *Cochrane Database Syst. Rev.* 8 (8), Cd013359. doi: 10.1002/14651858.CD013359.pub2

Khan, A. S., Ali, S., Khan, M. T., Ahmed, S., Khattak, Y., Abduljabbar,, et al. (2018). Comparison of GeneXpert MTB/RIF assay and LED-FM microscopy for the diagnosis of extra pulmonary tuberculosis in Khyber pakhtunkhwa, Pakistan. *Braz. J. Microbiol.* 49 (4), 909–913. doi: 10.1016/j.bjm.2018.02.011

Khan, E. A., and Starke, J. R. (1995). Diagnosis of tuberculosis in children: increased need for better methods. *Emerg. Infect. Dis.* 1 (4), 115–123. doi: 10.3201/eid0104.950402

Kim, Y. W., Kwak, N., Seong, M. W., Kim, E. C., Yoo, C. G., Kim, Y. W., et al. (2015). Accuracy of the xpert® MTB/RIF assay for the diagnosis of extra-pulmonary tuberculosis in south Korea. *Int. J. Tuberc Lung Dis.* 19 (1), 81–86. doi: 10.5588/ijtld.14.0500

Kohli, M., Schiller, I., Dendukuri, N., Dheda, K., Denkinger, C. M., Schumacher, S. G., et al. (2018). Xpert(®) MTB/RIF assay for extrapulmonary tuberculosis and rifampicin resistance. *Cochrane Database Syst. Rev.* 8 (8), Cd012768. doi: 10.1002/14651858.CD012768.pub2

Kohli, M., Schiller, I., Dendukuri, N., Yao, M., Dheda, K., Denkinger, C. M., et al. (2021). Xpert MTB/RIF ultra and xpert MTB/RIF assays for extrapulmonary tuberculosis and rifampicin resistance in adults. *Cochrane Database Syst. Rev.* 1 (1), Cd012768. doi: 10.1002/14651858.CD012768.pub3

Lamb, G. S., and Starke, J. R. (2017). Tuberculosis in infants and children. *Microbiol. Spectr.* 5 (2). doi: 10.1128/microbiolspec.TNMI7-0037-2016

Lee, J., and Song, J. U. (2021). Diagnostic accuracy of the Cepheid xpert xpress and the Abbott ID NOW assay for rapid detection of SARS-CoV-2: a systematic review and meta-analysis. *J. Med. Virol.* 93 (7), 4523–4531. doi: 10.1002/jmv.26994

Li, Y., Jia, W., Lei, G., Zhao, D., Wang, G., and Qin, S. (2018). Diagnostic efficiency of xpert MTB/RIF assay for osteoarticular tuberculosis in patients with inflammatory arthritis in China. *PLoS One* 13 (6), e0198600. doi: 10.1371/journal.pone.0198600

Ligthelm, L. J., Nicol, M. P., Hoek, K. G., Jacobson, R., van Helden, P. D., Marais, B. J., et al. (2011). Xpert MTB/RIF for rapid diagnosis of tuberculous lymphadenitis from fine-needle-aspiration biopsy specimens. *J. Clin. Microbiol.* 49 (11), 3967–3970. doi: 10.1128/jcm.01310-11

Litao, L., Hongmin, L., Yuanzhen, M., Dawei, L., Da, P., Xiaobo, L., et al. (2014). Assessment of the xpert MTB/RIF assay for the detection of m.tuberculosis and rifampicin resistance in spinal tuberculosis specimens: a retrospective validation study. *Chin. J. Orthopaedics* 34 (2), 211–215.

Liu, X., Huang, Z., and Du, J. (2015). Rapid diagnosis of pleural tuberculosis by xpert MTB/RIF assay. *Zhonghua Jie He He Hu Xi Za Zhi.* 38 (10), 741–745.

Liu, X. H., Xia, L., Song, B., Wang, H., Qian, X. Q., Wei, J. H., et al. (2021). Stool-based xpert MTB/RIF ultra assay as a tool for detecting pulmonary tuberculosis in children with abnormal chest imaging: a prospective cohort study. *J. Infect.* 82 (1), 84–89. doi: 10.1016/j.jinf.2020.10.036

Lu, J., Li, H., Dong, F., Shi, J., Yang, H., Han, S., et al. (2017). The feasibility of xpert MTB/RIF testing to detect rifampicin resistance among childhood tuberculosis for prevalence surveys in northern China. *BioMed. Res. Int.* 2017, 5857369. doi: 10.1155/2017/5857369

Lu, Y., Zhu, Y., Shen, N., Tian, L., and Sun, Z. (2018). Evaluating the diagnostic accuracy of the xpert MTB/RIF assay on bronchoalveolar lavage fluid: a retrospective study. *Int. J. Infect. Dis.* 71, 14–19. doi: 10.1016/j.ijid.2018.01.030

Lusiba, J. K., Nakiyingi, L., Kirenga, B. J., Kiragga, A., Lukande, R., Nsereko, M., et al. (2014). Evaluation of cepheid's xpert MTB/Rif test on pleural fluid in the diagnosis of pleural tuberculosis in a high prevalence HIV/TB setting. *PLoS One* 9 (7), e102702. doi: 10.1371/journal.pone.0102702

Maharjan, B., Thapa, J., Shah, D. K., Shrestha, B., Avsar, K., Suzuki, Y., et al. (2021). Comparison of xpert MTB/RIF to microscopy and culture for the diagnosis of tuberculosis in a referral laboratory in Nepal. *Jpn J. Infect. Dis.* 74 (6), 517–521. doi: 10.7883/yoken.JJID.2020.921

Mai, N. T., and Thwaites, G. E. (2017). Recent advances in the diagnosis and management of tuberculous meningitis. *Curr. Opin. Infect. Dis.* 30 (1), 123–128. doi: 10.1097/qco.0000000000000331

Malbruny, B., Le Marrec, G., Courageux, K., Leclercq, R., and Cattoir, V. (2011). Rapid and efficient detection of mycobacterium tuberculosis in respiratory and non-respiratory samples. *Int. J. Tuberc Lung Dis.* 15 (4), 553–555. doi: 10.5588/ijtld.10.0497

Marcy, O., Ung, V., Goyet, S., Borand, L., Msellati, P., Tejiokem, M., et al. (2016). Performance of xpert MTB/RIF and alternative specimen collection methods for the diagnosis of tuberculosis in HIV-infected children. *Clin. Infect. Dis.* 62 (9), 1161–1168. doi: 10.1093/cid/ciw036

Massi, M. N., Biatko, K. T., Handayani, I., Pratama, M. Y., Septriani, S., Nurdin, G. M., et al. (2017). Evaluation of rapid GeneXpert MTB/RIF method using DNA tissue specimens of vertebral bones in patients with suspected spondylitis TB. *J. Orthop.* 14 (1), 189–191. doi: 10.1016/j.jor.2016.12.003

Mazzola, E., Arosio, M., Nava, A., Fanti, D., Gesu, G., and Farina, C. (2016). Performance of real-time PCR xpert ®MTB/RIF in diagnosing extrapulmonary tuberculosis. *Infez Med.* 24 (4), 304–309.

McGuinness, L. A., and Higgins, J. P. T. (2021). Risk-of-bias VISualization (robvis): an r package and shiny web app for visualizing risk-of-bias assessments. *Res. Synth Methods* 12 (1), 55–61. doi: 10.1002/jrsm.1411

Meldau, R., Peter, J., Theron, G., Calligaro, G., Allwood, B., Symons, G., et al. (2014). Comparison of same day diagnostic tools including gene xpert and unstimulated IFN-γ for the evaluation of pleural tuberculosis: a prospective cohort study. *BMC Pulm Med.* 14, 58. doi: 10.1186/1471-2466-14-58

Meyer, A. J., Atuheire, C., Worodria, W., Kizito, S., Katamba, A., Sanyu, I., et al. (2017). Sputum quality and diagnostic performance of GeneXpert MTB/RIF among smear-negative adults with presumed tuberculosis in Uganda. *PLoS One* 12 (7), e0180572. doi: 10.1371/journal.pone.0180572

Mohapatra, P. R., and Janmeja, A. K. (2009). Tuberculous lymphadenitis. *J. Assoc. Physicians India.* 57, 585–590.

Moure, R., Martín, R., and Alcaide, F. (2012). Effectiveness of an integrated real-time PCR method for detection of the mycobacterium tuberculosis complex in smear-negative extrapulmonary samples in an area of low tuberculosis prevalence. *J. Clin. Microbiol.* 50 (2), 513–515. doi: 10.1128/jcm.06467-11

Myo, K., Zaw, M., Swe, T. L., Kyaw, Y. Y., Thwin, T., Myo, T. T., et al. (2018). Evaluation of xpert(®) MTB/RIF assay as a diagnostic test for pulmonary tuberculosis in children in Myanmar. *Int. J. Tuberc Lung Dis.* 22 (9), 1051–1055. doi: 10.5588/ijtld.18.0024

Pang, Y., Wang, Y., Zhao, S., Liu, J., Zhao, Y., and Li, H. (2014). Evaluation of the xpert MTB/RIF assay in gastric lavage aspirates for diagnosis of smear-negative childhood pulmonary tuberculosis. *Pediatr. Infect. Dis. J.* 33 (10), 1047–1051. doi: 10.1097/inf.0000000000000403

Parigi, S., Venturini, E., Galli, L., and Chiappini, E. (2021). Xpert(®) MTB/RIF ultra performance in diagnosing paediatric pulmonary TB in gastric aspirates. *Int. J. Tuberc Lung Dis.* 25 (1), 75–77. doi: 10.5588/ijtld.20.0499

Peize, Z., Junfeng, Z., Liang, F., Tianpin, L., Xingliao, Y., Houming, L., et al. (2019). Diagnostic accuracy of xpert MTB/RIF ultra for tuberculous meningitis. *J. Tuberc Lung Health* 8 (1), 42–47.

Pereira, G. R., Barbosa, M. S., Dias, N. J. D., Almeida, C. P. B., and Silva, D. R. (2018). Impact of introduction of xpert MTB/RIF test on tuberculosis (TB) diagnosis in a city with high TB incidence in Brazil. *PLoS One* 13 (3), e0193988. doi: 10.1371/journal.pone.0193988

Perez-Risco, D., Rodriguez-Temporal, D., Valledor-Sanchez, I., and Alcaide, F. (2018). Evaluation of the xpert MTB/RIF ultra assay for direct detection of mycobacterium tuberculosis complex in smear-negative extrapulmonary samples. *J. Clin. Microbiol.* 56 (9), 631-637. doi: 10.1128/jcm.00659-18

Phetsuksiri, B., Klayut, W., Rudeeaneksin, J., Srisungngam, S., Bunchoo, S., Toonkomdang, S., et al. (2020). The performance of an in-house loop-mediated isothermal amplification for the rapid detection of mycobacterium tuberculosis in sputum samples in comparison with xpert MTB/RIF, microscopy and culture. *Rev. Inst Med. Trop. Sao Paulo.* 62, e36. doi: 10.1590/s1678-9946202062036

Phillips, B., Stewart, L. A., and Sutton, A. J. (2010). 'Cross hairs' plots for diagnostic meta-analysis. *Res. Synth Methods* 1 (3-4), 308–315. doi: 10.1002/jrsm.26

Pierre-Louis, M. H., Rouzier, V., Rivera, V., Systrom, H. K., Julma, P., Jean, E., et al. (2021). Diagnosis of tuberculosis using gastric aspirates in pediatric patients in Haiti. *J. Pediatr. Infect. Dis. Soc* 10 (1), 22–26. doi: 10.1093/jpids/piaa012

Piersimoni, C., Gherardi, G., Gracciotti, N., and Pocognoli, A. (2019). Comparative evaluation of xpert MTB/RIF and the new xpert MTB/RIF ultra with respiratory and extra-pulmonary specimens for tuberculosis case detection in a low incidence setting. *J. Clin. Tuberc Other Mycobact Dis.* 15, 100094. doi: 10.1016/j.jctube.2019.100094

Porcel, J. M., Palma, R., Valdés, L., Bielsa, S., San-José, E., and Esquerda, A. (2013). Xpert® MTB/RIF in pleural fluid for the diagnosis of tuberculosis. *Int. J. Tuberc Lung Dis.* 17 (9), 1217–1219. doi: 10.5588/ijtld.13.0178

Rahman, S. M. M., Maliha, U. T., Ahmed, S., Kabir, S., Khatun, R., Shah, J. A., et al. (2018). Evaluation of xpert MTB/RIF assay for detection of mycobacterium tuberculosis in stool samples of adults with pulmonary tuberculosis. *PLoS One* 13 (9), e0203063. doi: 10.1371/journal.pone.0203063

Rasheed, W., Rao, N. A., Adel, H., Baig, M. S., and Adil, S. O. (2019). Diagnostic accuracy of xpert MTB/RIF in sputum smear-negative pulmonary tuberculosis. *Cureus.* 11 (8), e5391. doi: 10.7759/cureus.5391

Reechaipichitkul, W., Phetsuriyawong, A., Chaimanee, P., and Ananta, P. (2016). DIAGNOSTIC TEST OF SPUTUM GENEXPERT MTB/RIF FOR SMEAR NEGATIVE PULMONARY TUBERCULOSIS. *Southeast Asian J. Trop. Med. Public Health* 47 (3), 457–466.

Rufai, S. B., Singh, A., Kumar, P., Singh, J., and Singh, S. (2015). Performance of xpert MTB/RIF assay in diagnosis of pleural tuberculosis by use of pleural fluid samples. *J. Clin. Microbiol.* 53 (11), 3636–3638. doi: 10.1128/jcm.02182-15

Rufai, S. B., Singh, S., Singh, A., Kumar, P., Singh, J., and Vishal, A. (2017). Performance of xpert MTB/RIF on ascitic fluid samples for detection of abdominal tuberculosis. *J. Lab. Physicians.* 9 (1), 47–52. doi: 10.4103/0974-2727.187927

Samuel, B. P., Michael, J. S., Chandrasingh, J., Kumar, S., Devasia, A., and Kekre, N. S. (2018). Efficacy and role of xpert(®) mycobacterium tuberculosis/rifampicin assay in urinary tuberculosis. *Indian J. Urol.* 34 (4), 268–272. doi: 10.4103/iju.IJU_189_18

Sauzullo, I., Rodio, D. M., Facchinetti, S., Puggioni, G., De Angelis, M., Goldoni, P., et al. (2016). Diagnostic accuracy of xpert MTB/RIF versus smear microscopy in the early diagnosis tuberculosis in the real life of "Umberto i" hospital Rome. *New Microbiol.* 39 (4), 304–306.

Scott, L. E., Beylis, N., Nicol, M., Nkuna, G., Molapo, S., Berrie, L., et al. (2014). Diagnostic accuracy of xpert MTB/RIF for extrapulmonary tuberculosis specimens: establishing a laboratory testing algorithm for south Africa. *J. Clin. Microbiol.* 52 (6), 1818–1823. doi: 10.1128/jcm.03553-13

Shao, L., Qiu, C., Zheng, L., Yang, Y., Yang, X., Liang, Q., et al. (2020). Comparison of diagnostic accuracy of the GeneXpert ultra and cell-free nucleic acid assay for tuberculous meningitis: a multicentre prospective study. *Int. J. Infect. Dis.*, 98:441–98:446. doi: 10.1016/j.ijid.2020.06.076

Sharma, S., Dahiya, B., Sreenivas, V., Singh, N., Raj, A., Sheoran, A., et al. (2018). Comparative evaluation of GeneXpert MTB/RIF and multiplex PCR targeting mpb64 and IS6110 for the diagnosis of pleural TB. *Future Microbiol.* 13, 407–413. doi: 10.2217/fmb-2017-0147

Sharma, S., Shulania, A., Achra, A., Jeram, H., Kansra, S., and Duggal, N. (2020). Diagnosis of pulmonary tuberculosis from gastric aspirate samples in nonexpectorating pediatric patients in a tertiary care hospital. *Indian J. Pathol. Microbiol.* 63 (2), 210–213. doi: 10.4103/ijpm.Ijpm_694_19

Sharma, V., Soni, H., Kumar, M. P., Dawra, S., Mishra, S., Mandavdhare, H. S., et al. (2021). Diagnostic accuracy of the xpert MTB/RIF assay for abdominal tuberculosis: a systematic review and meta-analysis. *Expert Rev. Anti Infect. Ther.* 19 (2), 253–265. doi: 10.1080/14787210.2020.1816169

Singh, S., Singh, A., Prajapati, S., Kabra, S. K., Lodha, R., Mukherjee, A., et al. (2015). Xpert MTB/RIF assay can be used on archived gastric aspirate and induced sputum samples for sensitive diagnosis of paediatric tuberculosis. *BMC Microbiol.*, 15:191. doi: 10.1186/s12866-015-0528-z

Solanki, A. M., Basu, S., Biswas, A., Roy, S., and Banta, A. (2020). Sensitivity and specificity of gene xpert in the diagnosis of spinal tuberculosis: a prospective controlled clinical study. *Global Spine J.* 10 (5), 553–558. doi: 10.1177/2192568219858310

Solomons, R. S., Visser, D. H., Friedrich, S. O., Diacon, A. H., Hoek, K. G., Marais, B. J., et al. (2015). Improved diagnosis of childhood tuberculous meningitis using more than one nucleic acid amplification test. *Int. J. Tuberc Lung Dis.* 19 (1), 74–80. doi: 10.5588/ijtld.14.0394

Ssengooba, W., Iragena, J. D., Nakiyingi, L., Mujumbi, S., Wobudeya, E., Mboizi, R., et al. (2020). Accuracy of xpert ultra in diagnosis of pulmonary tuberculosis among children in Uganda: a substudy from the SHINE trial. *J. Clin. Microbiol.* 58 (9), e00410-20. doi: 10.1128/jcm.00410-20

Steingart, K. R., Schiller, I., Horne, D. J., Pai, M., Boehme, C. C., and Dendukuri, N. (2014). Xpert® MTB/RIF assay for pulmonary tuberculosis and rifampicin resistance in adults. *Cochrane Database Syst. Rev.* 2014 (1), Cd009593. doi: 10.1002/14651858.CD009593.pub3

Sun, L., Qi, X., Liu, F., Wu, X., Yin, Q., Guo, Y., et al. (2019). A test for more accurate diagnosis of pulmonary tuberculosis. *Pediatrics* 144 (5), e20190262. doi: 10.1542/peds.2019-0262

Sun, L., Zhu, Y., Fang, M., Shi, Y., Peng, X., Liao, Q., et al. (2020). Evaluation of xpert MTB/RIF ultra assay for diagnosis of childhood tuberculosis: a multicenter accuracy study. *J. Clin. Microbiol.* 24, 58(9). doi: 10.1128/jcm.00702-20

Tadesse, M., Abebe, G., Bekele, A., Bezabih, M., Yilma, D., Apers, L., et al. (2019). Xpert MTB/RIF assay for the diagnosis of extrapulmonary tuberculosis: a diagnostic evaluation study. *Clin. Microbiol. Infect.* 25 (8), 1000–1005. doi: 10.1016/j.cmi.2018.12.018

Talib, A., Bhatty, S., Mehmood, K., Naim, H., Haider, I., Lal, H., et al. (2019). GeneXpert in stool: diagnostic yield in intestinal tuberculosis. *J. Clin. Tuberc Other Mycobact Dis.* 17, 100131. doi: 10.1016/j.jctube.2019.100131

Tang, L., Feng, S., Gao, R., Han, C., Sun, X., Bao, Y., et al. (2017). A comparative study on the role of xpert MTB/RIF in testing different types of spinal tuberculosis tissue specimens. *Genet. Test Mol. Biomarkers.* 21 (12), 722–726. doi: 10.1089/gtmb.2017.0149

Tang, T., Liu, F., Lu, X., and Huang, Q. (2017). Evaluation of GeneXpert MTB/RIF for detecting mycobacterium tuberculosis in a hospital in China. *J. Int. Med. Res.* 45 (2), 816–822. doi: 10.1177/0300060517698618

Theron, G., Peter, J., Calligaro, G., Meldau, R., Hanrahan, C., Khalfey, H., et al. (2014). Determinants of PCR performance (Xpert MTB/RIF), including bacterial load and inhibition, for TB diagnosis using specimens from different body compartments. *Sci. Rep.* 4, 5658. doi: 10.1038/srep05658

Tiamiyu, A. B., Iliyasu, G., Dayyab, F. M., Habib, Z. G., Tambuwal, S. H., Galadanci, H., et al. (2020). Evaluation of GeneXpert MTB/RIF as a diagnostic tool in patients with sputum smear-negative TB in a high HIV burden region in Nigeria. *Trans. R Soc. Trop. Med. Hyg.* 114 (9), 690–692. doi: 10.1093/trstmh/traa019

Tortoli, E., Russo, C., Piersimoni, C., Mazzola, E., Dal Monte, P., Pascarella, M., et al. (2012). Clinical validation of xpert MTB/RIF for the diagnosis of extrapulmonary tuberculosis. *Eur. Respir. J.* 40 (2), 442–447. doi: 10.1183/09031936.00176311

Trajman, A., da Silva Santos Kleiz de Oliveira, E. F., Bastos, M. L., Belo Neto, E., Silva, E. M., da Silva Lourenço, M. C., et al. (2014). Accuracy of polimerase chain reaction for the diagnosis of pleural tuberculosis. *Respir. Med.* 108 (6), 918–923. doi: 10.1016/j.rmed.2014.04.007

Ullah, I., Javaid, A., Masud, H., Ali, M., Basit, A., Ahmad, W., et al. (2017). Rapid detection of mycobacterium tuberculosis and rifampicin resistance in extrapulmonary tuberculosis and sputum smear-negative pulmonary suspects using xpert MTB/RIF. *J. Med. Microbiol.* 66 (4), 412–418. doi: 10.1099/jmm.0.000449

Vadwai, V., Boehme, C., Nabeta, P., Shetty, A., Alland, D., and Rodrigues, C. (2011). Xpert MTB/RIF: a new pillar in diagnosis of extrapulmonary tuberculosis? *J. Clin. Microbiol.* 49 (7), 2540–2545. doi: 10.1128/jcm.02319-10

Van Rie, A., Page-Shipp, L., Mellet, K., Scott, L., Mkhwnazi, M., Jong, E., et al. (2013). Diagnostic accuracy and effectiveness of the xpert MTB/RIF assay for the diagnosis of HIV-associated lymph node tuberculosis. *Eur. J. Clin. Microbiol. Infect. Dis.* 32 (11), 1409–1415. doi: 10.1007/s10096-013-1890-0

Vitoria, M., Granich, R., Gilks, C. F., Gunneberg, C., Hosseini, M., Were, W., et al. (2009). The global fight against HIV/AIDS, tuberculosis, and malaria: current status and future perspectives. *Am. J. Clin. Pathol.* 131 (6), 844–848. doi: 10.1309/ajcp5xhdb1pnaeyt

Walters, E., van der Zalm, M. M., Palmer, M., Bosch, C., Demers, A. M., Draper, H., et al. (2017). Xpert MTB/RIF on stool is useful for the rapid diagnosis of tuberculosis in young children with severe pulmonary disease. *Pediatr. Infect. Dis. J.* 36 (9), 837–843. doi: 10.1097/inf.0000000000001563

Wang, G., Wang, S., Jiang, G., Yang, X., Huang, M., Huo, F., et al. (2019). Xpert MTB/RIF ultra improved the diagnosis of paucibacillary tuberculosis: a prospective cohort study. *J. Infect.* 78 (4), 311–316. doi: 10.1016/j.jinf.2019.02.010

Wang, G., Wang, S., Yang, X., Sun, Q., Jiang, G., Huang, M., et al. (2020). Accuracy of xpert MTB/RIF ultra for the diagnosis of pleural TB in a multicenter cohort study. *Chest.* 157 (2), 268–275. doi: 10.1016/j.chest.2019.07.027

Weyer, K., Mirzayev, F., Migliori, G. B., Van Gemert, W., D'Ambrosio, L., Zignol, M., et al. (2013). Rapid molecular TB diagnosis: evidence, policy making and global implementation of xpert MTB/RIF. *Eur. Respir. J.* 42 (1), 252–271. doi: 10.1183/09031936.00157212

WHO Guidelines Approved by the Guidelines Review Committee (2011). *Policy statement: automated real-time nucleic acid amplification technology for rapid and simultaneous detection of tuberculosis and rifampicin resistance: xpert MTB/RIF system* Vol. 2011 (Geneva: World Health Organization Copyright © World Health Organization).

Wu, X., Tan, G., Gao, R., Yao, L., Bi, D., Guo, Y., et al. (2019). Assessment of the xpert MTB/RIF ultra assay on rapid diagnosis of extrapulmonary tuberculosis. *Int. J. Infect. Dis.* 81, 91–96. doi: 10.1016/j.ijid.2019.01.050

Xia, L., Liu, X., Qian, X., Li, T., Xi, X., Fan, X., et al. (2020). Performance of Xpert/MTB/RIF assay for childhood pulmonary tuberculosis among HIV negative children with real world evidence in China. *J. Infect. Public Health* 13 (11), 1762–1767. doi: 10.1016/j.jiph.2020.08.006

Yang, C. Q., Liu, X. Y., Du, R. H., Cao, T. Z., and Dai, X. Y. (2017). Diagnosis value with xpert Mtb/RIF assay for cervical tuberculous lymphadenitis. *Lin Chung Er Bi Yan Hou Tou Jing Wai Ke Za Zhi.* 31 (17), 1338–1340. doi: 10.13201/j.issn.1001-1781.2017.17.010

Yeong, C., Byrne, A. L., Cho, J. G., Sintchenko, V., Crighton, T., and Marais, B. J. (2020). Use of GeneXpert MTB/RIF on a single pooled sputum specimen to exclude pulmonary tuberculosis among hospital inpatients placed in respiratory isolation. *Int. J. Infect. Dis.* 92, 175–180. doi: 10.1016/j.ijid.2019.12.024

Yu, Y., Kong, Y., Ye, J., and Wang, A. (2020). Performance of conventional histopathology and GeneXpert MTB/RIF in the diagnosis of spinal tuberculosis from bone specimens: a prospective clinical study. *Clin. Biochem.* 85, 33–37. doi: 10.1016/j.clinbiochem.2020.08.010

Yu, G., Ye, B., Chen, D., Zhong, F., Chen, G., Yang, J., et al. (2017). Comparison between the diagnostic validities of xpert MTB/RIF and interferon-γ release assays for tuberculous pericarditis using pericardial tissue. *PLoS One* 12 (12), e0188704. doi: 10.1371/journal.pone.0188704

Zhou, Z., Li, C., Zhu, R., Wang, D., Liu, T., Jia, J., et al. (2020a). Combination of percutaneous lung biopsy and xpert MTB/RIF ultra enhances the differential diagnosis of tuberculosis: a prospective cohort study. *Infect. Dis. Ther.* 9 (4), 797–806. doi: 10.1007/s40121-020-00327-0

Zhou, Z., Zheng, Y., and Wang, L. (2020b). A comparative study on the value of xpert MTB/RIF and T-SPOT.TB tests in the diagnosis of bone and joint tuberculosis. *Clin. Chim. Acta* 500, 115–119. doi: 10.1016/j.cca.2019.09.026

Zhou, Z., Zheng, Y., and Wang, L. (2021). Diagnostic accuracy of the xpert MTB/RIF assay for bone and joint tuberculosis using tissue specimens. *Int. J. Infect. Dis.* 105, 224–229. doi: 10.1016/j.ijid.2021.02.030

Zmak, L., Jankovic, M., and Jankovic, V. K. (2013). Evaluation of xpert MTB/RIF assay for rapid molecular diagnosis of tuberculosis in a two-year period in Croatia. *Int. J. Mycobacteriol.* 2 (3), 179–182. doi: 10.1016/j.ijmyco.2013.05.003

frontiers | Frontiers in Cellular and Infection Microbiology

TYPE Original Research
PUBLISHED 02 May 2023
DOI 10.3389/fcimb.2023.1153544



OPEN ACCESS

EDITED BY
Antonella Mencacci,
University of Perugia, Italy

REVIEWED BY
Kamiar Zomorodian,
Shiraz University of Medical Sciences, Iran
Min Chen,
Shanghai Changzheng Hospital, China

*CORRESPONDENCE
Ying Zhao
zhaoying28062806@163.com
Yingchun Xu
xycpumch@139.com

RECEIVED 29 January 2023
ACCEPTED 14 April 2023
PUBLISHED 02 May 2023

CITATION
Yu J, He C, Wang T, Zhang G, Li J, Zhang J, Kang W, Xu Y and Zhao Y (2023) Rapid automated antifungal susceptibility testing system for yeasts based on growth characteristics.
*Front. Cell. Infect. Microbiol.* 13:1153544.
doi: 10.3389/fcimb.2023.1153544



# Rapid automated antifungal susceptibility testing system for yeasts based on growth characteristics

Jinhan Yu[1,2,3], Chun He[4], Tong Wang[1,3], Ge Zhang[1,3], Jin Li[1,3], Jingjia Zhang[1,3], Wei Kang[1,3], Yingchun Xu[1,3]* and Ying Zhao[1,3]*

[1]Department of Clinical Laboratory, State Key Laboratory of Complex Severe and Rare Diseases, Peking Union Medical College Hospital, Chinese Academy of Medical Science and Peking Union Medical College, Beijing, China, [2]Graduate School, Chinese Academy of Medical Sciences and Peking Union Medical College, Beijing, China, [3]Beijing Key Laboratory for Mechanisms Research and Precision Diagnosis of Invasive Fungal Diseases, Beijing, China, [4]Department of Clinical Laboratory, Peking University School and Hospital of Stomatology, Beijing, China

Fungal pathogens are a major threat to public health, as they are becoming increasingly common and resistant to treatment, with only four classes of antifungal medicines currently available and few candidates in the clinical development pipeline. Most fungal pathogens lack rapid and sensitive diagnostic techniques, and those that exist are not widely available or affordable. In this study, we introduce a novel automated antifungal susceptibility testing system, Droplet 48, which detects the fluorescence of microdilution wells in real time and fits growth characteristics using fluorescence intensity over time. We concluded that all reportable ranges of Droplet 48 were appropriate for clinical fungal isolates in China. Reproducibility within ±2 two-fold dilutions was 100%. Considering the Sensititre YeastOne Colorimetric Broth method as a comparator method, eight antifungal agents (fluconazole, itraconazole, voriconazole, caspofungin, micafungin, anidulafungin, amphotericin B, and 5-flucytosine) showed an essential agreement of >90%, except for posaconazole (86.62%). Category agreement of four antifungal agents (fluconazole, caspofungin, micafungin, and anidulafungin) was >90%, except for voriconazole (87.93% agreement). Two *Candida albicans* isolates and anidulafungin showed a major discrepancy (MD) (2.60%), and no other MD or very MD agents were found. Therefore, Droplet 48 can be considered as an optional method that is more automated and can obtain results and interpretations faster than previous methods. However, the optimization of the detection performance of posaconazole and voriconazole and promotion of Droplet 48 in clinical microbiology laboratories still require further research involving more clinical isolates in the future.

KEYWORDS

**antifungal susceptibility testing, growth characteristics, discrepancy, minimum inhibitory concentration, epidemiological cutoff value, clinical breakpoints, Droplet 48, Sensititre YeastOne**

# 1 Introduction

In recent years, an increasing number of patients have developed risk factors for invasive fungal infection, and resistant fungal pathogens have become more widespread, particularly in medical centers that attend to patients with complex underlying diseases, such as immunocompromised patients, patients exposed to long courses of broad-spectrum antibiotics, and patients with implanted medical devices (Bassetti et al., 2020; Fisher et al., 2022). Key interventions to combat the spread and emergence of antifungal resistance include rapid detection and quantification of resistance, as well as antimicrobial stewardship (van Belkum et al., 2020). Antifungal susceptibility testing (AFST) provides minimal inhibitory concentration (MIC) of an antifungal agent to support clinicians in managing fungal infections, thereby tracking the emergence and spread of resistance and allowing comparison of agent activities (Berkow et al., 2020).

For over 30 years, only a few AFST methods have been developed and widely implemented (Berkow et al., 2020; van Belkum et al., 2020). There are several AFST methods for the detection of MICs for fungal isolates, including the broth microdilution (BMD) reference methods by the Clinical and Laboratory Standards Institute (CLSI) (Clinical and Laboratory Standards Institute, 2022a) and Antifungal Subcommittee of the European Committee on Antimicrobial Susceptibility Testing (EUCAST) (http://www.eucast.org/ast_of_fungi/). The BMD methods, as gold standards for AFST, are labor-intensive during microdilution plate preparation and have expensive antifungal powders; therefore, it is impractical for routine use in clinical microbiology laboratories (Berkow et al., 2020).

Commercial systems are more standardized, practical, and easy to use in clinical microbiology laboratories, and their interpretation is less subjective than that of standard BMD (Delma et al., 2020). Currently, a few methodologies, such as the Sensititre YeastOne (SYO) colorimetric antifungal panel (Thermo Fisher Scientific, Waltham, MA [formerly TREK Diagnostic Systems]), Vitek 2 yeast susceptibility panel (bioMérieux, Hazelwood, MO, USA), and gradient diffusion strips (bioMérieux, Hazelwood, MO; Liofilchem, Waltham, MA), are widely used for AFST in clinical laboratories (Berkow et al., 2020; Delma et al., 2020). Nevertheless, these methods require many manual operations or a limited number of drugs to be tested (Berkow et al., 2020; Durand et al., 2021). Miscellaneous methods are constantly emerging to better meet clinical laboratory application scenarios. In-fiber antibiotic susceptibility testing is fast, highly sensitive, and compatible with the Food and Drug Administration (FDA)-approved workflow in clinical settings (Farid et al., 2022). A rapid ultrasensitive detector uses a high reflectance coefficient at high incidence angles when light travels from low- to high-refractive-index media. It can detect extremely low cell densities (optical density $\geq 5 \times 10^{7}$) that correspond to approximately 20 bacterial cells, or a single fungal cell in the detection volume (Cansizoglu et al., 2019). The new detection methods listed above exhibit good theoretical feasibility.

Fluorescent dye-based detection technologies have been widely used for clinical detection. However, the cost of SYO is too high for clinical application, and it is necessary to purchase a supporting sample-loading device; otherwise, the operation is cumbersome.

In this study, we introduced a novel, rapid, automated AFST system for yeasts based on growth characteristics. This method also uses fluorescent dyes, such as SYO, and is more automated and cheaper than the existing methods. The automated system of antimicrobial susceptibility testing, Droplet 48 (D48), uses a unique fluorescence detection technology to feed back the growth of pathogens through continuous detection of changes in fluorescence intensity of the panel; it reports the results in real time. It also avoids the subjectivity of interpreting results by reading MICs manually, and is simple to apply in clinical microbiology laboratories.

The primary modes of propagation of pathogenic fungi are fission and proliferation, and their overall growth is exponential with a characteristic growth curve. Resazurin (blue) is a water-soluble dye that can be transformed into a fluorescent colorimetric indicator (pink) using metabolically active cells. When resazurin concentration was sufficient, the fluorescence intensity produced by resazurin was proportional to the number of viable cells (Zhang et al., 2017). Based on this principle, D48 uses resazurin as a redox indicator to detect fluorescence intensity and reflects the growth characteristics of pathogenic fungi in real time. Droplet 48 uses a reflective fluorescence detection device to obtain changes in fluorescence intensity in microdilution wells containing different concentrations of antifungal agents. Processed analysis software collected fluorescence data using various algorithms to fit a characteristic growth curve (Figure 1). Assuming that certain concentrations of antifungal agents can inhibit or kill microorganisms, the growth characteristics in this well will be significantly different from those of the control wells (antifungal agent-free), according to the threshold, slope, and acceleration algorithms (Figure 2A). The concentration of the antifungal agent in each well was considered the MIC. Considering *Candida krusei* as an example, the D48 detector fitted the acquired fluorescence signal to the growth curve and determined the MIC using various algorithms (Figures 2B–D).

Additionally, different species of fungi exhibit slightly different growth characteristics under the same growth conditions. For example, *Candida albicans* entered the logarithmic growth phase at approximately 15 h, while *Exophiala dermatitidis* reaches it at approximately 45 h (Figure 3). To improve the accuracy of the assay, D48 combined the growth characteristics of the species to establish individualized parameters to interpret the threshold, slope, and acceleration values of the agent, thereby accurately interpret the antifungal susceptibility of the strain.

As required by the Clinical Laboratory Improvement Amendments U.D.o.H.a.H.S. (2023) each laboratory must verify whether it can obtain performance specifications comparable to those of the manufacturer (accuracy, precision [reproducibility], and reportable range of test results) before performing patient testing with a commercial AFST. Therefore, this study aimed to assess the concordance between the two methods for detecting AFST in commonly found clinical *Candida*, *Cryptococcus*, and some relatively rare fungi.

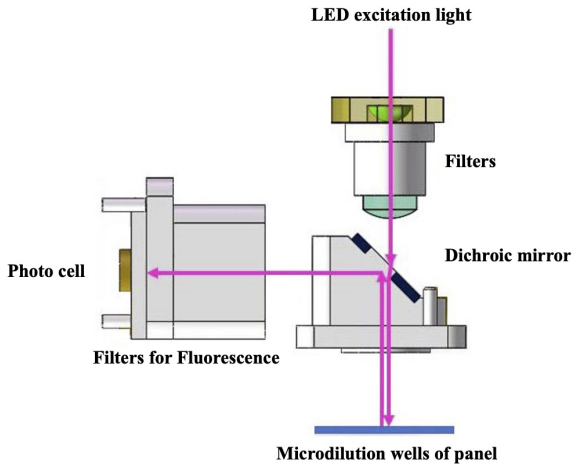


FIGURE 1
Automated antimicrobial susceptibility testing system, Droplet 48, uses the reflection fluorescence detection device to obtain fluorescence intensity change in microdilution wells. The fluorescence detection device has advantages of fast detection speed and avoidance of stray light interference. A stable light source with fixed band generated by monochromatic LED light source is used as an excitation light to illuminate the detection microdilution wells of the panel after filtering stray light using a filter and splitting by dichroic mirror. The panel continuously sampled the reflected light during the rotation process, and the fluorescence intensity was obtained through a high-sensitivity photocell. Software analysis processes the collected fluorescence data through a variety of algorithms to fit a characteristic growth curve.

# 2 Materials and methods

## 2.1 Identification of strains and species

A total of 144 clinical fungal strains were randomly analyzed from the Peking Union Medical College Hospital and Peking University School and Hospital of Stomatology. Species of these strains were commonly found in patients with systemic infections, including 16 *Candida albicans*, 16 *Candida krusei*, 13 *Candida tropicalis*, 13 *Candida parapsilosis*, 13 *Candida lusitaniae*, 10 *Candida glabrata*, 10 *Candida guilliermondii*, and 10 *Cryptococcus neoformans*. All isolates were cultured from the blood or other sterile body sites (brain abscess and intra-abdominal samples). To fully validate the performance of D48, we included 10 strains of *Trichosporon asahii* isolated from patients with bloodstream infections, 22 strains of *Exophiala dermatitidis* causing oral mucosal infections, and 11 randomly selected isolates from patients with rare bloodstream infections.

The CHROMagar Candida chromogenic agar medium was used for initial identification. Species identification was further confirmed using matrix-assisted laser desorption ionization-time of flight mass spectrometry and sequencing of the nuclear ribosomal internal transcribed spacer region and large subunit of the 28S ribosomal DNA gene (D1/D2).

## 2.2 Antifungal susceptibility testing

The AFST with nine antifungal agents (fluconazole, voriconazole, itraconazole, posaconazole, caspofungin, micafungin, anidulafungin, amphotericin B, and 5-flucytosine) was performed, according to the manufacturer's instructions. To prepare the inoculum, all the strains were subcultured onto sabouraud dextrose agar or potato dextrose agar at 35°C and subcultured again to ensure purity and viability (Figure 4A). Approximately five colonies of at least 1 mm in diameter were picked, suspended in sterile saline or water (Figure 4B), vortexed, and adjusted using a spectrophotometer to a transmittance equal to a 0.5 McFarland standard at a wavelength of 530 nm as a stock solution (Figure 4C). Further, 20 µL and 6 µL of stock solution were transferred to the SYO and D48 broth medium, and the final density of the working solution was $1.5–8 \times 10^3$ CFU/mL and $0.5–2.5 \times 10^3$ CFU/mL, respectively (Figure 4D). We ensured that the same stock solution tube was used in the experimental process of the two methods. Approximately 100 uL of stock solution was transferred into each microdilution well broth suspension to SYO panels and incubated without agitation at 35°C for 24 h before reading. An exception is *Cryptococcus* species isolates, which were maintained for 72 h before reading. Control wells were inspected for the presence and absence of growth. To get an accurate reading, plates with insufficient growth in the control well may be held for further 24 h. Between 3–3.2 mL of broth was transferred to the detection panel and added to the microdilution wells using the microfluidics technique. The instrument automatically completed the loading steps, quantitative sample addition, incubation, reporting of the results, and withdrawal (Figure 4E). To assess the reproducibility of the two methods, the AFST was repeated for isolates exhibiting MICs that differed by >1–2 two-fold dilutions. Quality control strains included *Candida parapsilosis* ATCC 22019 and *Candida krusei* ATCC 6258.

## 2.3 Data analysis

The MIC ranges, $MIC_{50}$, and $MIC_{90}$ were calculated using Microsoft Excel 2016 software. Clinical breakpoints (CBs) and epidemiology cut-off values (ECVs) in the 2022 CLSI files [M57S 4th Edition (Clinical and Laboratory Standards Institute, 2022b) and M27M44S 3rd Edition (Clinical and Laboratory Standards Institute, 2022a)] were used as the judging criteria for classification. When no CLSI CBs were used, specie-specific ECVs were used to define the isolates as wild type (WT) or non-WT. According to the CLSI guideline M52, essential agreement (EA) is the MIC obtained with D48 within two two-fold dilution steps from the MIC values detected by the SYO method. Categorical agreement (CA) was assessed and defined as the percentage of isolates classified in the same category (i.e., susceptible, intermediate, susceptible-dose-dependent, and resistant) by both methods. "Discrepancy" is used in a new AFST system when two systems are in disagreement, while "error" is used when the AFST result does not agree with the reference method result (such as BMD). Very major discrepancy (VMD) was defined as a test result when the D48 result is susceptible and SYO result is resistant. Major discrepancy (MD) was defined as a discrepancy in test results interpreted by D48 as resistant, and the comparator method result was susceptible. Minor discrepancy (mD) was intermediate, and the other was susceptible or resistant. The agreement between

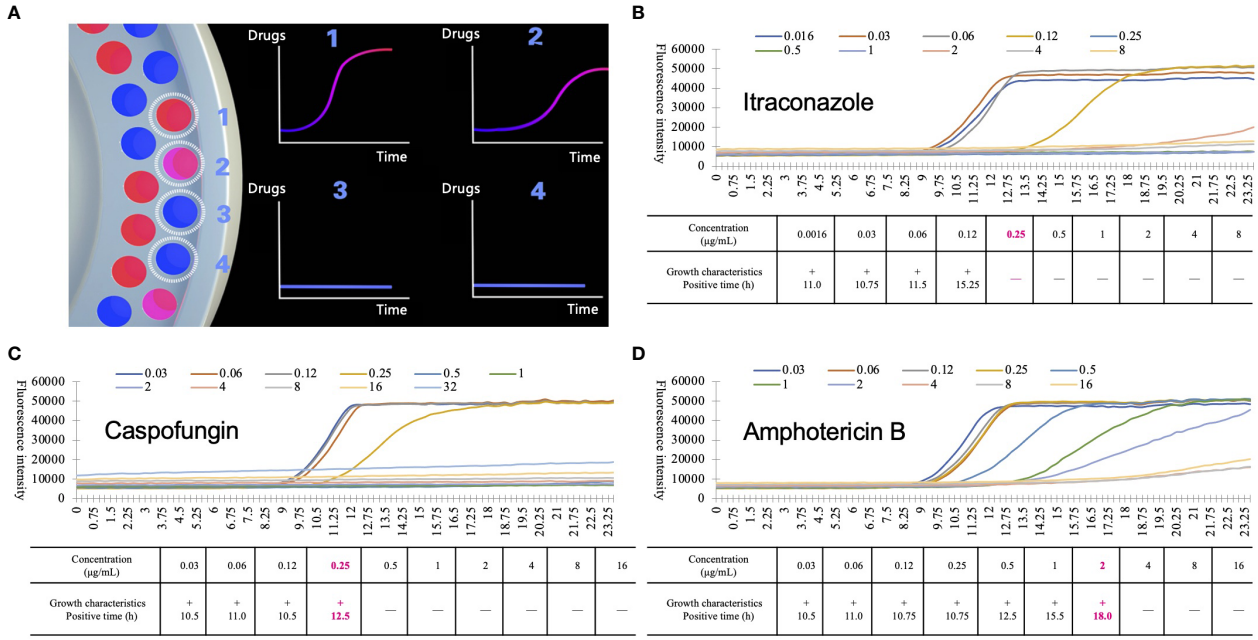


FIGURE 2
Detection principle of automated antimicrobial susceptibility testing system, Droplet 48 (D48). **(A)** the working mode diagram of D48: D48 monitors the fluorescence of microdilution wells containing different concentrations of antifungal agents in real-time and fits the growth characteristics of the strains by the fluorescence intensity over time. If the concentration of antifungal agents was higher than the minimum inhibitory concentration (MIC) of the tested strains (No.3 and No.4), the growth characteristics of the strains changed significantly compared to the microdilution wells containing lower MICs (No.1 and No.2, No.2 grows slightly slower than No.1); **(B-D)** growth characteristics of *Candida krusei* under different concentrations of itraconazole **(B)**, caspofungin **(C)** and amphotericin B **(D)**. During D48 testing, some substances will interfere with the fluorescence signal. Based on a large number of previous data, the MIC value of the agents were finally obtained by excluding the background signal and adding different correction algorithms. Boldfaced and red numbers indicate the MIC and positive reporting time of the antifungal agents.

the D48 and SYO results was also assessed by calculating the Cohen's kappa coefficient. The scale used to assess the degree of agreement was as follows: Kappa of ≤0.2, slight; 0.21–0.40, fair; 0.41–0.60, moderate; 0.61–0.80, substantial; and 0.81–1, almost perfect agreement (Wang et al., 2019).

This study was conducted in accordance with the Declaration of Helsinki and approved by the Ethics Committee of Peking Union Medical College Hospital (protocol code HS-3371, February 2022).

## 3 Results

The MICs for the quality control strains were within the recommended ranges of the CLSI for both assays. This study included 144 strains. Owing to inadequate growth, one *Saccharomyces cerevisiae* strain could not produce the desired results using the D48 method, and one *Rhodotorula mucilaginosa* strain could not obtain the desired results using the SYO method. Therefore, 142 samples were included in the statistical analyses.

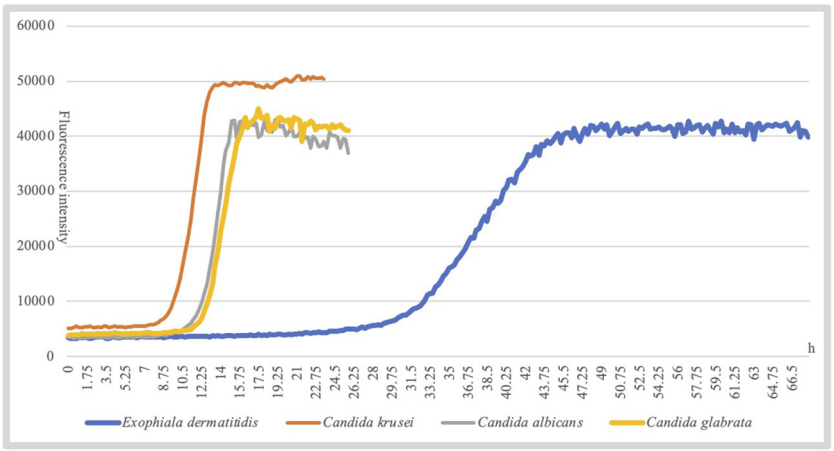


FIGURE 3
Different species of fungi slightly have different growth characteristics.

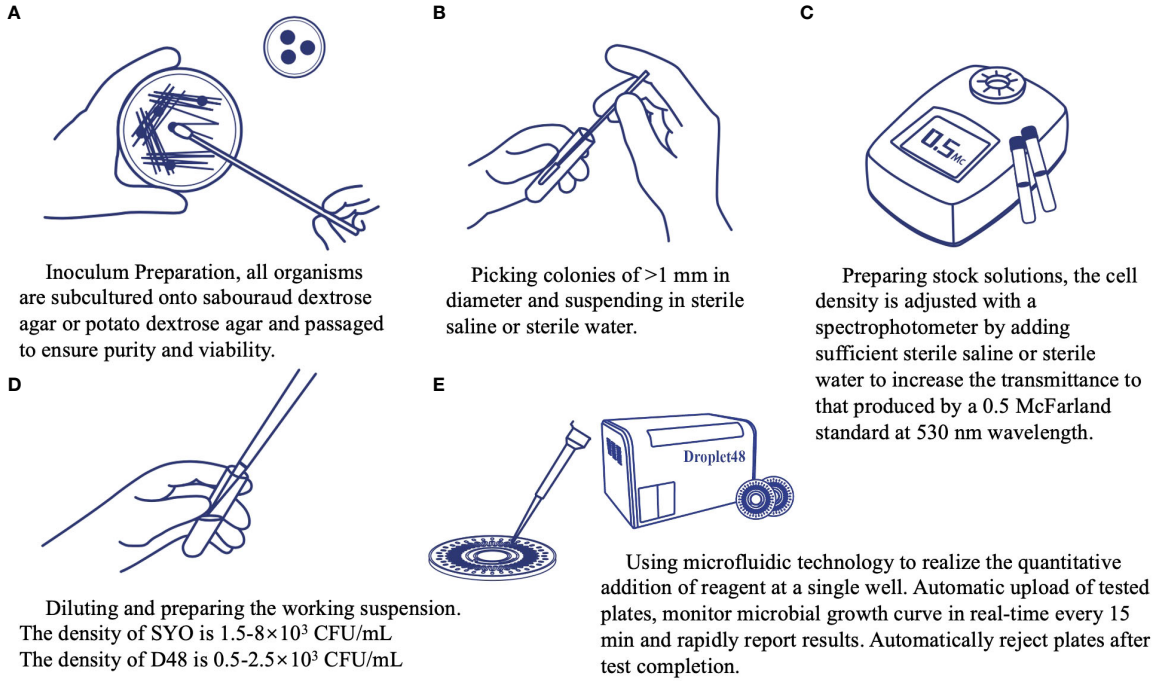


FIGURE 4
Operation procedure of the automated antimicrobial susceptibility testing system, Droplet 48.

The reportable range of D48 fully covered the CBs, ECVs, and quality control ranges of common clinically pathogenic fungi. Combined with microfluidics and other technologies to increase the concentration gradient of more drugs, D48 realizes simultaneous detection of 96 different drug concentrations. Except for 5-flucytosine and voriconazole, there was a slight difference in the reportable ranges between the two methods; however, the ranges were appropriate for clinical fungal isolates from China (Table 1). The reproducibility within ±2 two-fold dilutions was 100% for all the methods. An analysis of the agreement between D48 and SYO identification results is presented in Table 1. The EA (within two two-fold dilutions) between the two methods was best for fluconazole and micafungin (98.59%), followed by itraconazole (97.89%), voriconazole (97.18%), amphotericin B (95.07%), and caspofungin (92.96%). Posaconazole (86.62%) had the lowest EA, which was <90%. The CA of the four antifungal agents (fluconazole, caspofungin, micafungin, and anidulafungin) was >90%, except for voriconazole (87.93%). The highest CA value (98.72%) was observed for micafungin.

We also assessed the discrepancy between the SYO (comparator method) and D48 (Table 1). Two *Candida albicans* and anidulafungin showed MD (2.60%); no other MD or VMD agents were found. Voriconazole (12.07%), fluconazole (7.69%), caspofungin (6.41%), anidulafungin (3.85%), and micafungin (1.28%) were the agents with CBs that all showed mD. Categorical agreement analyses were performed for strains and agents with CBs only, and we used the Cohen's kappa coefficient for further analysis of all the strains and agents with CBs or ECVs. We noticed an almost perfect degree of detection agreement between the D48 and SYO for fluconazole, voriconazole, itraconazole, caspofungin, micafungin, anidulafungin, and 5-flucytosine (Cohen's kappa coefficient ≥0.81). Posaconazole (Cohen's kappa coefficient: 0.06) showed slight agreement, whereas amphotericin B (Cohen's kappa coefficient: 0.47) showed moderate agreement (Table 1).

In recent years, there has been growing interest in cases of uncommon and unknown "superfungal" diseases. In our study, 11 uncommon clinical fungal isolates from the bloodstream were included, and Table 2 displays their MIC values. It is noteworthy that D48's detection of *Trichosporon mucoides* and caspofungin/posaconazole, *Candida norvegensis* and anidulafungin, *Saccharomyces cerevisiae* and amphotericin B/fluconazole was more significant than two two-fold dilutions with SYO. The remaining samples (EA) were 100%. Although we could not interpret the consistency of the two detection methods due to the small number of strains, the MIC values of the tested strains were relatively consistent, which could provide a therapeutic option for patients with clinically rare fungal infections.

## 4 Discussion

A novel automated antimicrobial susceptibility testing system, D48 (Shanghai Fosun Long March Medical Science Co., Ltd.), based

TABLE 1 Reportable range and geometric mean of antifungal agents used in this study and analysis on the agreement of D48 and SYO detection results.

| Antifungal Agents | Reportable Range (μg/mL) | | Geometric Mean (μg/mL) | | % | | | | | Cohen's kappa coefficient [95% confidence interval] |
|---|---|---|---|---|---|---|---|---|---|---|
| | D48 | SYO | D48 | SYO | EA [$N_{EA}/N_T$] | CA [$N_{CA}/N_{CBs}$] | VMD [$N_{VMD}/N_R$] | MD [$N_{MD}/N_S$] | mD [$N_{mD}/N_T$] | |
| Amphotericin B | 0.03–16 | 0.12-8 | 0.76 | 0.54 | 95.07 [135/142] | — | — | — | — | 0.47 [0.11–0.83] |
| Itraconazole | 0.016–8 | 0.015-16 | 0.39 | 0.18 | 97.89 [139/142] | — | — | — | — | 0.85 [0.57–1.14] |
| 5-Flucytosine | 0.06–64 | 0.06-64 | 0.09 | 0.31 | 92.25 [131/142] | — | — | — | — | — |
| Caspofungin | 0.03–32 | 0.008-8 | 0.28 | 0.11 | 92.96 [132/142] | 92.59 [73/78] | 0 | 0 | 6.41 [5/78] | 0.83 [0.70–0.97] |
| Fluconazole | 0.25–256 | 0.12-256 | 1.84 | 2.41 | 98.59 [140/142] | 92.30 [48/52] | 0 | 0 | 7.69 [4/52] | 0.89 [0.82–0.97] |
| Voriconazole | 0.008–8 | 0.008-8 | 0.12 | 0.08 | 97.18 [138/142] | 87.93 [51/58] | 0 | 0 | 12.07 [7/58] | 0.81 [0.70–0.92] |
| Anidulafungin | 0.016–16 | 0.015-8 | 0.36 | 0.09 | 90.85 [129/142] | 93.59 [73/78] | 0 | 2.60 [2/77] | 3.85 [3/78] | 0.83 [0.69–0.97] |
| Micafungin | 0.03-32 | 0.008-8 | 0.06 | 0.07 | 98.59 [140/142] | 98.72 [77/78] | 0 | 0 | 1.28 [1/78] | 0.93 [0.85–1.00] |
| Posaconazole | 0.016–2 | 0.008-8 | 0.15 | 0.12 | 86.62 [123/142] | — | — | — | — | 0.06 [-0.16–0.27] |

EA, essential agreement; minimal inhibitory concentration (MIC) result obtained with Droplet 48 (D48) that is within two two-fold dilution of the MIC value determined by the Sensititre YeastOne (SYO) method. $N_{EA}$ is the number of tests that resulted in EA; CA, categorical agreement; agreement of susceptible, intermediate, susceptible-dose-dependent, and resistant results between the D48 and SYO methods. $N_{CA}$ is the number of tests that result in CA, $N_{CBs}$ is the number of tests that have the Clinical and Laboratory Standards Institute clinical breakpoints, very major discrepancy (VMD) is the major discrepancy, and VMD = $(N_{VMD} \times 100)/N_R$. $N_{VMD}$ is the number of tests that result in a VMD, and $N_R$ is the number of resistant microbial isolates as determined by SYO; MD, major discrepancy; MD = $(N_{MD} \bullet 100)/N_S$. $N_{MD}$ is the number of tests that resulted in an MD; $N_S$ is the number of susceptible microbial isolates as determined by SYO; mD, minor discrepancy, mD = $(N_{mD} \bullet 100)/N_T$, where $N_{mD}$ is the number of tests that result in an mD, and $N_T$ is the total number of isolates tested. If the MIC value of a method was identified as a range value (e.g., ≤2 or >4), the MIC value of another method that differed from its critical value within ±2 two-fold dilutions or within its range was also considered consistent (e.g., 8 vs. >2, 0.016 vs. ≤2, 2 vs. ≤4; 32 vs. >4); a horizontal thin line indicates no data available.

on the growth characteristics of pathogenic fungi, was evaluated in this study. It is real-time, quick, affordable, and simple to promote in clinical pathogenic microbiology laboratories, and avoids the subjectivity of manually reading MICs. The Fungi and Mycosis Research Center of Peking University compared the detection results of D48 and CLSI BMD methods when applied to the China Medical Device Product Registration Certificate (No.20192220368 and No.20192400349), and the EA of nine antifungal drugs were all >90%, which is consistent. Therefore, this study did not compare D48 with the BMD reference method.

According to the CLSI criteria for the verification of commercial antimicrobial susceptibility testing systems, SYO approved by the U.S. FDA was chosen as the comparator method. Importantly, the CLSI M52 document stipulates that when a clinical laboratory desires to implement a new AFST system, it should be compared with the commercial method that the laboratory is already using and meets the criteria.

The D48 should be verified for specific agent/fungus combinations tested when 1) CA and EA (if reporting MICs) are ≥90% compared to that in the current system; 2) VMD rate was <3% of total resistant isolates; and 3) MD rate was <3% for all susceptible isolates (Clinical and Laboratory Standards Institute, 2015). According to our study, all the agents and strains met the CLSI laboratory criteria, except for posaconazole (EA rate, 86.62%) and voriconazole (CA rate, 87.93%).

The Cohen's kappa coefficient for amphotericin B was 0.47, while the EA rate was 95.07%. The Cohen's kappa coefficient was calculated for strains with ECVs values, which reduced the sample data size compared with the EA included in all samples for calculation. Additionally, one *Candida albicans*, one *Cryptococcus neoformans*, and one *Trichosporon asahii* had inconsistent amphotericin B ECVs between the two methods, thereby leading to this discrepancy. Because the EA of the two methods was better than 90% for amphotericin B, we believe that the D48 has excellent performance in detecting amphotericin B.

TABLE 2 Minimal inhibitory concentration (μg/mL) detection results of D48 and SYO for quality control strains and rare clinical infection fungi .

| Isolates | Amphotericin B | | Itraconazole | | 5-flucytosine | | Caspofungin | | Fluconazole | | Voriconazole | | Anidulafungin | | Micafungin | | Posaconazole | |
|---|---|---|---|---|---|---|---|---|---|---|---|---|---|---|---|---|---|---|
| | D48 | SYO | D48 | SYO | D48 | SYO | D48 | SYO | D48 | SYO | D48 | SYO | D48 | SYO | D48 | SYO | D48 | SYO |
| ATCC 22019 | 0.5 | 0.5 | 0.12 | 0.12 | 0.25 | 0.5 | 0.5 | 0.25 | 2 | 2 | 0.06 | 0.03 | 0.5 | 0.5 | 0.5 | 1 | 0.06 | 0.06 |
| ATCC 6258 | 2 | 1 | 0.5 | 0.25 | 8 | 8 | 0.5 | 0.25 | 16 | 32 | 0.25 | 0.25 | 0.12 | 0.06 | 0.25 | 0.25 | 0.25 | 0.25 |
| *Saccharomyces cerevisiae* | **4** | **0.5** | 0.25 | 0.12 | ≤0.06 | ≤0.06 | 0.25 | 0.12 | **16** | **2** | 0.06 | 0.03 | 0.25 | 0.12 | *0.25* | *0.06* | 0.12 | 0.25 |
| | **16** | **0.5** | 0.25 | 0.25 | *0.25* | *≤0.06* | 0.25 | 0.25 | 2 | 2 | *0.25* | *.06* | 0.12 | 0.12 | 0.25 | 0.12 | *1* | *0.25* |
| | — | 0.5 | — | 0.5 | — | ≤0.06 | — | 0.5 | — | 4 | — | 0.12 | — | 0.25 | — | 0.12 | — | 0.5 |
| *Kodamaea ohmeri* | 0.5 | 0.5 | *0.5* | *0.12* | ≤0.06 | ≤0.06 | 0.25 | 0.12 | 8 | 4 | 0.12 | 0.06 | *0.5* | *0.12* | 0.12 | 0.12 | 0.12 | 0.06 |
| | 0.5 | 0.5 | 0.25 | 0.12 | ≤0.06 | ≤0.06 | 0.25 | 0.25 | 8 | 16 | 0.12 | 0.06 | 0.25 | 0.25 | 0.06 | 0.12 | 0.12 | 0.06 |
| *Pichia pastoris* | *4* | *1* | 0.5 | 0.5 | 16 | 8 | 0.25 | 0.5 | 64 | 128 | *0.25* | *1* | 0.12 | 0.06 | 0.12 | 0.12 | 0.25 | 0.5 |
| *Rhodotorula mucilaginosa* | 1 | — | 4 | — | ≤0.06 | — | 0.12 | — | ≤0.25 | — | 4 | — | >16 | — | 2 | — | ≤0.016 | — |
| *Candida nivariensis* | 2 | 1 | 0.25 | 0.5 | *1* | *0.25* | 0.12 | 0.06 | 4 | 4 | 0.06 | 0.12 | *0.06* | *≤0.015* | ≤0.03 | 0.015 | *0.12* | *0.5* |
| *Candida norvegensis* | *1* | *0.25* | *0.5* | *0.12* | *16* | *4* | *0.12* | *0.03* | 16 | 16 | 0.25 | 0.12 | **0.12** | **≤0.015** | 0.06 | 0.03 | 0.12 | 0.06 |
| *Trichosporon mucoides* | 1 | 0.5 | 0.25 | 0.25 | 16 | 32 | **2** | **>8** | 4 | 4 | 0.25 | 0.12 | >16 | >8 | >32 | >8 | **1** | **0.12** |
| *Lodderomyces elongisporus* | 0.5 | 0.25 | 0.06 | 0.12 | 1 | 0.5 | 0.12 | 0.06 | 0.5 | 0.5 | 0.016 | ≤0.008 | *0.06* | *≤0.015* | ≤0.03 | 0.03 | 0.06 | 0.12 |

"—" Indicates failure to detect minimal inhibitory concentration (MIC) of the isolate and antifungal agents; Italicized numbers indicate the discrepancy between the two antifungal susceptibility testing (AFST) methods was within ±2 two-fold dilutions for antifungal agents; Boldfaced numbers indicate the discrepancy was more than ±2 two-fold dilutions for antifungal agents. SYO, Sensititre YeastOne; D48, Droplet 48.





10.3389/fcimb.2023.1153544

The agreement between the two methods has also been evaluated in different species. The lowest CA rate (70%) was found for *Candida glabrata* and caspofungin, followed by 75% for *Candida albiacans* and voriconazole, 81.25% for *Candida albicans* and anidulafungin, 84.62% for *Candida parapsilosis* and fluconazole, and 87.50% for *Candida krusei* and voriconazole/caspofungin. The CA of the other strains and agents were >90%. Except for *Candida albicans* and anidulafungin whose MD was 12.5%, none of the isolates showed VMD or MD. *Candida glabrata* and caspofungin were associated with up to 30% mD, followed by *Candida albicans* and voriconazole (25.0%), *Candida parapsilosis* and fluconazole (15.38%), and *Candida krusei* and voriconazole (12.50%). The test range, $MIC_{50}$, $MIC_{90}$, and agreement rate between D48 and SYO for each species are shown in Supplementary Table 1. Since a sample size <30 is insufficient to identify discrepancies around the CBs while testing to verify the new antifungal susceptibility testing system, the agreement rate between some strains and antifungal agents was <90%, or MD was >3%, possibly because the number of tested strains was too small. The detection accuracy of different species should be verified by testing additional isolates.

In our study, the MIC was occasionally not determined accurately by the SYO because of "trailing growth" (Luna-Tapia et al., 2019). This phenomenon was mainly observed in *Candida albicans* and *Candida tropicalis*, which appeared as slight color changes and persisted in microdilution wells with concentrations greater than the MIC value (Figures 5A, B). According to several studies, *Candida tropicalis* has distinct phenotypes and genotypes for azole resistance and trailing (Astvad et al., 2018; Chen et al., 2021a; Chen et al., 2021b). Heavy trailing isolates were less susceptible to voriconazole, although weak trailing isolates (<25% of the positive growth control) were common and did not impair voriconazole efficacy (Astvad et al., 2018). Our research found that it is more challenging to precisely estimate how much "trailing growth" has occurred, and that this problem still has to be addressed in future development of the AFST technology.

Some strains can occasionally survive and grow in concentrations above the MIC, a phenomenon described as the "paradoxical growth effect" or "Eagle Effect" (Wagener and Loiko, 2017) of itraconazole and voriconazole (Figures 5C-F). It has been about 70 years since the "Eagle Effect" was first described for bacterial species. However, the "caspofungin paradoxical effect" (CPE) and other echinocandins have been frequently reported (Wagener and Loiko, 2017; Valero et al., 2020; Valero et al., 2022). However, its occurrence in azoles has not been reported. Because of the importance of the calcium/calcineurin/transcription factor-CrzA pathway in the regulation of CPE, one study on *Aspergillus fumigatus* discovered that 100% of ΔcrzAAf293 conidia did not exhibit CPE, while all ΔcrzACEA17 conidia did. A phenotype that should be regarded as antifungal tolerant is called CPE, a genetically encoded adaptive trait (Zhao et al., 2022). To determine whether the "paradoxical growth effect" can prevent invasive fungal diseases from being treated effectively in clinical settings, it is necessary to have a thorough understanding of the mechanisms underlying this phenomenon, as well as additional research on whether it exists in the human body.

In conclusion, we developed an innovative AFST system, D48, based on the growth characteristics of pathogenic fungi for the rapid determination of antifungal susceptibility profiles of fungal strains. Fluconazole, itraconazole, caspofungin, micafungin, anidulafungin, amphotericin B, and 5-flucytosine are seven regularly used clinical antifungal agents, and that D48's sensitivity detection performance was highly consistent with that of SYO. Therefore, D48 can be considered an optional assay that is more automated than the currently widely used commercial methods, and can provide results and interpretation more quickly than the traditional methods. However, further research involving more clinical isolates is required to optimize the detection performance of posaconazole/voriconazole and establish the validity of the D48 assay.

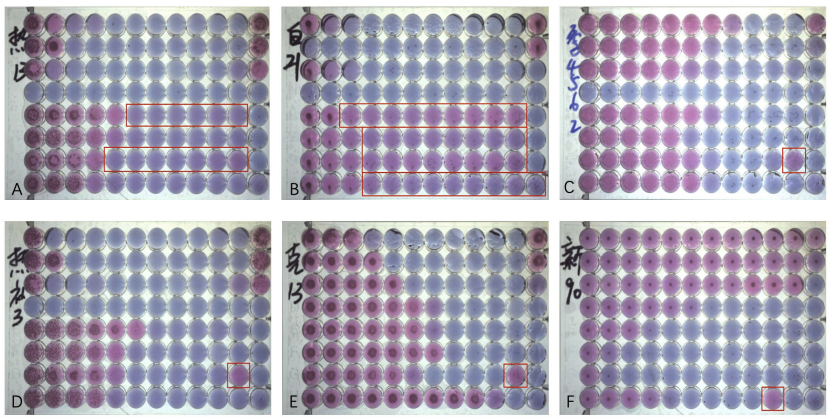


FIGURE 5
Antifungal Susceptibility Testing using Sensititre YeastOne (SYO) colorimetric antifungal panel (Thermo Fisher Scientific). **(A)** Weak "trailing growth" of posaconazole and itraconazole in *Candida tropicalis*. **(B)** Heavy "trailing growth" of posaconazole, voriconazole, itraconazole, and fluconazole in *Candida albicans*; **(C)** "Eagle effect" with itraconazole in *Candida guilliermondii*; **(D)** "Eagle effect" with itraconazole in Candida tropicalis. **(E)** "Eagle effect" with itraconazole in *Candida krusei*; and **(F)** "Eagle effect" with fluconazole in *Cryptococcus neoforman*.

## Data availability statement

The original contributions presented in the study are included in the article/Supplementary Material. Further inquiries can be directed to the corresponding author.

## Ethics statement

The study was conducted in accordance with the Declaration of Helsinki and approved by the Ethics Committee of Peking Union Medical College Hospital (protocol code HS-3371, February 2022).

## Author contributions

All authors listed have made a substantial, direct, and intellectual contribution to the work, and approved it for publication.

## Funding

This research was funded by the National High Level Hospital Clinical Research Funding [2022-PUMCH-C-052], National Natural Science Foundation of China (grant numbers 82202592 and 82002258), and the Beijing Natural Science Foundation (grant number 7222125).

## Acknowledgments

Fosun Diagnostics Technology (Shanghai) Co., Ltd. provided instruments and technical support to support this study.

## Conflict of interest

The authors declare that the research was conducted in the absence of any commercial or financial relationships that could be construed as a potential conflict of interest.

## Publisher's note

All claims expressed in this article are solely those of the authors and do not necessarily represent those of their affiliated organizations, or those of the publisher, the editors and the reviewers. Any product that may be evaluated in this article, or claim that may be made by its manufacturer, is not guaranteed or endorsed by the publisher.

## Supplementary material

The Supplementary Material for this article can be found online at: https://www.frontiersin.org/articles/10.3389/fcimb.2023.1153544/full#supplementary-material

## References

Astvad, K. M. T., Sanglard, D., Delarze, E., Hare, R. K., and Arendrup, M. C. (2018). Implications of the EUCAST trailing phenomenon in candida tropicalis for the *In Vivo* susceptibility in invertebrate and murine models. *Antimicrobial. Agents Chemother.* 62 (12), e01624–18. doi: 10.1128/AAC.01624-18

U.D.o.H.a.H.S *Centers for Medicare & Medicaid services, laboratory requirements; standard: establishment and verification of performance specifications* (US Government Printing Office). Available at: https://www.cms.gov/Regulations-and-Guidance/Legislation/CLIA.

Bassetti, M., Vena, A., Bouza, E., Peghin, M., Muñoz, P., Righi, E., et al. (2020). Antifungal susceptibility testing in candida, aspergillus and cryptococcus infections: are the MICs useful for clinicians? *Clin. Microbiol. Infection* 26, 1024–1033. doi: 10.1016/j.cmi.2020.02.017

Berkow, E. L., Lockhart, S. R., and Ostrosky-Zeichner, L. (2020). Antifungal susceptibility testing: current approaches. *Clin. Microbiol. Rev.* 33 (3), e00069–19. doi: 10.1128/CMR.00069-19

Cansizoglu, M. F., Tamer, Y. T., Farid, M., Koh, A. Y., and Toprak, E. (2019). Rapid ultrasensitive detection platform for antimicrobial susceptibility testing. *PloS Biol.* 17, e3000291. doi: 10.1371/journal.pbio.3000291

Chen, P. Y., Chuang, Y. C., Wu, U. I., Sun, H. Y., Wang, J. T., Sheng, W. H., et al. (2021a). Mechanisms of azole resistance and trailing in candida tropicalis bloodstream isolates. *J. Fungi (Basel)* 7 (11), 932932. doi: 10.3390/jof7080612

Chen, P.-Y., Chuang, Y.-C., Wu, U.-I., Sun, H.-Y., Wang, J.-T., Sheng, W.-H., et al. (2021b). Correction: Chen et al. mechanisms of azole resistance and trailing in candida tropicalis bloodstream isolates. *J. Fungi* 7, 612. doi: 10.3390/jof7080612

Clinical and Laboratory Standards Institute (2015). "Verification of commercial microbial identification and antimicrobial susceptibility testing systems," in *Approved standard. CLSI guideline M52, 1st Ed* (Wayne, PA: Clinical and Laboratory Standards Institute).

Clinical and Laboratory Standards Institute (2022a). "Performance standards for antifungal susceptibility testing of yeasts," in *Approved standard. CLSI supplement M27M44S, 3rd Ed* (Wayne, PA: Clinical and Laboratory Standards Institute).

Clinical and Laboratory Standards Institute (2022b). "Epidemiological cutoff values for antifungal susceptibility testing," in *Approved standard. CLSI supplement M57S, 4th Ed* (Wayne, PA: Clinical and Laboratory Standards Institute).

Delma, F. Z., Al-Hatmi, A. M. S., Buil, J. B., van der Lee, H., Tehupeiory-Kooreman, M., de Hoog, G. S., et al. (2020). Comparison of MIC test strip and sensititre YeastOne with the CLSI and EUCAST broth microdilution reference methods for *In Vitro* antifungal susceptibility testing of cryptococcus neoformans. *Antimicrobial. Agents Chemother* 64 (4), e02261–19. doi: 10.1128/AAC.02261-19

Durand, C., Maubon, D., Cornet, M., Wang, Y., Aldebert, D., and Garnaud, C. (2021). Can we improve antifungal susceptibility testing? *Front. Cell Infect. Microbiol.* 11, 720609. doi: 10.3389/fcimb.2021.720609

Farid, M., Rodrigues, M., England, R., and Toprak, E. (2022). Label-free optical detection of pathogenic bacteria and fungi at extremely low cell densities for rapid antibiotic susceptibility testing. *Front. Bioeng. Biotechnol.* 10, 884200. doi: 10.3389/fbioe.2022.884200

Fisher, M. C., Alastruey-Izquierdo, A., Berman, J., Bicanic, T., Bignell, E. M., Bowyer, P., et al. (2022). Tackling the emerging threat of antifungal resistance to human health. *Nat. Rev. Microbiol.* 20, 557–571. doi: 10.1038/s41579-022-00720-1

Luna-Tapia, A., Butts, A., and Palmer, G. E. (2019). Loss of c-5 sterol desaturase activity in candida albicans: azole resistance or merely trailing growth? *Antimicrob. Agents Chemother.* 63 (1), e01337–18. doi: 10.1128/AAC.01337-18

U.D.o.H.a.H.S. (2023). Centers for Medicare & Medicaid services, laboratory requirements; standard: Establishment and verification of performance specifications (US Government Printing Office). Available at: https://www.cms.gov/Regulations-and-Guidance/Legislation/CLIA (Accessed January 23, 2023).

Valero, C., Colabardini, A. C., de Castro, P. A., Amich, J., Bromley, M. J., and Goldman, G. H. (2022). The caspofungin paradoxical effect is a tolerant "Eagle effect" in the filamentous fungal pathogen aspergillus fumigatus. *mBio* 13, e0044722. doi: 10.1128/mbio.00447-22

Valero, C., Colabardini, A. C., Chiaratto, J., Pardeshi, L., de Castro, P. A., Ferreira Filho, J. A., et al. (2020). Aspergillus fumigatus transcription factors involved in the caspofungin paradoxical effect. *mBio* 11 (3), e00816–20. doi: 10.1128/mBio.00816-20

van Belkum, A., Burnham, C.-A. D., Rossen, J. W. A., Mallard, F., Rochas, O., and Dunne, W. M. (2020). Innovative and rapid antimicrobial susceptibility testing systems. *Nat. Rev. Microbiol.* 18, 299–311. doi: 10.1038/s41579-020-0327-x

Wagener, J., and Loiko, V. (2017). Recent insights into the paradoxical effect of echinocandins. *J. Fungi (Basel)* 4 (1), 5. doi: 10.3390/jof4010005

Wang, Y., Andriampamonjy, A. N., Bailly, S., Garnaud, C., Maubon, D., Cornet, M., et al. (2019). New antifungal susceptibility test based on chitin detection by image cytometry. *Antimicrob. Agents Chemother* 64 (1), e01101–19. doi: 10.1128/AAC.01101-19

Zhang, H., Aonbangkhen, C., Tarasovetc, E. V., Ballister, E. R., Chenoweth, D. M., and Lampson, M. A. (2017). Optogenetic control of kinetochore function. *Nat. Chem. Biol.* 13, 1096–1101. doi: 10.1038/nchembio.2456

Zhao, S., Martin-Vicente, A., Colabardini, A. C., Pereira Silva, L., Rinker, D. C., Fortwendel, J. R., et al. (2022). Genomic and molecular identification of genes contributing to the caspofungin paradoxical effect in aspergillus fumigatus. *Microbiol. Spectr.* 10, e0051922. doi: 10.1128/spectrum.00519-22

frontiers | Frontiers in Cellular and Infection Microbiology

TYPE Brief Research Report
PUBLISHED 17 May 2023
DOI 10.3389/fcimb.2023.1165017



OPEN ACCESS

EDITED BY
Michael Marceau,
Université Lille Nord de France, France

REVIEWED BY
Andrew McDowell,
Ulster University, United Kingdom
Llanos Salar Vidal,
University Hospital Fundación Jiménez Díaz, Spain

*CORRESPONDENCE
Holger Brüggemann
brueggemann@biomed.au.dk

RECEIVED 13 February 2023
ACCEPTED 02 May 2023
PUBLISHED 17 May 2023

CITATION
Ponraj DS, Lund M, Lange J, Poehlein A, Himmelbach A, Falstie-Jensen T, Jørgensen NP, Ravn C and Brüggemann H (2023) Shotgun sequencing of sonication fluid for the diagnosis of orthopaedic implant-associated infections with *Cutibacterium acnes* as suspected causative agent.
*Front. Cell. Infect. Microbiol.* 13:1165017.
doi: 10.3389/fcimb.2023.1165017



# Shotgun sequencing of sonication fluid for the diagnosis of orthopaedic implant-associated infections with *Cutibacterium acnes* as suspected causative agent

Diana Salomi Ponraj[1], Michael Lund[2], Jeppe Lange[1,3], Anja Poehlein[4], Axel Himmelbach[5], Thomas Falstie-Jensen[6], Nis Pedersen Jørgensen[7], Christen Ravn[6] and Holger Brüggemann[2*]

[1]Department of Clinical Medicine, Aarhus University, Aarhus, Denmark, [2]Department of Biomedicine, Aarhus University, Aarhus, Denmark, [3]Department of Orthopaedic Surgery, Regional Hospital, Horsens, Denmark, [4]Department of Genomic and Applied Microbiology, Institute of Microbiology and Genetics, University of Göttingen, Göttingen, Germany, [5]Leibniz Institute of Plant Genetics and Crop Plant Research (IPK), Gatersleben, Germany, [6]Department of Orthopaedic Surgery, Aarhus University Hospital, Aarhus, Denmark, [7]Department of Infectious Diseases, Aarhus University Hospital, Aarhus, Denmark

Orthopaedic implant-associated infections (OIAIs) due to *Cutibacterium acnes* can be difficult to diagnose. The aim of this pilot study was to determine if metagenomic next-generation sequencing (mNGS) can provide additional information to improve the diagnosis of *C. acnes* OIAIs. mNGS was performed on sonication fluid (SF) specimens derived from 24 implants. These were divided into three groups, based on culture results: group I, culture-negative (n = 4); group II, culture-positive for *C. acnes* (n = 10); and group III, culture-positive for other bacteria (n = 10). In group I, sequence reads from *C. acnes* were detected in only one SF sample, originating from a suspected case of OIAIs, which was SF and tissue culture-negative. In group II, *C. acnes* sequences were detected in 7/10 samples. In group III, *C. acnes* sequence reads were found in 5/10 samples, in addition to sequence reads that matched the bacterial species identified by culture. These samples could represent polymicrobial infections that were missed by culture. Taken together, mNGS was able to detect *C. acnes* DNA in more samples compared to culture and could be used to identify cases of suspected *C. acnes* OIAIs, in particular regarding possible polymicrobial infections, where the growth of *C. acnes* might be compromised due to a fast-growing bacterial species. However, since SF specimens are usually low-biomass samples, mNGS is prone to DNA contamination, possibly introduced during DNA extraction or sequencing procedures. Thus, it is advisable to set a sequence read count threshold, taking into account project- and NGS-specific criteria.

KEYWORDS

***Cutibacterium acnes*, shotgun sequencing, metagenomics, orthopaedic implant-associated infections, prosthetic infections, sonication fluid**

# 1 Introduction

*Cutibacterium acnes* (formerly known as *Propionibacterium acnes*) is a Gram-positive slow-growing anaerobic bacterium (SGAB). It is a skin commensal that has also been implicated in various implant-associated infections, including orthopaedic implant-associated infections (OIAIs) (Zeller et al., 2007; McDowell et al., 2013; Achermann et al., 2014; Aubin et al., 2014; Ponraj et al., 2021). However, the diagnosis of OIAIs caused by SGAB such as *C. acnes* is complicated because of non-specific or even absent clinical, radiological, histopathological, and laboratory diagnostic features (Achermann et al., 2014; Aubin et al., 2014; Ponraj et al., 2021). Microbiological diagnosis based on culture can also be constrained by the need for prolonged incubation, due to the bacterium's slow-growing nature, along with the attendant increased risk of sample contamination (Butler-Wu et al., 2011).

Culture-independent methods can potentially help to offset this problem (Gu et al., 2019). Culture-independent microbiological methods contain polymerase chain reaction (PCR)-based methods and sequencing-based methods; the latter comprise amplicon-based next-generation sequencing (aNGS) and metagenomic NGS (mNGS) (Tande and Patel, 2014; Ponraj et al., 2021). The utility of mNGS in the diagnosis of OIAIs from various specimens including synovial fluid aspirates and tissue samples has been reported previously (Ivy et al., 2018; Weaver et al., 2019; Cai et al., 2020; Fang et al., 2020; Huang et al., 2020; Kildow et al., 2021; Tan et al., 2022). However, only a few mNGS studies have so far been reported regarding the use of sonication fluid (SF) to support the diagnosis of OIAIs (Street et al., 2017; He et al., 2021) and, to the best of our knowledge, none with a specific focus on *C. acnes*.

In our previous study, we reported on the sonication of 100 orthopaedic implants that were removed for both presumed aseptic reasons and suspected infection (Ponraj et al., 2022). SF samples were further subjected to culture-dependent and culture-independent analyses. Thereby, an aNGS approach was employed to detect and phylotype *C. acnes*, and this along with the patients' clinical information as well as whole-genome sequencing of the *C. acnes* isolates was used to differentiate *C. acnes* contamination from true infection.

The aim of this pilot study was to determine if mNGS of SF provides an additional value in the diagnosis of OIAIs due to *C. acnes*. Therefore, mNGS of SF from 24 implants was carried out, and the mNGS data were compared to other data available regarding these implants, including aNGS and tissue culture results. The results show that *C. acnes* was more often detected by mNGS than by culture and could potentially help to identify cases of *C. acnes* OIAIs that might be missed by culture alone.

# 2 Methods

## 2.1 Sample selection

In a previous study, 100 implants removed during revision surgery were collected between August 2019 and September 2020 and processed by sonication (Ponraj et al., 2022). SF specimens from 24 of the 100 implants were included in this pilot study. The selection was based on the SF culture results, and the included specimens were divided into three groups: group I, culture-negative (n = 4); group II, culture-positive for *C. acnes* (n = 10); and group III, culture-positive for other bacteria, i.e., staphylococci and *Finegoldia magna* (n = 10). In addition, normal saline that was sonicated and processed like SF from implants was included as the negative control.

## 2.2 DNA extraction from sonication fluid

Implants removed during revision surgeries were processed by the previously described vortex-sonication method (Borens et al., 2013). The resultant SF was split into two samples, one for culture-dependent analyses and another for culture-independent analyses. The samples for culture-independent analyses were stored at −20°C until processing. DNA extraction of the SF and the negative control was described previously (Ponraj et al., 2022). In brief, SF (40 ml) stored at −20°C was thawed overnight at 4°C, concentrated by centrifugation (15,000 × *g* for 1 h at 16°C using rotor F 13–14 × 50 Cy, Thermo Scientific™ Sorvall™ RC 6 Plus Centrifuge), and DNA extraction was performed using the DNeasy PowerSoil Kit (QIAGEN, Hilden, Germany) as per manufacturer's instructions. DNA concentrations were measured using the Qubit dsDNA HS Assay (Thermo Fisher Scientific, Waltham, MA, USA) with a Qubit fluorometer. The same DNA extraction kit was used for the 24 samples to exclude any possible batch effect.

## 2.3 Library preparation and Illumina HiSeq sequencing

Illumina shotgun libraries were prepared using the Illumina DNA Prep Tagmentation Kit and Nextera DNA CD Indexes for multiplexing as recommended by the manufacturer (Illumina, San Diego, CA, USA). To assess the quality and size of the libraries, samples were run on an Agilent Bioanalyzer 2100 using an Agilent High Sensitivity DNA Kit as recommended by the manufacturer (Agilent Technologies, Waldbronn, Germany). The concentration of the libraries was determined using the Qubit dsDNA HS Assay Kit as recommended by the manufacturer (Life Technologies GmbH, Darmstadt, Germany). Sequencing was performed by using the NovaSeq6000 instrument (Illumina Inc., San Diego, CA, USA) using the NovaSeq6000 SP Reagent Kit (v. 1.5) and the NovaSeq XP 2-Lane Kit (v. 1.5) for sequencing in the paired-end mode 2 × 250 cycles.

## 2.4 Bioinformatics

The raw sequencing data were paired, and the paired-end reads along with metadata were uploaded and analysed using the publicly available web-based MG-RAST pipeline (https://www.mg-rast.org/)

(Meyer et al., 2019). The workflow involves the following steps: 1) normalization or quality control where artificial duplicate reads are removed along with quality- and length-based trimming; 2) screening of sequences for potential protein-coding genes using a BLASTX search against multiple databases; 3) functional assignments and taxonomic distributions using the matches to external databases. To further analyse sequence reads that were assigned to *Cutibacterium* sp. or *Finegoldia* sp., the reads were extracted in MG-RAST and mapped to their corresponding genomes. Complete genomes of *C. acnes* KPA171202, *Cutibacterium avidum* 44067, *F. magna* ATCC29328, and "*Finegoldia nericia*" 09T494 were used as reference genomes and subsequently indexed using Bowtie2 (v. 2.5.0) (Langmead and Salzberg, 2012). The extracted query reads were mapped to the reference genomes using Bowtie2, and the resulting SAM-files were converted into BAM-files and indexed using Samtools (v. 1.6) (Li et al., 2009). Resulting BAM-files and reference genomes were imported into Geneious Prime (v. 2023.0.1) to visualize mapping results.

In an additional analysis, the mNGS data were analysed using Kraken2/Bracken. First, human DNA reads were removed as follows: paired-end reads were mapped against the Genome Reference Consortium human genome build 38 (GRCh38) using Bowtie2 (v. 2.5.1) (Langmead and Salzberg, 2012). Any reads concordantly or discordantly mapped to the human reference genome were removed from the samples using Samtools (v. 1.6) and Bedtools (v. 2.30.0). The resulting filtered FASTQ-files were classified using Kraken2 (v. 2.1.2) (Wood et al., 2019) using a database consisting of bacteria, archaea, viruses, and plasmids with a minimum hit group of 3. The classification was subsequently re-estimated using Bracken (v. 2.5.0) (Lu et al., 2017). Since the Kraken2/Bracken analysis is more sensitive, resulting in more taxonomically assigned reads than MG-RAST, we introduced a minimum read count threshold of 150 (corresponding to approx. 0.1% of the total amount of bacterial reads per sample). Four samples had *C. acnes* reads <150, i.e., samples 2 and 3 in group II, and samples 9 and 10 in group III.

## 2.5 Amplicon NGS control PCR

To test the sensitivity of the aNGS approach (in detail described previously in Ponraj et al., 2022), a PCR was performed with the single-locus sequence typing (SLST) primers (5′-TTGCTCGCAACTGC AAGCA-3′ and 5′-CCGGCTGGCAAATGAGGCAT-3′) and different amounts (1,000 to 0.001 pg) of *C. acnes* genomic DNA (strain 266). The PCR contained 5 µl of genomic DNA template, 2.5 µl of AccuPrime PCR Buffer II (Invitrogen, Waltham, MA, USA), 1.5 µl of each primer (10 µM; DNA Technology, Risskov, Denmark), 0.15 µl of AccuPrime Taq DNA Polymerase High Fidelity (Invitrogen, Waltham, MA, USA), and 14.35 µl of PCR-grade water. The PCR was performed using the following cycle conditions: initial denaturation at 94°C for 2 min, 35 cycles of denaturation at 94°C for 20 s, annealing at 55°C for 30 s, elongation at 68°C for 1 min, and final elongation step at 72°C for 5 min.

## 2.6 Ethical approval

The study was registered with Region Midtjylland with reference number 661624. The Central Denmark Region ethical committee waived the need for ethical approval.

## 2.7 Statistical analyses

Data were entered in Excel, and graphs and charts were prepared using Prism GraphPad.

# 3 Results

Sequencing (mNGS) of SF specimens from 24 implants, divided into three groups (group I, culture-negative (n = 4); group II, culture-positive for *C. acnes* (n = 10); group III, culture-positive for other bacteria (n = 10)) was performed. The anatomical locations of the selected 24 implants from the three groups are shown in Figure 1. The majority of the implants were from the shoulder, followed by the hip.

Shotgun sequencing of DNA extracted from the 24 SF samples resulted in an average of 8,437,406 sequence reads per sample (range, 5,898,825–12,907,838). The data were first analysed with MG-RAST for taxonomic assignment of sequence reads. The total numbers of sequence reads, and sequence reads that passed quality control are given in Table S1. The average number of reads that passed quality control was 778,496 (range, 443,276–1,424,198) (9.2%). The top 10 genera assigned by MG-RAST for the 24 SF samples as well as the number of reads and percentage of total reads for each genus are given in Table S2. No sequence reads were obtained from the saline control sample.

Overall, the percentage of human DNA across the 24 SF samples in the three groups was higher than the percentage of bacterial DNA (Figures 2A, B). Reads that matched non-bacterial genera like *Canis*, *Macaca*, *Drosophila*, and *Danio* were also detected in all SF samples (Table S2). In addition, several SF samples showed the apparent presence of DNA from gut bacteria like the genera *Coprobacillus* (n = 23), *Bacteroides* (n = 13), *Prevotella* (n = 10), and *Clostridium* (n = 7). We also used an alternative approach to analyse the data, by first filtering and discarding reads that matched the human genome and subsequently analysing the remaining reads with Kraken2/Bracken for taxonomic assignment (Table 1).

In the following, mNGS results are outlined for the three groups and presented in the context of other results, i.e., SF culture and aNGS data regarding the detection of *C. acnes*.

- Group I—culture negative: in three out of four SF specimens in group I, no sequence reads matching *C. acnes* were detected by mNGS. This corresponded with aNGS results, as all three samples were negative for *C. acnes* by SLST PCR (Ponraj et al., 2022). In one SF sample (group I #4), *C. acnes* DNA was detected (793 reads (MG-RAST);

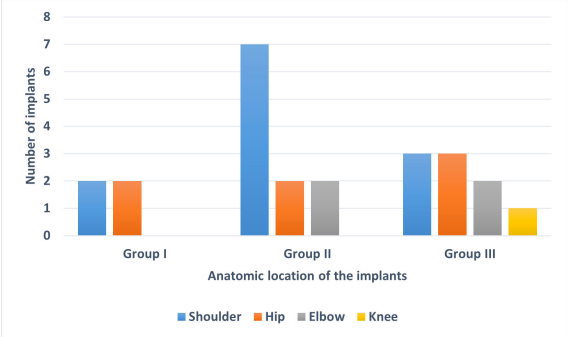


FIGURE 1
Anatomic location of the 24 implants used in this study. The implants were divided into three groups based on sonication fluid culture results: Group I: culture-negative, Group II: culture-positive for *C. acnes* and Group III: culture-positive for organisms other than *C. acnes*.

1,240 reads (Kraken2/Bracken)) (Table 1). The corresponding implant was both SF and tissue culture-negative; aNGS was not performed for this SF specimen. The implant was removed due to suspected infection diagnosed by the presence of a sinus tract, so *C. acnes* could potentially represent the causative agent that was missed by culture.

- Group II—culture-positive for *C. acnes*: group II included 10 samples that were SF culture-positive for *C. acnes* (Table 1). mNGS detected sequence reads matching *C. acnes* in seven of the 10 samples in this group. In these seven samples, 401 to 2,918 *C. acnes* sequence reads (average 1,271 reads) were identified with MG-RAST, corresponding to 2.5% to 20.5% of all detected bacterial reads. A slightly higher number of *C. acnes* reads were found with the Kraken2/Bracken approach (average 2,256 reads). Regarding the three samples, for which no *C. acnes* reads were obtained, one of them (group II #1) was also aNGS-negative (Table 1). In addition, the SF culture showed *C. acnes* growth with a low colony-forming unit (CFU) count of only 20 CFU/ml, and the five tissue cultures from that implant had no bacterial growth. Thus, *C. acnes* in this case could likely be a contaminant, possibly obtained at the cultivation step. The second sample (group II #2) with no *Cutibacterium* sp. reads was aNGS-positive. However, tissue culture results were not available for this sample (Table 1). The third sample (group II #3) was tissue culture-positive for *C. acnes*. This sample had a low *C. acnes* read count (49 and 81 reads assigned by MG-RAST and Kraken2/Bracken, respectively), which was under the applied read count threshold.
- Group III—culture-positive for other bacteria: 10 SF samples that were SF culture-positive for bacteria other than *C. acnes* were included in group III. The bacterial species identified from SF culture (*Staphylococcus epidermidis*, *Staphylococcus aureus*, *F. magna*, and *C. avidum*) and their corresponding tissue culture results are listed in Table 1. In eight out of 10 samples in this group, the bacterial genus determined by mNGS matched the bacterial genus detected by SF culture (Table 1). The two samples (group III #2 and #3) with discordant results had both growth of *S. epidermidis* on SF culture, albeit with a low CFU count of 20–30 CFU/ml. Interestingly, in four samples (group III #4, #6, #7, and #8), in addition to the bacteria

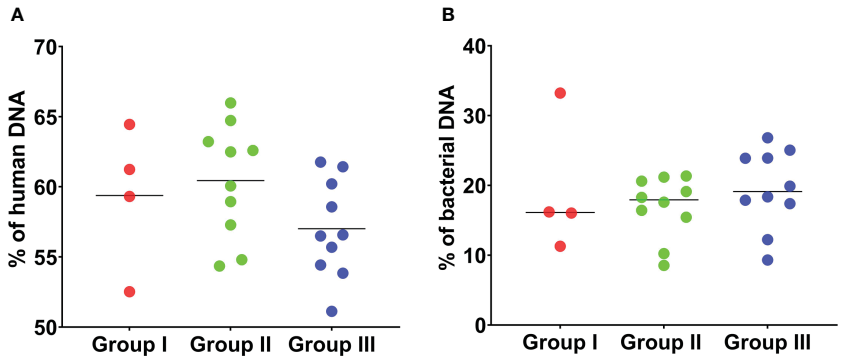


FIGURE 2
Percentage of human and bacterial DNA detected by mNGS of 24 sonication fluid samples. **(A)** The percentage of human DNA detected by mNGS in the 24 SF samples in the three groups is shown. The percentage of human DNA is similar across the three groups. **(B)** The percentage of bacterial DNA detected by mNGS is shown. The percentage of bacterial DNA across the three groups is much lower than the percentage of human DNA in the three groups. This analysis is based on MG-RAST assignment results.

10.3389/fcimb.2023.1165017

detected by SF culture (3 × *S. aureus*; 1 × *F. magna*), sequence reads from *C. acnes* (395 to 2,449 reads (MG-RAST); 2.2% to 10.6% of bacterial reads) were detected. In two of these samples (group III #7 and #8), there were twice as many *C. acnes* reads detected than staphylococcal reads, according to the MG-RAST analysis (Table 1). Three of the samples (group III #4, #7, and #8) were negative by aNGS, while aNGS was not performed in the remaining sample

TABLE 1 Comparison of SF culture results with results of mNGS and aNGS of SF of the 24 implants included in this pilot study.

| S. no. | Reason for implant removal* | Tissue culture | SF culture | | aNGS of SF | mNGS of SF | | |
|---|---|---|---|---|---|---|---|---|
| | | | Microorganism | CFU/ml ** | | Microorganism | MG-RAST: reads (% of total bacteria) | Kraken2: reads (% of total bacteria) |
| Group I—SF culture-negative | | | | | | | | |
| 1 | Pain from plate/ screw | n.g. | n.g. | – | Neg. | *Cutibacterium acnes* | – | – |
| 2 | Aseptic loosening | CoNS (1/5) *C. acnes* (1/5) | n.g. | – | Neg. | *C. acnes* | – | – |
| 3 | Unknown | n.d. | n.g. | – | Neg. | *C. acnes* | – | – |
| 4 | Suspected OIAIs | n.g. | n.g. | – | n.d. | *C. acnes* | 793 (8.4) | 1,240 (1) |
| Group II—Culture-positive for *C. acnes* | | | | | | | | |
| 1 | Aseptic failure | n.g. | *C. acnes* | (20) | Neg. | *C. acnes* | – | – |
| 2 | Pain from plate | n.d. | *C. acnes* | 170 | Pos. | *C. acnes* | – | – |
| 3 | Aseptic loosening | *C. acnes* (4/5) | *C. acnes* | 100 | Pos. | *C. acnes* | – | – |
| 4 | Aseptic loosening | *C. acnes* (2/5) *Staphylococcus epidermidis* (2/5) | *C. acnes* | >250 | Pos. | *C. acnes* | 463 (2.5) | 821 (0.8) |
| 5 | Aseptic failure | *C. acnes* (2/5) | *C. acnes* | 60 | Neg. | *C. acnes* | 545 (3.0) | 961 (1) |
| 6 | Pain from plate | n.d. | *C. acnes* | 90 | Pos. | *C. acnes* | 488 (4.2) | 890 (0.4) |
| 7 | Suspected OIAIs | n.g. | *C. acnes* | (10) | Pos. | *C. acnes* | 2,918 (13.1) | 5,113 (4) |
| 8 | Aseptic failure | *C. acnes* (5/5) | *C. acnes* | (20) | Pos. | *C. acnes* | 2,204 (12.0) | 4,101 (4) |
| 9 | Suspected OIAIs | *C. acnes* (4/5) | *C. acnes* | 100 | Pos. | *C. acnes* | 401 (3.2) | 652 (1) |
| 10 | Pain from plate | n.d. | *C. acnes* | >250 | Pos. | *C. acnes* | 1,883 (20.5) | 3,257 (3) |
| Group III—Culture-positive for other bacteria | | | | | | | | |
| 1 | Suspected OIAIs | *S. epidermidis* (5/5) | *S. epidermidis* | >250 | Neg. | *S. epidermidis* | 395 (1.9) | 574 (0.8) |
| 2 | Aseptic failure | n.g. | *S. epidermidis* | (20) | n.d. | *S. epidermidis* | – | – |
| 3 | Glenoid attrition | n.g. | *S. epidermidis* | (30) | n.d. | *S. epidermidis* | – | – |
| 4 | Suspected OIAIs | *Staphylococcus aureus* (4/5) | *S. aureus* | >250 | Neg. | *S. aureus* *C. acnes* | 5,322 (29.5) 395 (2.2) | 11,620 (11) 583 (0.6) |
| 5 | Aseptic failure | n.g. | *Cutibacterium avidum* | (200) *** | n.d. | *C. acnes* | 3,140 (14.2) | 5,932 (4) |
| 6 | Suspected OIAIs | *Finegoldia magna* (2/5) | *F. magna* | >250 | n.d. | *F. magna* *C. acnes* | 9,184 (41.7) 564 (2.6) | 15,340 (17) 923 (1) |
| 7 | Suspected OIAIs | *S. aureus* (3/5) | *S. aureus* | >250 | Neg. | *S. aureus* *C. acnes* | 1,208 (5.2) 2,449 (10.6) | 5,544 (4) 3,760 (3) |
| 8 | Pain from plate | n.d. | *S. aureus* | >250 | Neg. | *S. aureus* *C. acnes* | 217 (2.5) 458 (5.3) | 2,862 (4) 723 (1) |

*(Continued)*

TABLE 1 Continued

| S. no. | Reason for implant removal* | Tissue culture | SF culture | | aNGS of SF | mNGS of SF | | |
|---|---|---|---|---|---|---|---|---|
| | | | Microorganism | CFU/ml ** | | Microorganism | MG-RAST: reads (% of total bacteria) | Kraken2: reads (% of total bacteria) |
| 9 | Suspected OIAIs | *S. aureus* (5/5) | *S. aureus* | >250 | Neg. | *S. aureus* | 5,932 (40.3) | 12,221 (14) |
| 10 | Fracture | n.g. | *S. epidermidis* | >250 | n.d. | *S. epidermidis* | 187 (3.0) | 347 (0.5) |

n.g., no growth; n.d., not determined; CoNS, coagulase-negative Staphylococcus; SF, sonication fluid; mNGS, metagenomic next-generation sequencing; aNGS, amplicon-based next-generation sequencing; CFU, colony-forming unit; OIAIs, orthopaedic implant-associated infections; EBJIS, European Bone and Joint Infection Society.
*Based on pre-operative diagnosis of the operating surgeon.
**CFU counts below the cutoff described in the latest EBJIS criteria (>50 CFU/ml for uncentrifuged SF; >200 CFU/ml for centrifuged SF) are in brackets.
***Centrifuged SF.

(group III #6). This raised the question of how sensitive the aNGS approach is. We therefore tested the aNGS PCR with different amounts of genomic DNA of *C. acnes*. The PCR detection limit was determined to be a minimum amount of 0.1 pg *C. acnes* template DNA, which corresponded to ca. 37 genome copies (Supplementary Figure 1).

To test whether the obtained sequence reads by mNGS were originating from the entire bacterial genome or were potential artefacts, we mapped extracted sequence reads to reference genomes. Four samples (group I #4 and group II #5, #7, and #8) with *C. acnes* reads were selected and mapped against the *C. acnes* reference genome of strain KPA171202 (Figure 3A). The results showed that the sequence reads obtained by mNGS originated from the entire *C. acnes* genome and not only from certain conserved parts, such as rRNA genes. In one sample (group III #5), whose SF was culture-positive for *C. avidum*, mNGS detected 3,140 and 5,932 sequence reads assigned to *C. acnes* based on MG-RAST and Kraken2/Bracken analysis, respectively. To test if these reads originated from *C. acnes* or *C. avidum*, as culture results suggested, sequence reads were mapped against the genomes of *C. avidum* 44067 and *C. acnes* KPA171202 (Figure 3B). Results indicated that most reads originated from *C. acnes* and not from *C. avidum*. In another sample (group III #6), *F. magna* was identified by culture. *F. magna* is closely related to the tentative species "*F. nericia*" (Brüggemann et al., 2018). The 9,184 sequence reads assigned to *Finegoldia* sp. by MG-RAST were mapped against the genomes of *F. magna* ATCC29328 and "*F. nericia*" 09T494 (Figure 3C). Results showed that the detected DNA originated mainly, if not entirely, from "*F. nericia*".

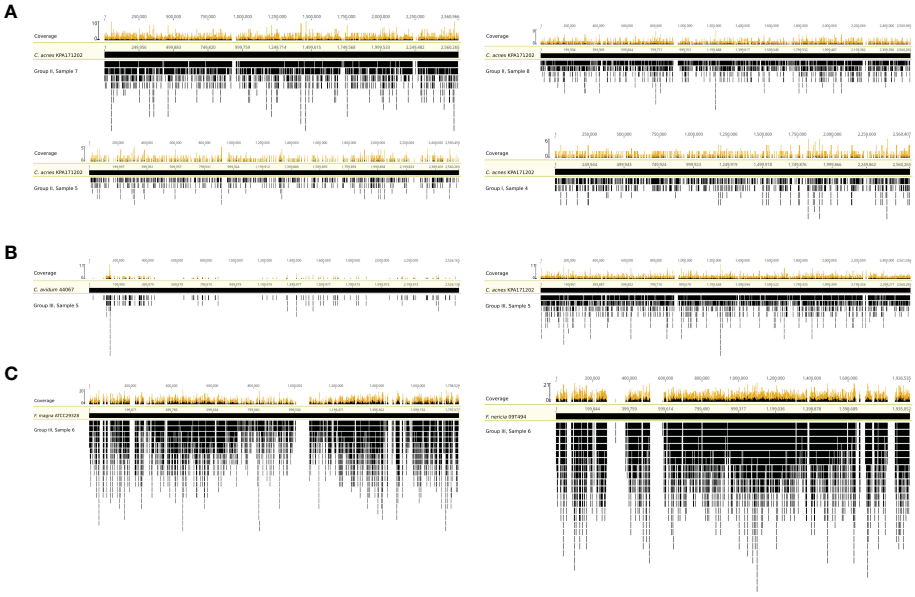


FIGURE 3
Mapping of sequence reads assigned to *Cutibacterium* sp. and/or *Finegoldia* sp. to their corresponding reference genomes. **(A)** Mapping of sequence reads assigned to *Cutibacterium* sp. from four samples (sample 4 from group I, samples 5,7 and 8 from group II) to the reference genome of *C. acnes* KPA171202. **(B)** Mapping of sequence reads assigned to *Cutibacterium* sp. from sample 5 in group III to the genome of *C. avidum* 44067 and to the genome of *C. acnes* KPA171202. **(C)** Mapping of sequence reads corresponding to *Finegoldia* sp. from sample 6 in group III to the genome of *Finegoldia magna* ATCC29328 and "*Finegoldia nericia*" 09T494. This analysis is based on MG-RAST assignment results.

## 4 Discussion

The significance of *C. acnes* isolated from removed orthopaedic implants and their surrounding tissues, including the possibility of overdiagnosis due to the interpretation of contamination or commensal colonization as infection, has often been debated (Hudek et al., 2014; Patel et al., 2020; Falstie-Jensen et al., 2021; Hudek et al., 2021). At the same time, the risk of underdiagnosing *C. acnes* OIAIs because of the slow-growing nature of the bacterium has also been discussed (Butler-Wu et al., 2011; Aubin et al., 2014; Bossard et al., 2016).

In this pilot study, a shotgun sequencing approach of SF was used that could potentially help to identify cases of *C. acnes* OIAIs that were not detected by culture. A total of 24 SF samples, based on their SF culture results, were included and divided into three groups. A large number of microbial sequence reads were obtained in all SF samples including the SF culture-negative samples. As pointed out in several recent studies, particular care needs to be taken when applying mNGS to low-biomass samples, as low-biomass samples are prone to contamination derived from DNA that could be present in liquids or reagents used, such as DNA extraction kits or reagents used for NGS library preparations (Weiss et al., 2014; Street et al., 2017; Thoendel et al., 2017; Thoendel et al., 2018; Eisenhofer et al., 2019). In our study, no DNA was detected by mNGS when a mock sample was sequenced, i.e., the saline used for sonication.

In all SF specimens, sequence reads that originated from gut bacteria were detected by mNGS (Table S2). The origin of these sequence reads in SF samples remains to be investigated. DNA of the gut microbiome in SF could potentially be due to gut permeability, which has been linked to OIAIs *via* the "gut–immune–joint axis" (Chisari et al., 2022), but this does not explain the presence of gut microbial DNA in culture-negative samples with no clinical indication of infection. Another possibility is that DNA of gut bacteria could be present in the normal joint microenvironment, as some studies suggested the presence of bacteria or DNA thereof in native joints (Torchia et al., 2020; Clarkson et al., 2022).

Regarding *C. acnes* in particular, several previous studies suggested that *C. acnes* or rather its DNA is a common contaminant in mNGS data, where it is assumed that *C. acnes* DNA is present in reagents needed for DNA isolation (e.g., DNA extraction kits) and sequence library preparation (Mollerup et al., 2016; Street et al., 2017). However, we did not detect *C. acnes* DNA in the control sample (saline). Moreover, *C. acnes* DNA was only detected in 14/24 samples and not in all samples, as would be expected if *C. acnes* DNA is a common contaminant. This speaks against a general contamination issue with *C. acnes* DNA in the used saline solution or DNA extraction kit or sequencing reagents. However, it cannot be excluded that *C. acnes* could have contaminated the implant in the process of surgery/implant removal in some but not all cases. Such surgery-related contamination is very difficult to prove or disprove. It has previously been reported that carriage of *C. acnes* on human skin can vary substantially from patient to patient and from body site to body site, which can lead to *C. acnes* wound contamination in some but not all patients (McLorinan et al., 2005; Patrick et al., 2017; Patel et al., 2020; Shroff et al., 2023). For example, the shoulder site is usually more heavily colonized with *C. acnes*, especially in male patients (Patel et al., 2020; Hudek et al., 2021; Shroff et al., 2023). A potential possibility to reduce wound contamination could be to wash the removed implants before sonication; this was not performed in this study due to logistic reasons. Here, the implants were placed in sterile, airtight, single-use plastic containers in the operating room and covered with sterile saline before being transported to the lab (Ponraj et al., 2022).

In the culture-negative group, sequence reads from *C. acnes* were obtained in only one sample that was both SF and tissue culture-negative. Clinically, the respective implant was defined as infected due to the presence of a sinus tract. Thus, it could potentially represent a *C. acnes* infection that was missed by culture. Alternatively, *C. acnes* or its DNA contaminated the sample at the DNA extraction step or later. Both explanations are possible, as the risk of contamination in low-biomass mNGS studies (as outlined above) as well as the ability of mNGS to identify organisms not detected by culture has been described previously in multiple studies (Street et al., 2017; Ivy et al., 2018; Sanderson et al., 2018; Weaver et al., 2019; Cai et al., 2020; Wang et al., 2020; He et al., 2021; Noone et al., 2021; Street et al., 2022; Tan et al., 2022).

Of the 10 samples in group II that had growth of *C. acnes* in SF culture, reads from *C. acnes* were obtained in seven samples. *C. acnes* isolates from two of the remaining three samples (#1 and #2) had been classified as likely contamination in our previous study (Ponraj et al., 2022), in which a combined analysis of genome sequencing and SLST typing of *C. acnes* isolates, aNGS of SF, tissue culture results, and pre-operative clinical diagnosis was used to determine the significance of *C. acnes* detection.

In four samples from group III that included SF culture-positive samples for bacteria other than *C. acnes*, mNGS detected *C. acnes* reads in addition to the reads from the bacteria also detected by SF culture, i.e., *S. aureus* in three cases and *F. magna* in one case. This could either represent *C. acnes* DNA contamination during mNGS or be a polymicrobial infection that was not detected in culture because the slow-growing *C. acnes* was overgrown or inhibited by the other faster-growing organism, i.e., *S. aureus* and *F. magna*. Interestingly, in two samples, there were twice as many *Cutibacterium* sp. reads detected than *S. aureus* reads (using the MG-RAST pipeline), albeit only *S. aureus* was identified by SF culture. This suggests that a polymicrobial infection could be present, which was missed by culture since *S. aureus* grows rapidly and possibly inhibits the growth of *C. acnes*.

It is challenging to determine and compare the detection limit of the two methods, mNGS and aNGS. Here, we determined in a mock setting that the aNGS method has a detection limit of ca. 37 *C. acnes* genome copies. However, in real samples, such as SF specimens, which potentially contain much DNA of human origin that could interfere with the *C. acnes* SLST PCR, the number of *C. acnes* genome copies needed to obtain a positive PCR result will likely be higher. Regarding the mNGS method, the detection limit has not been experimentally determined so far; it will depend on

many internal and external factors, such as the sequencing specificities (platform, materials, sequencing depths, and bioinformatics pipeline) as well as the relative abundance of *C. acnes* DNA in a given sample. Our data here suggested that mNGS is more sensitive than aNGS since four out of 10 aNGS-negative samples had actually *C. acnes* reads above the read count threshold. Like in other mNGS projects, a read count threshold was set (150 reads, corresponding to approx. 0.1% of the total amount of bacterial reads per sample) to eliminate potential false positives (Street et al., 2017). Some samples had read counts below the threshold, e.g., MG-RAST and Kraken2/Bracken detected one and four samples with low *C. acnes* read count (on average 51 reads) and four and 13 samples with low *S. epidermidis* read count (on average 37 reads). This might represent NGS-derived contamination, as low counts of *S. epidermidis* and *C. acnes* reads were previously reported in negative controls used in shotgun sequencing projects (Sanabria et al., 2020).

This pilot study has several limitations. The number of samples is limited due to the exploratory nature of the study. Optimal read count thresholds to filter out potential contaminant reads were not established in the study due to the lack of mock community mNGS data (with defined *C. acnes* genome copy numbers) and also hampered by the lack of detecting bacterial reads in negative control samples. Tissue sample culture and aNGS were not performed for all samples included in the study, and finally, due to lack of clinical follow-up, the significance of *C. acnes* reads detected by mNGS, especially in groups I and III, could not be determined. Further studies with the inclusion of clinical follow-up are needed before mNGS can be recommended for the diagnosis of OIAIs due to *C. acnes*.

## 5 Conclusions

The current study shows that *C. acnes* DNA was detected in more samples by mNGS compared to the culture of SF. Additional identification of *C. acnes* was seen in one culture-negative SF sample and in four SF samples that were culture-positive for other bacteria. Thus, mNGS could possibly be used to identify cases of potential *C. acnes* OIAIs, especially in polymicrobial infections that might be overlooked or misinterpreted by culture-based detection alone.

## Data availability statement

The datasets presented in this study can be found in online repositories. The names of the repository/repositories and accession number(s) can be found below: SRA with the accession number PRJNA940664.

## Ethics statement

The studies involving human participants were reviewed and approved by Ethical Committee Region Midtjylland, Denmark. The patients/participants provided their written informed consent to participate in this study.

## Author contributions

DP, JL, TF-J, NJ, CR, and HB contributed to the conception and design of the study. DP performed wet lab benchwork. DP analysed the data. ML, AP, AH, and HB contributed to sequence data generation and data analyses. DP and HB wrote the manuscript. All authors contributed to the article and approved the submitted version.

## Funding

This research was supported with funds from the A. P. Møller Foundation (no. 30903) for running costs and the "Fabrikant Vilhelm Pedersen og Hustrus Legat" (by the recommendation from the Novo Nordisk Foundation) for running costs and personnel (no. 30658).

## Acknowledgments

The authors would like to thank Kristine Schweinshaut and Lise Hald Schultz for their excellent technical assistance.

## Conflict of interest

The authors declare that the research was conducted in the absence of any commercial or financial relationships that could be construed as a potential conflict of interest.

## Publisher's note



## Supplementary material

The Supplementary Material for this article can be found online at: https://www.frontiersin.org/articles/10.3389/fcimb.2023.1165017/full#supplementary-material

SUPPLEMENTARY FIGURE 1
SLST-PCR with different concentrations of *C. acnes* genomic DNA as template. *C. acnes* strain 266 was used. The lanes: 1, DNA ladder (EasyLadder I); 2, 1000 pg; 3, 100 pg; 4, 10 pg; 5, 1 pg; 6, 0.1 pg; 7, 0.01 pg; 8, 0.001 pg; 9, negative control; 10, positive control (1 ng *C. acnes* DNA).

# References


Achermann, Y., Goldstein, E. J., Coenye, T., and Shirtliff, M. E. (2014). *Propionibacterium acnes*: from commensal to opportunistic biofilm-associated implant pathogen. *Clin. Microbiol. Rev.* 27, 419–440. doi: 10.1128/CMR.00092-13

Aubin, G. G., Portillo, M. E., Trampuz, A., and Corvec, S. (2014). *Propionibacterium acnes*, an emerging pathogen: from acne to implant-infections, from phylotype to resistance. *Med. Mal. Infect.* 44, 241–250. doi: 10.1016/j.medmal.2014.02.004

Borens, O., Yusuf, E., Steinrücken, J., and Trampuz, A. (2013). Accurate and early diagnosis of orthopedic device-related infection by microbial heat production and sonication. *J. Orthop. Res.* 31, 1700–1703. doi: 10.1002/jor.22419

Bossard, D. A., Ledergerber, B., Zingg, P. O., Gerber, C., Zinkernagel, A. S., Zbinden, R., et al. (2016). Optimal length of cultivation time for isolation of *Propionibacterium acnes* in suspected bone and joint infections is more than 7 days. *J. Clin. Microbiol.* 54, 3043–3049. doi: 10.1128/JCM.01435-16

Brüggemann, H., Jensen, A., Nazipi, S., Aslan, H., Meyer, R. L., Poehlein, A., et al. (2018). Pan-genome analysis of the genus *Finegoldia* identifies two distinct clades, strain-specific heterogeneity, and putative virulence factors. *Sci. Rep.* 8, 266. doi: 10.1038/s41598-017-18661-8

Butler-Wu, S. M., Burns, E. M., Pottinger, P. S., Magaret, A. S., Rakeman, J. L., Matsen, F. A., et al. (2011). Optimization of periprosthetic culture for diagnosis of *Propionibacterium acnes* prosthetic joint infection. *J. Clin. Microbiol.* 49, 2490–2495. doi: 10.1128/JCM.00450-11

Cai, Y., Fang, X., Chen, Y., Huang, Z., Zhang, C., Li, W., et al. (2020). Metagenomic next generation sequencing improves diagnosis of prosthetic joint infection by detecting the presence of bacteria in periprosthetic tissues. *Int. J. Infect. Dis.* 96, 573–578. doi: 10.1016/j.ijid.2020.05.125

Chisari, E., Cho, J., Wouthuyzen-Bakker, M., and Parvizi, J. (2022). Gut permeability may be associated with periprosthetic joint infection after total hip and knee arthroplasty. *Sci. Rep.* 12, 15094. doi: 10.1038/s41598-022-19034-6

Clarkson, S. J., Goswami, K., and Parvizi, J. (2022). "The microbiome of the joint," in *Essentials of cemented knee arthroplasty*. Eds. E. Hansen and K.-D. Kühn (Berlin, Heidelberg: Springer Berlin Heidelberg), 101–107.

Eisenhofer, R., Minich, J. J., Marotz, C., Cooper, A., Knight, R., and Weyrich, L. S. (2019). Contamination in low microbial biomass microbiome studies: issues and recommendations. *Trends Microbiol.* 27, 105–117. doi: 10.1016/j.tim.2018.11.003

Falstie-Jensen, T., Lange, J., Daugaard, H., Sørensen, A. K. B., Ovesen, J., and Søballe, K. (2021). Unexpected positive cultures after revision shoulder arthroplasty: does it affect outcome? *J. Shoulder Elbow Surg.* 30, 1299–1308. doi: 10.1016/j.jse.2020.12.014

Fang, X., Cai, Y., Shi, T., Huang, Z., Zhang, C., Li, W., et al. (2020). Detecting the presence of bacteria in low-volume preoperative aspirated synovial fluid by metagenomic next-generation sequencing. *Int. J. Infect. Dis.* 99, 108–116. doi: 10.1016/j.ijid.2020.07.039

Gu, W., Miller, S., and Chiu, C. Y. (2019). Clinical metagenomic next-generation sequencing for pathogen detection. *Annu. Rev. Pathol.* 14, 319–338. doi: 10.1146/annurev-pathmechdis-012418-012751

He, R., Wang, Q., Wang, J., Tang, J., Shen, H., and Zhang, X. (2021). Better choice of the type of specimen used for untargeted metagenomic sequencing in the diagnosis of periprosthetic joint infections. *Bone Joint J.* 103-B, 923–930. doi: 10.1302/0301-620X.103B5.BJJ-2020-0745.R1

Huang, Z., Li, W., Lee, G. C., Fang, X., Xing, L., Yang, B., et al. (2020). Metagenomic next-generation sequencing of synovial fluid demonstrates high accuracy in prosthetic joint infection diagnostics: mNGS for diagnosing PJI. *Bone Joint Res.* 9, 440–449. doi: 10.1302/2046-3758.97.BJR-2019-0325.R2

Hudek, R., Brobeil, A., Brüggemann, H., Sommer, F., Gattenlöhner, S., and Gohlke, F. (2021). Cutibacterium acnes is an intracellular and intra-articular commensal of the human shoulder joint. *J. Shoulder Elbow Surg.* 30, 16–26. doi: 10.1016/j.jse.2020.04.020

Hudek, R., Sommer, F., Kerwat, M., Abdelkawi, A. F., Loos, F., and Gohlke, F. (2014). *Propionibacterium acnes* in shoulder surgery: true infection, contamination, or commensal of the deep tissue? *J. Shoulder Elbow Surg.* 23, 1763–1771. doi: 10.1016/j.jse.2014.05.024

Ivy, M. I., Thoendel, M. J., Jeraldo, P. R., Greenwood-Quaintance, K. E., Hanssen, A. D., Abdel, M. P., et al. (2018). Direct detection and identification of prosthetic joint infection pathogens in synovial fluid by metagenomic shotgun sequencing. *J. Clin. Microbiol.* 56, e00402–e00418. doi: 10.1128/JCM.00402-18

Kildow, B. J., Ryan, S. P., Danilkowicz, R., Lazarides, A. L., Penrose, C., Bolognesi, M. P., et al. (2021). Next-generation sequencing not superior to culture in periprosthetic joint infection diagnosis. *Bone Joint J.* 103-B, 26–31. doi: 10.1302/0301-620X.103B1.BJJ-2020-0017.R3

Langmead, B., and Salzberg, S. L. (2012). Fast gapped-read alignment with bowtie 2. *Nat. Methods* 9, 357–359. doi: 10.1038/nmeth.1923

Li, H., Handsaker, B., Wysoker, A., Fennell, T., Ruan, J., Homer, N., et al. (2009). The sequence Alignment/Map format and SAMtools. *Bioinformatics* 25, 2078–2079. doi: 10.1093/bioinformatics/btp352

Lu, J., Breitwieser, F. P., Thielen, P., and Salzberg, S. L. (2017). Bracken: estimating species abundance in metagenomics data. *PeerJ Comput. Sci.* 3, e104. doi: 10.7717/peerj-cs.104

McDowell, A., Nagy, I., Magyari, M., Barnard, E., and Patrick, S. (2013). The opportunistic pathogen *Propionibacterium acnes*: insights into typing, human disease, clonal diversification and CAMP factor evolution. *PloS One* 8, e70897. doi: 10.1371/journal.pone.0070897

McLorinan, G. C., Glenn, J. V., McMullan, M. G., and Patrick, S. (2005). Propionibacterium acnes wound contamination at the time of spinal surgery. *Clin. Orthop. Relat. Res.* 437, 67–73. doi: 10.1097/00003086-200508000-00012

Meyer, F., Bagchi, S., Chaterji, S., Gerlach, W., Grama, A., Harrison, T., et al. (2019). MG-RAST version 4-lessons learned from a decade of low-budget ultra-high-throughput metagenome analysis. *Brief. Bioinform.* 20, 1151–1159. doi: 10.1093/bib/bbx105

Mollerup, S., Friis-Nielsen, J., Vinner, L., Hansen, T. A., Richter, S. R., Fridholm, H., et al. (2016). *Propionibacterium acnes*: disease-causing agent or common contaminant? detection in diverse patient samples by next-generation sequencing. *J. Clin. Microbiol.* 54, 980–987. doi: 10.1128/JCM.02723-15

Noone, J. C., Helmersen, K., Leegaard, T. M., Skråmm, I., and Aamot, H. V. (2021). Rapid diagnostics of orthopaedic-Implant-Associated infections using nanopore shotgun metagenomic sequencing on tissue biopsies. *Microorganisms* 9, 97. doi: 10.3390/microorganisms9010097

Patel, M. S., Singh, A. M., Gregori, P., Horneff, J. G., Namdari, S., and Lazarus, M. D. (2020). *Cutibacterium acnes*: a threat to shoulder surgery or an orthopedic red herring? *J. Shoulder Elbow Surg.* 29, 1920–1927. doi: 10.1016/j.jse.2020.02.020

Patrick, S., McDowell, A., Lee, A., Frau, A., Martin, U., Gardner, E., et al. (2017). Antisepsis of the skin before spinal surgery with povidone iodine-alcohol followed by chlorhexidine gluconate-alcohol versus povidone iodine-alcohol applied twice for the prevention of contamination of the wound by bacteria: a randomised controlled trial. *Bone Joint J.* 99-B, 1354–1365. doi: 10.1302/0301-620X.99B10.BJJ-2017-0291.R1

Ponraj, D. S., Falstie-Jensen, T., Jørgensen, N. P., Ravn, C., Brüggemann, H., and Lange, J. (2021). Diagnosis of orthopaedic-implant-associated infections caused by slow-growing gram-positive anaerobic bacteria – a clinical perspective. *J. Bone Joint Infect.* 6, 367–378. doi: 10.5194/jbji-6-367-2021

Ponraj, D. S., Lange, J., Falstie-Jensen, T., Jørgensen, N. P., Ravn, C., Poehlein, A., et al. (2022). Amplicon-based next-generation sequencing as a diagnostic tool for the detection of phylotypes of *Cutibacterium acnes* in orthopedic implant-associated infections. *Front. Microbiol.* 13, 866893. doi: 10.3389/fmicb.2022.866893

Sanabria, A., Hjerde, E., Johannessen, M., Sollid, J. E., Simonsen, G. S., and Hanssen, A. M. (2020). Shotgun-metagenomics on positive blood culture bottles inoculated with prosthetic joint tissue: a proof of concept study. *Front. Microbiol.* 11, 1687. doi: 10.3389/fmicb.2020.01687

Sanderson, N. D., Street, T. L., Foster, D., Swann, J., Atkins, B. L., Brent, A. J., et al. (2018). Real-time analysis of nanopore-based metagenomic sequencing from infected orthopaedic devices. *BMC Genomics* 19, 714. doi: 10.1186/s12864-018-5094-y

Shroff, J. B., Hanna, P., Levy, B. J., Jimenez, A. E., Grimm, N. L., Cote, M. P., et al. (2023). Is there value in the routine practice of discarding the incision scalpel from the surgical field to prevent deep wound contamination with cutibacterium acnes? an update. *J. Shoulder Elbow Surg.*, S1058–S2746. doi: 10.1016/j.jse.2023.02.130

Street, T. L., Sanderson, N. D., Atkins, B. L., Brent, A. J., Cole, K., Foster, D., et al. (2017). Molecular diagnosis of orthopedic-Device-Related infection directly from sonication fluid by metagenomic sequencing. *J. Clin. Microbiol.* 55, 2334–2347. doi: 10.1128/JCM.00462-17

Street, T. L., Sanderson, N. D., Kolenda, C., Kavanagh, J., Pickford, H., Hoosdally, S., et al. (2022). Clinical metagenomic sequencing for species identification and antimicrobial resistance prediction in orthopedic device infection. *J. Clin. Microbiol.* 60, e0215621. doi: 10.1128/jcm.02156-21

Tan, J., Liu, Y., Ehnert, S., Nüssler, A. K., Yu, Y., Xu, J., et al. (2022). The effectiveness of metagenomic next-generation sequencing in the diagnosis of prosthetic joint infection: a systematic review and meta-analysis. *Front. Cell. Infect. Microbiol.* 12, 875822. doi: 10.3389/fcimb.2022.875822

Tande, A. J., and Patel, R. (2014). Prosthetic joint infection. *Clin. Microbiol. Rev.* 27, 302–345. doi: 10.1128/CMR.00111-13

Thoendel, M., Jeraldo, P., Greenwood-Quaintance, K. E., Yao, J., Chia, N., Hanssen, A. D., et al. (2017). Impact of contaminating DNA in whole-genome amplification kits used for metagenomic shotgun sequencing for infection diagnosis. *J. Clin. Microbiol.* 55, 1789–1801. doi: 10.1128/JCM.02402-16

Thoendel, M. J., Jeraldo, P. R., Greenwood-Quaintance, K. E., Yao, J. Z., Chia, N., Hanssen, A. D., et al. (2018). Identification of prosthetic joint infection pathogens using a shotgun metagenomics approach. *Clin. Infect. Dis.* 67, 1333–1338. doi: 10.1093/cid/ciy303

Torchia, M. T., Amakiri, I., Werth, P., and Moschetti, W. (2020). Characterization of native knee microorganisms using next-generation sequencing in patients undergoing primary total knee arthroplasty. *Knee* 27, 1113–1119. doi: 10.1016/j.knee.2019.12.013

Wang, C., Huang, Z., Li, W., Fang, X., and Zhang, W. (2020). Can metagenomic next-generation sequencing identify the pathogens responsible for culture-negative prosthetic joint infection? *BMC Infect. Dis.* 20, 253. doi: 10.1186/s12879-020-04955-2

Weaver, A. A., Hasan, N. A., Klaassen, M., Karathia, H., Colwell, R. R., and Shrout, J. D. (2019). Prosthetic joint infections present diverse and unique microbial

communities using combined whole-genome shotgun sequencing and culturing methods. *J. Med. Microbiol.* 68, 1507–1516. doi: 10.1099/jmm.0.001068

Weiss, S., Amir, A., Hyde, E. R., Metcalf, J. L., Song, S. J., and Knight, R. (2014). Tracking down the sources of experimental contamination in microbiome studies. *Genome Biol.* 15, 564. doi: 10.1186/s13059-014-0564-2

Wood, D. E., Lu, J., and Langmead, B. (2019). Improved metagenomic analysis with kraken 2. *Genome Biol.* 20, 257. doi: 10.1186/s13059-019-1891-0

Zeller, V., Ghorbani, A., Strady, C., Leonard, P., Mamoudy, P., and Desplaces, N. (2007). *Propionibacterium acnes*: an agent of prosthetic joint infection and colonization. *J. Infect.* 55, 119–124. doi: 10.1016/j.jinf.2007.02.006

frontiers | Frontiers in Cellular and Infection Microbiology

TYPE Original Research
PUBLISHED 17 May 2023
DOI 10.3389/fcimb.2023.1142426



OPEN ACCESS

EDITED BY
Floriana Campanile,
University of Catania, Italy

REVIEWED BY
Davide Carcione,
ASST Valle Olona, Italy
Yu Xia,
Southern University of Science and Technology, China
Ruichao Li,
Yangzhou University, China

*CORRESPONDENCE
Yunhe Xiong
xiongyunhe@whu.edu.cn
Sixing Yang
sxyang@whu.edu.cn

†These authors have contributed equally to this work and share first authorship

RECEIVED 11 January 2023
ACCEPTED 28 April 2023
PUBLISHED 17 May 2023

CITATION
Jiang S, Wei Y, Ke H, Song C, Liao W, Meng L, Sun C, Zhou J, Wang C, Su X, Dong C, Xiong Y and Yang S (2023) Building a nomogram plot based on the nanopore targeted sequencing for predicting urinary tract pathogens and differentiating from colonizing bacteria. *Front. Cell. Infect. Microbiol.* 13:1142426. doi: 10.3389/fcimb.2023.1142426



# Building a nomogram plot based on the nanopore targeted sequencing for predicting urinary tract pathogens and differentiating from colonizing bacteria

Shengming Jiang[1†], Yangyan Wei[2†], Hu Ke[1†], Chao Song[1], Wenbiao Liao[1], Lingchao Meng[1], Chang Sun[1], Jiawei Zhou[1], Chuan Wang[1], Xiaozhe Su[1], Caitao Dong[1], Yunhe Xiong[1*] and Sixing Yang[1*]

[1]Department of Urology, Renmin Hospital of Wuhan University, Wuhan, China, [2]Department of Cardiovascular Surgery, The Affiliated Hospital of Qingdao University, Qingdao, China

**Background:** The identification of uropathogens (UPBs) and urinary tract colonizing bacteria (UCB) conduces to guide the antimicrobial therapy to reduce resistant bacterial strains and study urinary microbiota. This study established a nomogram based on the nanopore-targeted sequencing (NTS) and other infectious risk factors to distinguish UPB from UCB.

**Methods:** Basic information, medical history, and multiple urine test results were continuously collected and analyzed by least absolute shrinkage and selection operator (LASSO) regression, and multivariate logistic regression was used to determine the independent predictors and construct nomogram. Receiver operating characteristics, area under the curve, decision curve analysis, and calibration curves were used to evaluate the performance of the nomogram.

**Results:** In this study, the UPB detected by NTS accounted for 74.1% (401/541) of all urinary tract microorganisms. The distribution of ln(reads) between UPB and UCB groups showed significant difference (OR = 1.39; 95% CI, 1.246–1.551, $p < 0.001$); the reads number in NTS reports could be used for the preliminary determination of UPB (AUC=0.668) with corresponding cutoff values being 7.042. Regression analysis was performed to determine independent predictors and construct a nomogram, with variables ranked by importance as ln(reads) and the number of microbial species in the urinary tract of NTS, urine culture, age, urological neoplasms, nitrite, and glycosuria. The calibration curve showed an agreement between the predicted and observed probabilities of the nomogram. The decision curve analysis represented that the nomogram would benefit clinical interventions. The performance of nomogram with ln(reads) (AUC = 0.767; 95% CI, 0.726–0.807) was significantly better (Z = 2.304, p-value = 0.021) than that without ln(reads) (AUC = 0.727; 95% CI, 0.681–0.772).

The rate of UPB identification of nomogram was significantly higher than that of ln(reads) only ($\chi^2$ = 7.36, p-value = 0.009).

**Conclusions:** NTS is conducive to distinguish uropathogens from colonizing bacteria, and the nomogram based on NTS and multiple independent predictors has better prediction performance of uropathogens.

KEYWORDS

**nomogram, nanopore sequencing, LASSO regression, urinary tract infections, asymptomatic infections**

# 1 Introduction

Urinary tract infection (UTI) is among the most frequent infectious diseases in the community and healthcare setting and usually classified into asymptomatic bacteriuria (ABU), uncomplicated UTI, and complicated UTI (cUTI) to assess the infectious severity and decide whether to apply antimicrobial drugs actively (Wagenlehner et al., 2020). ABU in adults without risk factors corresponds to commensal colonization, and active treatment is not recommended in the latest European Association of Urology (EAU) guidelines (Bonkat, 2022). Similarly, pathogenic detection is not strongly recommended for uncomplicated UTI patients unless empirical antimicrobial therapy is ineffective (Hooton et al., 2021). Despite that the obvious benefits of antibiotic use to cUTI patients has been testified, the more sobering reality is that overuse and misuse have led to a growing problem of drug resistance in uropathogens (Eliakim-Raz et al., 2019; Quan et al., 2021). As can be seen, recent guidelines and consensus have distinguished between urinary tract pathogenic bacteria (UPB) and colonizing bacteria (UCB), as their handling attitudes are markedly different.

Urine dipstick and microscopic analysis are often used for qualitative preliminary screening, after which etiological detection is still required. Urine culture is of great significance for the pathogenic diagnosis and effective treatment of UTI (Bonkat, 2022). However, culture methods are not always sensitive and accurate but always with a huge time cost (McDonald et al., 2017; Dauwalder et al., 2021). Statistically, the sensitivity of culture is approximately 30%, and negative results cannot completely rule out UTI; even multiple tests are not uncommon. Moreover, further studies showed that the small counts of *Escherichia coli* in midstream urine were too low to form sufficient colony unit (CFU) for diagnosis in urine culture and were still highly predictive of acute cystitis. In contrast, the enterococci and group B streptococci frequently cultured from midstream urine were rarely isolated from urine sampled from the bladder through catheterization (Gupta et al., 2017). Therefore, urine culture cannot effectively differentiate UPB from UCB. Clinicians make a diagnosis, heavily relying on a combined analysis of clinical and medical history and test manifestations. Previous studies have constructed nomograms, a simple and accurate visualization tool, based on multi-factors for predicting UTI, but there are problems of poor performance and cumbersome variables. Li et al. used culture results strictly as a diagnostic criterion for UTI; the UTI patients was only 13.5% (171/1271), and negative results of urine culture could not completely exclude UTI (Li et al., 2023). Yang et al. established a preoperative nomogram to predict postoperative urosepsis for negative preoperative urine culture patients. Unfortunately, there is no postoperative etiological detection to verify urosepsis (Yang et al., 2023). It is not recommended to predict UPB completely out of touch with etiological detection.

Recent genomic sequencing techniques allow the highly sensitive detection of every microorganism in any specimen, and their expanded application in urine testing has changed the traditional dogma that urine of healthy individuals is sterile (Gu et al., 2021). The latest Nanopore Targeted Sequencing (NTS) offers a powerful option to overcome the above clinical diagnostic challenges, which has been reported for the rapid, accurate, and comprehensive detection of respiratory viruses and endophthalmitis pathogens (Rusk, 2019; Wang et al., 2020; Huang et al., 2021). There is an article documenting the first clinical attempt of NTS to detect multi-system pathogens, where the mentioned NTS detected 20 common UPB, but the urine sample size was extremely limited (n=74), much less the interpretation of the sequencing results for determining the pathogenicity of detected bacteria (Fu et al., 2022). Therefore, this study is the first to analyze NTS data of urinary tract microorganisms in detail. To ensure that the NTS data reflected uropathogens as accurately as possible, we innovatively combined NTS results with clinical information related to uropathogenic infections to screen out independent predictors for the identification of UPB or UCB and constructed a visualized nomogram to calculate the likelihood of infection with uropathogens.

# 2 Materials and methods

## 2.1 Study population

The study was a retrospective analysis consisting of consecutive patients in the Department of Urology, Renmin Hospital of Wuhan

University from June 2020 to August 2021. The inclusion criteria were patients whose urine had been detected by NTS, urine culture and routine tests before antibacterial therapy at admission, and NTS indicated that there may be urinary microorganism(s) or even uropathogen(s), no matter one kind or more. Potential factors associated with UTI including possible baseline characteristics, medical history, and laboratory test data were collected for regression analysis.

The exclusion criteria were as follows: (1) anti-infective treatment before admission or sample collection; (2) clinical data obtained from non-midstream urine and cystostomy or nephrostomy status; (3) lack of urine routine or culture on admission; (4) patients whose urine collections for NTS, urine culture, and urine routine tests were performed at different time periods; (5) the urine culture suggested a contaminated sample or was completely inconsistent with NTS; and (6) patients with incomplete clinical data.

All personal information was masked during the process of analysis and publication. This retrospective study has obtained the informed consent from the Ethics Committee of the Renmin Hospital of Wuhan University (WDRY2022-KS006), which abandoned the requested written informed consent.

## 2.2 Etiological detection methods and routine variables

### 2.2.1 NTS technology

After specimen collection, the work was carried out according to the following steps. Professional operators extracted samples' DNA using Sanure DNA extraction kit (Sansure Biotech, China). Second, library preparation through polymerase chain reaction (PCR) process target amplified bacterial 16s rRNA and fungal internally transcribed spacer 1/2 (ITS1/2), and then, 1D ligation kit SQK-LSK109 (Oxford Nanopore, UK) was used to mixed amplification products in the ratio of 10:3. Libraries were sequenced using MinION platform (Oxford Nanopore, UK). Finally, software including Guppy software (version 6.0.0), Porechop software (version 0.2.4), and Blast software (version 2.9.0) were used to process sequencing data and map to NCBI FTP 16S rDNA/ITS reference database. Through sequencing and data processing, a urine sample generated abundant sequencing reads.

Reads number represented the number of sequencing reads with >90% identity matched to each target region of the genome in database used to describe corresponding bacteria or fungi. To facilitate the calculation and display of data differences, the number of reads is converted to its logarithmic form, abbreviated as ln(reads).

The number of urinary tract microbiological species (NUP) was determined by the classification of sequencing reads if there were multiple matches referring to bioinformatic analysis above.

### 2.2.2 Urine culture

The pathogenic bacteria were cultured and isolated according to the standard procedure, and the isolated UPB were identified and tested for drug sensitivity by applying the automatic microbiological analyzer Phoenix-100 (Becton, Dickinson and Company, USA) and auxiliary identification card or drug sensitivity card. Bacteriuria was defined as the presence of at least $10^5$ colony-forming units per milliliter. Results were categorized as positive and negative.

### 2.2.3 Routine variables

Potential predictive variables were chosen based upon review of the literature and guidelines, including the fasting plasma glucose (FPG) and routine urine test at admission (Eliakim-Raz et al., 2019; Bonkat, 2022). FPG, urine pH, urine white blood cells (WBCs), epithelial cells count, urine casts, and pathological casts were continuous numeric variables. The color, clarity, urine glucose, ketonuria, protein, occult blood, nitrite, and leukocyte enzymes of urine were collected by categories.

## 2.3 Diagnosis and definitions

The clinical diagnosis of UTI is referred to clinical guidelines and published literature and based on a combination of clinical features and results of laboratory testing (Wagenlehner et al., 2020; Bonkat, 2022).

### 2.3.1 Identification of UPB

Primary microorganism in NTS was considered as UPB in patients who was required to have at least one sign or symptom of UTI, lower urinary tract symptoms (LUTS) involving frequency or urgency or dysuria, flank pain including costovertebral angle tenderness, fever of 37.3°C or worse, with any one of the following positive urine laboratory test results, nitrites, leukocyte esterase, protein quantification >2 g/24 h, centrifugal urine sediment WBC count more than five cells/HP, and midstream urine culture showing bacterial growth over $10^5$ CFU/ml.

### 2.3.2 Diagnosis of UCB

The patient with the single presence of potential symptoms above or a positive urine test result alone was considered to have ABU or non-UTI symptoms, whose primary microorganisms in NTS are defined as UCB.

## 2.4 Statistical analysis

The continuous numeric variables that coincided with normal distribution were expressed as mean ± standard deviation (X ± SD). Categorical variables were described as count and percentage. Univariate logistic regression and McNemar–Bowker test were used for intergroup statistical analysis.

All study indexes and variables were introduced into the least absolute shrinkage and selection operator (LASSO) regression to screen out potential predictors for the identification of UPB and UCB. Subsequently, multivariate logistic regression was used to determine the independent predictors and build a model using stepwise backward regression analysis, which visualized with a nomogram. The model was internally validated by resampling K-

fold cross-validation (K = 5, times = 400) and calculating the resampled AUC.

The receiver operating characteristic curve (ROC), area under the ROC curve (AUC), and the decision curve analysis (DCA) were used to graphically assess the discriminating performance and clinical utility of the nomogram. Plotting calibration curves were used to assess the relationship between the actual and predicted probabilities of UPB infections. Each predictor's contribution in the nomogram was measured by the partial chi-square statistic minus the predictor degrees of freedom and visually shown in a bar chart. DeLong's test was used for comparison of two correlated ROC curves. Data were analyzed by SPSS software (version 26.0) and R software (version 4.1.2), and two-tailed $p<0.05$ was considered statistically significant.

# 3 Results

## 3.1 Patient characteristics

In the study, 541 patients at admission were consecutively enrolled for analysis. According to diagnostic criteria and detecting results, the primary microorganisms detected by NTS in 401 (74.1%) patients were UPB, and 140 (25.9%) people were UCB. Baseline characteristics of two groups patients are presented in Table 1.

In the basic information, the mean age of the enrolled patients was 58.3 ± 14.3 years, and 339 patients (62.7%) were men. In terms of chronic underlying diseases and specific medical history, 147 (27.2%) people suffered from hypertension and 74 (13.7%) from diabetes, 358 (66.2%) patients had urinary tract calculi, 125 (23.1%) patients had benign prostatic hyperplasia (BPH), 85 (15.7%) had urologic neoplasms, 87 (16.1%) had urological anatomical and functional abnormalities (UAFA), 160 (29.6%) had a history of urological endoscopic surgery, and 14 (2.6%) patients had nephrostomy or cystostomy. Some patients had existing more than one urogenital disease or chronic comorbidities. Flank pain was recorded in 209 (38.6%) patients, LUTS in 115 (21.3%), hematuria in 63 (11.7%), and fever (>37.3°C) in 21 (3.9%).

## 3.2 NTS detection results

In univariate logistic regression, ln(reads) and NUP were significantly different between the UPB and UCB groups. To further explore the NTS test results and urinary tract microorganisms, we showed ln(reads) distribution of primary microorganisms classified by genus in 541 urine samples. According to above criteria, microorganisms were divided into UPB and UCB groups, classified by genus, and ranked according to the mean value of ln(reads) (Figure 1). At the genus level, in order of detection rate, *Escherichia* spp., *Candida* spp., *Enterococcus* spp., *Gardnerella vaginalis*, *Streptococcus pneumoniae*, *Klebsiella* spp., *Proteus* spp., *Ureaplasma* spp., *Pseudomonas* spp., *Acinetobacter* spp., and *Staphylococcus aureus* were the most common UPB groups found in NTS. Consistent with previous studies, *E. coli* was still the highest detection rate pathogen at the level of species. UCB groups did not belong to the UPB group as mentioned above and were not deemed to cause symptoms of infections, including non-uropathogenic *Streptococcus* spp., e.g. *Streptococcus mitis*, *Lactobacillus* spp., *Prevotella* spp., non-uropathogenic *Staphylococcus* spp., e.g., *Staphylococcus epidermidis*, *Finegoldia magna*, and *Anaerococcus* spp.

There was a significant difference in ln(reads) between the UPB and UCB groups graphically displayed with a symmetrical histogram (Figure 2), which possessed a preliminary ability to identify UPB and UCB (AUC=0.668), and the corresponding cutoff value was 7.042 (Figure 3). AUC value was not entirely satisfactory, and we tried to find independent predictors to identify UPB from UCB to improve diagnostic efficiency.

## 3.3 Predictor selection

In order to determine, to the extent possible, the clinical indicators that have an association with the predicted outcome, we performed regression analysis with all the above-mentioned indicators that may be associated with UPB infections. First, 33 UTI-related features were subjected to LASSO regression (Figures 4, 5). UPB infections may be associated with 14 variables: age, LUTS, fever (>37.3°C), urological neoplasms, urological endoscopic surgery, ln(reads), NUP, urine culture, urine clarity, urine glucose, urine protein, urine occult blood, nitrites, and urine casts. These 14 variables were included in a multifactorial logistic regression model, yielding seven variables as independent predictors for distinguishing UPB from UCB, including age, urological neoplasms, NUP in NTS testing, ln(reads), urine culture, urine glucose, and nitrites. Their OR values and 95% confidence interval (CI) are shown in Figure 6.

## 3.4 Nomogram construction and verification

A nomogram was constructed with the seven independent predictors to distinguish between UPB and UCB in admitted patients. The nomogram assigned scores to each of the seven variables, and the risk score was calculated based on the coefficients of the logistic model and the values of the expressions corresponding to the seven candidates in the model; the probability of UPB infections for a given patient was computed by summing the allocations for each variable (Figure 7).

The discriminating degree and performance of the prediction model was evaluated by the ROC curve test (AUC = 0.767; 95% CI, 0.726–0.807; Figure 8, Model 1), so did internal validation and the resampling K-fold cross-validation (K = 5, times = 400) of the model (AUC = 0.750). The calibration curve of the model (Figure 9) showed an agreement between the predicted and observed probabilities of the nomogram without undesirable deviations. The DCA (Figure 10) representing the net benefit of clinical interventions relying on nomogram were higher than that of full or no intervention without the help of nomogram and indicated

TABLE 1 The baseline characteristics of included patients with UTI at admission.

| Characteristics | Overall | UCB (140) | UPB (401) | OR | CI | p |
|---|---|---|---|---|---|---|
| Age, means (SD) | 58.3 (14.3) | 55.2 (16.5) | 59.4 (13.2) | 1.02 | 1.007–1.035 | 0.003 |
| Man, n (%) | 339 (62.7) | 96 (68.6) | 243 (60.6) | 0.7 | 0.468–1.061 | 0.094 |
| Hypertension, n (%) | 147 (27.2) | 34 (24.3) | 113 (28.2) | 1.22 | 0.785–1.906 | 0.373 |
| Diabetes, n (%) | 74 (13.7) | 14 (10.0) | 60 (15.0) | 1.58 | 0.855–2.934 | 0.144 |
| LUTS, n (%) | 115 (21.3) | 17 (12.1) | 98 (24.4) | 2.34 | 1.342–4.08 | 0.003 |
| Hematuria, n (%) | 63 (11.6) | 18 (12.9) | 45 (11.2) | 0.86 | 0.478–1.536 | 0.604 |
| Flank pain, n (%) | 209 (38.6) | 63 (45.0) | 146 (36.4) | 0.7 | 0.474–1.034 | 0.073 |
| Fever (>37.3°C), n (%) | 21 (3.9) | 2 (1.4) | 19 (4.7) | 3.43 | 0.789–14.923 | 0.1 |
| Urinary calculi, n (%) | 358 (66.2) | 100 (71.4) | 258 (64.3) | 0.72 | 0.474–1.098 | 0.128 |
| BPH, n (%) | 125 (23.1) | 30 (21.4) | 95 (23.7) | 1.14 | 0.715–1.812 | 0.585 |
| Urological neoplasms, n (%) | 85 (15.7) | 25 (17.9) | 60 (15.0) | 0.81 | 0.485–1.351 | 0.418 |
| UAFA, n (%) | 87 (16.1) | 24 (17.1) | 63 (15.7) | 0.9 | 0.538–1.508 | 0.691 |
| Urological endoscopic surgery, n (%) | 160 (29.6) | 35 (25.0) | 125 (31.2) | 1.36 | 0.878–2.103 | 0.169 |
| Nephrostomy or cystostomy, n (%) | 14 (2.6) | 2 (1.4) | 12 (3.0) | 2.13 | 0.47–9.631 | 0.327 |
| NUP, means (SD) | 1.9 (1.1) | 2.2 (1.2) | 1.9 (1.1) | 0.77 | 0.651–0.906 | 0.002 |
| Ln(reads), means (SD) | 7.6 (1.9) | 6.8 (1.8) | 7.9 (1.8) | 1.39 | 1.246–1.551 | 0 |
| Positive urine culture, n (%) | 167 (30.9) | 16 (11.4) | 151 (37.7) | 4.68 | 2.678–8.182 | 0 |
| FPG, means (SD) | 5.3 (1.7) | 5.2 (1.6) | 5.4 (1.7) | 1.1 | 0.954–1.276 | 0.183 |
| Gross hematuria, n (%) | 36 (6.7) | 10 (7.1) | 26 (6.5) | 0.9 | 0.423–1.92 | 0.788 |
| Cloudy urine, n (%) | 446 (82.4) | 121 (86.4) | 325 (81.0) | 0.67 | 0.39–1.157 | 0.152 |
| Glycosuria, n (%) | 46 (8.5) | 5 (3.6) | 41 (10.2) | 3.07 | 1.19–7.945 | 0.02 |
| Ketonuria, n (%) | 39 (7.2) | 8 (5.7) | 31 (7.7) | 1.38 | 0.62–3.084 | 0.429 |
| PH, means (SD) | 6.2 (0.7) | 6.2 (0.5) | 6.3 (0.8) | 1.21 | 0.922–1.586 | 0.171 |
| Proteinuria, n (%) | 281 (51.9) | 60 (42.9) | 221 (55.1) | 1.64 | 1.11–2.414 | 0.013 |
| Occult blood, n (%) | 420 (77.6) | 100 (71.4) | 320 (79.8) | 1.58 | 1.017–2.454 | 0.042 |
| Nitrite, n (%) | 85 (15.7) | 8 (5.7) | 77 (19.2) | 3.92 | 1.842–8.348 | 0 |
| Leukocyte enzymes, n (%) | 391 (72.3) | 94 (67.1) | 297 (74.1) | 1.4 | 0.921–2.122 | 0.116 |
| WBC count, means (SD) | 699.8 (2315.7) | 324.1 (1481.8) | 830.9 (2531.7) | 1 | 1–1 | 0.043 |
| Epithelial cells count, means (SD) | 8.8 (15.8) | 8.3 (17.5) | 9.0 (15.2) | 1 | 0.99–1.016 | 0.641 |
| Urine casts, means (SD) | 0.4 (1.0) | 0.3 (0.6) | 0.5 (1.1) | 1.29 | 0.958–1.724 | 0.094 |
| Pathological casts, means (SD) | 0.2 (0.6) | 0.1 (0.2) | 0.2 (0.7) | 1.52 | 0.773–3.001 | 0.223 |

LUTS, lower urinary tract symptoms, BPH, benign prostatic hyperplasia; UAFA, urological anatomical and functional abnormalities; NUP, number of urinary tract microbiological species; FPG, fasting plasma glucose; WBC, urine white blood cells

that the use of this nomogram to identify UPB infections to intervene may provide more benefit than the original treatment strategy. According to the analysis, there would be higher risk of infections with UPB for patients whose total score of all indicators is ≥148, and in turn, <148 means higher likelihood of microbial colonizing in urinary tract. The validation results demonstrated that the nomogram score could be used as a predictor of UPB infections and clinical intervention accordingly.

## 3.5 The role of ln(reads) in nomogram

Building the bar chart to identify the importance of seven predictor variables found ln(reads) came out on top (Figure 11). Following the above methods, we tried to remove the ln(reads) in the model and only used the rest six variables, namely, age, UN, NUP, urine culture, urine glucose, and nitrites, to repeat the modeling process again constructing the simple model

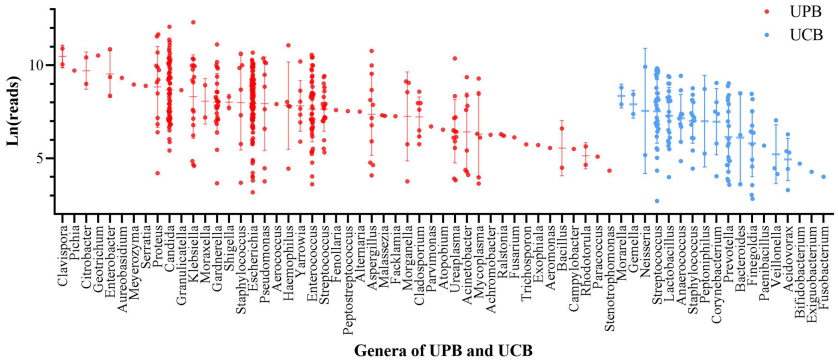


FIGURE 1
The ln(reads) distribution of primary microorganism of 541 enrolled patient. Microorganisms were divided into urinary tract pathogens (UPB) and colonizing bacteria (UCB) groups, classified by genus, and ranked according to the mean value of ln(reads). Each dot represented one sample, red for UPB and blue for UCB.

(Figure 8, Model 2) and compared their predictive performance. The prediction efficiency of nomogram with ln(reads) (AUC = 0.767, 95% CI 0.726–0.807) was significantly better (Z = 2.304, p-value = 0.021) than that without ln(reads) (AUC = 0.727; 95% CI, 0.681–0.772). The ln(reads) of NTS could significantly improve the predictive effect of nomogram. Dividing into two groups according to the cutoff value, it can be found that the nomogram based on NTS can cover more UPB than ln(reads) only (Figure 12). The nomogram incorporating multiple factors can further expand the scope of identification based on ln(reads) only ($\chi^2$ = 7.36, p-value = 0.009).

## 4 Discussion

Nowadays, the popularization of sequencing technology has proved that there are still microorganisms in the bladder urine of healthy individuals; even the concepts of urinary microflora and urinary microbiome have been proposed (Markowski et al., 2019; Yacouba et al., 2022). More than one reference stresses the importance of distinguishing between pathogens and colonizers in the urinary tract environment (Yoshimura et al., 2021; Zhao et al., 2021). Timely and accurate detection of pathogens will contribute to targeted treatment of UTI patients, which can significantly reduce the occurrence of multi-drug-resistant uropathogens and life-threatening urosepsis (Quan et al., 2021). This study was the first to use nanopore targeted sequencing (NTS) for urinary microbiota detection in a large clinical sample size and made the first attempt at interpretation in detail of sequencing results for distinguishing UPB from UCB. The results suggested that NTS could be used to identify UPB to some extent and that a nomogram constructed by combining NTS with other infection-independent predictors could achieve better performance in prediction.

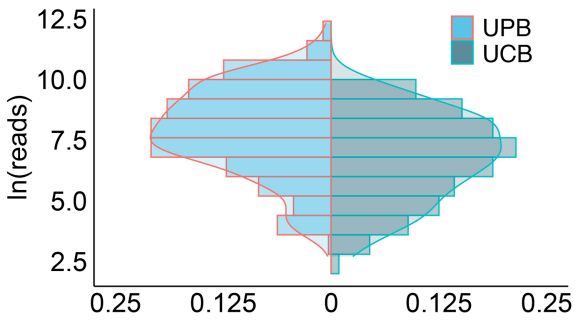


FIGURE 2
The histogram symmetrically displayed the distribution of ln(reads) in the UPB and UCB groups. The horizontal coordinate represented the percentage, the vertical coordinate represented ln(reads), the red line represented uropathogens, the blue line represented colonizers, and the two sets of ln(reads) data were symmetrically distributed on both sides of X=0.

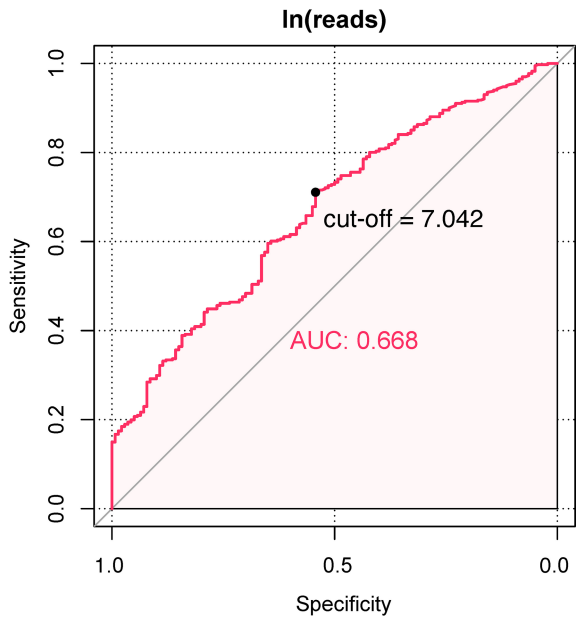


FIGURE 3
The ROC and AUC of ln(reads) to distinguish UPB or UCB.

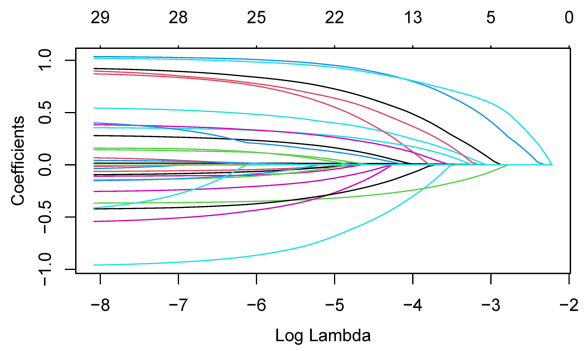


FIGURE 4
Plots for coefficient distribution of 33 variables in LASSO regression. The horizontal coordinate indicates the logarithm of the penalty parameter λ, the vertical coordinate represents the coefficient of potential predictor, and colored curves represents the coefficients changing trajectories of the predictors as the penalty parameter λ increasing.

Sequencing technologies are better suited to this job than urine culture (Petersen et al., 2019; Marshall et al., 2021). Some studies have pointed out that reads of metagenomic next generation sequencing (mNGS) can diagnose lower respiratory tract infections and identify the true-positive pathogenic bacteria; however, there is still a hot topic of discussion about efficient clinical applications or precision of mNGS for its short read length (Gasiorek et al., 2019; Liu et al., 2022). Compared with the previous sequencing technologies, nanopore sequencing achieves high throughput and long read length (≥150 kbp), with the advantages of large-scale multiplex sequencing and real-time analysis and can realize timely and comprehensive visualization overall urinary tract microbes (Noakes et al., 2019; Moss et al., 2020). In addition, targeted amplification during library preparation can reduce human host interference and enhance the genomic abundance of microorganisms (Kovaka et al., 2021). To some extent, the advantages of NTS with long read length to sensitively, comprehensively, and accurately detect multi-system microorganisms have been demonstrated (Charalampous et al., 2019; Burgess, 2020; Gilpatrick et al., 2020). Although the value

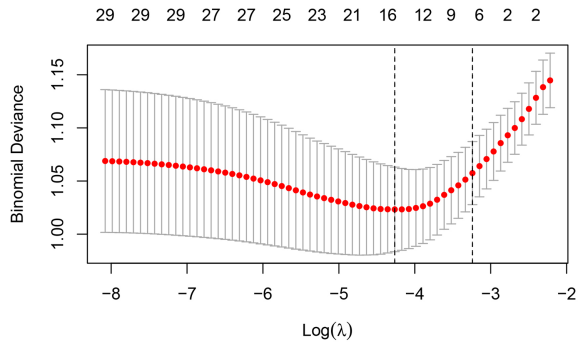


FIGURE 5
Cross-validation results for the penalty parameter in LASSO regression. The left dashed line corresponded to the value of the parameter log(λ) and the number of variables with the minimum variable loss error. When log(λ) = −4.26, 14 variables were filtered out.

of reads in the identification of UPB and UCB was not extremely satisfactory, the ln(reads) and NUP of NTS occupied the top 2 positions in the variable importance ranking, which effectively validated NTS as a determinant of model's validity. Hence, the preliminary determination of UPB from NTS results has become possible from a clinical perspective, especially when culture results are not available; the clinical value of the nomogram is more easily demonstrated.

Multi-species of microorganisms in the urinary tract environment were found to be a protective factor in our study; the greater the variety of urinary tract microorganisms, the less likely to be infected with UPB. Horwitz proved that colonization with *E. coli* did not impact bacterial bladder diversity, but subjects who developed infections were all associated with overgrowth of a urinary pathogen and had less diverse bladder microbiota (Horwitz et al., 2015). Florian suggested that while polymicrobial colonization was considered a pre-infection state from a pathophysiological perspective, however, compared to the healthy, the increased risk of UTI was usually due to reduced clearance of UPB or increased UCB (Wagenlehner et al., 2020). Therefore, maintaining a stable UCB group for people who cannot avoid the growth of UCB will help reduce the incidence of UPB infections. As described in the EAU guidelines, urinary growth of bacteria in an asymptomatic individual may protect against superinfecting symptomatic UTI (Neugent et al., 2020; Bonkat, 2022).

We collected UTI-related clinical data for regression analysis and screened out seven independent predictors to construct the nomogram, which showed favorable performance in UPB identification. The two items described above indicates that NTS is the major contributor to this nomogram, and beyond that, urine culture, age, urological neoplasms, urine glucose, and nitrites are additional independent predictors of UPB infections.

In this study, the role of urine culture was to diagnose typical UPB with a pathogen detection rate of 37.7% (151/401); negative results still have the possibility of infection. There is no doubt that urine culture is still an independent factor in determining the pathogenic organism but not the most important with positive results scoring approximately 20 in the nomogram, even negligible in certain cases, while NTS score was apparently higher and dominant. Multi-study results consistent with clinical experience showed that culture methods always seem to lag, and the positive rate would be influenced by potential applications of empirical antibiotics therapy (Wang et al., 2022). Gupta suggested that the role of urine culture is to retrospectively confirm and emphasized the definition of "contaminants" and the threshold of bacteriuria required for the diagnosis needed to be re-discussed (Gupta et al., 2017).

Age was an important risk predictor for the infections with UPB; the likelihood of infections with UPB increased by 1.6% for each additional year of age in patients. Similarly, a study demonstrated that older age was an independent predictor of treatment failure for cUTI patients and risk factors for 30-day mortality (Eliakim-Raz et al., 2019). It might be associated with miscellaneous underlying diseases, dysregulated immune status of host, and the variability in antibiotic resistance pattern (Frisbie et al., 2021). Hence, differentiating UPB from urinary tract

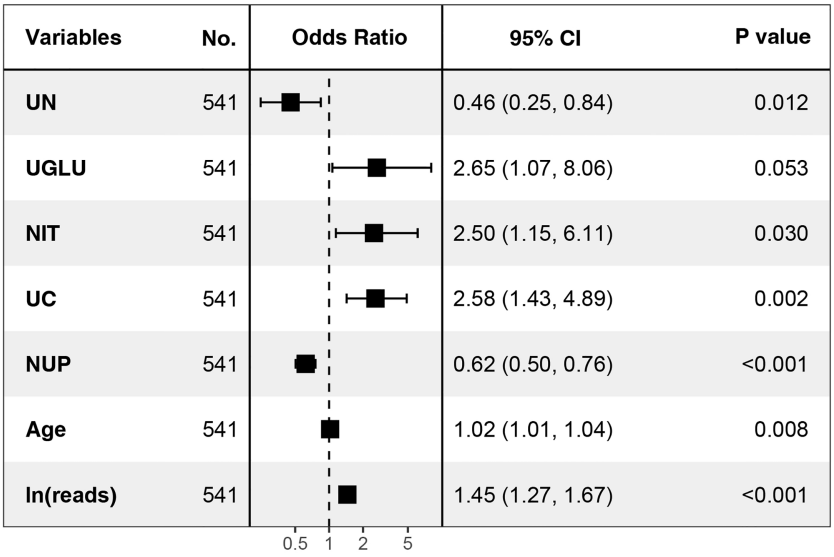


FIGURE 6
Seven independent predictors in multi-factor logistic regression. UN, urological neoplasms; UGLU, urine glucose; NIT, urine nitrite; UC, urine culture; NUP, number of urinary tract microbiological species.

microbiota in elderly patients will help to avoid the overuse of antibiotics and reduce the generation of multidrug-resistant strains (Bonkat, 2022).

Regression analysis results found that UCB were more likely to be detected in the urine of patients with urological neoplasms. It is perhaps related to adjuvant intravesical chemotherapy instillations for re-hospitalized bladder urothelial carcinoma patients (Bajic et al., 2019). This result is consistent with Peng's finding that bacterial richness was increased in genitourinary cancer groups classified at a higher risk of recurrence or progression, indicating that microbial composition may help predict the prognosis of cancer patients (Wu et al., 2018). Notably, available evidence suggests an association between the differences in genitourinary microbial composition or diversity and the development or progression of genitourinary malignancies, with both pathogenic factors and cofactors among microbiota members. Unfortunately, the number of relevant articles has been limited, and the types of differential flora found in different studies vary widely (Yacouba et al., 2022). The more readily accepted view is that the chronic inflammatory response after the early acute UPB infection may be a carcinogenic factor, making the search for preventive factors in UCB group particularly necessary, similar to the preventive role of *Lactobacillus vaginalis* in controlling UPB colonization in women and reducing UTI (Markowski et al., 2019). What is clear is that sequencing technology and statistical analysis will help to study the

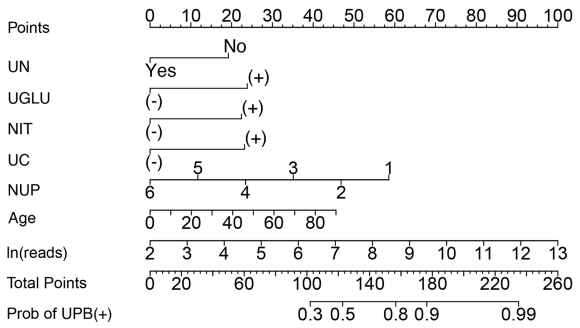


FIGURE 7
Nomogram to distinguish between UPB and UCB of patients suspected with UTI by calculating the sum of the corresponding scores for each indicator. UN, urological neoplasms; UGLU, urine glucose; NIT, urine nitrite; UC, urine culture; NUP, number of urinary tract microbiological species. '+' or '–' represents positive or negative result for corresponding laboratory test indicator.

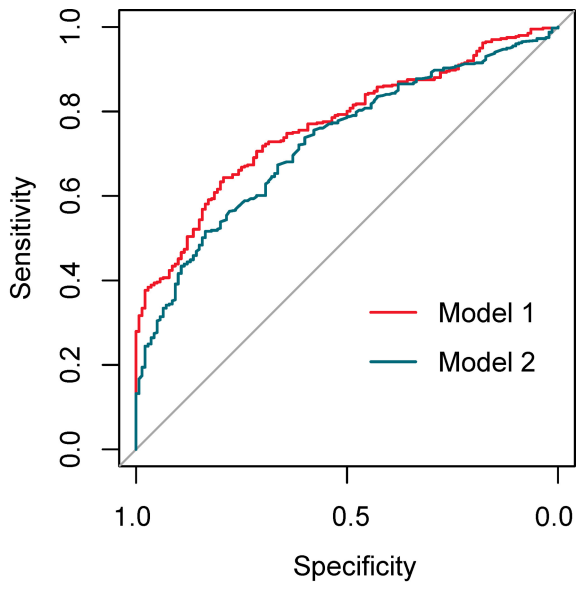


FIGURE 8
The ROC curves of the models with ln(reads) (Model 1) and without ln(reads) (Model 2).

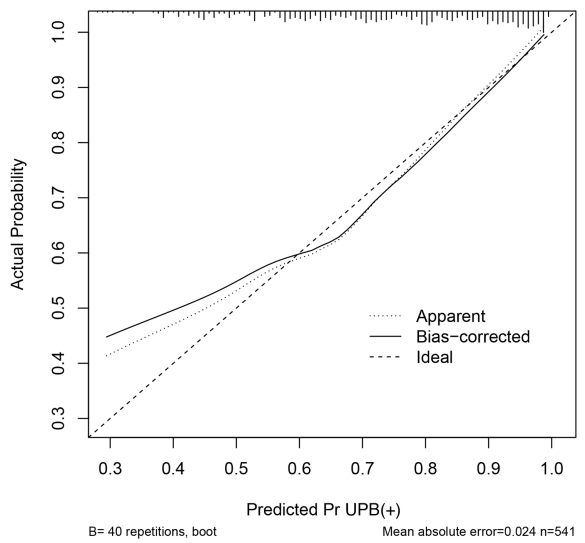


FIGURE 9
Calibration curve of the nomogram. The horizontal and vertical coordinates represent the predicted probability of uropathogens infection by the nomogram and actual probability of infection, the diagonal line is a reference line representing the predicted probability equaled to the actual probability, and the black line indicates the degree of matching between the predicted and actual results of this nomogram.

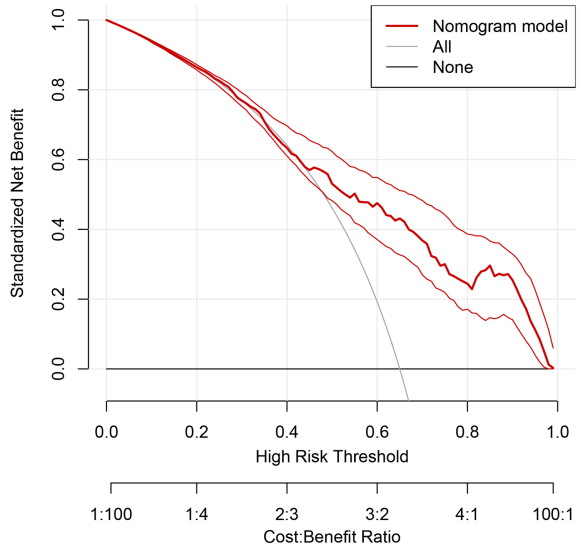


FIGURE 10
Decision curve analysis (DCA) of the nomogram. The horizontal coordinate represents the threshold probability, above which the predicted outcome was a true positive; the clinical intervention at this point would benefit, there are drawbacks conversely, and the vertical coordinate represented the net benefit after the benefit minus the drawback. The gray curve is the net benefit of clinical intervention for all enrolled patients, the black line at Y=0 represents no clinical intervention for any outcome, so the net benefit is always 0. The thick red line represents the benefit of clinical interventions with reference to the predicted results of the nomogram.

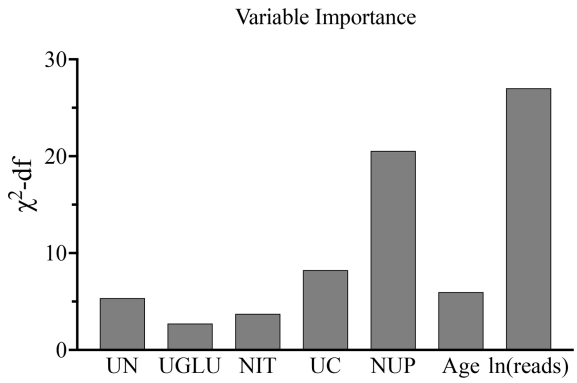


FIGURE 11
The bar chart showed importance ranking of seven independent predictors of the nomogram.

relationship between the urinary tract microbiota and genitourinary neoplasms, and forthcoming clinical application of NTS will contribute to the subsequent research on this subject.

It has been adequately demonstrated that urine nitrite was beneficial in predicting the infections of UPB, most of which were Gram-negative *Bacillus* in Florian's statistics concerning the prevalence of uropathogenic bacterial species in cUTI, converting nitrates to nitrites (Wagenlehner et al., 2020). Multiple studies have reported that urine nitrite is associated with UTIs; even preoperative positive urine nitrite is an independent risk factor for postoperative fever after ureteroscopy (Velasco et al., 2020; Ma et al., 2021).

It should be noted that it was glycosuria rather than blood glucose that could predict the infections of UPB in this study; the latter was not significantly different in the two data sets, so did diabetes. Diabetes has been shown to increase the risk of all classification of UTIs, from ASB to cUTI (Gupta et al., 2017). However, glycosuria is believed to provide an optimal environmental condition for bacterial growth (Mohanty et al., 2022). Research showed that glycosuria exposure augmented group B *Streptococcus* epithelial adherence and hemolysis and

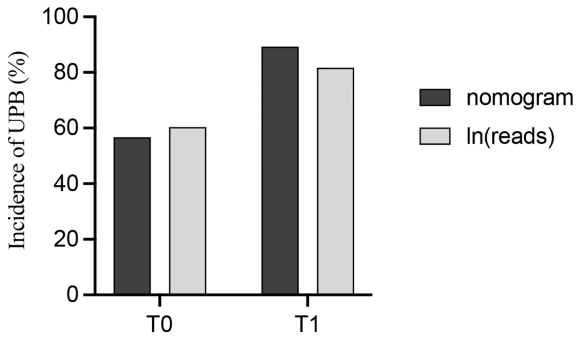


FIGURE 12
The probability of identifying UPB was compared between the nomogram and ln(reads) alone after grouping with the cutoff value of ln(reads).

antimicrobial peptide resistance (John et al., 2021). Islam found that glycosuria rapidly increased gene expression encoding biofilm formation and central metabolic virulence of uropathogenic *E. coli* (Islam et al., 2022). Whether urine glucose plays a greater role in identifying uropathogenic bacteria from colonizers needs more data to be supported.

### 4.1 Limitation

First, it should not be overlooked that NTS is currently unable to perform drug-resistant strain prediction, but the potential exists to identify drug-resistant genes (Arango-Argoty et al., 2019; Xu et al., 2021). Second, there are differences in colonization of different parts in the urinary tract, which cannot be identified in the midstream urine. Third, there is still the possibility of infection caused by colonizing bacteria, and even non-first bacteria in the microorganisms cause disease. For opportunistic pathogens, there should be two states of colonization and pathogenicity, which have not been discussed in this study. Hence, the conclusions of this study cannot be directly used to guide the prevention of infection of UPB from healthy individuals, and better prediction models need to be further developed.

## 5 Conclusions

We dug deeper into NTS data than ever before and demonstrated that NTS was conducive to distinguish uropathogens from colonizing bacteria. Through LASSO and multivariate logistic regression, we screened out seven independent predictors and established a nomogram to determine whether the patient has uropathogenic infection, which showed good performance in internal verification and better prediction effect than NTS only.

NTS was the primary contributor to the validity of this nomogram and showed great potential in etiological detection. The nomogram might contribute to timely detecting uropathogens, in-depth interpretation for clinical applications of NTS, and the research on urinary tract microorganisms.

## Data availability statement

The datasets presented in this article are not readily available because: The full data belongs to the Renmin hospital of Wuhan University, it is not in a public repository. Data is included in part in Supplementary Table 1, and further inquiries can be directed to the corresponding authors.

## Ethics statement

The studies involving human participants were reviewed and approved by The Ethics Committee of the Renmin Hospital of Wuhan University. Written informed consent for participation was not required for this study in accordance with the national legislation and the institutional requirements.

## Author contributions

SJ, YW, YX, and SY contributed to conception and design of the study. HK, CSu, JZ, and LM collected the clinical data. YW, CW, and XS performed the statistical analysis. SJ wrote the first draft of the manuscript. CSo, CD, and WL wrote sections of the manuscript. All authors contributed to the article and approved the submitted version.

## Acknowledgments

We are grateful to Wuhan Dgensee Medical Laboratory Co., Ltd. for their contribution and support in data collection and technical guidance of this study.

## Conflict of interest

The authors declare that the research was conducted in the absence of any commercial or financial relationships that could be construed as a potential conflict of interest.

## Publisher's note



## Supplementary material

The Supplementary Material for this article can be found online at: https://www.frontiersin.org/articles/10.3389/fcimb.2023.1142426/full#supplementary-material

## References

Arango-Argoty, G. A., Dai, D., Pruden, A., Vikesland, P., Heath, L. S., and Zhang, L. (2019). NanoARG: a web service for detecting and contextualizing antimicrobial resistance genes from nanopore-derived metagenomes. *Microbiome* 7 (1), 88. doi: 10.1186/s40168-019-0703-9

Bajic, P., Wolfe, A. J., and Gupta, G. N. (2019). Old instillations and new implications for bladder cancer: the urinary microbiome and intravesical BCG. *BJU Int.* 124 (1), 7–8. doi: 10.1111/bju.14683

Bonkat, G. (2022). *EAU guidelines* (Amsterdam, The Netherlands: EAU Guidelines Office).

Burgess, D. J. (2020). Expanding applications for nanopore sequencing. *Nat. Rev. Genet.* 21 (2), 67. doi: 10.1038/s41576-019-0204-5

Charalampous, T., Kay, G. L., Richardson, H., Aydin, A., Baldan, R., Jeanes, C., et al. (2019). Nanopore metagenomics enables rapid clinical diagnosis of bacterial lower respiratory infection. *Nat. Biotechnol.* 37 (7), 783–792. doi: 10.1038/s41587-019-0156-5

Dauwalder, O., Michel, A., Eymard, C., Santos, K., Chanel, L., Luzzati, A., et al. (2021). Use of artificial intelligence for tailored routine urine analyses. *Clin. Microbiol. Infection* 27 (8), 1161–1168. doi: 10.1016/j.cmi.2020.09.056

Eliakim-Raz, N., Babitch, T., Shaw, E., Addy, I., Wiegand, I., Vank, C., et al. (2019). Risk factors for treatment failure and mortality among hospitalized patients with complicated urinary tract infection: a multicenter retrospective cohort study (RESCUING study group). *Clin. Infect. Dis.* 68 (1), 29–36. doi: 10.1093/cid/ciy418

Frisbie, L., Weissman, S. J., Kapoor, H., D'Angeli, M., Salm, A., Radcliff, J., et al. (2021). Antimicrobial resistance patterns of urinary escherichia coli among outpatients in Washington state, 2013-2017: associations with age and sex. *Clin. Infect. Dis.* 73 (6), 1066–1074. doi: 10.1093/cid/ciab250

Fu, Y., Chen, Q., Xiong, M., Zhao, J., Shen, S., Chen, L., et al. (2022). Clinical performance of nanopore targeted sequencing for diagnosing infectious diseases. *Microbiol. Spectr.* 10 (2), e27022. doi: 10.1128/spectrum.00270-22

Gasiorek, M., Hsieh, M. H., and Forster, C. S. (2019). Utility of DNA next-generation sequencing and expanded quantitative urine culture in diagnosis and management of chronic or persistent lower urinary tract symptoms. *J. Clin. Microbiol.* 58 (1), e204–e219. doi: 10.1128/JCM.00204-19

Gilpatrick, T., Lee, I., Graham, J. E., Raimondeau, E., Bowen, R., Heron, A., et al. (2020). Targeted nanopore sequencing with Cas9-guided adapter ligation. *Nat. Biotechnol.* 38 (4), 433–438. doi: 10.1038/s41587-020-0407-5

Gu, W., Deng, X., Lee, M., Sucu, Y. D., Arevalo, S., Stryke, D., et al. (2021). Rapid pathogen detection by metagenomic next-generation sequencing of infected body fluids. *Nat. Med.* 27 (1), 115–124. doi: 10.1038/s41591-020-1105-z

Gupta, K., Grigoryan, L., and Trautner, B. (2017). Urinary tract infection. *Ann. Internal Med.* 167 (7), C49. doi: 10.7326/AITC201710030

Hooton, T. M., Roberts, P. L., and Stapleton, A. E. (2021). Asymptomatic bacteriuria and pyuria in premenopausal women. *Clin. Infect. Dis.* 72 (8), 1332–1338. doi: 10.1093/cid/ciaa274

Horwitz, D., McCue, T., Mapes, A. C., Ajami, N. J., Petrosino, J. F., Ramig, R. F., et al. (2015). Decreased microbiota diversity associated with urinary tract infection in a trial of bacterial interference. *J. Infect.* 71, 3, 358–367. doi: 10.1016/j.jinf.2015.05.014

Huang, Q., Fu, A., Wang, Y., Zhang, J., Zhao, W., and Cheng, Y. (2021). Microbiological diagnosis of endophthalmitis using nanopore targeted sequencing. *Clin. Exp. Ophthalmol.* 49 (9), 1060–1068. doi: 10.1111/ceo.13992

Islam, M. J., Bagale, K., John, P. P., Kurtz, Z., and Kulkarni, R. (2022). Glycosuria alters uropathogenic escherichia coli global gene expression and virulence. *mSphere* 7 (3), e422. doi: 10.1128/msphere.00004-22

John, P. P., Baker, B. C., Paudel, S., Nassour, L., Cagle, H., and Kulkarni, R. (2021). Exposure to moderate glycosuria induces virulence of group b streptococcus. *J. Infect. Dis.* 223 (5), 843–847. doi: 10.1093/infdis/jiaa443

Kovaka, S., Fan, Y., Ni, B., Timp, W., and Schatz, M. C. (2021). Targeted nanopore sequencing by real-time mapping of raw electrical signal with UNCALLED. *Nat. Biotechnol.* 39 (4), 431–441. doi: 10.1038/s41587-020-0731-9

Li, S. C., Chi, H., Huang, F. Y., Chiu, N. C., Huang, C. Y., Chang, L., et al. (2023). Building nomogram plots for predicting urinary tract infections in children less than three years of age. *J. Microbiol. Immunol. Infect.* 56 (1), 111–119. doi: 10.1016/j.jmii.2022.08.006

Liu, H., Zhang, Y., Yang, J., Liu, Y., and Chen, J. (2022). Application of mNGS in the etiological analysis of lower respiratory tract infections and the prediction of drug resistance. *Microbiol. Spectr.* 10 (1), e250221. doi: 10.1128/spectrum.02502-21

Ma, Y. C., Jian, Z. Y., Li, H., and Wang, K. J. (2021). Preoperative urine nitrite versus urine culture for predicting postoperative fever following flexible ureteroscopic lithotripsy: a propensity score matching analysis. *World J. Urol* 39 (3), 897–905. doi: 10.1007/s00345-020-03240-w

Markowski, M. C., Boorjian, S. A., Burton, J. P., Hahn, N. M., Ingersoll, M. A., Maleki, V. S., et al. (2019). The microbiome and genitourinary cancer: a collaborative review. *Eur. Urol.* 75 (4), 637–646. doi: 10.1016/j.eururo.2018.12.043

Marshall, C. W., Kurs-Lasky, M., McElheny, C. L., Bridwell, S., Liu, H., and Shaikh, N. (2021). Performance of conventional urine culture compared to 16S rRNA gene amplicon sequencing in children with suspected urinary tract infection. *Microbiol. Spectr.* 9 (3), e186121. doi: 10.1128/spectrum.01861-21

McDonald, M., Kameh, D., Johnson, M. E., Johansen, T., Albala, D., and Mouraviev, V. (2017). A head-to-Head comparative phase II study of standard urine culture and sensitivity versus DNA next-generation sequencing testing for urinary tract infections. *Rev. Urol.* 19 (4), 213–220. doi: 10.3909/riu0780

Mohanty, S., Kamolvit, W., Scheffschick, A., Björklund, A., Tovi, J., Espinosa, A., et al. (2022). Diabetes downregulates the antimicrobial peptide psoriasin and increases e. coli burden in the urinary bladder. *Nat. Commun.* 13 (1), 4983. doi: 10.1038/s41467-022-32636-y

Moss, E. L., Maghini, D. G., and Bhatt, A. S. (2020). Complete, closed bacterial genomes from microbiomes using nanopore sequencing. *Nat. Biotechnol.* 38 (6), 701–707. doi: 10.1038/s41587-020-0422-6

Neugent, M. L., Hulyalkar, N. V., Nguyen, V. H., Zimmern, P. E., and De Nisco, N. J. (2020). Advances in understanding the human urinary microbiome and its potential role in urinary tract infection. *mBio* 11 (2), e218–e220. doi: 10.1128/mBio.00218-20

Noakes, M. T., Brinkerhoff, H., Laszlo, A. H., Derrington, I. M., Langford, K. W., Mount, J. W., et al. (2019). Increasing the accuracy of nanopore DNA sequencing using a time-varying cross membrane voltage. *Nat. Biotechnol.* 37 (6), 651–656. doi: 10.1038/s41587-019-0096-0

Petersen, L. M., Martin, I. W., Moschetti, W. E., Kershaw, C. M., and Tsongalis, G. J. (2019). Third-generation sequencing in the clinical laboratory: exploring the advantages and challenges of nanopore sequencing. *J. Clin. Microbiol.* 58 (1), e1315-e1319. doi: 10.1128/JCM.01315-19

Quan, J., Dai, H., Liao, W., Zhao, D., Shi, Q., Zhang, L., et al. (2021). Etiology and prevalence of ESBLs in adult community-onset urinary tract infections in East China: a prospective multicenter study. *J. Infect.* 83 (2), 175–181. doi: 10.1016/j.jinf.2021.06.004

Rusk, N. (2019). More accurate nanopore sequencing. *Nat. Methods* 16 (6), 460. doi: 10.1038/s41592-019-0449-0

Velasco, R., Gomez, B., de la Torre, M., Benito, J., and Mintegi, S. (2020). A positive nitrite test was an independent risk factor for invasive bacterial infections in infants under 90 days of age with fever without source. *Acta Paediatr.* 109 (11), 2316–2323. doi: 10.1111/apa.15230

Wagenlehner, F., Bjerklund, J. T., Cai, T., Koves, B., Kranz, J., Pilatz, A., et al. (2020). Epidemiology, definition and treatment of complicated urinary tract infections. *Nat. Rev. Urol* 17 (10), 586–600. doi: 10.1038/s41585-020-0362-4

Wang, M., Fu, A., Hu, B., Tong, Y., Liu, R., Liu, Z., et al. (2020). Nanopore targeted sequencing for the accurate and comprehensive detection of SARS-COV-2 and other respiratory viruses. *Small* 16 (32), e2002169. doi: 10.1002/smll.202002169

Wang, C., You, Z., Fu, J., Chen, S., Bai, D., Zhao, H., et al. (2022). Application of metagenomic next-generation sequencing in the diagnosis of pulmonary invasive fungal disease. *Front. Cell Infect. Microbiol.* 12, 949505. doi: 10.3389/fcimb.2022.949505

Wu, P., Zhang, G., Zhao, J., Chen, J., Chen, Y., Huang, W., et al. (2018). Profiling the urinary microbiota in Male patients with bladder cancer in China. *Front. Cell. Infection Microbiol.* 8. doi: 10.3389/fcimb.2018.00167

Xu, Y., Lewandowski, K., Downs, L. O., Kavanagh, J., Hender, T., Lumley, S., et al. (2021). Nanopore metagenomic sequencing of influenza virus directly from respiratory samples: diagnosis, drug resistance and nosocomial transmission, united kingdom, 2018/19 influenza season. *Euro Surveill* 26 (27), 2000004. doi: 10.2807/1560-7917.ES.2021.26.27.2000004

Yacouba, A., Tidjani, A. M., Lagier, J. C., Dubourg, G., and Raoult, D. (2022). Urinary microbiota and bladder cancer: a systematic review and a focus on uropathogens. *Semin. Cancer Biol.* 86 (Pt 3), 875–884. doi: 10.1016/j.semcancer.2021.12.010

Yang, M., Li, Y., and Huang, F. (2023). A nomogram for predicting postoperative urosepsis following retrograde intrarenal surgery in upper urinary calculi patients with negative preoperative urine culture. *Sci. Rep.* 13 (1), 2123. doi: 10.1038/s41598-023-29352-y

Yoshimura, J., Yamakawa, K., Umemura, Y., Nishida, T., Ooi, Y., and Fujimi, S. (2021). Impact of beta-lactamase detection reagent on rapid diagnosis of ESBL-producing pathogens using urine samples of patients with gram-negative bacteriuria. *Int. J. Infect. Dis.* 113, 18–22. doi: 10.1016/j.ijid.2021.09.059

Zhao, N., Cao, J., Xu, J., Liu, B., Liu, B., Chen, D., et al. (2021). Targeting RNA with next- and third-generation sequencing improves pathogen identification in clinical samples. *Adv. Sci.* 8 (23), 2102593. doi: 10.1002/advs.202102593

frontiers | Frontiers in Cellular and Infection Microbiology

TYPE Perspective
PUBLISHED 27 June 2023
DOI 10.3389/fcimb.2023.1188684



OPEN ACCESS

EDITED BY
Elisabetta Blasi,
University of Modena and Reggio Emilia, Italy

REVIEWED BY
Antonella Lupetti,
University of Pisa, Italy

*CORRESPONDENCE
Antonella Mencacci
antonella.mencacci@unipg.it

RECEIVED 17 March 2023
ACCEPTED 05 June 2023
PUBLISHED 27 June 2023

CITATION
Mencacci A, De Socio GV, Pirelli E, Bondi P and Cenci E (2023) Laboratory automation, informatics, and artificial intelligence: current and future perspectives in clinical microbiology. *Front. Cell. Infect. Microbiol.* 13:1188684. doi: 10.3389/fcimb.2023.1188684



# Laboratory automation, informatics, and artificial intelligence: current and future perspectives in clinical microbiology

Antonella Mencacci [1,2*], Giuseppe Vittorio De Socio [3], Eleonora Pirelli [1], Paola Bondi [1] and Elio Cenci [1,2]

[1]Microbiology and Clinical Microbiology, Department of Medicine and Surgery, University of Perugia, Perugia, Italy, [2]Microbiology, Perugia General Hospital, Perugia, Italy, [3]Clinic of Infectious Diseases, Perugia General Hospital, Perugia, Italy

Clinical diagnostic laboratories produce one product—information—and for this to be valuable, the information must be clinically relevant, accurate, and timely. Although diagnostic information can clearly improve patient outcomes and decrease healthcare costs, technological challenges and laboratory workflow practices affect the timeliness and clinical value of diagnostics. This article will examine how prioritizing laboratory practices in a patient-oriented approach can be used to optimize technology advances for improved patient care.

KEYWORDS

**laboratory automation, artificial intelligence, informatics, laboratory workflow, Kiestra, WASPLab**

## Introduction

Patterns of infectious diseases have changed dramatically: patients are frequently immunocompromised and often have complicating comorbidities, infections with multi-drug-resistant organisms (MDRO) are a global problem, new antibiotics are available, but it is mandatory to preserve their efficacy. It is estimated that at least 700,000 people die worldwide every year with infections caused by MDRO, and it is predicted that by 2050, 10 million deaths might be due to these organisms (O'Neill, 2016). Administration of rapid, broad-spectrum empiric therapy is essential to improve patient outcome (Levy et al., 2018), but this is often inappropriate (Kumar et al., 2009; Zilberberg et al., 2017). A meta-analysis assessing the impact of antibiotic therapy on Gram-negative sepsis showed that inappropriate therapy was associated with 3.3-fold increased risk of mortality, longer hospitalization, and higher costs (Raman et al., 2015). Thus, rapid, accurate diagnostics are critical for the selection of the most appropriate therapy.

Advanced, sophisticated technologies such as mass spectrometry and molecular diagnostics are rapidly changing our ability to diagnose infections (Trotter et al., 2019),

although they should be viewed as complementary to traditional growth-based diagnostics. Laboratory automation and applications of intelligent use of informatics also have a transformative impact of microbiology diagnostics. These tools have the potential to accelerate clinical decision-making and positively impact the management of infections, improve patient outcome, and facilitate diagnostic and antimicrobial stewardship (AS) programs (Messacar et al., 2017). However, it is a challenge for clinical microbiologists to implement these technologies because it requires changing well-established workflow practices. This paper will focus on the impact of automation and informatics combined with workflow changes on laboratory, patient, and hospital management (Figure 1).

## Impact on laboratory management

In clinical microbiology, the term "total laboratory automation" (TLA) is used to describe the automation of the entire diagnostic workflow: inoculation of the agar plates, incubation, reading of culture results, identification (ID), and antimicrobial susceptibility testing (AST). All these steps in a conventional laboratory are performed manually, usually according to a sample-centered approach. At present, two laboratory automation (LA) systems are available: the BD Kiestra™ system (Becton Dickinson, Sparks, MD) and the WASPLab® system (Copan Diagnostics, Murrieta, CA) (Croxatto et al., 2016).

### Inoculation

Quality and precision of inoculation are improved by automation. Instruments work in a standardized and consistent mode, not achievable with a manual procedure, and independent of operator variability. Indeed, LA allows better isolation of colonies compared to manual inoculation, with decreased need of subcultures for follow-up work, mainly AST, resulting in a more rapid report (Croxatto et al., 2015; Burckhardt, 2018). It was found that WASP automated streaking of urines using a sterile loop was superior to manual streaking, yielding a higher number of single colonies and of detected morphologies, species, and pathogens (Quiblier et al., 2016). The BD Kiestra™ system, based on a rolling magnetic bead streaking technology, has been shown to improve the accuracy of quantitative culture results and the recovery of discrete colonies from polymicrobial samples, compared to manual and automated WASP streaking (Croxatto et al., 2015; Iversen et al., 2016). This implies a reduction of bacterial subcultures to perform ID and AST, thus shortening time to results, as evidenced for urines (Croxatto et al., 2017) and both methicillin-resistant *Staphylococcus aureus* (MRSA) and carbapenem-resistant *Enterobacterales* screening samples (Cheng et al., 2020).

### Incubation

Closed incubators with digital imaging of cultures allow more rapid growth than conventional incubators that are opened frequently throughout the day. Moreover, in TLA, plates are fully tracked as long as they stay within the system, so that it is possible to define by hours and minutes incubation times and plate examination in contrast with the traditional system in which incubation times are defined in days. Burckhardt et al. showed that first growth of MRSA, multi-drug-resistant (MDR) Gram-negative bacteria, and vancomycin-resistant enterococci (VRE) on selective chromogenic plates was visible as early as after 4 h of inoculation, although the bacterial mass was not sufficient for follow-up work (Burckhardt et al., 2019). Also, growth of *Escherichia coli*, *Pseudomonas aeruginosa*, *Enterococcus faecalis*, and *S. aureus* on chromogenic plates was 3 to 4 hours faster in the automated than in classic system (Moreno-Camacho et al., 2017). Implementation of BD Kiestra TLA significantly improved turnaround times (TAT) for positive and negative urine cultures (Theparee et al., 2017). Similarly, WASPLab automation enabled a reduction of the culture reading time for different specimens without affecting performances (Cherkaoui et al., 2019). However,

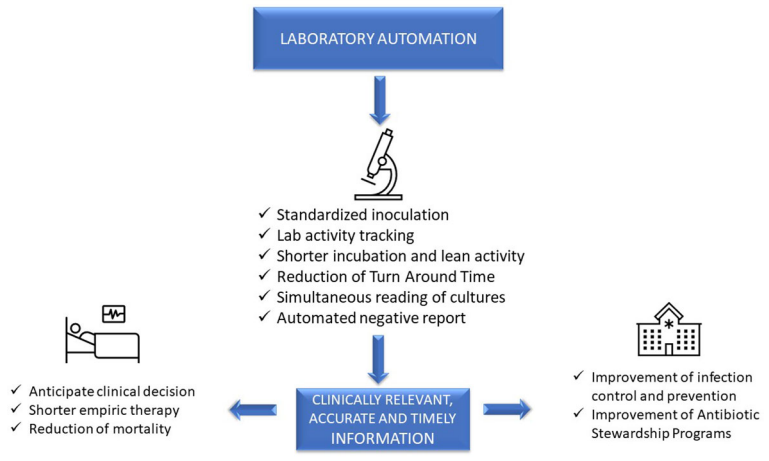


FIGURE 1

Impact of automation on laboratory, patient, and hospital management.

minimum incubation times for each type of specimen, for a timely and accurate positive or negative report, are not yet defined and additional studies are needed.

## Reading

Kiestra LA system, through a real-time dashboard, times tasks as they are scheduled. Thus, each technician perfectly knows when the culture plates will be ready for reading and when a follow-up work can be performed. This strongly facilitates laboratory workflow management, avoiding wasted time and allowing results to be delivered to the clinician as soon as possible. In addition, while in the classical system plates are read one-by-one, digital reading allows simultaneous viewing of all the plate images from the same sample, and even of different samples from the same patient. This greatly facilitates and speeds up the interpretation of culture results, either for monomicrobial or polymicrobial infections.

## ID and AST

The implementation of TLA in clinical microbiology has leveraged the advancement brought by matrix-assisted laser desorption/ionization time-of-flight mass spectrometry (MALDI-TOF/MS) (Thomson and McElvania, 2019; Cherkaoui and Schrenzel, 2022). Furthermore, Copan's TLA has recently integrated an automated device (Colibri™) that can reproducibly prepare the MALDI target for microbial identification. A recent study conducted by Cherkaoui et al. established that the WASPLab coupled to MALDI-TOF/MS significantly reduces the TAT for positive blood cultures (Cherkaoui et al., 2023). Similarly, the BD Kiestra™ IdentifA/SusceptA, a prototype for automatic colony picking, bacterial suspension preparation, MALDI-TOF target plates spotting, and Phoenix™ M50 AST panel preparation, exhibited high ID and AST performances (Jacot et al., 2021). In particular, the IdentifA showed excellent identification rates for Gram-negative bacteria, outperforming manual processing for *Enterobacterales* identification (Jacot et al., 2021), but not for streptococci, coagulase-negative staphylococci (CoNS), and yeasts (Jacot et al., 2021).

Finally, an automated solution for disk diffusion AST was developed and integrated with the Copan WASPLab system. It prepares inoculum suspensions, inoculates culture media plates, dispenses appropriate antibiotic disks according to predefined panels, transports the plates to the incubators, takes digitalized images of the media plates, and measures and interprets the inhibition zones' diameters. Cherkaoui et al., evaluating 718 bacterial strains including *S. aureus*, CoNS, *E. faecalis*, *Enterococcus faecium*, *P. aeruginosa*, and different species of *Enterobacterales*, found 99.1% overall categorical agreement between this automated AST and Vitek2 (Cherkaoui et al., 2021).

## Artificial Intelligence

The development of intelligent image analysis based on tailored algorithms designed on type of specimens and patient characteristics allows automated detection of microbial growth, release of negative samples, presumptive ID, and quantification of bacterial colonies. This represents a major innovation that has the potential to increase laboratory quality and productivity while reducing TAT (Croxatto et al., 2017). Promising results have been obtained on urine samples, with a 97%–99% sensitivity and 85%–94% specificity by the BD Kiestra system (Burckhardt et al., 2019). By a different approach, the WASPLab Chromogenic Detection Module has developed automated categorization of agar plates as "negative" (i.e., sterile) or "non-negative", comparing the same plate at time point zero to the plate after the established incubation time. With this system, an optimal diagnostic accuracy in MRSA (Faron et al., 2016a), VRE (Faron et al., 2016b), and carbapenemase-producing Enterobacteriaceae (Foschi et al., 2020) detection has been observed.

## Other functions of LA

LA can greatly facilitate to implement an effective quality system, which is required to ensure that reliable results are reported for patients. LA systems automatically track and record all the useful information for quality control: user credentials, media (lot number and expiration date), inoculation (volumes of samples, patterns, and times of streaking), incubation (atmosphere, temperature, and times) and imaging (digital images of plates and times) data (Dauwalder et al., 2016). Thus, a proper integration of LA with laboratory information system allows for complete traceability of the analytical process, from sample receipt to the final report.

Moreover, the possibility to access and review any taken image represents an invaluable tool from a diagnostic point of view (e.g., comparing morphology of colonies in recent and old samples from the same patient) and also for other activities such as monitoring laboratory quality, teaching, training, and discussing culture results with colleagues and clinicians.

# Impact on patient management

Clinical impact of an assay, a technology, or a modified workflow can be defined based on its added value for patient management. In the case of sepsis, this can be measured as time to targeted therapy and, hopefully, a decrease in the mortality rate. In manual processing laboratories, the activities are performed in batches, usually based on the type of sample and of activity (inoculation, reading, ID, AST, technical validation, and clinical validation), and the results are usually delivered mostly during the morning hours. Indeed, a study evaluating the TAT for positive blood cultures (BC) in 13 US acute care hospitals demonstrated a significant discrepancy between times of BC collection and reporting laboratory test results. While only 25% of specimens were collected between 6:00 a.m. and 11:59 a.m., approximately 80% of laboratory ID and AST results were reported in this time interval (Tabak et al., 2018). This can have a negative impact on septic patient management, delaying clinical decision-making for optimal targeted therapy.

In contrast, in automated laboratories, the activity can be organized according to lean principles, creating a continuous "flow" and producing "just-in-time" results. De Socio et al. evaluated the impact of LA on septic patient management. Positive BC were processed by fully automatic inoculation on solid media and digital reading after 8 h of incubation, followed by ID and AST. The authors found that a reduction of time to report (TTR) of about 1 day led to a significant reduction of the duration of empirical therapy (from approximately 87 h to approximately 55 h) and of 30-day crude mortality rate (from 29.0% to 16.7%) (De Socio et al., 2018).

Therefore, provided that the laboratory is open 24 h a day, or taking advantage of telemedicine systems for clinical validation, LA has a potential great impact on patient management. However, the success of such organization lies in the responsiveness of the medical teams, who should act upon the results soon after delivery by the laboratory (Vandenberg et al., 2020).

## Impact on hospital management

LA can improve the laboratory ability to characterize MDRO and produce quality results, permitting a more standardized workflow, and leaving more time for laboratory staff to focus on second-level phenotypic and/or genotypic tests. Indeed, the large diffusion of MDRO and the expanding spectrum of resistance mechanisms among pathogens pointed out the limitations of commercial routine methods for susceptibility testing of selected antibiotics, increasing the demand for cumbersome and time-consuming reference methods. For example, in the case of MDRO Gram-negative isolates, colistin MIC should be determined by the broth microdilution method (Kulengowski et al., 2019); fosfomycin MIC, by the agar-dilution method (Camarlinghi et al., 2019); and cefiderocol, a novel siderophore-conjugated cephalosporin, by the broth microdilution method using an iron-depleted cation-adjusted Mueller-Hinton broth (Simner and Patel, 2020). Moreover, in the case of detection of uncommon resistance phenotypes, molecular methods, gene sequencing, or other next-generation sequencing methods are often required (Antonelli et al., 2019).

Accuracy is not sufficient *per se* for a result to be useful. Information must be given to clinicians or other healthcare providers (e.g., pharmacists and the patient's primary care nurse) as quickly as possible. Timely report can affect hospital conditions in at least two ways: permitting to rapidly control the spread of MDRO (contact precautions, investigation of clusters of colonized/infected patients) and reducing the duration of broad-spectrum antibiotic therapy (positive results) or unnecessary empiric antibiotic therapy (negative results).

In a study proposing a cumulative antimicrobial resistance index as a tool to predict antimicrobial resistance (AR) trend in a hospital, a reversion of AR trend was observed in 2018, in comparison with the 2014–2017 period (De Socio et al., 2019). The authors speculate that this could have been a consequence of some changes in the management of infections in their hospital: (i) incubation of all BC within 1 h from collection using satellite incubators, (ii) a significant reduction in TTR after the introduction of molecular technologies and LA, and (iii) an established close collaboration between infectious disease clinicians and clinical microbiologists (De Socio et al., 2019).

Finally, Culbreath et al. demonstrated that the implementation of TLA increased laboratory productivity by up to 90%, while reducing the cost per specimen by up to 47%, provided an excellent elaboration of the efficiencies and cost-savings is achievable by implementation of full LA in the bacteriology laboratory (Culbreath et al., 2021).

## Possible improvements

A detailed wish list of technical issues to be evaluated in order to improve the performance and workflow of LA systems has been recently published (Burckhardt, 2018). Here, we will focus on facts that, in our opinion, could affect laboratory, patient, and hospital management.

To facilitate the reading of the plates according to a patient-centered approach, it would be useful to view the specimens' Gram stains in the same screen of cultured plates. The images could also be shared with clinicians, improving clinician–microbiologist interplay. Further improvement can be made by automated microscopy systems, which can significantly reduce the workload of the technical staff (Zimmermann, 2021).

The availability of digital images lays the foundation for telebacteriology, intended as the use of digital imaging and file storage for on-screen reading and decision-making (Croxatto et al., 2016). It makes it possible to geographically dissociate plate manipulation from reading and validation of the results. This could promote the microbiologist counseling activity and interaction with clinicians, as the images could be shared between consultants located at different sites. Also, it could support a 24/7 laboratory activity, allowing the plates to be read outside the laboratory in a hub-laboratory or even at home, with follow-up work performed in real time where the plates are incubated.

To make these technological innovations fully operational, a middleware information technology (IT) solution is needed to connect all the laboratory instruments (Zimmermann, 2021).

## Discussion

The main reason to introduce automation in a laboratory is to increase productivity and to face limited budgets and personnel shortages. However, implementation of LA can represent an exceptional opportunity to change laboratory organization, improve quality, and reduce TTR, with a potential positive impact on laboratory, patient, and hospital management.

One of the most relevant innovations of LA regards the reading phase, with the possibility to read simultaneously all the plates inoculated from one of even more samples from the same patient. Moreover, taking advantage of informatics, it is also possible to view patient microbiological, hematological, and even clinical and therapeutic data while reading the plates. This patient-oriented

approach provides meaningful clinical interpretation of results and decision-making.

By continuously tracing all the analytical steps, LA ensures that the microbiologist knows in real time the work to be carried out. This concept fully adheres to the so-called "lean" organization that, initially envisaged for industry (Womack et al., 1990), is increasingly applied to healthcare processes. "Lean" means to do only valuable activities, without any delay, avoiding "waste" or unnecessary work. This implies a dramatic revolution in the mentality of microbiologists, transitioning from exclusively sample-centered laboratory work towards a more clinically oriented activity, shortening TTR and prioritizing diagnosis of time-dependent infections. Taking advantage of workflow optimization, about 24 h reduction in TTR has been observed for positive BC processed by LA, with a significant decrease of duration of empirical therapy and mortality (De Socio et al., 2018). Similar results were observed for urines (Yarbrough et al., 2018) and nasal MRSA surveillance (Burckhardt et al., 2018) and all types of specimens (Croxatto et al., 2017; Theparee et al., 2017).

An artificial intelligence algorithm to interpret culture results is another important tool applicable to LA: automated reporting of negative samples can be done without delay and further human assistance, so that clinicians can receive earlier results to rule out MDRO colonization or a urinary tract infection and reduce the need for patient isolation or antibiotic treatment (Faron et al., 2016a; Faron et al., 2016b; Cherkaoui and Schrenzel, 2022).

Beside LA, a variety of technologies are revolutionizing clinical microbiology. These include MALDI-TOF MS (Seng et al., 2009), time-lapse microscopy for ID and phenotypic AST (Charnot-Katsikas et al., 2018), molecular diagnostic tests and syndromic panels (Arena et al., 2017; Trotter et al., 2019), and next-generation sequencing (Mitchell and Simner, 2019; Pitashny et al., 2022). All of them can significantly improve the diagnosis and therapy of infections, but as stated above, they are primarily complementary to culture (Trotter et al., 2019). Thus, in an advanced laboratory, the goal will be to implement the use of all these technologies in a coordinated and timely program of diagnostic stewardship (DS). For example, for active surveillance of MDRO, both molecular and culture methods should be available in the laboratory (Anandan et al., 2015). Indeed, active surveillance of carbapenem-resistant Enterobacteriaceae can limit and prevent their spread and infections, which is crucially relevant to AS (Ambretti et al., 2019). In high-risk patients, rapid molecular methods are more appropriate, but cannot replace culture-based methods, as the latter can detect all types of carbapenem-resistant organisms, perform phenotypic susceptibility testing, and collect and store the isolates (Ambretti et al., 2019). An interesting algorithm, based on a multi-parametric score including clinical, microbiological, and biochemical parameters, has been recently proposed to establish patient priority, including information on infection or colonization by MDRO (Mangioni et al., 2019). It is reasonable to think that by combining DS and AS programs with a strict collaboration between laboratory and clinicians, the impact of modern microbiology on the management of infection can progressively increase.

In this line, rapid and effective communication from laboratory to wards and back is essential for optimal patient care. A recent study showed that many barriers exist, like verbal reporting of results, poorly integrated information systems, mutual lack of insight into each other's area of expertise, and limited laboratory services (Skodvin et al., 2017). Electronic reporting improves communication between microbiologists and clinical staff, but a sort of alarm for the right physician (i.e., the treating clinician, an infectious diseases specialist, or a sepsis team member) to look up the data immediately should be integrated. Nevertheless, we believe that direct microbiologist/clinician interplay remains crucial for an optimal patient management: positive BC, detection of MDRO, isolation of alert organisms from sterile fluids, and acid-fast bacilli in respiratory samples must be immediately reported to someone who will act on the results.

Moreover, as microbiological methods become increasingly sophisticated, good clinical practice should be for the microbiologist to report the results with comments to facilitate the clinician's interpretation of the significance of the data (Arena et al., 2017). In our experience, after LA implementation, a closer relationship with clinicians has been established, providing an opportunity to convey insight into microbiology and microbiological work processes to clinical staff. On the other hand, patients are increasingly complex and heterogeneous and management of severe and MDRO infections is challenging, often requiring a multidisciplinary approach for optimal personalized diagnostics and therapy (Tiseo et al., 2022). Therefore, to integrate DS with AS, microbiologists should broaden their knowledge of patient care by working closely with physicians.

Information from the microbiology laboratory is essential for the control and management of infections in a hospital. In particular, timely and accurate data on the antibiotic susceptibility profiles for pathogens isolated from different wards and on MDRO colonization/infection are the basis for setting up hospital infection control and AS programs, which can ultimately affect patient outcome. Unfortunately, laboratories are not always able to provide timely information due to lack of specific expertise, personnel, user-friendly software, and optimized workflow practices. The implementation of LA and informatics can support integration into routine practice monitoring specimens' quality, isolation of specific pathogens, alert reports for infection control practitioners, and real-time collection of lab trend data, all essential for the prevention and control of infections and epidemiological studies.

In conclusion, timely, accurate, and clinically relevant information is the basis for prevention and treatment of infections. LA and informatics can greatly improve the accuracy of diagnostic procedures, TTR, and laboratory workflow. However, to exploit these technologies for the benefit of the patients, clinical microbiologists need to change their way of working, according to a lean workflow and a patient-centered approach, and their way of thinking, working more closely with clinical staff.

## Data availability statement

The original contributions presented in the study are included in the article/supplementary material. Further inquiries can be directed to the corresponding author.

## Author contributions

Study concept: AM, GD, EC. Critical revision of manuscript: PB, EP. Approval of manuscript: AM, GD, EC, PB, EP. All authors contributed to the article and approved the submitted version.

## Conflict of interest

AM has received funds for speaking at a symposium organized on behalf of Becton-Dickinson.

The remaining authors declare that the research was conducted in the absence of any commercial or financial relationships that could be construed as a potential conflict of interest.

## Publisher's note



## References

Ambretti, S., Bassetti, M., Clerici, P., Petrosillo, N., Tumietto, F., Viale, P., et al. (2019). Screening for carriage of carbapenem-resistant enterobacteriaceae in settings of high endemicity: a position paper from an Italian working group on CRE infections. *Antimicrob. Resist. Infect. Control.* 8, 136. doi: 10.1186/s13756-019-0591-6

Anandan, S., Damodaran, S., Gopi, R., Bakthavatchalam, Y. D., and Veeraraghavan, B. (2015). Rapid screening for carbapenem resistant organisms: current results and future approaches. *J. Clin. Diagn. Res.* 9 (9), DM01–DM03. doi: 10.7860/JCDR/2015/14246.6530

Antonelli, A., Giani, T., Di Pilato, V., Riccobono, E., Perriello, G., Mencacci, A., et al. (2019). KPC-31 expressed in a ceftazidime/avibactam-resistant klebsiella pneumoniae is associated with relevant detection issues. *J. Antimicrob. Chemother.* 74 (8), 2464–2466. doi: 10.1093/jac/dkz156

Arena, F., Giani, T., Pollini, S., Viaggi, B., Pecile, P., and Rossolini, G. M. (2017). Molecular antibiogram in diagnostic clinical microbiology: advantages and challenges. *Future Microbiol.* 12, 361–364. doi: 10.2217/fmb-2017-0019

Burckhardt, I. (2018). Laboratory automation in clinical microbiology. *Bioengineering (Basel).* 5 (4), 102. doi: 10.3390/bioengineering5040102

Burckhardt, I., Horner, S., Burckhardt, F., and Zimmermann, S. (2018). Detection of MRSA in nasal swabs-marked reduction of time to report for negative reports by substituting classical manual workflow with total lab automation. *Eur. J. Clin. Microbiol. Infect. Dis.* 37 (9), 1745–1751. doi: 10.1007/s10096-018-3308-5

Burckhardt, I., Last, K., and Zimmermann, S. (2019). Shorter incubation times for detecting multi-drug resistant bacteria in patient samples: defining early imaging time points using growth kinetics and total laboratory automation. *Ann. Lab. Med.* 39 (1), 43–49. doi: 10.3343/alm.2019.39.1.43

Camarlinghi, G., Parisio, E. M., Antonelli, A., Nardone, M., Coppi, M., Giani, T., et al. (2019). Discrepancies in fosfomycin susceptibility testing of KPC-producing klebsiella pneumoniae with various commercial methods. *Diagn. Microbiol. Infect. Dis.* 93 (1), 74–76. doi: 10.1016/j.diagmicrobio.2018.07.014

Charnot-Katsikas, A., Tesic, V., Love, N., Hill, B., Bethel, C., Boonlayangoor, S., et al. (2018). Use of the accelerate pheno system for identification and antimicrobial susceptibility testing of pathogens in positive blood cultures and impact on time to results and workflow. *J. Clin. Microbiol.* 56 (1), e01166–e01117. doi: 10.1128/JCM.01166-17

Cheng, C. W. R., Ong, C. H., and Chan, D. S. G. (2020). Impact of BD kiestra InoqulA streaking patterns on colony isolation and turnaround time of methicillin-resistant staphylococcus aureus and carbapenem-resistant enterobacterales surveillance samples. *Clin. Microbiol. Infect.* 26 (9), 1201–1206. doi: 10.1016/j.cmi.2020.01.006

Cherkaoui, A., Renzi, G., Vuilleumier, N., and Schrenzel, J. (2019). Copan WASPLab automation significantly reduces incubation times and allows earlier culture readings. *Clin. Microbiol. Infect.* 25 (11), 1430.e5–1430.e12. doi: 10.1016/j.cmi.2019.04.001

Cherkaoui, A., Renzi, G., Vuilleumier, N., and Schrenzel, J. (2021). Performance of fully automated antimicrobial disk diffusion susceptibility testing using copan WASP colibri coupled to the radian in-line carousel and expert system. *J. Clin. Microbiol.* 59 (9), e0077721. doi: 10.1128/JCM.00777-21

Cherkaoui, A., Riat, A., Renzi, G., Fischer, A., and Schrenzel, J. (2023). Diagnostic test accuracy of an automated device for the MALDI target preparation for microbial identification. *Eur. J. Clin. Microbiol. Infect. Dis.* 42 (2), 153–159. doi: 10.1007/s10096-022-04531-3

Cherkaoui, A., and Schrenzel, J. (2022). Total laboratory automation for rapid detection and identification of microorganisms and their antimicrobial resistance profiles. *Front. Cell Infect. Microbiol.* 12. doi: 10.3389/fcimb.2022.807668

Croxatto, A., Dijkstra, K., Prod'hom, G., and Greub, G. (2015). Comparison of inoculation with the InoqulA and WASP automated systems with manual inoculation. *J. Clin. Microbiol.* 53 (7), 2298–2307. doi: 10.1128/JCM.03076-14

Croxatto, A., Marcelpoil, R., Orny, C., Morel, D., Prod'hom, G., and Greub, G. (2017). Towards automated detection, semi-quantification and identification of microbial growth in clinical bacteriology: a proof of concept. *BioMed. J.* 40 (6), 317–328. doi: 10.1016/j.bj.2017.09.001

Croxatto, A., Prod'hom, G., Faverjon, F., Rochais, Y., and Greub, G. (2016). Laboratory automation in clinical bacteriology: what system to choose? *Clin. Microbiol. Infect.* 22 (3), 217–235. doi: 10.1016/j.cmi.2015.09.030

Culbreath, K., Piwonka, H., Korver, J., and Noorbakhsh, M. (2021). Benefits derived from full laboratory automation in microbiology: a tale of four laboratories. *J. Clin. Microbiol.* 59, e01969–e01920. doi: 10.1128/JCM.01969-20

Dauwalder, O., Landrieve, L., Laurent, F., de Montclos, M., Vandenesch, F., and Lina, G. (2016). Does bacteriology laboratory automation reduce time to results and increase quality management? *Clin. Microbiol. Infect.* 22 (3), 236–243. doi: 10.1016/j.cmi.2015.10.037

De Socio, G. V., Di Donato, F., Paggi, R., Gabrielli, C., Belati, A., Rizza, G., et al. (2018). Laboratory automation reduces time to report of positive blood cultures and improves management of patients with bloodstream infection. *Eur. J. Clin. Microbiol. Infect. Dis.* 37 (12), 2313–2322. doi: 10.1007/s10096-018-3377-5

De Socio, G. V., Rubbioni, P., Botta, D., Cenci, E., Belati, A., Paggi, R., et al. (2019). Measurement and prediction of antimicrobial resistance in bloodstream infections by ESKAPE pathogens and escherichia coli. *J. Glob Antimicrob. Resist.* 19, 154–160. doi: 10.1016/j.jgar.2019.05.013

Faron, M. L., Buchan, B. W., Coon, C., Liebregts, T., van Bree, A., Jansz, A. R., et al. (2016b). Automatic digital analysis of chromogenic media for vancomycin-Resistant-Enterococcus screens using copan WASPLab. *J. Clin. Microbiol.* 54 (10), 2464–2469. doi: 10.1128/JCM.01040-16

Faron, M. L., Buchan, B. W., Vismara, C., Lacchini, C., Bielli, A., Gesu, G., et al. (2016a). Automated scoring of chromogenic media for detection of methicillin-resistant staphylococcus aureus by use of WASPLab image analysis software. *J. Clin. Microbiol.* 54 (3), 620–624. doi: 10.1128/JCM.02778-15

Foschi, C., Gaibani, P., Lombardo, D., Re, M. C., and Ambretti, S. (2020). Rectal screening for carbapenemase-producing enterobacteriaceae: a proposed workflow. *J. Glob Antimicrob. Resist.* 21, 86–90. doi: 10.1016/j.jgar.2019.10.012

Iversen, J., Stendal, G., Gerdes, C. M., Meyer, C. H., Andersen, CØ, and Frimodt-Møller, N. (2016). Comparative evaluation of inoculation of urine samples with the copan WASP and BD kiestra InoqulA instruments. *J. Clin. Microbiol.* 54 (2), 328–332. doi: 10.1128/JCM.01718-15

Jacot, D., Sarton-Lohéac, G., Coste, A. T., Bertelli, C., Greub, G., Prod'hom, G., et al. (2021). Performance evaluation of the becton Dickinson kiestra™ IdentifA/SusceptA. *Clin. Microbiol. Infect.* 27 (8), 1167.e9–1167.e17. doi: 10.1016/j.cmi.2020.09.050

Kulengowski, B., Ribes, J. A., and Burgess, D. S. (2019). Polymyxin b etest® compared with gold-standard broth microdilution in carbapenem-resistant enterobacteriaceae exhibiting a wide range of polymyxin b MICs. *Clin. Microbiol. Infect.* 25 (1), 92–95. doi: 10.1016/j.cmi.2018.04.008

Kumar, A., Ellis, P., Arabi, Y., Roberts, D., Light, B., Parrillo, J. E., et al. (2009). Cooperative antimicrobial therapy of septic shock database research group. initiation of inappropriate antimicrobial therapy results in a fivefold reduction of survival in human septic shock. *Chest* 136 (5), 1237–1248. doi: 10.1378/chest.09-0087

Levy, M. M., Evans, L. E., and Rhodes, A. (2018). The surviving sepsis campaign bundle: 2018 update. *Intensive Care Med.* 44 (6), 925–928. doi: 10.1007/s00134-018-5085-0

Mangioni, D., Viaggi, B., Giani, T., Arena, F., D'Arienzo, S., Forni, S., et al. (2019). Diagnostic stewardship for sepsis: the need for risk stratification to triage patients for fast microbiology workflows. *Future Microbiol.* 14, 169–174. doi: 10.2217/fmb-2018-0329

Messacar, K., Parker, S. K., Todd, J. K., and Dominguez, S. R. (2017). Implementation of rapid molecular infectious disease diagnostics: the role of diagnostic and antimicrobial stewardship. *J. Clin. Microbiol.* 55 (3), 715–723. doi: 10.1128/JCM.02264-16

Mitchell, S. L., and Simner, P. J. (2019). Next-generation sequencing in clinical microbiology: are we there yet? *Clin. Lab. Med.* 39 (3), 405–418. doi: 10.1016/j.cll.2019.05.003

Moreno-Camacho, J. L., Calva-Espinosa, D. Y., Leal-Leyva, Y. Y., Elizalde-Olivas, D. C., Campos-Romero, A., and Alcántar-Fernández, J. (2017). Transformation from a conventional clinical microbiology laboratory to full automation. *Lab. Med.* 49 (1), e1–e8. doi: 10.1093/labmed/lmx079

O'Neill, J. (2016). Tackling drug-resistant infections globally: final report and recommendations. Review on Antimicrobial Resistance. Wellcome Trust and HM Government. Available at: https://amr-review.org/sites/default/files/160525_Final%20paper_with%20cover.pdf

Pitashny, M., Kadry, B., Shalaginov, R., Gazit, L., Zohar, Y., Szwarcwort, M., et al. (2022). NGS in the clinical microbiology settings. *Front. Cell Infect. Microbiol.* 12. doi: 10.3389/fcimb.2022.955481

Quiblier, C., Jetter, M., Rominski, M., Mouttet, F., Böttger, E. C., Keller, P. M., et al. (2016). Performance of copan WASP for routine urine microbiology. *J. Clin. Microbiol.* 54 (3), 585–592. doi: 10.1128/JCM.02577-15

Raman, G., Avendano, E., Berger, S., and Menon, V. (2015). Appropriate initial antibiotic therapy in hospitalized patients with gram-negative infections: systematic review and meta-analysis. *BMC Infect. Dis.* 15, 395. doi: 10.1186/s12879-015-1123-5

Seng, P., Drancourt, M., Gouriet, F., La Scola, B., Fournier, P. E., Rolain, J. M., et al. (2009). Ongoing revolution in bacteriology: routine identification of bacteria by matrix-assisted laser desorption ionization time-of-flight mass spectrometry. *Clin. Infect. Dis.* 49 (4), 543–551. doi: 10.1086/600885

Simner, P. J., and Patel, R. (2020). Cefiderocol antimicrobial susceptibility testing considerations: the achilles' heel of the Trojan horse? *J. Clin. Microbiol.* 17, 59(1): e00951–20. doi: 10.1128/JCM.00951-20

Skodvin, B., Aase, K., Brekken, A. L., Charani, E., Lindemann, P. C., and Smith, I. (2017). Addressing the key communication barriers between microbiology laboratories and clinical units: a qualitative study. *J. Antimicrob. Chemother.* 72 (9), 2666–2672. doi: 10.1093/jac/dkx163

Tabak, Y. P., Vankeepuram, L., Ye, G., Jeffers, K., Gupta, V., and Murray, P. R. (2018). Blood culture turnaround time in U.S. acute care hospitals and implications for laboratory process optimization. *J. Clin. Microbiol.* 56 (12), e00500–e00518. doi: 10.1128/JCM.00500-18

Theparee, T., Das, S., and Thomson, R. B.Jr (2017). Total laboratory automation and matrix-assisted laser desorption ionization-time of flight mass spectrometry improve turnaround times in the clinical microbiology laboratory: a retrospective analysis. *J. Clin. Microbiol.* 56 (1), e01242–e01217. doi: 10.1128/JCM.01242-17

Thomson, R. B.Jr, and McElvania, E. (2019). Total laboratory automation: what is gained, what is lost, and who can afford it? *Clin. Lab. Med.* 39 (3), 371–389. doi: 10.1016/j.cll.2019.05.002

Tiseo, G., Brigante, G., Giacobbe, D. R., Maraolo, A. E., Gona, F., Falcone, M., et al. (2022). Diagnosis and management of infections caused by multidrug-resistant bacteria: guideline endorsed by the Italian society of infection and tropical diseases (SIMIT), the Italian society of anti-infective therapy (SITA), the Italian group for antimicrobial stewardship (GISA), the Italian association of clinical microbiologists (AMCLI) and the Italian society of microbiology (SIM). *Int. J. Antimicrob. Agents* 60 (2), 106611. doi: 10.1016/j.ijantimicag.2022.106611

Trotter, A. J., Aydin, A., Strinden, M. J., and O'Grady, J. (2019). Recent and emerging technologies for the rapid diagnosis of infection and antimicrobial resistance. *Curr. Opin. Microbiol.* 51, 39–45. doi: 10.1016/j.mib.2019.03.001

Vandenberg, O., Durand, G., Hallin, M., Diefenbach, A., Gant, V., Murray, P., et al. (2020). Consolidation of clinical microbiology laboratories and introduction of transformative technologies. *Clin. Microbiol. Rev.* 33 (2), e00057–e00019. doi: 10.1128/CMR.00057-19

Womack, J. P., Jones, D. T., and Roos, D. (1990). *The machine that changed the world* (New York, NY, USA: Free Press).

Yarbrough, M. L., Lainhart, W., McMullen, A. R., Anderson, N. W., and Burnham, C. D. (2018). Impact of total laboratory automation on workflow and specimen processing time for culture of urine specimens. *Eur. J. Clin. Microbiol. Infect. Dis.* 37 (12), 2405–2411. doi: 10.1007/s10096-018-3391-7

Zilberberg, M. D., Nathanson, B. H., Sulham, K., Fan, W., and Shorr, A. F. (2017). Carbapenem resistance, inappropriate empiric treatment and outcomes among patients hospitalized with enterobacteriaceae urinary tract infection, pneumonia and sepsis. *BMC Infect. Dis.* 17 (1), 279. doi: 10.1186/s12879-017-2383-z

Zimmermann, S. (2021). Laboratory automation in the microbiology laboratory: an ongoing journey, not a tale? *J. Clin. Microbiol.* 59 (3), e02592–e02520. doi: 10.1128/JCM.02592-20

frontiers | Frontiers in Cellular and Infection Microbiology

TYPE Original Research
PUBLISHED 01 July 2023
DOI 10.3389/fcimb.2023.1183078



OPEN ACCESS

EDITED BY
Joseph Oliver Falkinham,
Virginia Tech, United States

REVIEWED BY
Min Chen,
Shanghai Changzheng Hospital, China
Weida Liu,
Chinese Academy of Medical Sciences, China

*CORRESPONDENCE
Lianjuan Yang
lianjuanyang@163.com

†These authors have contributed equally to this work

RECEIVED 09 March 2023
ACCEPTED 12 June 2023
PUBLISHED 01 July 2023

CITATION
Yu Q, Wang Y, Gao Z, Yang H, Liu S, Tan J and Yang L (2023) DNA microarray chip assay in new use: early diagnostic value in cutaneous mycobacterial infection. *Front. Cell. Infect. Microbiol.* 13:1183078. doi: 10.3389/fcimb.2023.1183078



# DNA microarray chip assay in new use: early diagnostic value in cutaneous mycobacterial infection

Qian Yu†, Yuanyuan Wang†, Zhiqin Gao, Hong Yang, Siyu Liu, Jingwen Tan and Lianjuan Yang*

Department of Medical Mycology, Shanghai Skin Disease Hospital, Tongji University School of Medicine, Shanghai, China

**Introduction:** The clinical practicability of DNA microarray chip in detecting the presence of mycobacterial species/isolates directly in the skin tissues has not been evaluated, nor the efficacy of DNA microarray chip as a novel diagnostic tool for the early diagnosis of cutaneous mycobacterial infections is known.

**Methods:** The present study analyzed the incidence of cutaneous mycobacterial infections in Shanghai and explored the efficacy of a novel DNA microarray chip assay for the clinical diagnosis of the disease from skin tissue specimens compared to traditional detection methods. A total of 60 participants fulfilling the defined diagnostic criteria and confirmed positive for cutaneous mycobacterial infections from 2019 to 2021 were enrolled in the study. Subsequent to recording the participants' medical history and clinical characteristics, the skin tissue specimens were collected for analyses. The specimens underwent histopathological analyses, skin tissue culture, and DNA microarray chip assay.

**Results:** Increased incidence of cutaneous mycobacterial infection was detected from 2019 to 2021. The most common infecting pathogen was *M. marinum* followed by *M. abscessus*. The sensitivity, specificity and accuracy of the skin tissue culture method were 70%, 100% and 76.62%, respectively, while that of the DNA microarray chip assay were 91.67%, 100% and 93.51%, respectively. The sensitivity and accuracy of the DNA microarray chip assay were significantly higher than those of the skin tissue culture method. The positive likelihood and diagnostic odds ratio were >10 and >1, respectively for both the methods. The negative likelihood ratio was significantly higher (30% vs 8.33%) and the Youden's index was significantly lower (70.00% vs 91.67%) in the skin culture method compared to that of the DNA microarray chip assay. There was a significant association of false negative results with a history of antibiotic use in the skin tissue culture method.

**Discussion:** Given the increasing incidence of cutaneous mycobacterial infections, early diagnosis remains a prime clinical focus. The DNA microarray chip assay provides a simple, rapid, high-throughput, and reliable method for the diagnosis of cutaneous mycobacterial infections with potential for clinical application.

KEYWORDS

DNA microarray chip, early diagnosis, cutaneous mycobacterial infection, nontuberculous mycobacteria, skin tissue culture

# 1 Introduction

Cutaneous mycobacterial infection is an infectious granuloma of the skin and subcutaneous soft tissue caused by pathogens commonly found in clinical settings, *Nontuberculous mycobacteria* (NTM) and *Mycobacterium tuberculosis* (MTB) (Gardini et al., 2022). The incidence of cutaneous mycobacterial infections has been steadily increasing over the past 10 years, with a higher rate of occurrence due to factors such as the rising prevalence of HIV infection, increased use of immunosuppressants, growing geriatric population, and cosmetic or surgical procedures (Mei et al., 2019). This group of diseases are frequently underdiagnosed and delayed treatment results in significant stigma, disfigurement, deformity, and disability.

Diagnosis of cutaneous mycobacterial infection is challenging because of the wide spectrum of nonspecific clinical manifestations and histopathological similarities including the granulomatous reaction pattern (Min et al., 2012; Franco-Paredes et al., 2018). Conventional culture methods are considered the 'gold standard,' but they are often time-consuming and have a lower positivity rate, resulting in delayed patient care (Kromer et al., 2019). Recently, several studies have reported the use of various molecular diagnostic techniques, such as gene sequencing, PCR analysis, and high-performance liquid chromatography, that could used for the rapid identification of mycobacterial species/isolates (Kim et al., 2015; Kim et al., 2018; Shen et al., 2020). These have been gradually accepted by dermatologists as an auxiliary in the diagnosis of cutaneous mycobacterial infections. However, the clinical application of these techniques is limited due to their being labor-intensive, less efficient, and expensive. Thus, development of a rapid, simple, high-throughput, and accurate diagnostic method for the detection of mycobacterial species/isolates remains the need of the hour.

DNA microarray chip technology has emerged as a promising tool for the rapid detection of mycobacterial species (Tobler et al., 2006; Gaballah et al., 2022). Zhu et al. established a DNA microarray platform based on the principle of polymorphism in the 16S rRNA space region for multi-target, rapid, and simultaneous detection of 17 pathogenic mycobacteria associated with pulmonary mycobacterial infection, including NTM and MTB (Zhu et al., 2010; Shi et al., 2012). As a diagnostic tool for pulmonary mycobacterial infections, DNA microarray chip technology enables high throughput and rapid detection of mycobacterial isolates in sputum specimens. However, their widespread application for the clinical diagnosis of dermatological diseases, still needs to be explored.

This retrospective study aimed to investigate the incidence and clinical characteristics of cutaneous mycobacterial infections, explore the clinical practicability of DNA microarray chip in detecting the presence of mycobacterial species/isolates directly in the skin tissues, and performs a comparative study with traditional methods to analyze the efficacy of DNA microarray chip as a novel diagnostic tool for the early diagnosis of cutaneous mycobacterial infections.

# 2 Materials and methods

## 2.1 Clinical sample collection

The present retrospective study was conducted at the Shanghai Dermatology Hospital, China. Patients admitted to the hospital from January 2019 to December 2021, who were suspected to be positive for cutaneous mycobacterial infection were included in the study. The study was reviewed and approved by the Ethics Committee of Shanghai Dermatology Hospital. The participants provided their written informed consent to participate in the study and for the publication of any potentially identifiable images or data included in this article. Details of participants, including age, sex, signs and symptoms of disease, medical history, contributing factors, therapeutic schedule, and prognosis were documented. Clinical samples were taken from participants and evaluated for hematology and blood chemistry, skin biopsy, skin tissue culture, identification of microbial isolates, and DNA microarray chip assay. Skin tissue specimens from participants were divided into three parts (6×6×6 mm, each) and processed for histopathological analyses, tissue culture and pathogen identification, and DNA microarray chip assay. Contaminated skin tissue specimens that were extremely small were excluded from the study.

Control group: The 17 mycobacterial reference strains were used as positive controls. The negative controls were skin samples from 8 patients who were diagnosed with deep dermatophytosis, 5 with pigmented nevus, 2 with epidermoid cysts and 2 with seborrheic keratosis.

## 2.2 Culture and gene sequencing

Skin tissues were excised, ground, and decontaminated with N-acetyl-L-cysteine-2% sodium hydroxide (pH 6.8) according to the

standard protocol. Bacteria suspended in phosphate buffered saline (PBS) were concentrated by centrifugation at 3000 x *g* for 15 min and the sediment was resuspended in 0.5 mL of sterile water for use as skin tissue homogenates for standby application. Further, skin tissue homogenates were cultured in Lowenstein-Jensen media at 30 °C and 37 °C in 5% $CO_2$ and in Sabouraud dextrose agar (SDA) at 26 °C and 35 °C. Although NTM species grow within 2-3 weeks on subculturing, the cultures in the present study were incubated for 6 weeks. The suspected samples with *M. ulcerans* or *M. genavense* were stored for 8-12 weeks. Cutaneous MTB cultures were cultured for 8-12 weeks. The cultured organisms were characterized as acid-fast bacilli by Ziehl-Neelsen staining. Subsequently, mycobacterial genomic DNA was extracted, 16S rRNA gene was amplified by polymerase chain reaction (PCR), sequenced, and the obtained sequences were compared using BLAST for the identification of mycobacterial species.

## 2.3 DNA microarray biochip assay

The DNA microarray biochip (CapitalBio Company Ltd, Beijing, China) used in the study could identify 17 mycobacterial species, including *M. tuberculosis*, *M. intracellulare*, *M. avium*, *M. gordonae*, *M. kansasii*, *M. fortuitum*, *M. scrofulaceum*, *M. gilvum*, *M. terrae*, *M. chelonae/M. abscessus*, *M. phlei*, *M. nonchromogenicum*, *M. marinum/M. ulcerans*, *M. aurum*, *M. szulgai/M. malmoense*, *M. xenopi*, and *M. smegmatis*. The DNA microarray biochip test was performed as described previously (Zhu et al., 2010). Firstly, skin tissue homogenates were processed for DNA extraction and target gene fragments were amplified by PCR using 16S rRNA. PCR was performed in two amplification rounds, with an initial activation step at 37 °C for 10 min, denaturation at 94 °C for 10 min, followed by 35 cycles of first round exponential amplification at 94 °C for 30 s, 60 °C for 30 s, and 72 °C for 40 s, followed by 10 cycles of second round linear amplification at 94 °C for 30 s and 72 °C for 60 s, and final extension at 72 °C for 5 min. Secondly, the amplified and fluorescently labeled gene fragments were hybridized with probes on the DNA microarray chip. Probes represented species-specific 16S rRNA gene sequences for the identification of different Mycobacterial species. Thirdly, the chip images were analyzed using a LuxScan Dx24 microarray scanner (CapitalBio Company Ltd, Beijing, China) and the fluorescent intensities were quantified by the mycobacteria identification array test system software (CapitalBio Company Ltd, Beijing, China).

## 2.4 Diagnostic criteria

In the present study, diagnosis of cutaneous mycobacterial infection was based on the combination of clinical and microbiological evidence. A participant was defined as positive for cutaneous mycobacterial infection, if they met all of the following diagnostic criteria: suspected of having cutaneous mycobacterial infection; skin biopsy indicated infectious granuloma irrespective of the Ziehl-Neelsen staining; one or more positive result confirming mycobacterial infection with any of the microbiological detection methods used, including skin tissue culture and DNA microarray chip or macrogenomic detection of pathogenic microorganisms; and participant cured after combined anti-mycobacterial therapy.

## 2.5 Statistical analysis

Data were analyzed using the SPSS version 20.0 software (Armonk, IBM Corp., NY). The median and interquartile range (IQR) was calculated using descriptive statistics. Sensitivity, specificity, and accuracy of clinical diagnosis between two categories of samples were calculated and compared. The effectiveness of the methods used to diagnose cutaneous mycobacterial infection was compared using the likelihood ratio, the Youden's index, and the diagnostic odds ratio. The sensitivity, accuracy, negative likelihood ratios, and Youden's indices were compared between the groups using Chisquare tests. For the skin tissue culture method, risk factors associated with false-negative results were identified using logistic regression analysis. All statistical tests were two-sided, and results were considered significant at a $P < 0.05$.

# 3 Results

## 3.1 Predominance of NTM over MTB infections in cutaneous mycobacterial infected participants

A total of 77 suspected cutaneous mycobacterial infection cases were enrolled for the study, of which 60 cases were confirmed with cutaneous mycobacterial infection as they met the specified diagnostic criteria, 12 cases were diagnosed with cutaneous deep dermatophytosis through skin tissue culture, and 5 cases were diagnosed with non-infectious granuloma by skin biopsy. The number of cutaneous mycobacterial infection cases was in general increased during the study period (Supplementary Figure 1). Cutaneous NTM infections were more prominent than MTB infections in the study population (91.67% and 8.33%, respectively). The most common NTM species detected were *M. marinum* (58.33%), followed by *M. abscessus* (30.00%), and *M. chelonae* (3.33%), respectively (Table 1).

## 3.2 Clinical features of participants with cutaneous mycobacterial infections

Clinical features and causative factors of cutaneous mycobacterial infection of participants are summarized in Table 2. The infected male-to female ratio was 1:2.75, indicating a selective predominance of infection in females. The median age of participants was 52.5 years (range: 10-82 years). The time lapse between the onset and diagnosis ranged from 1 month to 40 years. The median course of cutaneous mycobacterial infection was 4 months (range: 1-480 months) and the causative factors were recorded in 53 participants. Aquatic trauma was reported by 24

10.3389/fcimb.2023.1183078

TABLE 1 Profile of mycobacterial species detected in participants with cutaneous mycobacterial infection (n = 60).

| | Year of diagnosis, No. (%) of isolates | | | |
|---|---|---|---|---|
| | 2019 (n = 8) | 2020 (n = 16) | 2021 (n = 36) | Total (n = 60) |
| Mycobacterium species | n (%) | n (%) | n (%) | n (%) |
| ***M. tuberculosis*** | 1 (12.50) | 2 (12.50) | 2 (5.56) | 5 (8.33) |
| **NTM** | | | | |
| ***M. marinum*** | 6 (75.00) | 10 (62.50) | 19 (52.78) | 35 (58.33) |
| ***M. abscessus*** | 1 (12.50) | 3 (18.75) | 14 (38.89) | 18 (30.00) |
| ***M. chelonae*** | 0 | 1 (6.25) | 1 (2.78) | 2 (3.33) |

participants (40.00%, 23 cases of *M. marinum* and a case of *M. chelonae* infection), while non-aquagenic trauma was found in 7 cases (11.67%, 5 cases of *M. marinum* and 2 cases of MTB infection). Cosmetic procedure preceded infection in 19 participants (31.67%, 18 cases of *M. abscessus* and a case of *M. chelonae* infection). BCG vaccination preceded one case of MTB infection (1.67%), while tuberculosis was associated with 2 cases of MTB infection (3.33%). Several participants had a history of antibiotic use before consultation, either in the form of systemic administration or tropical ointment (23 cases (38.33%) and 15 cases (25.00%), respectively.

The skin lesions were initially localized on the hand (55.00%) followed by the face (30.00%). These predilection sites were mainly located on vulnerability or injection sites. The following skin presentations were documented: nodules (63.33%, Figure 1A), abscesses (33.33%, Figure 1B), ulcers (5.00%, Figure 1C), and papules and plaques (6.67% and 21.67%, respectively, Figure 1D). Of the participants, 13 (21.67%) had single lesions, while 47 (78.33%) had multiple lesions. Lymphocutaneous lesions were present in 23 participants (45.8%), of whom 22 were infected with *M. marinum* and one with *M. chelonae*. Non-lymphocutaneous lesions were seen in 29 participants (37.5%), of whom 12 were infected with *M. marinum*, 15 with *M. abscessus*, one case each with MTB and *M. chelonae*. Deep infection was seen in four participants, two of whom were infected with MTB and *M. abscessus*. Disseminated cutaneous lesions were present in 4 participants, of whom 2 cases were infected with MTB and one each with *M. marinum* and *M. abscessus*.

## 3.3 Diverse manifestation of laboratory findings in participants with cutaneous mycobacterial infections

Histopathological examination of the specimens revealed epidermal changes in the form of acanthosis, pseudoepitheliomatous hyperplasia, or exocytosis (Figure 1E). Diffuse inflammatory cell infiltration was seen in the dermis comprising multinucleated giant cells, lymphocytes, neutrophils, and plasmocytes (Figure 1F), which was manifested in the form of an infectious granuloma (Figures 1E, F). The Ziehl-Neelsen staining and Periodic-acid-Schiff were negative in all the analyzed skin biopsy specimens.

TABLE 2 Clinical features of participants with cutaneous mycobacterial infection (n = 60).

| Characteristics | n | % |
|---|---|---|
| Sex | | |
| Male | 16 | 26.67 |
| Female | 44 | 73.33 |
| Age | | |
| 0~39 years | 23 | 38.33 |
| 40~59 years | 21 | 35 |
| ≥60 years | 16 | 26.67 |
| Median (range) | 52.5 (10~82) | |
| Duration, mo. | | |
| ≤3 | 26 | 43.33 |
| >3,≤6 | 15 | 25 |
| >6 | 19 | 31.67 |
| Median (range) | 4 (1~480) | |
| Causative factor | | |
| Aquatic trauma | 24 | 40 |
| Nonaquatic Trauma | 7 | 11.67 |
| Cosmetic procedures | 19 | 31.67 |
| Iatrogenic procedures | 1 | 1.67 |
| Internal focus | 2 | 3.33 |
| None | 7 | 11.67 |
| History of antibiotic usage | | |
| Systemic antibiotic | 23 | 38.33 |
| Topical antibiotic | 15 | 25 |
| None | 22 | 36.67 |
| Initial location of skin lesion | | |
| Hand | 33 | 55 |
| Face | 18 | 30 |

(Continued)

TABLE 2 Continued

| Characteristics | n | % |
|---|---|---|
| Forearm | 3 | 5 |
| Neck | 2 | 3.33 |
| Lower limb | 1 | 1.67 |
| Trunk | 1 | 1.67 |
| Multiple sites | 2 | 3.33 |
| Type of lesion | | |
| Nodules | 38 | 63.33 |
| Papules | 4 | 6.67 |
| Plaques | 13 | 21.67 |
| Abscesses | 20 | 33.33 |
| Ulcers | 3 | 5 |
| No. of sites | | |
| Single | 13 | 21.67 |
| Multiple | 47 | 78.33 |
| Pattern of distribution | | |
| Lymphocutaneous | 23 | 45.8 |
| Non-lymphocutaneous | 29 | 37.5 |
| Deep infection | 4 | 8.3 |
| Disseminated cutaneous | 4 | 8.3 |

Identification of pathogens from skin tissues subjected to mycobacterial culture for 4-12 weeks revealed distinct growth rate for diverse mycobacterial species. Yellowish-white wet colonies were observed in the Lowenstein-Jensen media cultures, while all isolates showed red club-shaped filaments in Ziehl-Neelsen staining (Figure 1G).

For the DNA microarray chip assay, the mapped images of MTB and 16 NTM were as described previously, with each of the 17 mycobacteria having their own graphic features (Zhu et al., 2010). Analysis of the images from the present study that were directly detected in the skin tissue compared to that of the mapped images revealed the presence of pathogenic mycobacterial species, such as *M. marinum* (Figure 1H), *M. abscessus* (Figure 1I), MTB (Figure 1J), and *M. chelonae* (Figure 1K).

## 3.4 Enhanced diagnostic sensitivity of DNA microarray chip assay over the skin tissue culture method in detecting cutaneous mycobacterial infections

According to the defined diagnostic criteria for cutaneous mycobacterial infections, 42 cases (70%) were diagnosed positive with the skin tissue culture method and 55 cases (91.67%) using the DNA microarray chip assay, while both assays together detected 56 (93.33%) positive cases. Among the 56 cases, 41 were positive for both the culture and DNA microarray chip assay, 14 were positive for DNA microarray chip assay but negative for culture, and one case was positive for culture but negative for DNA microarray chip assay. Four cases were negative with both culture and DNA microarray chip assay but were confirmed as positive by macrogenomic detection of pathogenic microorganisms.

The reference standard of cutaneous mycobacterial infection calculated based on the defined diagnostic criteria indicated the sensitivity, specificity and accuracy of the skin tissue culture to be 70.00% (95% CI: 56.63-80.80%), 100% (95% CI: 77.08-100%), 76.62% (67.17-86.07%), respectively, and that of the DNA microarray chip assay as 91.67% (95% CI: 80.88-96.89%), 100% (95% CI: 77.08-100%), and 93.51% (95% CI: 88.01-99.01%), respectively (Table 3). The sensitivity and accuracy of DNA microarray chip assay were significantly higher than those of the culture method ($P = 0.003$ and $P= 0.003$, respectively). The positive likelihood ratio of both the skin tissue culture method and DNA microarray chip assay was >10. The negative likelihood ratio of the skin tissue culture method was 30.00% (95% CI: 20.38-44.16%) and that of the DNA microarray chip assay was 8.33% (95% CI: 3.60-19.29%), indicating a statistically significant difference ($P = 0.032$). The Youden's index of skin tissue culture method was significantly lower (70.00%, 95% CI: 56.63-80.80%) than that of the DNA microarray chip assay (91.67%, 95%CI: 80.88-96.89%) ($P = 0.003$) (Table 4).

## 3.5 Antibiotic use associated with false-negative results in the skin tissue culture method based diagnosis of cutaneous mycobacterial infections

Among the 60 cases of cutaneous mycobacterial infection confirmed, 42 were identified as positive by the skin tissue culture method, while 18 were falsely negative. Logistic regression analysis was performed to identify factors associated with the occurrence of false negative results in the skin tissue culture method. The results revealed a significant association with antibiotic usage, but no significant associations were observed with gender, age, duration, or pattern of distribution of skin lesions. Participants with a history of topical or systemic antibiotic use had an 11.81-fold (95% CI: 1.71-81.59) and 36.22-fold (95% CI: 3.63-361.09) increased risk of false negative results, respectively, compared to those with no history of antibiotic use in the skin tissue culture method (Table 5).

# 4 Discussion

The genus mycobacterium is the only entity within the Mycobacteriaceae family (order Actinomycetales, phylum Actinobacteria) that consists of a distinct group of aerobic, nonmotile, nonspore-forming, Gram-positive bacilli (Grange, 1996). Lack of efficient diagnostic methods overlook the detection of Mycobacterium as causative agents of cutaneous and subcutaneous infection in clinical practice (Peters et al., 2016). The present study identified 5 MTB and 55 NTM positive

10.3389/fcimb.2023.1183078

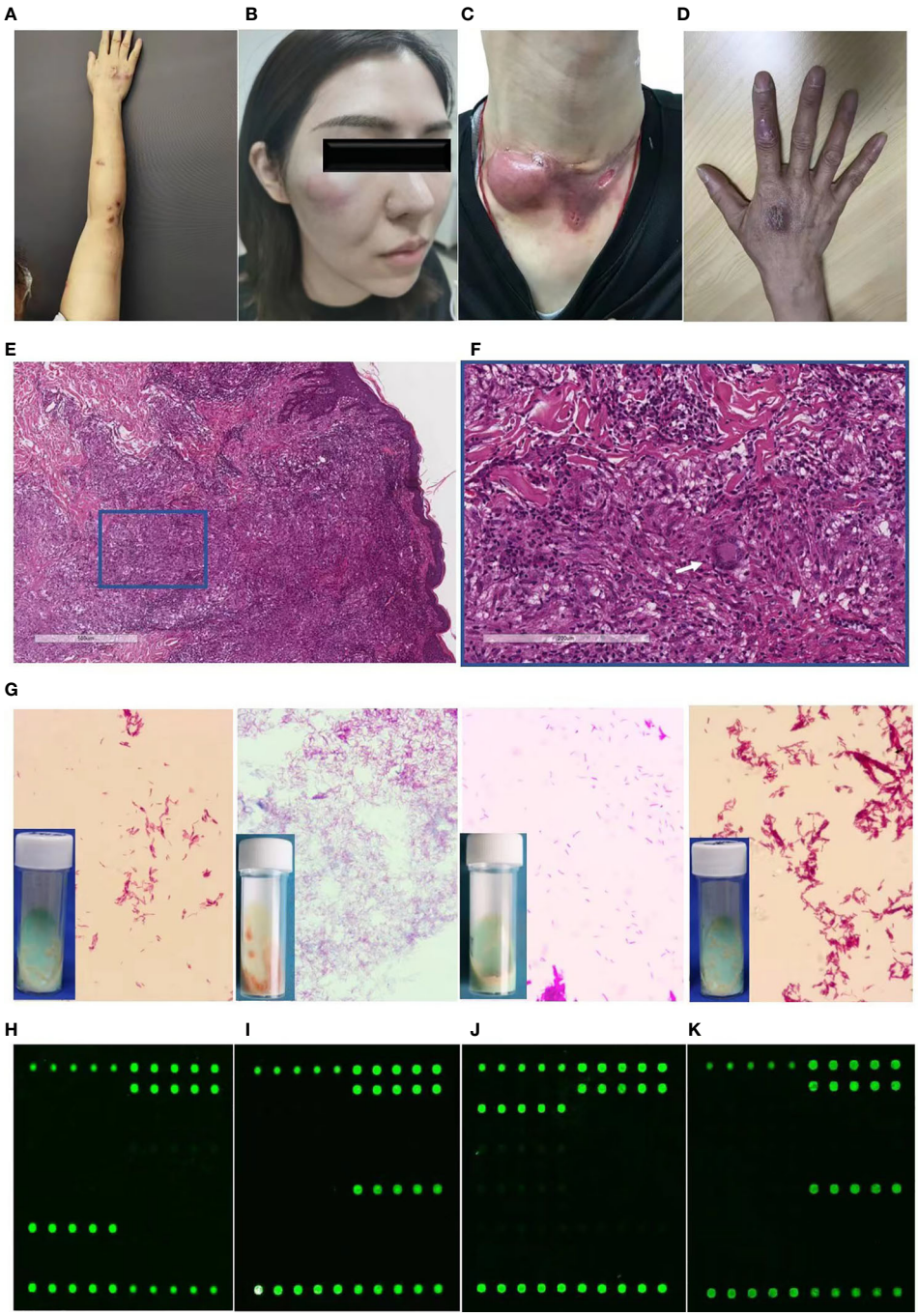


FIGURE 1
Diagnostic profile of clinical images, histopathological findings, Ziehl-Neelsen staining, and DNA microarray chip assay of participants with cutaneous mycobacterial infections. **(A-C)** Skin lesions of participants with cutaneous infection of *M. marinum* **(A)**, *M. abscessus* **(B)**, MTB **(C)**, and *M. chelonae* **(D)**. **(E, F)** Hematoxylin and eosin staining revealing acanthosis, pseudoepitheliomatous hyperplasia or exocytosis, diffuse inflammatory cells infiltration in the dermis, including multinucleated giant cells (white arrow), lymphocytes, neutrophils, and plasmocytes (magnification: A, 40×; B, 200×). **(G)** Ziehl-Neelsen staining of isolates from skin tissue culture showing red club-shaped filaments. **(H-K)** Mapped images of the DNA microarray chip assay of skin tissue confirming infection with *M. marinum* **(H)**, *M. abscessus* **(I)**, MTB **(J)**, and *M. chelonae* **(K)**.

cutaneous infections by combining clinical spectrum and etiological examination. In general, the incidence of NTM infections has been on the rise (Wentworth et al., 2013; Mei et al., 2019; Yeo et al., 2019) and the same was evidenced by the increased number of cutaneous mycobacterial infection cases detected from 2019 to 2021 in our hospital. In addition to the general increase of infections, improved diagnostic accuracy was responsible for the augmented incidence of cutaneous mycobacterial infections (Wang and Pancholi, 2014). The present three-year study found that *M. marinum* infections were predominant over other mycobacterial species in causing cutaneous mycobacterial infections, a trend that has been previously reported (Mei et al., 2019). The surge of *M. abscessus*

TABLE 3 Sensitivities, specificity and accuracy of the skin culture method and DNA microarray chip assay in the diagnosis of cutaneous mycobacterial infections.

| | | Gold standard | | | | | |
|---|---|---|---|---|---|---|---|
| | | Positive [a] (n = 60) | Negative [b] (n = 17) | Total (n = 77) | Sensitivity [c] (95% CI) | Specificity (95% CI) | Accuracy [d] (95% CI) |
| **Skin tissue culture** | Positive | 42 | 0 | 42 | 70.00% (56.63-80.80%) | 100% (77.08-100%) | 76.62% (67.17-86.07%) |
| | Negative | 18 | 17 | 35 | | | |
| **DNA microarray chip** | Positive | 55 | 0 | 55 | 91.67% (80.88-96.89%) | 100% (77.08-100%) | 93.51% (88.01-99.01%) |
| | Negative | 5 | 17 | 22 | | | |

[a]Positive consists of 60 patients with cutanrous mycobacterial infections, who met diagnostic criteria in **2.4**.
[b]Negative consists of 17 skin samples from 8 patients who were diagnosed with deep dermatophytosis, 5 with pigmented nevus, 2 with epidermoid cysts and 2 with seborrheic keratosis.
[c]Comparison of sensitivity between the skin tissue culture and DNA microarray chip assay in the diagnosis of cutaneous mycobacterial infections, P = 0.003.
[d]Comparison of accuracy between the skin tissue culture and DNA microarray chip assay in diagnosis of cutaneous mycobacterial infection, P = 0.003.

TABLE 4 PLR, NLR, Youden's index and OR of the skin tissue culture method and DNA microarray chip assay.

| | PLR (95% CI) | NLR [a] (95% CI) | Youden's index [b] (%) | OR |
|---|---|---|---|---|
| **Skin tissue culture** | >10 | 30.00% (20.38-44.16%) | 70.00% (56.63-80.80%) | >1 |
| **DNA microarray chip** | >10 | 8.33% (3.60-19.29%) | 91.67% (80.88-96.89%) | >1 |

PLR, positive likelihood ratio; NLR, negative likelihood ratio; OR, odds ratio.
[a]Comparison of NLR between the skin tissue culture method and DNA microarray chip assay in the diagnosis of cutaneous mycobacterial infections, P = 0.032.
[b]Comparison of OR between the skin tissue culture method and DNA microarray chip assay in the diagnosis of cutaneous mycobacterial infections, P = 0.003.

infection among young women, with the emergence of diverse unscheduled cosmetic infections, made it the second most causative pathogen of cutaneous mycobacterial infections (Eustace et al., 2016, Yang et al., 2017).

Cutaneous mycobacterial infection usually follows inoculation through contact of damaged skin with environmental niches such as tap water or through invasive medical methods (Bartralot et al., 2005). Infection with *M. marinum* was the most frequent cause of aquatic trauma localized on the hand and forearm, while infection with *M. abscessus* mostly occurred after cosmetic procedures and was restricted to the face. Clinical manifestation and incubation period of these infections were heterogeneous depending on the modality of mycobacterial acquisition, bacterial load, virulence, and host immune status. While cutaneous *M. marinum* infection was manifested as an isolated lesion at the site of trauma or in the form of lymphocutaneous localized infections, *M. abscessus* infections were seen in the form of multiple abscesses upon onset at cosmetic injection sites. In the current study, among the detected 5 cases of MTB infections, 2 were of lupus vulgaris, 2 of scrofulphyma, and a case was of scrofuloderma. Of the two *M. chelonae* infections, a case was similar to *M. marinum* infection presenting lymphocutaneous pattern after aquatic trauma, while the other resembled *M. abscessus* infection and appeared at sites of latrogenic injection. Thus, clinical manifestations of cutaneous mycobacterial infections lack significant pathognomonic characteristics, leaving the diagnosis to be based largely on etiological examination. Cutaneous mycobacterial infections are frequently underdiagnosed because of the limited laboratory facilities and examinations. The traditional detection techniques (Kromer et al., 2019) mostly include histopathology, skin tissue culture, and PCR-bases methods (Abdalla et al., 2009). Histopathologic analyses are nonspecific usually manifesting in the form of granulomatous inflammatory cell infiltrates that are difficult to differentiate from syphilis, granulomatous rosacea, skin tumor (Teh et al., 2013), cutaneous leishmaniasis (Vanlier et al., 2021) and deep dermatophytosis. Thus, histopathologic diagnosis is generally combined with Ziehl-Neelsen staining, particularly for lesions that have a high bacterial load. Although positive Ziehl-Neelsen staining supports the diagnosis of cutaneous mycobacterial infection, it fails to identify the pathogenic bacterial species based on morphological characteristics. Identification of clinical mycobacterium isolates at the species level is pivotal for the formulation of antibiotic treatment regimens. Presently, skin tissue culture is considered the sole reliable method for determining and identifying the presence of mycobacterial species and their respective sensitivity to drugs (Samper and González-Martin, 2018). Diverse mycobacterial species exhibit distinct culture conditions with specific incubation temperatures and time (Wallace et al., 2021). Majority of the mycobacterium grow at 35-37°C. However, *M. ulcerans* and *M. marinum* grow best at 30-32°C, while *M. kansasii* grows at 31°C and 37°C with specific growth characteristics exhibited subsequent to light exposure. Furthermore, recovery of all mycobacterial species requires culturing for several weeks. Incubation period for cultures of *M. marinum*, MTB (Handog et al., 2008), and *M. ulcerans* are 2-4, 2-6, and 6-12 weeks, respectively. Thus, the overall operational process of the skin tissue culture method is time-consuming and labor-intensive. In addition, the participants have to endure long waiting period for

TABLE 5 Correlated factors for missed diagnosis of cutaneous mycobacterial infection in the skin tissue culture method.

| | Positive rate | Skin tissue culture | |
|---|---|---|---|
| | | OR (95% CI) | *P*-value |
| Sex | | | |
| Male | 13 (61.25%) | Reference | |
| Female | 29 (65.91%) | 0.36 (0.06-2.36) | 0.288 |
| Age | | | |
| 0~39 years | 15 (65.22%) | Reference | |
| 40~59 years | 15 (71.43%) | 1.22 (0.15-9.56) | 0.854 |
| ≥60 years | 12 (75.00%) | 0.69 (0.10-4.74) | 0.709 |
| Duration, mo. | | | |
| ≤3 | 22 (84.62%) | Reference | |
| >3,≤6 | 11 (74.33%) | 3.23(0.74-24.29) | 0.106 |
| >6 | 9 (47.37%) | 2.04(0.30-13.90) | 0.469 |
| History of antibiotic usage | | | |
| None | 22 (95.65%) | Reference | |
| Topical antibiotic | 11 (73.33%) | *11.81 (1.71-81.59)* | *0.012* |
| Systemic antibiotic | 9 (40.91%) | *36.22(3.63-361.09)* | *0.002* |
| Pattern of distribution | | | |
| Lesion restricted to primary sites | 21 (72.41%) | Reference | |
| Lesions progressed to distant sites | 21 (67.74%) | 2.27(0.40-12.94) | 0.356 |

OR, odds ratio.

results with probable aggravation of skin lesions during the interval. Hence, availability of rapid and simple molecular techniques for the diagnosis of cutaneous mycobacterial infections is the need of the hour.

The advent of molecular biology techniques that led to significant advances in DNA amplification and hybridization techniques has significantly aided the rectification of current flaws in the diagnosis of cutaneous mycobacterial infections (Jagielski et al., 2016). DNA sequencing, PCR-restriction fragment length polymorphism (RFLP) assays (Wong et al., 2003), gene chip assays (Chang et al., 2010), and commercial kits, such as GenoType and INNO-LiPA, are established nucleic acid-based assays for identification of mycobacterial infections (Zhu et al., 2010). DNA sequencing, especially metagenomic next-generation sequencing (mNGS) (Kong et al., 2022), has greater efficiency, sensitivity, and specificity in detection of pathogenic bacteria, and can even detect rare pathogens. However, the detection of non-specific pathogens by mNGS is possible, creating difficulties in differentiating between contaminants, colonizers, and pathogens; furthermore, mNGS is not cheap and could be prohibitively expensive for patients. A positive PCR-RFLP result (Wong et al., 2003) will only confirm mycobacterial infection, without identification of the pathogenic mycobacterial species. Previously used gene chip assays (Chang et al., 2010) and DNA probes (Chung et al., 2018) have limited detection ranges, and are also not available for most NTM species; moreover, these methods can only be used for detection in specific samples types, such as mycobacterial isolates, sputum, pus. Both the GenoType and the INNO-LiPA assay are line-probe assays and, because of the space limitations of the strip, it is difficult to include more probes for the identification of a greater variety of species in a single experiment. Since the molecular methods mentioned above have flawed including high price, low sensitivity, restricted detection range, and low efficiency (Yüksel and Tansel, 2009; Röltgen et al., 2012), it makes meeting the clinical diagnostic demand challenging.

The newly designed DNA microarray biochip system with species-specific 16S rRNA sequences for identifying 17 mycobacterial species could be promising for diagnosing mycobacterial infections (Zhu et al., 2010). Compared to other currently used diagnostic methods, the advantages of DNA microarray biochip-based diagnostic method are as follows: (i) It have simplified the procedure for nucleic acid extraction, convenient operation process, and concise interpretation of the result. The time span from the start of the DNA microarray chip assay to the acquisition of the results averages 6 h. Compared to traditional culture methods that can take 2-12 weeks, the use of the DNA microarray biochip greatly shortens the diagnostic procedure. (ii) Each DNA microarray chip can simultaneously and rapidly test

4 samples, while each experiment can test 24 chips simultaneously. This high-throughput feature reduces the need for repetitive work by the technician and can thus meet busy clinical requirements. (iii) The cost of mycobacterial detection by the DNA microarray biochip is about $30 per sample, which is much cheaper than that of other molecular diagnostic methods, especially mNGS. The low cost is more acceptable to patients and more conducive to clinical application. Thus, the DNA microarray biochip assay is a simple, rapid, high-throughput, and economical diagnostic detection method that is ideal for the clinical screening of large numbers of samples.

The DNA microarray chip technology had been widely used for the diagnosis of pulmonary mycobacterial infections employing sputum specimens (Shi et al., 2012). Skin represents the most common extrapulmonary organ involved in mycobacterial infections (Rajendran et al., 2021) and therefore warrants an urgent need for efficient and accurate diagnostic methods. In the present study, a novel DNA microarray chip was used for the detection of mycobacterial isolates in clinical skin tissue specimens and was found to be more sensitive and accurate compared to that of the conventional culture method (70.00% vs 91.67%; 77.92% vs 93.51%). The positive likelihood ratios for both DNA microarray chip and culture method were more than 10, which provided clear evidence that they were significantly more likely to diagnose cutaneous mycobacterial infection accurately. The negative likelihood ratio was significantly smaller for DNA microarray chip compared with the culture method, suggesting that the negative results of DNA microarray chip were more likely to true negative. The Youden's index for DNA microarray chip was superior to that for culture method, indicating that the results of DNA microarray chip were more reliable. Diagnostic detection sensitivity of the skin tissue culture method was susceptible to antibiotic usage, since 63.33% of the participants with cutaneous mycobacterial infection had a history of systemic or topical antibiotic abuse before he/she visited the hospital. Inappropriate use of antibiotics might have reduced mycobacterial infection to a certain extent lessening the mycobacterial load or activity and could have contributed to the false negative results in the skin tissue culture method. However, diagnosis of cutaneous mycobacterial infection by the DNA microarray chip assay was not influenced by antibiotic treatment, probably due to the detection of DNA sequences from bacterial debris or dead bacteria. Thus, the DNA microarray chip assay is a highly sensitive and reliable clinical diagnostic technique for the early etiological diagnosis of cutaneous mycobacterial infection that could facilitate timely intervention of pathogen-adapted antimicrobial therapy.

The results of the present study indicate DNA microarray chip assay as an effective method for the early diagnosis of cutaneous mycobacterial infections. However, the method is limited in differentiating *M. marinum-M. ulcerans* and *M. chelonae-M. abscessus* paired infections, as each of these paired NTMS have the same 16S rRNA sequences. Thus, the method is reliable as a diagnostic tool in combination with medical history and clinical symptoms. This limitation could potentially be overcome by using combined probes 16S rRNA and 23S rRNA, or 5S rRNA genes. Further, the DNA microarray chip assay is limited in providing information related to drug-resistance and is therefore inefficient in completely replacing the skin tissue culture method, which still remain an essential part of the diagnosis and treatment protocol. Future research is required to develop modified DNA chip related technologies for the detection of drug resistance in the diagnosis of cutaneous mycobacterial infections.

## 5 Conclusion

The present study reports on the incidence, clinical characteristics, and pathogenic profile of mycobacteria associated with cutaneous mycobacterial infections in Shanghai, China. Achieving accurate and rapid diagnosis of cutaneous mycobacterial infections remains a major clinical challenge that requires specific and timely intervention for effective treatment and improved prognosis. The DNA microarray chip assay evaluated in this study provides a simple, rapid, high-throughput, and reliable method for identifying 17 mycobacterial species, and overcomes the limitations associated with traditional detection methods for diagnosing cutaneous mycobacterial infections. Therefore, the DNA microarray chip assay holds great potential as a clinical tool for diagnosing cutaneous mycobacterial infections.

## Data availability statement

The datasets presented in this study can be found in online repositories. The names of the repository/repositories and accession number(s) can be found below: https://www.ncbi.nlm.nih.gov/, OQ594967 OQ594968 OQ594969 OQ594970 OQ594971 OQ594972 OQ594973 OQ594974 OQ594975 OQ594976 OQ594977 OQ594978 OQ594979 OQ594980 OQ594981 OQ594982 OQ594983 OQ594984 OQ594985 OQ594986 OQ594987 OQ594988 OQ594989 OQ594990 OQ594991 OQ594992 OQ594993 OQ594994 OQ594995 OQ594996 OQ594997 OQ594998 OQ594999 OQ595000 OQ595001 OQ595002 OQ595003 OQ595004 OQ595005 OQ595006 OQ595007 OQ595008.

## Ethics statement

Written informed consent was obtained from the individual(s) for the publication of any potentially identifiable images or data included in this article.

## Author contributions

QY and YW designed and drafted the work, contributed to the DNA microarray chip testing, analysis, acquisition, and interpretation of data; ZG, HY, and SL performed the laboratory tests and analyzed the data; JT reviewed the cases and provided clinical information; LY designed the study, revised, and finalized

the manuscript. All authors contributed to the article and approved the submitted version.

## Funding

This work was supported by the National Natural Science Foundation of China (Grant number 82173429 to LY), the Science and Technology Commission of Shanghai Municipality (Grant number 20Y11905600 and 21Y11904900 to QY and LY, respectively), and the Shanghai Municipal Commission of Health and Family Planning (Grant number 20194Y0337 and 201940476 to QY and LY, respectively).

## Acknowledgments

We thank Prof. Hai Wen (Shanghai Changzheng Hospital, Second Military Medical University) for his assistance in designing this study.

## Conflict of interest

The authors declare that the research was conducted in the absence of any commercial or financial relationships that could be construed as a potential conflict of interest.

## Publisher's note



## Supplementary material

The Supplementary Material for this article can be found online at: https://www.frontiersin.org/articles/10.3389/fcimb.2023.1183078/full#supplementary-material

## References

Abdalla, C. M. Z., de Oliveira, Z. N. P., Sotto, M. N., Leite, K. R. M., Canavez, F. C., and de Carvalho, C. M. (2009). Polymerase chain reaction compared to other laboratory findings and to clinical evaluation in the diagnosis of cutaneous tuberculosis and atypical mycobacteria skin infection. *Int. J. Dermatol.* 48, 27–35. doi: 10.1111/j.1365-4632.2009.03807.x

Bartralot, R., García-Patos, V., Sitjas, D., Rodríguez-Cano, L., Mollet, J., Martín-Casabona, N., et al. (2005). Clinical patterns of cutaneous nontuberculous mycobacterial infections. *Br. J. Dermatol.* 152, 727–734. doi: 10.1111/j.1365-2133.2005.06519.x

Chang, H. J., Huang, M. Y., Yeh, C. S., Chen, C. C., Yang, M. J., Sun, C. S., et al. (2010). Rapid diagnosis of tuberculosis directly from clinical specimens using a gene chip. *Clin. Microbiol. Infect.* 16, 1090–1096. doi: 10.1111/j.1469-0691.2009.03045.x

Chung, J., Ince, D., Ford, B. A., and Wanat, K. A. (2018). Cutaneous infections due to nontuberculosis mycobacterium: recognition and management. *Am. J. Clin. Dermatol.* 19 (6), 867–878. doi: 10.1007/s40257-018-0382-5

Eustace, K., Jolliffe, V., Sahota, A., and Gholam, K. (2016). Cutaneous mycobacterium abscessus infection following hair transplant. *Clin. Exp. Dermatol.* 41, 768–770. doi: 10.1111/ced.12900

Franco-Paredes, C., Marcos, L. A., Henao-Martínez, A. F., Rodríguez-Morales, A. J., Villamil-Gómez, W. E., Gotuzzo, E., et al. (2018). Cutaneous mycobacterial infections. *Clin. Microbiol. Rev.* 32, e00069–e00018. doi: 10.1128/CMR.00069-18

Gaballah, A., Ghazal, A., Almiry, R., Emad, R., Sades, N., Rahman, M. A., et al. (2022). Simultaneous detection of mycobacterium tuberculosis and atypical mycobacterium by DNA- microarray in Egypt. *Med. Princ. Pact.* 31, 246–253. doi: 10.1159/000524209

Gardini, G., Gregori, N., Matteelli, A., and Castelli, F. (2022). Mycobacterial skin infection. *Curr. Opin. Infect. Dis.* 35, 79–87. doi: 10.1097/QCO.0000000000000820

Grange, J. M. (1996). The biology of the genus mycobacterium. *Soc Appl. Bacteriol. Symp. Ser.* 25, 1S–9S.

Handog, E. B., Gabriel, T. G., and Pineda, R. T. (2008). Management of cutaneous tuberculosis. *Dermatol. Ther.* 21, 154–161. doi: 10.1111/j.1529-8019.2008.00186.x

Jagielski, T., Minias, A., van Ingen, J., Rastogi, N., Brzostek, A., Żaczek, A., et al. (2016). Methodological and clinical aspects of the molecular epidemiology of mycobacterium tuberculosis and other mycobacteria. *Clin. Microbiol. Rev.* 29, 239–290. doi: 10.1128/CMR.00055-15

Kim, Y. N., Kim, K. M., Choi, H. N., Lee, J. H., Park, H. S., Jang, K. Y., et al. (2015). Clinical usefulness of PCR for differential diagnosis of tuberculosis and nontuberculous mycobacterial infection in paraffin-embedded lung tissues. *J. Mol. Diagn.* 17, 597–604. doi: 10.1016/j.jmoldx.2015.04.005

Kim, J. U., Ryu, D. S., Cha, C. H., and Park, S. H. (2018). Paradigm for diagnosing mycobacterial disease: direct detection and differentiation of mycobacterium tuberculosis complex and non-tuberculous mycobacteria in clinical specimens using multiplex real-time PCR. *J. Clin. Pathol.* 71, 774–780. doi: 10.1136/jclinpath-2017-204945

Kong, M., Li, W., Kong, Q., Dong, H., Han, A., and Jiang, L. (2022). Application of metagenomic next-generation sequencing in cutaneous tuberculosis. *Front. Cell. Infect. Microbiol.* 12. doi: 10.3389/fcimb.2022.942073

Kromer, C., Fabri, M., Schlapbach, C., Schulze, M. H., Groß, U., Schön, M. P., et al. (2019). Diagnosis of mycobacterial skin infections. *J. Dtsch. Dermatol. Ges.* 17, 889–893. doi: 10.1111/ddg.13925

Mei, Y., Zhang, W., Shi, Y., Jiang, H., Chen, Z., Chokkakula, S., et al. (2019). Cutaneous tuberculosis and nontuberculous mycobacterial infections at a national specialized hospital in China. *Acta Derm. Venereol.* 99, 997–1003. doi: 10.2340/00015555-3283

Min, K. W., Ko, J. Y., and Park, C. K. (2012). Histopathological spectrum of cutaneous tuberculosis and non-tuberculous mycobacterial infections. *J. Cutan. Pathol.* 39, 582–595. doi: 10.1111/j.1600-0560.2012.01903.x

Peters, F., Batinica, M., Plum, G., Eming, S. A., and Fabri, M. (2016). Bug or no bug: challenges in diagnosing cutaneous mycobacterial infections. *J. Dtsch. Dermatol. Ges.* 14, 1227–1235. doi: 10.1111/ddg.13001

Rajendran, P., Padmapriyadarsini, C., and Mondal, R. (2021). Nontuberculous mycobacterium: an emerging pathogen: Indian perspective. *Int. J. Mycobacteriol.* 10, 217–227. doi: 10.4103/ijmy.ijmy_141_21

Röltgen, K., Assan-Ampah, K., Danso, E., Yeboah-Manu, D., and Pluschke, G. (2012). Development of a temperature-switch PCR-based SNP typing method for mycobacterium ulcerans. *PloS Negl. Trop. Dis.* 6, e1904. doi: 10.1371/journal.pntd.0001904

Samper, S., and González-Martin, J. (2018). Microbiological diagnosis of infections caused by the genus mycobacterium. *Enferm. Infecc. Microbiol. Clin. (Engl. Ed).* 36, 104–111. doi: 10.1016/j.eimc.2017.11.009

Shen, Y., Fang, L., Xu, X., Ye, B., and Yu, G. (2020). CapitalBio mycobacterium real-time polymerase chain reaction detection test: rapid diagnosis of mycobacterium tuberculosis and nontuberculous mycobacterial infection. *Int. J. Infect. Dis.* 98, 1–5. doi: 10.1016/j.ijid.2020.06.042

Shi, X. C., Liu, X. Q., Xie, X. L., Xu, Y. C., and Zhao, Z. X. (2012). Gene chip array for differentiation of mycobacterial species and detection of drug resistance. *Chin. Med. J. (Engl.)* 125, 3292–3297.

Teh, R. W., Feeney, K., Francis, R. J., Phillips, M., and Millward, M. J. (2013). Mycobacterium mimicking metastatic melanoma. *Intern. Med. J.* 43, 1342–1346. doi: 10.1111/imj.12209

Tobler, N. E., Pfunder, M., Herzog, K., Frey, J. E., and Altwegg, M. (2006). Rapid detection and species identification of mycobacterium spp. using real-time PCR and DNA-microarray. *J. Microbiol. Methods* 66, 116–124. doi: 10.1016/j.mimet.2005.10.016

Vanlier, C., Marot, L., Laranaga, E., D'abadie, P., Yombi, J. C., Yildiz, H., et al. (2021). A case report of cutaneous leishmaniasis: a misleading clinical presentation. *Infection* 49 (1), 177–180. doi: 10.1007/s15010-020-01517-1

Wallace, E., Hendrickson, D., Tolli, N., Mehaffy, C., Peña, M., Nick, J. A., et al. (2021). Culturing mycobacteria. *Methods Mol. Biol.* 2314, 1–58. doi: 10.1007/978-1-0716-1460-0_1

Wang, S. H., and Pancholi, P. (2014). Mycobacterial skin and soft tissue infection. *Curr. Infect. Dis. Rep.* 16, 438. doi: 10.1007/s11908-014-0438-5

Wentworth, A. B., Drage, L. A., Wengenack, N. L., Wilson, J. W., and Lohse, C. M. (2013). Increased incidence of cutaneous nontuberculous mycobacterial infection 1980 to 2009: a population-based study. *Mayo Clin. Proc.* 88, 38–45. doi: 10.1016/j.mayocp.2012.06.029

Wong, D. A., Yip, P. C., Tse, D. L., Tung, V. W., Cheung, D. T., and Kam, K. M. (2003). Routine use of a simple low-cost genotypic assay for the identification of mycobacteria in a high throughput laboratory. *Diagn. Microbiol. Infect. Dis.* 47 (2), 421–426. doi: 10.1016/s0732-8893(03)00133-0

Yang, P., Lu, Y., Liu, T., Zhou, Y., Guo, Y., Zhu, J., et al. (2017). Mycobacterium abscessus infection after facial injection with autologous fat: a case report. *Ann. Plast. Surg.* 78 (2), 138–140. doi: 10.1097/SAP.0000000000000837

Yeo, P. M., Lee, S. X., Tan, Y. E., Sng, L. H., and Ang, C. C. (2019). Epidemiology, risk factors, and outcomes of adult cutaneous non-tuberculous mycobacterial infection over a 10-year period in Singapore. *Int. J. Dermatol.* 58, 679–687. doi: 10.1111/ijd.14356

Yüksel, P., and Tansel, O. (2009). Characterization of pncA mutations of pyrazinamide-resistant mycobacterium tuberculosis in Turkey. *New Microbiol.* 32, 153–158.

Zhu, L., Jiang, G., Wang, S., Wang, C., Li, Q., Yu, H., et al. (2010). Biochip system for rapid and accurate identification of mycobacterial species from isolates and sputum. *J. Clin. Microbiol.* 48, 3654–3660. doi: 10.1128/JCM.00158-10

# Frontiers in
# Cellular and Infection Microbiology

**Investigates how microorganisms interact with their hosts**

Explores bacteria, fungi, parasites, viruses, endosymbionts, prions and all microbial pathogens as well as the microbiota and its effect on health and disease in various hosts.

---

## Discover the latest Research Topics

See more →

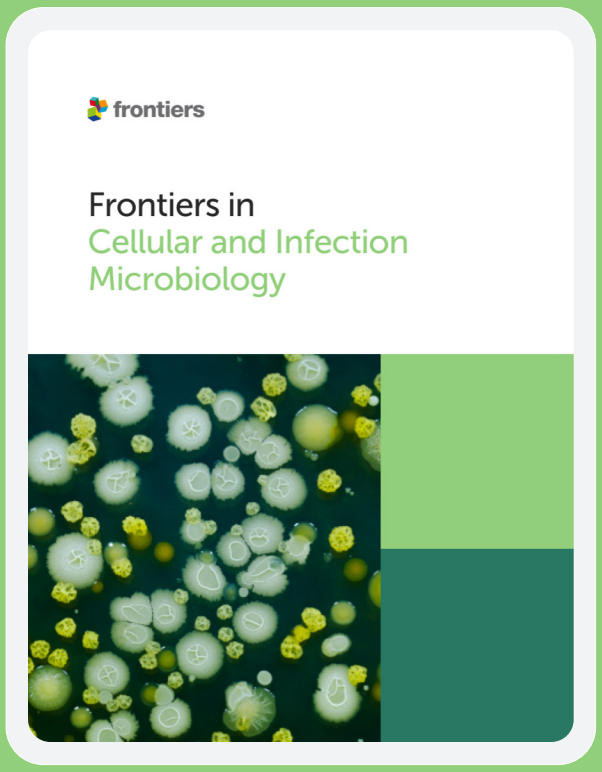


**Frontiers**

Avenue du Tribunal-Fédéral 34
1005 Lausanne, Switzerland
frontiersin.org

**Contact us**

+41 (0)21 510 17 00
frontiersin.org/about/contact